

mgr inż. Piotr Miądlicki

Rozprawa doktorska

**„Izomeryzacja alfa-pinenu na syntetycznych katalizatorach
tytanowo-silikatowych oraz na porowatych materiałach
pochodzenia naturalnego”**

**„Isomerization of alpha-pinene on synthetic titanium-silicate
catalysts and porous materials of natural origin”**

Rozprawa doktorska

napisana pod kierunkiem:

prof. dr hab. inż. Agnieszki Wróblewskiej

Katedra Inżynierii Materiałów Katalitycznych i Sorpcyjnych

Szczecin, 2022

*Niniejszą pracę pragnę zdedykować moim wspaniałym Rodzicom,
dzięki którym miałem możliwość kształcić się i zdobywać cenną wiedzę,
którzy stale mnie mobilizowali i wspierali przez okres trwania studiów*

*Z całego serca dziękuję
Prof. dr hab. inż. Agnieszce Wróblewskiej
za wsparcie i zaufanie w pracy badawczej
oraz stwarzanie niezwykłych możliwości rozwoju*

SPIS TREŚCI

Streszczenie.....	4
Ankieta dorobku naukowego	5
Przewodnik po publikacjach stanowiących rozprawę doktorską.....	24
1. Wstęp teoretyczny	24
2. Cel pracy	29
3. Omówienie wyników badań.....	30
4. Wnioski	40
5. Literatura	43
Kopie cyklu publikacji stanowiących osiągnięcia naukowe, o których mowa w art. 13 ust. 2 ustawy	50

Streszczenie

Terpeny stanowią naturalną alternatywę dla związków organicznych otrzymywanych na drodze syntezy chemicznej z surowców pochodzących z ropy naftowej. Biologiczna aktywność terpenów sprawia, że znalazły one bardzo liczne zastosowania w medycynie i w kosmetyce. Również pochodne terpenów, otrzymane na drodze modyfikacji ich struktur, znajdują liczne zastosowania jako związki biologicznie czynne, stosowane w nowoczesnych terapiach w medycynie lub są wykorzystywane w nowych preparatach kosmetycznych. Przykładem terpenu o bardzo cennych właściwościach jest α -pinen. Bogatym jego źródłem jest terpentyna. Ponadto otrzymuje się go jako produkt uboczny przy produkcji papieru. Jedną z dróg przekształceń terpenów (w tym α -pinenu) jest reakcja izomeryzacji, która przebiega w obecności odpowiednio dobranego katalizatora heterogenicznego. W celu otrzymania pożądaných produktów izomeryzacji α -pinenu, dąży się do otrzymania katalizatorów, które będą ekologiczne, selektywne, tanie w produkcji, stabilne termicznie oraz chemicznie i będą ulegały regeneracji.

Niniejsza rozprawa doktorska pt. „Izomeryzacja alfa-pinenu na syntetycznych katalizatorach tytanowo-silikatowych oraz na porowatych materiałach pochodzenia naturalnego” przedstawia badania dotyczące nowych katalizatorów wykorzystywanych w procesie izomeryzacji α -pinenu. W pracy przedstawiono sposoby otrzymywania syntetycznych katalizatorów tytanowo-silikatowych o różnej zawartości tytanu, takich jak: Ti-SBA-15, Ti-MCM-41, TS-1 oraz opisano również sposoby przygotowania katalizatorów, otrzymanych przez modyfikację naturalnego klinoptylolitu oraz komercyjnego węgla aktywnego DT0. W rozprawie doktorskiej zostały szczegółowo opisane właściwości fizyko-chemiczne otrzymanych materiałów porowatych oraz sprawdzono ich aktywność w procesie izomeryzacji α -pinenu. Najbardziej aktywny katalizator z każdej grupy badanych katalizatorów, posłużył do wyznaczenia najkorzystniejszych warunków prowadzenia izomeryzacji α -pinenu dla tej grupy katalizatorów.

Ankieta dorobku naukowego

mgr inż. Piotr Miądlicki

Wykaz opublikowanych prac naukowych lub twórczych prac zawodowych oraz informacja o osiągnięciach dydaktycznych, współpracy naukowej i popularyzacji nauki.

A. Wykaz publikacji stanowiących osiągnięcia naukowe, o którym mowa w art. 13 ust. 2 ustawy:

Rozprawa doktorska w oparciu o cykl publikacji na temat „Izomeryzacja alfa-pinenu na syntetycznych katalizatorach tytanowo-silikatowych oraz na porowatych materiałach pochodzenia naturalnego”

1. Agnieszka Wróblewska*, **Piotr Miądlicki**, Edyta Makuch, *The isomerization of α -pinene over the Ti-SBA-15 catalyst—the influence of catalyst content and temperature*, Reaction Kinetics, Mechanisms and Catalysis, 119 (2016), 641–654, **IF (2016)-1,264, 5-letni IF-1,762; punkty MNiSW – 40, liczba cytowań - 11**

Moim wkładem do tej pracy było przygotowanie katalizatora Ti-SBA-15 metodą zol-żel, identyfikacja produktów powstających w procesie izomeryzacji, opracowanie metody pozwalającej na określenie składu mieszanin poreakcyjnych, przeprowadzenie serii doświadczeń mających na celu zbadanie aktywności otrzymanego materiału, określenie składu mieszanin poreakcyjnych metodą chromatografii gazowej oraz wyznaczenie wartości głównych funkcji opisujących proces (selektywności produktów, konwersja α -pinenu), dyskusja wyników oraz współtworzenie pierwszej wersji publikacji.

Mój udział procentowy szacuje na 33%.

Udział procentowy pozostałych autorów: Agnieszka Wróblewska – 34%, Edyta Makuch – 33%

2. Agnieszka Wróblewska*, **Piotr Miądlicki***, Joanna Sreńscek-Nazzal, Marcin Sadłowski, Zvi C. Koren, Beata Michalkiewicz, *Alpha-pinene isomerization over Ti-SBA-15 catalysts obtained by the direct method: The influence of titanium content, temperature, catalyst amount and reaction time*, Microporous and Mesoporous Materials, 258 (2018), 72–82, **IF (2018)-4,182; 5-letni IF-4,862; punkty MNiSW – 100, liczba cytowań - 21**

Moim wkładem do tej pracy było przygotowanie serii katalizatorów Ti-SBA-15 o różnej zawartości tytanu metodą zol-żel, wykonanie analiz otrzymanych katalizatorów metodami UV-

VIS oraz FTIR wraz z ich interpretacja, przeprowadzenie serii doświadczeń mających na celu zbadanie aktywności otrzymanych materiałów oraz wyznaczenie najkorzystniejszych warunków prowadzenia reakcji, określenie składu mieszanin poreakcyjnych metodą chromatografii gazowej, przygotowanie wykresów, współudział w opisie i w dyskusji wyników oraz współtworzenie pierwszej wersji publikacji.

Mój udział procentowy szacuję na 30%.

Udział procentowy pozostałych autorów: Agnieszka Wróblewska – 38%, Joanna Sreńscek-Nazzal – 4%, Marcin Sadłowski – 4%, Zvi C. Koren – 4%, Beata Michalkiewicz - 20%

3. Agnieszka Wróblewska*, Piotr Miądlicki*, Jadwiga Tołpa, Joanna Sreńscek-Nazzal, Zvi C. Koren, Beata Michalkiewicz, *Influence of the titanium content in the Ti-MCM-41 catalyst on the course of the α -pinene isomerization process*, Catalysts, 9(5), 396, (2019),, **IF (2019)-3,520, 5-letni IF-4,399; punkty MNiSW – 100, liczba cytowań – 17**

Moim wkładem do tej pracy było przygotowanie serii katalizatorów Ti-MCM-41 o różnej zawartości tytanu metodą zol-żel, wykonanie analiz otrzymanych katalizatorów metodami UV-VIS oraz FTIR oraz ich interpretacja, przeprowadzenie serii doświadczeń mających na celu zbadanie aktywności otrzymanych materiałów oraz wyznaczenie najkorzystniejszych warunków prowadzenia reakcji, określenie składu mieszanin poreakcyjnych metodą chromatografii gazowej oraz wyznaczenie głównych funkcji opisujących proces (selektywności produktów, konwersja α -pinenu), współudział w opisie i w dyskusji wyników oraz współtworzenie pierwszej wersji publikacji.

Mój udział procentowy szacuję na 43%.

Udział procentowy pozostałych autorów: Agnieszka Wróblewska – 43%, Jadwiga Tołpa – 2%, Joanna Sreńscek-Nazzal – 4%, Zvi C. Koren – 2%, Beata Michalkiewicz - 6%

4. Piotr, Miądlicki*, Agnieszka Wróblewska*, Karolina Kiełbasa, Zvi C. Koren, and Beata Michalkiewicz, *Sulfuric acid modified clinoptilolite as a solid green catalyst for solvent-free α -pinene isomerization process*, Microporous and Mesoporous Materials, 324 (2021), **IF (2020)-5,455; 5-letni IF-4,862; punkty MNiSW – 100, liczba cytowań - 10**

Moim wkładem do tej pracy było przygotowanie serii katalizatorów na bazie naturalnego klinoptylolitu, wykonanie analiz otrzymanych katalizatorów metodami UV-VIS, XRD oraz FTIR, a także ich interpretacja, wyznaczenie ilości centrów kwasowych obecnych na powierzchni katalizatora, przeprowadzenie serii doświadczeń mających na celu zbadanie

aktywności otrzymanych materiałów oraz wyznaczenie najkorzystniejszych warunków prowadzenia reakcji, określenie składu mieszanin poreakcyjnych metodą chromatografii gazowej oraz wyznaczenie głównych funkcji opisujących proces (selektywności produktów, konwersja α -pinenu), przygotowanie wykresów, współudział w opisie i w dyskusji wyników oraz tworzenie pierwszej wersji publikacji. Współuczestniczyłem również w przygotowywaniu odpowiedzi na uwagi recenzentów do tego artykułu.

Mój udział procentowy szacuję na 70%.

Udział procentowy pozostałych autorów: Agnieszka Wróblewska – 15%, Karolina Kielbasa – 5 %, Zvi C. Koren – 2%, Beata Michalkiewicz - 8%

5. Joanna Sreńscek-Nazzal*, Adrianna Kamińska, **Piotr Miądlicki**, Agnieszka Wróblewska*, Karolina Kielbasa, Rafał Jan Wróbel, Jarosław Serafin, Beata Michalkiewicz, *Activated carbon modification towards efficient catalyst for high value-added products synthesis from alpha-pinene*, *Materials*, 14 (2021), 7811, **IF (2021)-3,623, 5-letni IF-3,920; punkty MNiSW – 140, liczba cytowań - 3**

Moim wkładem do tej pracy było przygotowanie serii katalizatorów na bazie węgla aktywnego DT0, wykonanie analiz otrzymanych katalizatorów metodami XRD oraz FTIR oraz ich interpretacja, przeprowadzenie serii doświadczeń mających na celu zbadanie aktywności otrzymanych materiałów oraz wyznaczenie najkorzystniejszych warunków prowadzenia reakcji, określenie składu mieszanin poreakcyjnych metodą chromatografii gazowej oraz wyznaczenie głównych funkcji opisujących proces (selektywności produktów, konwersja α -pinenu), przygotowanie wykresów, współudział w opisie i w dyskusji wyników oraz współtworzenie pierwszej wersji publikacji.

Mój udział procentowy szacuję na 65%.

Udział procentowy pozostałych autorów: Joanna Sreńscek-Nazzal – 5%, Adrianna Kamińska – 5%, Agnieszka Wróblewska – 5%, Karolina Kielbasa – 5%, Rafał Jan Wróbel – 5%, Jarosław Serafin – 5 %, Beata Michalkiewicz - 5%

Sumaryczny IF – 18,044

Sumaryczny 5-letni IF – 19,805

Sumaryczna liczba punktów MNiSW – 480

Sumaryczna liczba cytowań (Scopus) - 32

B. Wykaz innych (nie wchodzących w skład osiągnięcia wymienionego w pkt. I) prac naukowych:

1. Agnieszka Wróblewska, Edyta Makuch, Piotr Miądlicki, *The oxidation of limonene at raised pressure and over the various titanium-silicate catalysts*, Polish Journal of Chemical Technology, 17 (2015), 82–87, **IF (2015)-0,575; punkty MNiSW – 70**

Moim wkładem do tej pracy było przeprowadzenie serii reakcji utleniania limonenu w autoklawie oraz oznaczenie nieprzereagowanego nadtlenu wodoru metodą jodometryczną w mieszaninach poreakcyjnych.

Mój udział procentowy szacuję na 33%.

2. Agnieszka Wróblewska, Edyta Makuch, **Piotr Miądlicki**, *The studies on the limonene oxidation over the microporous TS-1 catalyst*, Catalysis Today, 268 (2016), 121–29, **IF (2016)-4,636; punkty MNiSW - 140**

Moim wkładem do tej pracy było przygotowanie katalizatorów TS-1 o różnej zawartości tytanu, przeprowadzenie serii reakcji utleniania limonenu nadtlakiem wodoru, wyznaczenie najkorzystniejszych warunków prowadzenia tej reakcji, określenie składu mieszanin poreakcyjnych metodą chromatografii gazowej oraz wyznaczenie głównych funkcji opisujących proces (selektywności produktów, konwersja limonenu), przygotowanie wykresów, współudział w opisie i w dyskusji wyników oraz współtworzenie pierwszej wersji publikacji.

Mój udział procentowy szacuję na 33%.

3. Mariusz Malko, Adrian Krzysztof Antosik, Agnieszka Wróblewska, Zbigniew Czech, Katarzyna Wilpiszewska, **Piotr Miądlicki**, Beata Michalkiewicz, *Montmorillonite as the catalyst in oxidation of limonene with hydrogen peroxide and in isomerization of limonene*, Polish Journal of Chemical Technology, 19 (2017), 50–58, **IF (2017)-0,550; punkty MNiSW – 70**

Moim wkładem do tej pracy było przeprowadzenie serii doświadczeń dotyczących utleniania limonenu nadtlakiem wodoru, wyznaczenie najkorzystniejszych warunków prowadzenia tej reakcji, określenie składu mieszanin poreakcyjnych metodą chromatografii gazowej oraz wyznaczenie głównych funkcji opisujących proces (selektywności produktów,

konwersja limonenu), przygotowanie wykresów, współudział w opisie i w dyskusji wyników oraz współtworzenie pierwszej wersji publikacji.

Mój udział procentowy szacuję na 15%.

4. Agnieszka Wróblewska, **Piotr Miądlicki**, Edyta Makuch, Natalia Benedyczak, *Epoxidation of natural limonene extracted from orange peels with hydrogen peroxide over Ti-MCM-41 catalyst*, Polish Journal of Chemical Technology, 20 (2018), 1–6, **IF (2018)-0,975; punkty MNiSW - 70**

Moim wkładem do tej pracy było przygotowanie wykresów, współudział w opisie i w dyskusji wyników oraz współtworzenie pierwszej wersji publikacji.

Mój udział procentowy szacuję na 25%.

5. Agnieszka Wróblewska, Katarzyna Janda, Edyta Makuch, Marika Walasek, **Piotr Miądlicki**, Karolina Jakubczyk, *Effect of extraction method on the antioxidative activity of ground elder (Aegopodium Podagraria L.)*, Polish Journal of Chemical Technology, 21 (2019), 13–18, **IF (2019)-1,193; punkty MNiSW - 70**

Moim wkładem do tej pracy było zbadanie składu otrzymanych ekstraktów metodą chromatografii gazowej.

Mój udział procentowy szacuję na 15%.

6. Anna Fajdek-Bieda, Agnieszka Wróblewska, **Piotr Miądlicki**, Alicja Szymańska, Małgorzata Dziecioł, Andy M. Booth, Beata Michalkiewicz, *Influence of technological parameters on the isomerization of geraniol using sepiolite*, Catalysis Letters, 150 (2020), 901–11, **IF (2020)-3,186; punkty MNiSW - 70**

Moim wkładem do tej pracy było określenie składu mieszanin poreakcyjnych metodą chromatografii gazowej, przygotowanie wykresów i współtworzenie pierwszej wersji publikacji.

Mój udział procentowy szacuję na 15%.

7. Agnieszka Wróblewska, Jarosław Serafin, Alicja Gawarecka, **Piotr Miądlicki**, Karolina Urbaś, Zvi C. Koren, Jordi Llorca, Beata Michalkiewicz, *Carbonaceous Catalysts from Orange Pulp for Limonene Oxidation*, Carbon Letters, 30 (2020), 189–98, **IF (2020)-1,917; punkty MNiSW - 40**

Moim wkładem do tej pracy było oznaczenie nieprzereagowanego nadtlenu wodoru metodą jodometryczną oraz przygotowanie wykresów.

Mój udział procentowy szacuję na 10%.

8. Beata Zielińska, Agnieszka Wróblewska, Klaudia Maślana, **Piotr Miądlicki**, Karolina Kielbasa, Anita Rozmysłowska-Wojciechowska, Mateusz Petrus, Jarosław Woźniak, Agnieszka Maria Jastrzębska, Beata Michalkiewicz, Ewa Mijowska, *High catalytic performance of 2D Ti₃C₂T_x MXene in α -pinene isomerization to camphene*, *Applied Catalysis A: General*, 604 (2020), 117765, **IF (2020)-5,706; punkty MNiSW - 100**

Moim wkładem do tej pracy było przeprowadzenie serii doświadczeń mających na celu zbadanie aktywności katalitycznej otrzymanych materiałów oraz wyznaczenie najkorzystniejszych warunków prowadzenia reakcji izomeryzacji, określenie składu mieszanin poreakcyjnych metodą chromatografii gazowej oraz wyznaczenie głównych funkcji opisujących proces (selektywności produktów, konwersja α -pinenu), przygotowanie wykresów, współudział w opisie wyników oraz współtworzenie pierwszej wersji publikacji.

Mój udział procentowy szacuję na 10%.

9. Agnieszka Wróblewska*, Jadwiga Tołpa, Dominika Kłosin, **Piotr Miądlicki**, Zvi C. Koren, Beata Michalkiewicz, *The application of TS-1 materials with different titanium contents as catalysts for the autoxidation of α -pinene*, *Microporous and Mesoporous Materials*, 305 (2020), 1–12, **IF (2020)-5,455; punkty MNiSW - 100**

Moim wkładem do tej pracy było współprzygotowanie serii katalizatorów TS-1 o różnej zawartości tytanu metodą zol-żel, wykonanie analiz otrzymanych katalizatorów metodami UV-VIS oraz FTIR oraz ich interpretacja. Przeprowadzenie badań wstępnych reakcji izomeryzacji α -pinenu, które wykazały brak aktywności w kierunku izomeryzacji, identyfikacja produktów reakcji metodą chromatografii gazowej sprzężonej ze spektrometrią mas i współtworzenie pierwszej wersji publikacji.

Mój udział procentowy szacuję na 20%.

10. Monika Retajczyk, Agnieszka Wróblewska, Zvi C. Koren, Beata Michalkiewicz, Alicja Szymańska, **Piotr Miądlicki**, Zvi C. Koren, Beata Michalkiewicz, *Synthesis, characterization, and catalytic applications of the Ti-SBA-16 porous material in the selective and green*

isomerizations of limonene and s-carvone, Catalysts, 10 (2020), 1–17, **IF (2020)-4,146; punkty MNiSW - 100**

Moim wkładem do tej pracy było przygotowanie wykresów oraz odpowiednie sformatowanie wykazu literatury.

Mój udział procentowy szacuję na 5%.

11. Adrianna Kamińska, Nikola Maciejewska, **Piotr Miądlicki**, Karolina Kiełbasa, Joanna Sreńscek-Nazzal, Beata Michalkiewicz, *Fe-modified activated carbon obtained from biomass as a catalyst for α -pinene autoxidation*, Polish Journal of Chemical Technology, 23 (2021), 73–80, **IF (2021)-1,125; punkty MNiSW - 70**

Moim wkładem do tej pracy było wykonanie analiz otrzymanych katalizatorów metodami XRD i FTIR oraz ich interpretacja, przygotowanie wykresów, współudział w opisie wyników oraz współtworzenie końcowej wersji publikacji.

Mój udział procentowy szacuję na 10%.

12. Adrian Antosik Krzysztof, **Piotr Miądlicki**, Katarzyna Wilpiszewska, Agata Markowska-Szczupak, Zvi C. Koren, Agnieszka Wróblewska, *Polysaccharide films modified by compounds of natural origin and silver having potential medical applications*, Cellulose, 28 (2021), 7257–71, **IF (2021)-5,044; punkty MNiSW - 100**

Moim wkładem do tej pracy było zbadanie pęcznienia otrzymanych materiałów, oznaczenie kąta zwilżalności, przygotowanie części wykresów, współudział w opisie i w dyskusji wyników oraz współtworzenie końcowej wersji publikacji.

Mój udział procentowy szacuję na 15%.

13. Anna Fajdek-Bieda, Agnieszka Wróblewska, **Piotr Miądlicki**, Jadwiga Tołpa, Beata Michalkiewicz, *Clinoptilolite as a natural, active zeolite catalyst for the chemical transformations of geraniol*, Reaction Kinetics, Mechanisms and Catalysis, 133 (2021), 997–1011, **IF (2021)-2,081; punkty MNiSW - 70**

Moim wkładem do tej pracy było określenie składu mieszanin poreakcyjnych metodą chromatografii gazowej, przygotowanie wykresów i współtworzenie końcowej wersji publikacji.

Mój udział procentowy szacuję na 20%.

14. Adrianna Kamińska, **Piotr Miądlicki**, Karolina Kielbasa, Marcin Kujbida, Joanna Sreńscek-Nazzal, Rafał Jan Wróbel, Agnieszka Wróblewska, *Activated carbons obtained from orange peels, coffee grounds, and sunflower husks - comparison of physicochemical properties and activity in the alpha-pinene isomerization process*, *Materials*, 14 (2021), 7448, **IF (2021)-3,623; punkty MNiSW - 140**

Moim wkładem do tej pracy było wykonanie analiz otrzymanych katalizatorów metodami XRD i FTIR oraz ich interpretacja, przygotowanie wykresów, współudział w opisie wyników oraz współtworzenie końcowej wersji publikacji.

Mój udział procentowy szacuję na 5%.

15. Agnieszka Wróblewska, Jadwiga Grzeszczak, **Piotr Miądlicki**, Karolina Kielbasa, Marcin Kujbida, Adrianna Kamińska, Beata Michalkiewicz, *The studies on α -pinene oxidation over the TS-1. The influence of the temperature, reaction time, titanium and catalyst content*, *Materials*, 14 (2021), 7799, **IF (2021)-3,623; punkty MNiSW - 140**

Moim wkładem do tej pracy było wykonanie analiz otrzymanych katalizatorów metodami XRD i FTIR oraz ich interpretacja, przygotowanie wykresów, współudział w opisie wyników oraz współtworzenie końcowej wersji publikacji.

Mój udział procentowy szacuję na 5%.

16. Adrianna Kamińska, **Piotr Miądlicki**, Karolina Kielbasa, Jarosław Serafin, Joanna Sreńscek-Nazzal, Rafał Jan Wróbel, Agnieszka Wróblewska, *FeCl₃-modified carbonaceous catalysts from orange peel for solvent-free alpha-pinene oxidation*, *Materials*, 14 (2021), 7729, **IF (2021)-3,623; punkty MNiSW - 140**

Moim wkładem do tej pracy było wykonanie analiz otrzymanych katalizatorów metodami XRD i FTIR oraz ich interpretacja, przygotowanie wykresów, współudział w opisie wyników oraz współtworzenie końcowej wersji publikacji.

Mój udział procentowy szacuję na 5%.

17. Agata Zubkiewicz, Izabela Irska, **Piotr Miądlicki**, Konrad Walkowiak, Zbigniew Rozwadowski, Sandra Paszkiewicz, *Structure, thermal and mechanical properties of copoly(ester amide)s based on 2,5 - furandicarboxylic acid*, *Journal of Materials Science*, 56 (2021), 19296–309, **IF (2021)-4,220; punkty MNiSW - 100**

Moim wkładem do tej pracy było określenie składu destylatu powstałego w trakcie syntezy polimeru metodą chromatografii gazowej, wykonanie analiz FTIR gotowych polimerów oraz interpretacja części wyników.

Mój udział procentowy szacuję na 10%.

18. Anna Fajdek-Bieda, Agnieszka Wróblewska*, **Piotr Miądlicki**, Anna Konstanciak*, *Conversion of geraniol into useful value-added products in the presence of catalysts of natural origin: diatomite and alum*, *Materials*, 15 (2022), 2449, **IF (2022)-3,623; punkty MNiSW - 140**

Moim wkładem do tej pracy było określenie składu mieszanin poreakcyjnych metodą chromatografii gazowej, przygotowanie wykresów i współtworzenie końcowej wersji publikacji.

Mój udział procentowy szacuję na 20%.

19. Piotr Rychtowski, **Piotr Miądlicki**, Bartłomiej Prowans, Beata Tryba*, *High performance fluidized bed photoreactor for ethylene decomposition*, *Polish Journal of Chemical Technology*, 24 (2022), 2, 50—56, **IF (2022)-1,115; punkty MNiSW - 70**

Moim wkładem do tej pracy było przygotowanie złoża katalitycznego, współkonstrukcja reaktora oraz współtworzenie końcowej wersji publikacji.

Mój udział procentowy szacuję na 25%.

20. Jadwiga Grzeszczak, Agnieszka Wróblewska*, Adrianna Kamińska, **Piotr Miądlicki**, Joanna Sreńscek-Nazzal, Rafał Wróbel, Zvi C. Koren, Beata Michalkiewicz, *Carbon catalysts from pine cones – Synthesis and testing of their activities*, *Catalysis Today*, online 24.08.2022 (2022), **IF (2022)-6,562; punkty MNiSW - 140**

Moim wkładem do tej pracy było wykonanie oraz opis analiz XRD otrzymanych materiałów.

Mój udział procentowy szacuję na 5%.

21. Sandra Paszkiewicz, Konrad Walkowiak, Izabela Irska, Sonia Mechowska, Katarzyna Stankiewicz, Agata Zubkiewicz, Elżbieta Piesowicz, **Piotr Miadlicki**, *Influence of the Multiple Injection Moulding and Composting Time on the Properties of Selected Packaging and Furan-*

Based Polyesters, Journal of Polymers and the Environment, online 03.10.2022 (2022), **IF (2022)-4,705; punkty MNiSW - 70**

Moim wkładem do tej pracy była analiza ekstraktów metanolowych otrzymanych polimerów metodą chromatografii gazowej oraz wykonanie analiz FTIR gotowych polimerów oraz interpretacja części wyników.

Mój udział procentowy szacuję na 5%.

22. Karolina Kielbasa, Şahin Bayar, Esin Apaydin Varol, Joanna Sreńscek-Nazzal, Monika Bosacka, **Piotr Miądlicki**, Jarosław Serafin, Rafał J. Wróbel, Beata Michalkiewicz, *Carbon Dioxide Adsorption over Activated Carbons Produced from Molasses Using H₂SO₄, H₃PO₄, HCl, NaOH, and KOH as Activating Agents*, *Molecules*, 27, 21:7467 (2022), **IF (2022)-4,927; punkty MNiSW - 140**

Moim wkładem do tej pracy było wykonanie analiz XRD oraz FTIR otrzymanych materiałów.

Mój udział procentowy szacuję na 5%.

C. Udzielone patenty oraz zgłoszenia patentowe międzynarodowe i krajowe

Patenty

1. Agnieszka Wróblewska, Edyta Makuch, **Piotr Miądlicki**, Sposób epoksydacji limonenu, Pat. 228408, 30.03.2018,

Mój udział procentowy wynosi: 25%.

2. Agnieszka Wróblewska, **Piotr Miądlicki**, Edyta Makuch, Sposób epoksydacji limonenu, Pat. 228408, 30.03.2017,

Mój udział procentowy wynosi: 35%.

3. Agnieszka Wróblewska, Beata Michalkiewicz, Alicja Gawarecka, **Piotr Miądlicki**, Jarosław Serafin, Sposób wytwarzania katalizatora do utleniania limonenu, Pat. 233634, 29.11.2019

Mój udział procentowy wynosi: 10%.

4. Agnieszka Wróblewska, Beata Michalkiewicz, Alicja Gawarecka, **Piotr Miądlicki**, Jarosław Serafin, Sposób utleniania limonenu, Pat. 231515, 29.03.2019

Mój udział procentowy wynosi: 10%.

5. Agnieszka Wróblewska, **Piotr Miądlicki**, Sposób izomeryzacji α -pinenu, Pat. 230167, 28.09.2018,

Mój udział procentowy wynosi: 40%.

6. Agnieszka Wróblewska, Beata Michalkiewicz, **Piotr Miądlicki**, Jarosław Serafin, Antoni Morawski, Sposób katalitycznego utleniania α -pinenu, Pat. 230992, 31.01.2019,

Mój udział procentowy wynosi: 25%.

7. Agnieszka Wróblewska, Beata Michalkiewicz, Jarosław Serafin, Jacek Młodzik, Alicja Gawarecka, **Piotr Miądlicki**, Sposób utleniania limonenu, Pat. 235721, 05.10.2020,

Mój udział procentowy wynosi: 10%.

8. Agnieszka Wróblewska, Beata Michalkiewicz, Jarosław Serafin, Jacek Młodzik, Alicja Gawarecka, **Piotr Miądlicki**, Zbigniew Czech, Adrian Antosik, Katarzyna Wilpiszewska, Sposób utleniania limonenu, Pat. 231108, 31.01.2019,

Mój udział procentowy wynosi: 11%.

9. Agnieszka Wróblewska, **Piotr Miądlicki**, Sposób izomeryzacji α -pinenu, Pat. 234253, 31.01.2020,

Mój udział procentowy wynosi: 40%.

10. Agnieszka Wróblewska, **Piotr Miądlicki**, Mariusz Malko, Zbigniew Czech, Adrian Antosik, Katarzyna Wilpiszewska, Sposób utleniania limonenu, Pat. 237107, 22.03.2021,

Mój udział procentowy wynosi: 20%.

11. Agnieszka Wróblewska, **Piotr Miądlicki**, Mariusz Malko, Zbigniew Czech, Adrian Antosik, Katarzyna Wilpiszewska, Sposób utleniania limonenu, Pat. 233642, 29.11.2019,

Mój udział procentowy wynosi: 20%.

12. Agnieszka Wróblewska, **Piotr Miądlicki**, Sposób izomeryzacji α -pinenu w obecności katalizatora tytanowo-silikatowego, Pat. 233955, 31.12.2019,

Mój udział procentowy wynosi: 40%.

13. Agnieszka Wróblewska, **Piotr Miądlicki**, Dominika Kłosin, Sposób utleniania α -pinenu, Pat. 237108, 22.03.2021,

Mój udział procentowy wynosi: 42%.

14. Agnieszka Wróblewska, **Piotr Miądlicki**, Sposób izomeryzacji α -pinenu w obecności haloizytu, Pat. 235284, 15.06.2020,

Mój udział procentowy wynosi: 50%.

15. Agnieszka Wróblewska, **Piotr Miądlicki**, Dominika Kłosin, Sposób utleniania α -pinenu w obecności katalizatora TS-1, Pat. 235283, 15.06.2020,

Mój udział procentowy wynosi: 42%.

16. Agnieszka Wróblewska, **Piotr Miądlicki**, Sposób izomeryzacji α -pinenu, Pat. 235725, 05.10.2020,

Mój udział procentowy wynosi: 50%.

17. Agnieszka Wróblewska, **Piotr Miądlicki**, Adrian Antosik, Zbigniew Czech, Magda Zdanowicz, Plaster do zastosowania jako opatrunek medyczny i sposób otrzymywania plastrów do zastosowania jako opatrunki medyczne, Pat. 238962, 25.10.2021,

Mój udział procentowy wynosi: 15%.

18. Agnieszka Wróblewska, **Piotr Miądlicki**, Adrian Antosik, Zbigniew Czech, Magda Zdanowicz, Opatrunek medyczny o właściwościach antyseptycznych i sposób otrzymywania opatrunków medycznych o właściwościach antyseptycznych, Pat. 238290, 02.08.2021,

Mój udział procentowy wynosi: 15%.

19. Agnieszka Wróblewska, **Piotr Miądlicki**, Sposób izomeryzacji α -pinenu w obecności haloizytu, Pat. 235726, 05.10.2020,

Mój udział procentowy wynosi: 50%.

20. Agnieszka Wróblewska, **Piotr Miądlicki**, Sposób izomeryzacji α -pinenu w obecności katalizatora, Pat. 236553, 25.01.2021,

Mój udział procentowy wynosi: 50%.

21. Agnieszka Wróblewska, **Piotr Miądlicki**, Sposób izomeryzacji α -pinenu w obecności katalizatora, Pat. 237110, 22.03.2021,

Mój udział procentowy wynosi: 50%.

22. Agnieszka Wróblewska, **Piotr Miądlicki**, Anna Fajdek-Bieda, Sposób izomeryzacji geraniolu, Pat. 239717, 27.12.2021,

Mój udział procentowy wynosi: 33%.

23. Agnieszka Wróblewska, **Piotr Miądlicki**, Anna Fajdek-Bieda, Sposób izomeryzacji geraniolu, Pat. 239718, 27.12.2021,

Mój udział procentowy wynosi: 33%.

24. Agnieszka Wróblewska, **Piotr Miądlicki**, Zuzanna Szeremeta, Sposób izomeryzacji α -pinenu w obecności katalizatora, Pat. 237700, 17.05.2021,

Mój udział procentowy wynosi: 40%.

25. Agnieszka Wróblewska, Jadwiga Tołpa, **Piotr Miądlicki**, Sposób utleniania α -pinenu na katalizatorze TS-1, Pat. 238459, 23.08.2021,

Mój udział procentowy wynosi: 33%.

26. Agnieszka Wróblewska, Jadwiga Tołpa, **Piotr Miądlicki**, Sposób utleniania α -pinenu na katalizatorze TS-1, Pat. 238460, 23.08.2021,

Mój udział procentowy wynosi: 33%.

Zgłoszenia patentowe

1. Agnieszka Wróblewska, **Piotr Miądlicki**, Anna Fajdek-Bieda, Sposób izomeryzacji geraniolu, Numer zgłoszenia: 431603, 25.10.2019,

Mój udział procentowy wynosi: 33%.

2. Agnieszka Wróblewska, **Piotr Miądlicki**, Anna Fajdek-Bieda, Sposób izomeryzacji geraniolu, Numer zgłoszenia: 431754, 12.11.2019,
Mój udział procentowy wynosi: 33%.

3. Agnieszka Wróblewska, **Piotr Miądlicki**, Anna Fajdek-Bieda, Aleksandra Radomska-Zalas, Andrzej Perec, Jadwiga Tołpa, Marcin Stefan Kujbida, Sposób izomeryzacji geraniolu w obecności katalizatora, Numer zgłoszenia: 433647, 23.04.2020,
Mój udział procentowy wynosi: 20%.

4. Agnieszka Wróblewska, Jadwiga Tołpa, **Piotr Miądlicki**, Beata Michalkiewicz, Sposób utleniania α -pinenu w obecności katalizatora ZSM-5, Numer zgłoszenia: 434540, 02.07.2020,
Mój udział procentowy wynosi: 15%.

5. Agnieszka Wróblewska, **Piotr Miądlicki**, Zuzanna Szeremeta, Sposób izomeryzacji α -pinenu w obecności wermikulitu jako katalizatora, Numer zgłoszenia: 434550, 02.07.2020,
Mój udział procentowy wynosi: 45%.

6. Agnieszka Wróblewska, **Piotr Miądlicki**, Zuzanna Szeremeta, Sposób izomeryzacji α -pinenu w obecności wermikulitu jako katalizatora, Numer zgłoszenia: 434550, 02.07.2020,
Mój udział procentowy wynosi: 45%.

7. Agnieszka Wróblewska, **Piotr Miądlicki**, Anna Fajdek-Bieda, Aleksandra Radomska-Zalas, Jadwiga Tołpa, Sposób izomeryzacji geraniolu w obecności haloizytu jako katalizatora, Numer zgłoszenia: 434907, 05.08.2020,
Mój udział procentowy wynosi: 28%.

8. Agnieszka Wróblewska, Jadwiga Tołpa, **Piotr Miądlicki**, Sposób otrzymywania katalizatora tytanowo-silikatowego i jego zastosowanie, Numer zgłoszenia: 435576, 05.10.2020,
Mój udział procentowy wynosi: 24%.

9. Paweł Herbin, Bartłomiej Szymczak, Marek Grudziński, Łukasz Marchewka, **Piotr Miądlicki**, Śluza do pomiaru temperatury oraz dezynfekcji ludzi, Numer zgłoszenia: 129611, 18.11.2020,

Mój udział procentowy wynosi: 5%.

10. Paweł Herbin, Beata Niesterowicz, Karol Miądlicki, Aleksandra Dembkowska, **Piotr Miądlicki**, Marcin Jasiewicz, Robot dezynfekujący, Numer zgłoszenia: 129624, 23.11.2020, Mój udział procentowy wynosi: 5%.

11. Agnieszka Wróblewska, **Piotr Miądlicki**, Anna Fajdek-Bieda, Aleksandra Radomska-Zalas, Jadwiga Tołpa, Sposób izomeryzacji geraniolu, Numer zgłoszenia: 436839, 02.02.2021, Mój udział procentowy wynosi: 28%.

12. Agnieszka Wróblewska, Jadwiga Tołpa, **Piotr Miądlicki**, Sposób otrzymywania katalizatora tytanowo-silikatowego i jego zastosowanie, Numer zgłoszenia: 437458, 30.03.2021, Mój udział procentowy wynosi: 16%.

13. Joanna Sreńscek-Nazzal, Agnieszka Wróblewska, Adrianna Kamińska, Jadwiga Tołpa, **Piotr Miądlicki**, Sposób wytwarzania katalizatora węglowego zawierającego żelazo i jego zastosowanie do utleniania α -pinenu, Numer zgłoszenia: 437859, 14.05.2021, Mój udział procentowy wynosi: 20%.

14. Agnieszka Wróblewska, **Piotr Miądlicki**, Anna Fajdek-Bieda, Aleksandra Radomska-Zalas, Jadwiga Tołpa, Sposób izomeryzacji geraniolu w obecności katalizatora, Numer zgłoszenia: 438254, 24.06.2021, Mój udział procentowy wynosi: 28%.

15. Joanna Sreńscek-Nazzal, Agnieszka Wróblewska, Adrianna Kamińska, Jadwiga Grzeszczak, **Piotr Miądlicki**, Sposób izomeryzacji α -pinenu w obecności katalizatora węglowego, Numer zgłoszenia: 439341, 28.10.2021, Mój udział procentowy wynosi: 20%.

D. Wskaźniki charakteryzujące dorobek naukowy

- Sumaryczny Impact Factor według listy Journal Citation Reports (JCR), zgodnie z rokiem opublikowania: **90,654**
- Liczba cytowań według bazy Scopus: **166**
- Indeks Hirscha według bazy Scopus: **9**

E. Aktywny udział w międzynarodowych i krajowych konferencjach naukowych:

1. *Sposoby pokrywania spienionego polistyrenu tlenkiem krzemu (IV) oraz tlenkiem tytanu (IV) w celu otrzymania złoża fluidalnego do badań fotokatalitycznych*, **Piotr Miądlicki**, Piotr Rychtowski, Rafał Wróbel, Beata Tryba, X Kongres Technologii Chemicznej, TECHEM10, 11-14.05.2022, Wrocław – wystąpienie.

2. *Isomerization of alpha-pinene over natural minerals and synthetic titanium-silicate catalysts – comparison of activity*, **P. Miądlicki**, A. Wróblewska, and M.W. Malko, 10th International Conference on the Occurrence Properties and Utilization of Natural Zeolites “ZEOLITE 2018” 24-29.06.2018, Kraków – poster.

3. *Isomerization of alpha-pinene over halloysite - the effect of temperature*. **P. Miądlicki**, A. Wróblewska, M. Malko, The 3rd International Conference on Nanomaterials: Fundamentals and Applications, October 09-11.10.2017, Strbske Pleso – poster.

4. *Isomerization of alpha-pinene over mesoporous Ti-MCM-41 catalyst – the effect of temperature*. **P. Miądlicki**, A. Wróblewska, M. Malko The 3rd International Conference on Nanomaterials: Fundamentals and Applications, October 09-11.10.2017, Strbske Pleso – poster.

5. *Epoxidation of natural limonene extracted from orange peels with hydrogen peroxide on Ti-MCM-41 catalyst*. **P. Miądlicki**, E. Makuch, A. Wróblewska, N. Benedyczak III Krajowa Konferencja „Grafen i inne materiały 2D” 3rd Polish Conference „Graphene and 2D materials”, 6-8.09.2017 r., Szczecin – poster.

6. *Mezoporowate materiały SBA-15 oraz Ti-SBA-15 – sposób otrzymywania, charakterystyka oraz zastosowania*. **P. Miądlicki**, A. Wróblewska, B. Michalkiewicz. Innowacyjni Naukowcy, 28.10.2016, Wrocław – poster.

7. *Material Ti-SBA-16 – właściwości, synteza oraz charakterystyka*, P. Miądlicki, A. Wróblewska, Postępy w technologii i inżynierii chemicznej, II Szczecińskie Sympozjum Młodych Chemików, 18.05.2017, Szczecin – poster.

8. *Otrzymywanie kamfenu w procesie izomeryzacji α -pinenu – porównanie aktywności katalizatorów Ti-SBA-15 oraz SBA-15*. P. Miądlicki, A. Wróblewska. I Szczecińskie Sympozjum Młodych Chemików, 17.06.2016, Szczecin – wystąpienie.

9. *Izomeryzacja α -pinenu na katalizatorze Ti-SBA-15 – wpływ zawartości katalizatora oraz temperatury*. P. Miądlicki, A. Wróblewska.; X Konferencja Technologie Bezodpadowe i Zagospodarowanie Odpadów w Przemysle i Rolnictwie, 14-17.06.2016, Międzyzdroje – poster.

10. *Wpływ zawartości tytanu w katalizatorze TS-1 na przebieg epoksydacji limonenu*. P. Miądlicki, A. Wróblewska, E. Makuch, BioOrg I Wielkopolskie Sympozjum Chemii Bioorganicznej, Organicznej i Biomateriałów, 05.12.2015, Poznań – poster.

11. *Wpływ zawartości tytanu w katalizatorze TS-1 na przebieg epoksydacji limonenu*, P. Miądlicki, A. Wróblewska, 58 Zjazd Naukowy Polskiego Towarzystwa Chemicznego w Gdańsku, 21-25.09.2015, Gdańsk – poster.

F. Udział w projektach badawczych:

1. Grant Narodowego Centrum Nauki OPUS nr PB 2020/39/B/ST8/01514 pt. „Badania fotokatalitycznego rozkładu lotnych związków organicznych (LZO) w reaktorze ze złożem fluidalnym” – stypendysta.

2. Grant Narodowego Centrum Nauki SONATA PB 506-06-084-8628/6 pt. „Badania korelacji między strukturą nadcząsteczkową a właściwościami funkcjonalnymi nowych kopoliamido-estrów opartych częściowo na surowcach odnawialnych” – stypendysta.

3. Projekt LIDER 0028/L-11/2019 pt. “Samoprzylepne kleje silikonowe do zastosowań specjalnych” – wykonawca.

4. Projekt: „Odpowiedzialny społecznie Proto_lab” finansowany w ramach Regionalnego Programu Operacyjnego Województwa Zachodniopomorskiego 2014-2020, pt. „Semi-autonomiczny robot dezynfekujący do walki z COVID-19” – wykonawca.

5. Projekt: „Odpowiedzialny społecznie Proto_lab” finansowany w ramach Regionalnego Programu Operacyjnego Województwa Zachodniopomorskiego 2014-2020, pt. „System zautomatyzowanej kontroli dostępu do obiektów użyteczności publicznej przeznaczony do przeciwdziałaniu rozprzestrzenianiu SARS-COV2” – wykonawca.

G. Osiągnięciach dydaktyczne oraz popularyzacja nauki:

1. Uczestnictwo w prowadzeniu zajęć dydaktycznych: bezpieczeństwo pracy i ergonomia, operacje jednostkowe w technologii chemicznej, laboratorium przeddyplomowe, technologia chemiczna organiczna, ochrona środowiska w technologii chemicznej.

2. Działania popularyzujące naukę - udział w przygotowaniu i przeprowadzeniu ćwiczeń laboratoryjnych dla 2 klasy Technikum Technologii Chemicznej Zespołu Szkół im. Ignacego Łukasiewicza, 22.02.2019 r.

3. Czynny udział w przygotowaniach i prowadzenie zajęć w ramach NOCY NAUKOWCÓW, 28.09.2018 r.

4. Działania popularyzujące naukę - uczestnictwo i przygotowanie warsztatów „Chemia znana i nieznaną” w ramach Regionalnego Festiwalu Naukowego E(X)PLORY w Szczecinie, 23.02.2018 r.

5. Działania popularyzujące naukę - udział w przygotowaniu i przeprowadzeniu ćwiczeń laboratoryjnych dla 3 klasy Technikum Technologii Chemicznej Zespołu Szkół im. Ignacego Łukasiewicza, 09.02.2018 r.

- 6.** Działania popularyzujące naukę - aktywny udział w Festiwalu Nauki organizowanym przez Szczecińskie Towarzystwo Naukowe przy współpracy szczecińskich szkół wyższych, 22.09.2017 r.
- 7.** Działania popularyzujące naukę - udział w przygotowaniu i w przeprowadzeniu warsztatów chemicznych „Świat Szalonego Chemika” w ramach imprezy „Moc Naukowców”, 31.03-01.04.2017 r.
- 8.** Działania popularyzujące naukę - udział w przygotowaniu i przeprowadzeniu warsztatów chemicznych pt. "Pachnące warsztaty" dla uczniów Technikum Chemicznego Zespołu Szkół im. Ignacego Łukasiewicza w Policach, 09.02.2017 r.
- 9.** Działania popularyzujące naukę - udział w przygotowaniu i przeprowadzeniu warsztatów chemicznych dla Zespołu Szkół Publicznych nr 4 w Świnoujściu, 06.12.2016 r.
- 10.** Działania popularyzujące naukę - aktywny udział w Festiwalu Nauki organizowanym przez Szczecińskie Towarzystwo Naukowe przy współpracy szczecińskich szkół wyższych, 19-24.09.2016 r.
- 11.** Działania popularyzujące naukę - udział w przygotowaniu i przeprowadzeniu warsztatów chemicznych dla uczniów Technikum Chemicznego Zespołu Szkół im. Ignacego Łukasiewicza w Policach, grudzień 2015 r.
- 12.** Działania popularyzujące naukę - udział w przygotowaniu i przeprowadzeniu w ramach działań promocyjnych ZUT cyklu 4 warsztatów nt. "Pachnące warsztaty", 01.10.2015 r.
- 13.** Działania popularyzujące naukę - aktywny udział w Festiwalu Nauki organizowanym przez Szczecińskie Towarzystwo Naukowe przy współpracy szczecińskich szkół wyższych, 22-25.09.2015 r.

Przewodnik po publikacjach stanowiących rozprawę doktorską

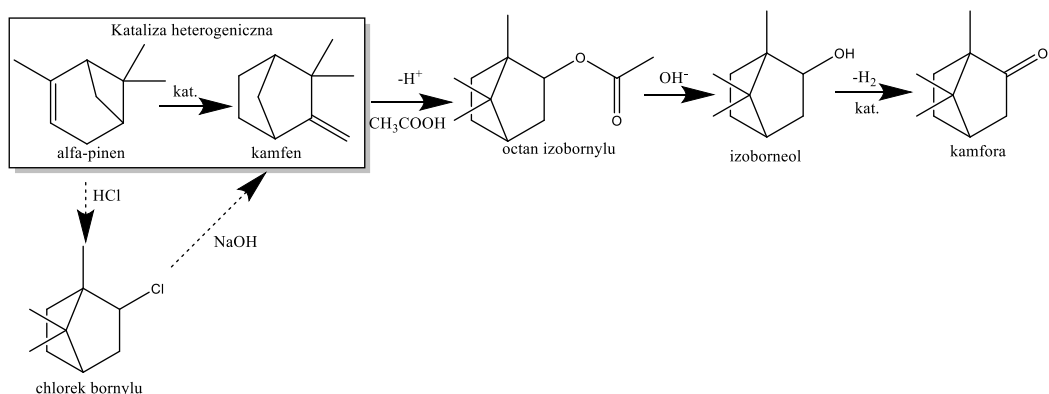
„Izomeryzacja alfa-pinenu na syntetycznych katalizatorach tytanowo-silikatowych oraz na porowatych materiałach pochodzenia naturalnego”

1. Wstęp teoretyczny

Surowce roślinne są bogatym źródłem związków biologicznie czynnych dla medycyny i kosmetyki. Ponadto, na bazie tych związków można otrzymywać bardziej skomplikowane struktury (np. pochodne tlenowe związków pochodzenia naturalnego), znajdujące zastosowania nie tylko w medycynie i w kosmetyce, ale również w przemyśle spożywczym, perfumeryjnym, czy w syntezie polimerów. Zróżnicowane struktury chemiczne związków pochodzenia naturalnego, a także ich pochodnych oraz ich cenne właściwości biologiczne, budzą coraz większe zainteresowanie naukowców na całym świecie [1].

α -Pinen jest jednym z najbardziej powszechnych w przyrodzie monoterpenu. Związek ten ma dwa enancjomery: (-)- α -pinen oraz (+)- α -pinen. α -Pinen jest metabolitem wielu roślin i znajduje się w składzie olejków eterycznych pozyskiwanych z tych roślin [2]. Przykładem takich roślin mogą być: sosna, świerk, jodła, eukaliptus, rozmaryn, mięta, bazylia i inne [3]. Przemysłowo α -pinen otrzymywany jest z terpentyny, która pozyskiwana jest przez destylację żywicy sosnowej. Otrzymany destylat różni się zawartością α -pinenu i jego skład zależy od gatunku sosny oraz miejsca, w którym została pozyskana żywica. Kolejnym źródłem, z którego pozyskuje się przemysłowe ilości terpentyny jest produkcja papieru z drewna sosny, jodły oraz świerku. Otrzymana w tym procesie terpentyna siarczanowa zawiera około 60-70% α -pinenu, a pozostałe związki to na przykład β -pinen, limonen, czy anetol [4].

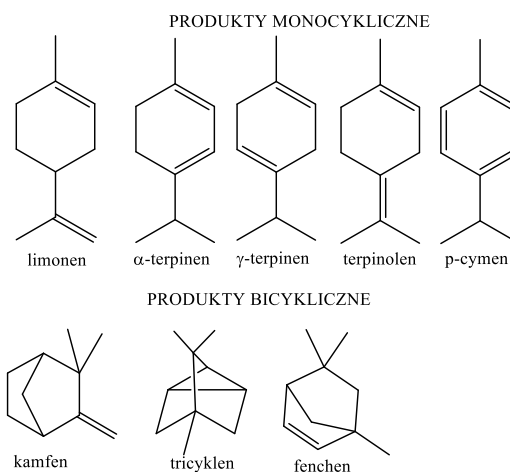
α -Pinen znalazł zastosowanie jako substrat do produkcji wielu cennych związków dla przemysłu perfumeryjnego. Przy czym największe znaczenie ma produkcja kamfory z α -pinenu. Wielkość tej produkcji to około 30 000 ton/rok (główni producenci to Chiny i Indie). Kamforę można otrzymać na dwa sposoby (Rys. 1)[5].



Rysunek 1. Metody otrzymywania kamfory z α -pinenu

Pierwszy sposób polega na otrzymaniu kamfenu poprzez chlorowanie α -pinenu do chlorku bornylu, który następnie ulega reakcji z wodorotlenkiem sodu, w wyniku tej reakcji powstaje kamfen. Metoda ta prowadzi do otrzymania wielu produktów ubocznych, które są trudne do oddzielenia od kamfenu. Ze względu na niekorzystny wpływ takiego sposobu prowadzenia reakcji na środowisko naturalne oraz ze względu na trudności związane z rozdzielaniem mieszaniny poreakcyjnej, dużą uwagę zwrócono na możliwości zastosowania katalizatorów heterogenicznych w otrzymywaniu kamfenu. Użycie katalizatorów heterogenicznych, związane jest z większą szybkością reakcji i wyższą selektywnością przemiany do kamfenu, jednocześnie użycie katalizatora heterogenicznego pozwala łatwo oddzielić go z mieszaniny reakcyjnej przez odfiltrowanie i wiąże się z łatwiejszą regeneracją tego katalizatora. Taki sposób prowadzenia reakcji otrzymywania kamfenu jest bardziej przyjazny dla środowiska naturalnego. W następnym etapie kamfen reaguje z kwasem octowym, w wyniku tej reakcji powstaje octanu izobornylu, który poddawany jest w ostatnim etapie hydrolizie, w wyniku której otrzymujemy izoborneol. Ostatnim etapem jest katalityczne odwodornienie izoborneolu do kamfory [5]. Wykorzystanie heterogenicznych katalizatorów do izomeryzacji α -pinenu pozwoliło zmniejszyć liczbę etapów w procesie produkcji kamfory. Ponadto nowa metoda pozwoliła na zmniejszenie ilości produktów ubocznych do minimum.

Izomeryzacja α -pinenu prowadzona jest na przemysłową skalę z wykorzystaniem TiO_2 modyfikowanego H_2SO_4 jako katalizatora. Reakcja ta prowadzona jest w temperaturze 145°C [6,7], a jej głównymi produktami są związki bicykliczne, w tym: kamfen, bornylen, tricyklen, fenchen oraz związki monocykliczne, w tym: limonen, terpineny, terpinolen oraz p-cymen (Rys. 2). Przy czym z największą selektywnością, wynoszącą łącznie ponad 80%, powstają w tym procesie kamfen oraz limonen.



Rysunek 2. Główne produkty izomeryzacji α -pinenu

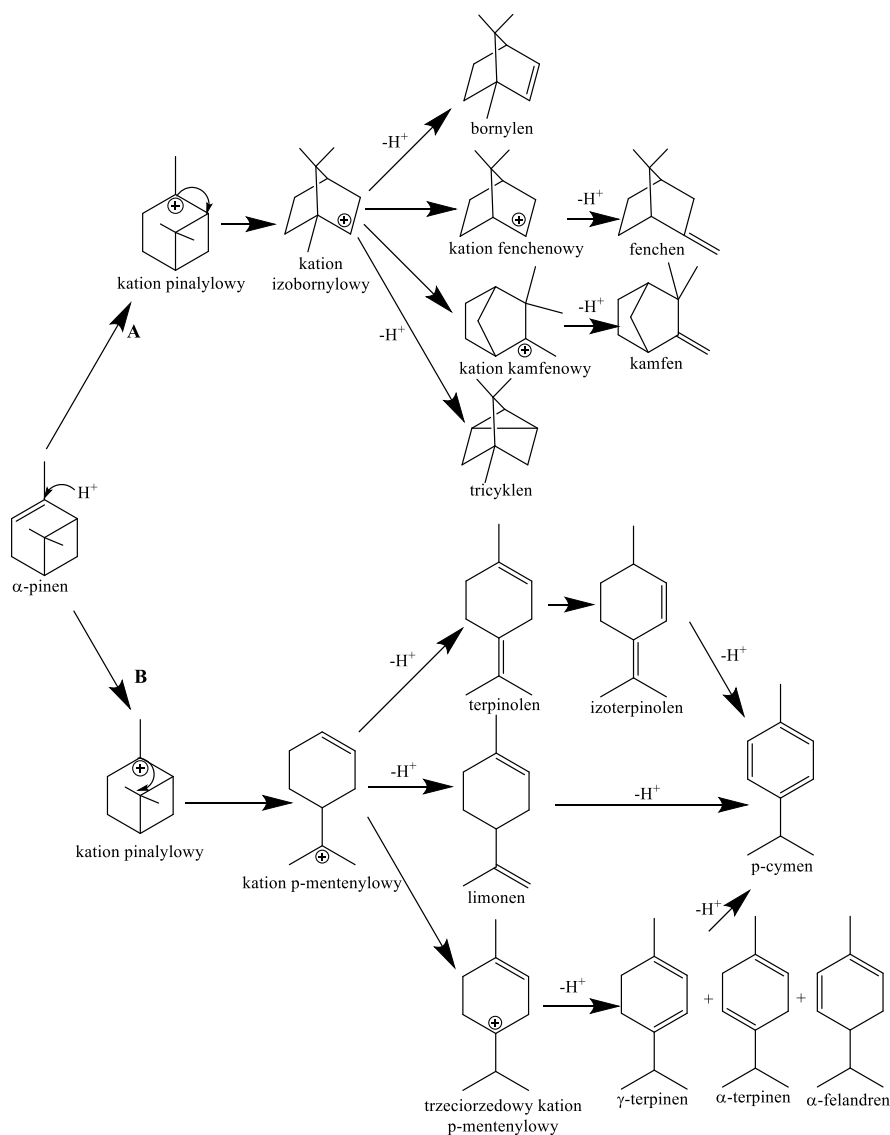
Główny produkt izomeryzacji α -pinenu – kamfen, nie tylko wykorzystywany jest w produkcji kamfory, znalazł on również zastosowanie do produkcji insektycydu – toksafenu [8]. Ponadto reakcja kamfenu z gwajakolem prowadzi do powstania cykloheksanoli, które mają charakterystyczny zapach drzewa sandałowego i znalazły zastosowanie jako syntetyczny zamiennik naturalnego olejku sandałowego [9]. Kamfen jest związkiem biologicznie czynnym, który posiada właściwość lecznicze, działa on: przeciwzapalnie [10], przeciwnowotworowo [11], antybakteryjnie [12], przeciwgrzybiczo [13], przeciwwirusowo [10] oraz ma właściwości przeciwutleniające [14] oraz antydiabetyczne [10]. Ponadto, ze względu na jego charakterystyczny zapach, wykorzystywany jest w przemyśle perfumeryjnym oraz jako aromat w przemyśle spożywczym [15].

Drugi produkt, powstający z największą selektywnością w izomeryzacji α -pinenu, to limonen. Związek ten jest szeroko stosowany w: przemyśle chemicznym, perfumeryjnym, kosmetycznym i spożywczym. Limonen znalazł też bardzo liczne zastosowania w medycynie, np. stwierdzono, że mieszanina limonenu, α -pinenu i 1,8-cyneolu wykazuje działanie terapeutyczne zbliżone do powszechnie stosowanych antybiotyków i leków mukolitycznych, które są stosowane w leczeniu zapalenia górnych dróg oddechowych [16]. Ponadto limonen wykazuje działanie przeciwbakteryjne oraz przeciwgrzybicze [17,18]. Stosuje się go również w leczeniu kamicy dróg żółciowych [19]. Badania wykazały, że limonen działa: przeciwzapalnie, przeciwnowotworowo, antydiabetycznie, antyalergicznie i antystresowo [20]. Jedną z najważniejszych reakcji z wykorzystaniem limonenu jest opracowana w latach pięćdziesiątych XX wieku metoda przekształcania (+)-limonenu w (-)-karwon, który jest używany jako aromat miętowy [21]. Badano również zastosowanie limonenu jako dodatku do tworzyw sztucznych mających kontakt z żywnością. Dodatek limonenu do polilaktydu (PLA)

polepszył m.in. właściwości plastyczne materiału oraz zmniejszył adsorpcję wody. Związek ten okazał się dobrym zamiennikiem syntetycznych plastyfikatorów [22].

Związki otrzymywane podczas izomeryzacji α -pinenu z mniejszymi selektywnościami, takie jak: terpinolen, α -terminen, γ -terpinen p-cymen, tricyklen oraz fenchen, są cennymi substancjami zapachowymi i znalazły szerokie zastosowania w przemyśle perfumeryjnym, spożywczym i chemicznym [23].

Mechanizm izomeryzacji α -pinenu jest bardzo skomplikowany ze względu na powstanie różnych produktów, w zależności od zastosowanego katalizatora (Rys. 3). Reakcja izomeryzacji α -pinenu może przebiegać dwoma ścieżkami. W pierwszej z nich (ścieżka (A)), powstają produkty bicykliczne: kamfen, fenchen, bornylen i tricyklen. Natomiast druga ścieżka (ścieżka (B)) prowadzi do powstania produktów monocykliczych, takich jak: limonen, terpinolen, izoterpinolen, terpineny, felandren oraz (w reakcji następczej) p-cymen [24,25].



Rysunek 3. Mechanizm izomeryzacji α -pinenu

W celu obniżenia temperatury prowadzenia reakcji oraz osiągnięcia, jak najwyższej selektywności przemiany do kamfenu, który jest najbardziej pożądanym produktem tego procesu (ze względu na swoje właściwości i zastosowania), wiele grup naukowych prowadzi intensywne poszukiwania nowych heterogenicznych katalizatorów izomeryzacji α -pinenu. W ostatnich dwóch dekadach opisano wiele z tych katalizatorów (Tabela 1), m.in. były to: tlenek cyrkonu [26], W_2O_3/Al_2O_3 [27], montmorylonit [28], illit modyfikowany kwasem [29], kalcynowany H-mordenit [30], zeolit beta [31], sita molekularne MSU-S [32], Al-MCM-41 [33], ciecze jonowe [34], heteropolikwasy fosfowolframowe [35], Ga-SBA-15 [36], Ti-SBA-15 [37,38], Ti-MCM-41 [39], eksfoliowany- Ti_3C_2 [40], klinoptylolit [41–45], węgle aktywne [46], Au/ γ - Al_2O_3 [47], kwas metatytanowy [48], żywica jonowymienna Amberlyst 35 [49], czy MCM-50 modyfikowany fosforanami [50].

Tabela 1. Wybrane katalizatory izomeryzacji α -pinenu opisane w literaturze

Katalizator	Temp. [°C]	Czas [h]	Konwersja α -pinenu [%]	Źródło
SO_4/Al_xZrO_2	85	6	32	[26]
$W_2O_3-Al_2O_3$	150	2	73	[27]
Montmorylonit modyfikowany kwasem	150	5	99	[28]
Illit modyfikowany kwasem	140	6	100	[29]
Kalcynowany H-Mordenit	130	4	98,5	[30]
Zeolit beta	70	0.5	91,4	[31]
Sita molekularne MSU-S	70	4	97	[32]
Al-MCM-41	160	2 min	98	[33]
$[HSO_3-(CH_2)_3-NEt_3]Cl-ZnCl_2$	140	4	97,6	[34]
$H_3PW_{12}O_{40}$ osadzony na krzemionce	60	1	98	[35]
Eksfoliowany Ti_3C_2	160	6	98,4	[40]
Słowacki klinoptylolit modyfikowany kwasem	120	2	100	[41]
Klinoptylolit modyfikowany Fe	155	8	93,7	[45]
Klinoptylolit kalcynowany	155	3	100	[43]
Klinoptylolit modyfikowany kwasem	155	2	100	[44]
Au/ γ - Al_2O_3	200	1	99,9	[47]
TiM	120	8	98,6	[48]
Żywica jonowymienna Amberlyst 35	120	6	99,7	[49]
MCM-50	110	10	68,1	[50]

Duże zainteresowanie naukowców tematem izomeryzacji α -pinenu prowadzonej w obecności katalizatorów heterogenicznych, a także bardzo liczne zastosowania produktów tego procesu, skłoniły mnie do podjęcia badań dotyczących tego procesu w ramach niniejszej rozprawy doktorskiej.

2. Cel pracy

Celem tej rozprawy doktorskiej było poszukiwanie nowych, heterogenicznych katalizatorów dla procesu izomeryzacji α -pinenu. W ramach pracy doktorskiej otrzymano do badań tego procesu następujące katalizatory: katalizatory tytanowo-silikatowe Ti-SBA-15, Ti-MCM-41 i TS-1 o różnej zawartości tytanu, zmodyfikowany poprzez przemywanie roztworami wodnymi kwasu siarkowego (VI) o różnym stężeniu klinoptylolit oraz zmodyfikowany poprzez przemywanie roztworami wodnymi kwasów (HNO_3 , HCl) węgiel aktywny DT0. Właściwości fizyko-chemiczne otrzymanych materiałów porowatych zostały scharakteryzowane z wykorzystaniem zaawansowanych metod instrumentalnych: XRD, FTIR, UV-Vis, SEM, TEM, ED-XRF, EDX, XPS i ICP.

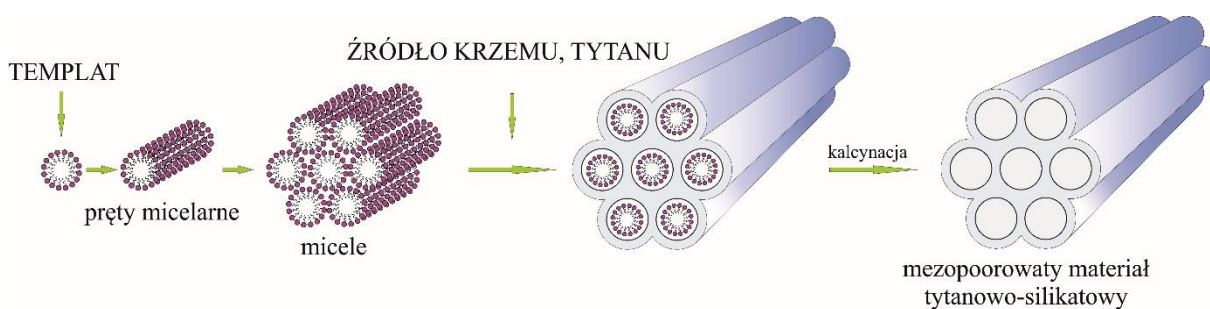
W celu sprawdzenia aktywności otrzymanych katalizatorów w procesie izomeryzacji α -pinenu wykonano szereg doświadczeń. Najbardziej aktywne katalizatory z każdej z grupy posłużyły do wyznaczenia najbardziej korzystnych warunków prowadzenia tego procesu. W tym celu zbadano wpływ wybranych parametrów technologicznych, takich jak: temperatura, ilość katalizatora oraz czas reakcji, na przebieg procesu izomeryzacji α -pinenu. Dla wybranych katalizatorów wyznaczono równanie kinetyczne, rząd reakcji oraz energię aktywacji.

3. Omówienie wyników badań

Krystaliczne materiały porowate nieustannie są obiektem zainteresowania naukowców ze względu na ich szerokie zastosowanie w petrochemii, w katalizie oraz w adsorpcji. Za sukces tych materiałów odpowiada kilka ich unikalnych cech, takich jak: jednorodne kanały i pory, miejsca aktywne o różnej sile i charakterze, duża zdolność adsorpcyjna, korzystne właściwości elektronowe, a także odporność termiczna oraz chemiczna. Najpopularniejszymi materiałami porowatymi są: zeolity (ZSM-5, Zeolit A i Silicate-1), uporządkowane materiały porowate (MCM-41, MCM-48, MCM-50 i SBA-15) oraz związki metaloorganiczne MOF. Wszystkie te materiały mają wiele cech wspólnych, jednak to szczególne różnice w ich właściwościach fizyko-chemicznych determinują zastosowania tych materiałów, zwłaszcza w katalizie [51].

Pierwsze uporządkowane materiały mezoporowate zostały otrzymywane pod koniec lat 80-tych, przez naukowców firmy Mobil. Były to mezoporowate krzemionki z rodziny M41S, takie jak: MCM-41 o budowie heksagonalnej, MCM-48 o budowie kubicznej oraz MCM-50 o budowie warstwowej [52]. W 1988 roku Zhao i współpracownicy otrzymali materiał SBA-15, który posiadał wysoką stabilność hydrotermalną oraz większą odporność chemiczną w porównaniu do materiałów z grupy M41S. Odkrycie tych materiałów wzbudziło bardzo duże zainteresowanie naukowców, którzy poprzez różne modyfikacje tych materiałów starali się otrzymać nowe materiały, o lepszych właściwościach oraz mogące znaleźć nowe zastosowania [53].

W pierwszej części pracy doktorskiej otrzymano mezoporowaty materiał Ti-SBA-15 o stosunku molowym krzemu do tytanu w żelu krystalizacyjnym 40:1 (katalizator Ti-SBA-15 40:1). Materiał ten otrzymano metodą zol-żel z wykorzystaniem templat (surfaktant - Pluronic P123), którego celem było wytworzenie odpowiedniej struktury. Schemat otrzymywania mezoporowatych materiałów tytanowo-silikatowych został przedstawiony na rysunku 4.



Rysunek 4. Schemat otrzymywania mezoporowatych materiałów tytanowo-silikatowych

Prekursorem krzemu w reakcji otrzymywania katalizatora Ti-SBA-15 40:1 był ortokrzemian tetraetylu, natomiast prekursorem tytanu był ortotytanian tetraizopropylu. Syntezę prowadzono w autoklawie w środowisku kwaśnym, w temperaturze 35°C i przez 24 godziny. Po tym czasie otrzymany katalizator przesączono, przemyto wodą dejonizowaną, suszono w 100°C, a następnie kalcynowano przez 5h w temperaturze 550°C.

Pierwszym etapem sprawdzenia aktywności katalitycznej otrzymanego materiału Ti-SBA-15 40:1 było przeprowadzenie badań wstępnych, przy czym reakcję izomeryzacji α -pinenu prowadzono bez użycia rozpuszczalnika. Zbadano wpływ temperatury w zakresie 80-140°C, czasu reakcji od 5 do 48 godzin oraz ilość katalizatora od 5 do 15 % wag. Identyfikację jakościową i ilościową produktów reakcji przeprowadzono z wykorzystaniem chromatografii gazowej. Bilans masowy pozwolił wyznaczyć następujące funkcje opisujące proces izomeryzacji: konwersję α -pinenu i selektywności głównych produktów: kamfenu oraz limonenu. Badania wykazały, że katalizator Ti-SBA-15 40:1 jest aktywnym katalizatorem w procesie izomeryzacji α -pinenu. Szczegółowe badania pozwoliły wyznaczyć najkorzystniejsze warunki prowadzenia procesu izomeryzacji α -pinenu: temperatura prowadzenia reakcji 140°C, czas reakcji 48 godzin oraz ilość katalizatora w stosunku do α -pinenu 15% wag. W tych warunkach konwersja α -pinenu wyniosła 60% mol, a selektywności kamfenu i limonenu wyniosły odpowiednio: 51 i 19% mol. Sumaryczna selektywności tych związków była więc bardzo wysoka i wynosiła około 70 mol%. Pełne wyniki zostały opublikowane w czasopiśmie naukowym *Reaction Kinetics, Mechanisms and Catalysis* 2016, 119, 641–654 [54].

W drugim etapie postanowiono zbadać wpływ zawartości tytanu w katalizatorze Ti-SBA-15 na jego aktywność w procesie izomeryzacji α -pinenu. Otrzymano serię katalizatorów Ti-SBA-15 o różnej zawartości tytanu (stosunek molowy krzemu do tytanu w żelu krystalizacyjnym od 10:1 do 40:1), które miały postać białego proszku. Zawartość tytanu w otrzymanych katalizatorach wynosiła: Ti-SBA-15 40:1 = 0,75% wag.; Ti-SBA-15 30:1 = 0,90% wag.; Ti-SBA-15 20:1 = 1,1% wag. oraz dla Ti-SBA-15 10:1 = 3,1% wag. Metoda syntezy była taka sama, jak w poprzedniej pracy. Uzyskane materiały poddano badaniom instrumentalnym, w celu otrzymania pełnej charakterystyki fizyko-chemicznej tych katalizatorów. W celu sprawdzenia zawartości tytanu wykonano mikroanalizę rentgenowską EDX oraz spektrometrię ICP-AES. Struktura otrzymanych materiałów została potwierdzona metodą spektroskopii rentgenowskiej - XRD. Pozyskane z tych badań instrumentalnych dane są zgodne z danymi literaturowymi i potwierdzają, że otrzymane materiały mają strukturę p6mm (2-D heksagonalną). Ponadto dla otrzymanych katalizatorów wykonano widma

spektroskopii fourierowskiej w podczerwieni, które również potwierdziły powstanie sieci krzemionkowej oraz włączenie tytanu w strukturę krzemionki. Natomiast widma UV-Vis potwierdziły koordynacyjne włączenie atomów tytanu (Ti^{4+}) w strukturę krzemionki, ponadto potwierdzono obecność ditlenku tytanu, dla materiału o najwyższej zawartości tytanu. Właściwości powierzchni określone zostały za pomocą badań adsorpcji/desorpcji azotu w temperaturze $-196^{\circ}C$. Wszystkie otrzymane katalizatory cechowały się rozwiniętą powierzchnią właściwą około $750\text{ m}^2/\text{g}$ oraz średnim rozmiarem porów, który wynosił około $5,3\text{ nm}$. Strukturę powierzchniową materiałów potwierdzono zdjęciami wykonanymi elektronowym mikroskopem skaningowym oraz mikroskopem sił atomowych. Dobrze rozwiniętą strukturę mezoporowatą potwierdzono wykonując zdjęcia transmisyjnym mikroskopem elektronowym. Pełne wyniki przedstawiające otrzymane materiały zostały opublikowane w czasopiśmie *Microporous and Mesoporous Materials*, 258, 72–82 [55]. W dalszej części badań otrzymane materiały zostały wykorzystane jako katalizatory w reakcji izomeryzacji α -pinenu. W tym celu przeprowadzono serię doświadczeń, a aktywność katalityczna otrzymanych katalizatorów była oceniana na podstawie konwersji α -pinenu i selektywności odpowiednich produktów. Ponadto, metodą chromatografii gazowej sprzężonej ze spektrometrią mas zidentyfikowano pozostałe produkty, powstające w trakcie izomeryzacji α -pinenu, takie jak: α -terpinen, γ -terpinen, terpinolen, p-cymen, α -felandren oraz aldehyd kamfolenowy. Na początku badań temperatura prowadzenia reakcji wynosiła $140^{\circ}C$, ilość katalizatora była równa 10% wag., natomiast czas reakcji zmieniał się w zakresie 1-48h. Warunki te zostały dobrane na podstawie wcześniejszych badań wstępnych. W następnym etapie najbardziej aktywny katalizator, biorąc pod uwagę konwersję α -pinenu, posłużył do wyznaczenia najkorzystniejszych warunków prowadzenia procesu izomeryzacji. W tym celu dla tego katalizatora przeprowadzono badania wpływu: temperatury w zakresie $20-200^{\circ}C$, zawartości katalizatora w zakresie 0,5-20% wag. i czasu reakcji od 15 min do 24 godzin. Przeprowadzone badania pokazały, że najkorzystniejsza zawartość tytanu w katalizator Ti-SBA-15 to 1,1% wag. (stosunek molowy krzemu do tytanu w żelu krystalizacyjnym 20:1). Z wykorzystaniem najbardziej aktywnego katalizatora wyznaczono najkorzystniejsze warunki prowadzenia procesu izomeryzacji α -pinenu: temperatura $180^{\circ}C$, czas reakcji 6 h, a zawartość katalizatora 15% wag. W tych warunkach konwersja α -pinenu wyniosła 97% mol, natomiast selektywności produktów osiągnęły następujące wartości (jednostka % mol): kamfen (25,9), limonen (23,5) i γ -terpinen (18,7), α -terpinen (8,0), terpinolen (12,9), p-cymen (4,7) oraz α -felandren (2,0). Warto podkreślić, że znaczne wydłużenie czasu reakcji powoduje

zachodzenie reakcji następczych, podczas których powstają produkty polimerowe. Szczegółowe wyniki badań katalitycznych otrzymanych 4 próbek katalizatorów Ti-SBA-15 zostały opublikowane w czasopiśmie naukowym *Microporous and Mesoporous Materials*, 258, 72–82 [55].

Kolejnymi katalizatorami zbadanymi w procesie izomeryzacji α -pinenu były materiały mezoporowate Ti-MCM-41 o różnej zawartości tytanu. W tym celu zmieniano stosunek molowy krzemu do tytanu podczas syntezy katalizatorów od 10:1 do 40:1. Zawartość tytanu dla otrzymanych katalizatorów wynosiła: Ti-MCM-41 40:1 = 3,12% wag.; Ti-MCM-41 30:1 = 4,51% wag.; Ti-MCM-41 20:1 = 5,58% wag. oraz dla Ti-MCM-41 10:1 = 12,09% wag. Materiały te otrzymano metodą zol-żel z wykorzystaniem bromku cetylotrimetyloamoniowego jako templaty [56]. Prekursorem krzemu był ortokrzemian tetraetylu, natomiast prekursorem tytanu był ortotytanian tetrabutylu. Syntezę katalizatorów prowadzono przez 18 godzin, w temperaturze pokojowej i w obecności amoniaku. Po tym czasie otrzymane katalizatory przesączano, przemywano wodą dejonizowaną, suszono, a następnie kalcynowano przez 5h w temperaturze 550°C w celu usunięcia związków organicznych z porów katalizatora. Podobnie, jak w przypadku badań nad katalizatorami Ti-SBA-15 o różnej zawartości tytanu, otrzymane materiały Ti-MCM-41 zostały scharakteryzowane z wykorzystaniem odpowiednio dobranych metod instrumentalnych, w celu otrzymania ich pełnej charakterystyki (XRF, UV-Vis, FTIR, SEM i XRD). Natomiast parametry teksturalne określone zostały za pomocą badań adsorpcji/desorpcji azotu w temperaturze -196°C. Badania te potwierdziły otrzymanie materiałów mezoporowatych o dobrze rozwiniętej powierzchni od 900 do 1060 m²/g. Metoda spektroskopii rentgenowskiej XRD potwierdziła otrzymanie uporządkowanej struktury heksagonalnej, charakterystycznej dla tej grupy materiałów. Analizując widma UV-Vis, nie zaobserwowano wytworzenia się ditlenku tytanu, natomiast potwierdzono wbudowanie się jonów tytanu w strukturę krzemionki. Dokładna charakterystyka otrzymanych materiałów została opublikowana w czasopiśmie naukowym *Catalysts* 2019, 9, 396 [57].

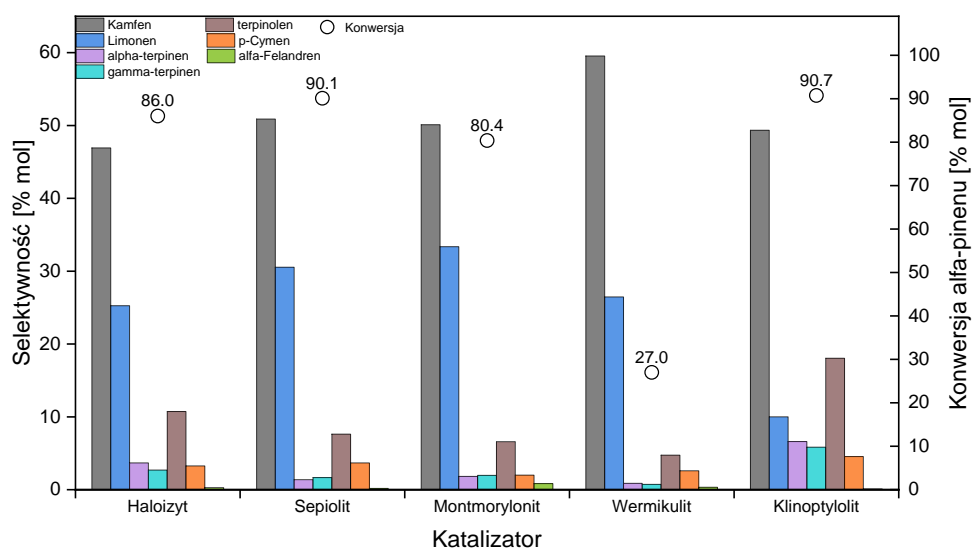
Badania aktywności katalitycznej w procesie izomeryzacji α -pinenu, materiałów Ti-MCM-41 o różnej zawartości tytanu prowadzone były w następujących warunkach: temperatura reakcji 160°C, zawartość katalizatora 7,5% wag. w stosunku do α -pinenu i czas reakcji 6 godz. Warunki do badań wstępnych dobrano, biorąc pod uwagę wcześniejsze badania tego procesu na katalizatorach Ti-SBA-15. Najwyższą konwersję α -pinenu otrzymano wykorzystując katalizator o największej zawartości tytanu (Ti-MCM-41 10:1 = 12,09% wag. Ti) i wynosiła ona 97% mol. Wraz ze zmniejszającą się zawartością tytanu obniżała się również

konwersja α -pinenu i dla kolejnych katalizatorów wynosiła ona odpowiednio: 49,5% mol (Si/Ti = 20:1, 5,58% wag. Ti), 45,3% mol (Si/Ti = 30:1, 4,51% wag. Ti) oraz 39,2 % mol (Si/Ti = 40:1, 3,12% wag. Ti). Selektywności przemiany do odpowiednich produktów były podobne dla czterech badanych katalizatorów Ti-MCM-41. Najwyższą selektywność osiągnięto dla takich produktów, jak kamfen (35% mol) oraz limonenu (37% mol), natomiast z niższą selektywnością powstawały: α - oraz γ -terpinen, terpinolen, p-cymen oraz α -felandren. Drugi etap badań z udziałem katalizatorów Ti-MCM-41 polegał na określeniu najkorzystniejszych warunków izomeryzacji α -pinenu z wykorzystaniem najbardziej aktywnego katalizatora Ti-MCM-41 (Si/Ti = 40:1). W tym celu przeprowadzono badania procesu izomeryzacji, zmieniając wartości następujących parametrów: temperatura 80-180°C, zawartość katalizatora 2,5-15% wag. w stosunku do α -pinenu i czas reakcji od 15 min do 24 godzin. Najwyższą konwersję α -pinenu (98% mol), z jednocześnie wysokimi selektywnościami głównych produktów (kamfen oraz limonen), udało się uzyskać w temperaturze 160°C, po czasie 7 godzin i przy zawartości katalizatora w mieszaninie reakcyjnej równej 7,5% wag. W tych warunkach kamfen oraz limonen powstawały z selektywnościami równymi odpowiednio: 35,5 oraz 21,3% mol. Podobnie, jak w przypadku katalizatora Ti-SBA-15, w mniejszych ilościach powstawały w badanym procesie: α - oraz γ -terpinen, terpinolen, α -felandren oraz p-cymen. Pełne badania katalityczne zostały przedstawione w czasopiśmie naukowym *Catalysts* 2019, 9, 396 [57].

Następne katalizatory, które miały posłużyć do badań izomeryzacji α -pinenu to syntetyczne zeolity tytanowo-silikatowe TS-1. Otrzymano serię materiałów o różnej zawartości tytanu, w tym celu zmieniano stosunek molowy krzemu do tytanu podczas syntezy katalizatorów od 10:1 do 40:1. Zawartość tytanu dla otrzymanych katalizatorów wynosiła: TS-1 40:1 = 3,08% wag.; TS-1 30:1 = 3,39% wag.; TS-1 20:1 = 5,42% wag. oraz dla TS-1 10:1 = 9,92% wag. Podczas badań wstępnych nieoczekiwanie okazało się, że otrzymane katalizatory są nieaktywne w procesie izomeryzacji α -pinenu, a ich zastosowanie powoduje zachodzenie procesów autoutleniania α -pinenu tlenem z powietrza. Potwierdzone to zostało przez przeprowadzenie izomeryzacji α -pinenu na tych katalizatorach, ale w obecności argonu. Doświadczenie to pokazało, że w atmosferze argonu reakcja izomeryzacji nie zachodziła. Główne produkty utleniania α -pinenu zostały zidentyfikowane z wykorzystaniem chromatografii gazowej ze spektrometrią mas i były to tlenek pinenu, werbenol, werbenon oraz aldehyd kamfoleinowy. Ze względu na brak aktywności otrzymanych katalizatorów TS-1 w procesie izomeryzacji α -pinenu, nie kontynuowano w tej pracy doktorskiej badań nad aktywnością tych materiałów w procesie izomeryzacji α -pinenu.

Kolejną grupą materiałów, które posłużyły jako katalizatory do izomeryzacji α -pinenu były materiały porowate pochodzenia naturalnego. Gromada krzemianów i glinokrzemianów jest największą wśród minerałów – obejmuje ona około 30% ogólnej liczby znanych minerałów. Materiały te stanowią około 75% skorupy ziemskiej, przy czym najpowszechniejszą grupą są skalenie potasowe – ich udział w litosferze wynosi 40-45% jej objętości. Głównymi pierwiastkami wchodzącymi w skład krzemianów i glinokrzemianów są: K, Na, Ca, Mg i Fe. Ważną rolę w tych materiałach odgrywa również Al, który w strukturze minerałów może występować zarówno jako kation, jak i jako część składowa anionu złożonego. Ze względu na swoje właściwości glinokrzemiany znalazły zastosowania w wielu gałęziach przemysłu, m.in.: w przemyśle przetwórczym, w rolnictwie, w inżynierii i w budownictwie, w rekultywacji środowiska oraz w geologii [58,59]. Glinokrzemiany wykazują również świetne właściwości katalityczne w procesie izomeryzacji α -pinenu [43] oraz w innych reakcjach np. w reakcji otrzymywania pirydo[2,1-a]izochinoliny [60], w alkiowaniu benzenu [61], w syntezie pochodnych benzimidazolu [62] oraz w nitrowaniu arenów [63].

Badania wstępne nad zastosowaniem wybranych glinokrzemianów w procesie izomeryzacji α -pinenu zostały przeprowadzone z wykorzystaniem: haloizytu (Polska), sepiolitu (Hiszpania), wermikulitu (Rosja), montmorylonitu (Japonia) i klinoptylolitu (Turcja). W tym celu przeprowadzono serię doświadczeń w jednakowych warunkach: ilość katalizatora 10% wag., temperatura 150°C oraz czas reakcji 5 godzin. Otrzymane wyniki przedstawiono na rysunku 5.



Rysunek 5. Porównanie aktywności materiałów pochodzenia naturalnego w procesie izomeryzacji α -pinenu

Najbardziej aktywny w roli katalizatora okazał się klinoptylolit - biorąc pod uwagę konwersję substratu organicznego. Dla tego katalizatora po 5 godzinach konwersja α -pinenu wyniosła 90,7% mol, a selektywność przemiany do kamfenu około 50% mol. Podobną aktywność wykazały sepiolit i haloizyt. Najwyższą selektywność dla kamfenu uzyskano na wermikulicie (59% mol), jednak ze względu na niską konwersję α -pinenu, konieczne byłoby zbadanie aktywności tego materiału w wyższej temperaturze. Biorąc pod uwagę wyniki przedstawione na rysunku 5, do dalszych badań wybrano klinoptylolit i postanowiono go poddać modyfikacji roztworami wodnymi kwasu siarkowego (VI) o różnych stężeniach. Metoda ta została wybrana ze względu na podobną modyfikację, która jest wykonywana dla przemysłowo stosowanego katalizatora izomeryzacji α -pinenu, jakim jest TiO_2 modyfikowany H_2SO_4 [7,64].

Surowy klinoptylolit modyfikowany był roztworami wodnymi kwasu siarkowego (VI) o stężeniu od 0,01 do 2M, w temperaturze 80°C i przez 4 godziny. Zmodyfikowane w ten sposób próbki klinoptylolitów sączono, a następnie suszono. Tak przygotowane modyfikowane klinoptylolity były scharakteryzowane z wykorzystaniem następujących metod instrumentalnych: XRF, UV-Vis, FTIR, SEM i XRD. Właściwości powierzchni tych materiałów porowatych określone zostały za pomocą badań adsorpcji/desorpcji azotu w temperaturze -196°C. Badania te pokazały, że przemycie próbek klinoptylolitu roztworami wodnymi kwasu siarkowego (VI) o stężeniu od 0,01 do 2M, pozwoliło na rozwinięcie ich powierzchni właściwej od 36 do 136 m²/g. Dodatkowo, dla tych materiałów określono stężenie centrów kwasowych metodą miareczkową. Metoda ta polegała na intensywnym wytrząsaniu badanego materiału z roztworem wodnym NaOH o odpowiednim stężeniu, a następnie odmiareczkowaniu nieprzereagowanego NaOH przy pomocy roztworu kwasu solnego wobec fenoloftaleiny jako wskaźnika. Maksymalne stężenie centrów kwasowych wynosiło około 1 mmol/g i wartość ta nie zmieniała się dla wszystkich próbek katalizatorów, dla których stężenie kwasu zastosowanego do przemywania wynosiło powyżej 0,5M. Szczegółowa charakterystyka otrzymanych materiałów została opublikowana w czasopiśmie naukowym *Microporous and Mesoporous Materials* 2021, 324, [65].

W pierwszej kolejności przeprowadzono badania mające na celu zbadanie wpływu przeprowadzonej modyfikacji na aktywność otrzymanych klinoptylolitów. Parametry reakcji izomeryzacji α -pinenu były następujące: temperatura 70°C, ilość katalizatora 7,5% wag. oraz czas 1h. Parametry te nie mogły być zbliżone do poprzednich badań ze względu na bardzo dużą aktywność otrzymanych materiałów i musiały być wyznaczone na nowo. Najbardziej aktywny okazał się klinoptylolit modyfikowany przez przemywanie roztworem wodnym kwasu

siarkowego (VI) o stężeniu 0,1M. Dla tego katalizatora konwersja α -pinenu wyniosła 88% mol, natomiast selektywności kamfenu i limonenu wynosiły odpowiednio: 54 oraz 31% mol. Wysoka aktywność katalityczna tych materiałów jest związana ze wzrostem ich powierzchni właściwej oraz ze zwiększeniem ilości centrów kwasowych na powierzchni tych materiałów. Należy również uwzględnić zmianę składu pierwiastkowego tych materiałów, ponieważ stosowanie do przemywania katalizatorów roztworów wodnych kwasu o zbyt wysokim stężeniu, powoduje wymywanie pierwiastków ze struktury, w szczególności glinu.

Celem drugiego etapu badań nad aktywnością modyfikowanych klinoptylolitów, było wyznaczenie najkorzystniejszych warunków prowadzenia izomeryzacji α -pinenu z wykorzystaniem najbardziej aktywnego z tych katalizatorów (klinoptylolit przemywany 0,1M roztworem H_2SO_4). Zbadano wpływ następujących parametrów na przebieg tego procesu: temperatury od 30 do 80°C, zawartości katalizatora od 2,5 do 12,5% wag. w stosunku do α -pinenu oraz czasu reakcji od 30 do 210 sekund. Temperatura, która pozwoliła na uzyskanie najwyższej konwersji α -pinenu, przy zachowaniu wysokiej selektywności kamfenu to 70°C. Uwzględniając konwersję oraz selektywność kamfenu, ilość katalizatora, którą uznano za najkorzystniejszą to 10% wag. W przypadku przeprowadzonych badań wpływu czasu reakcji należy podkreślić, że przy większych ilościach mieszaniny reakcyjnej, reakcja przebiega bardzo szybko. Wynika to z silnie egzotermicznego przebiegu reakcji. Podczas tych badań 100% konwersję α -pinenu uzyskano już po 210 sekundach, z zachowaniem wysokich wartości selektywności przemiany do kamfenu (50% mol) oraz do limonenu (31% mol). Przy tak dużej szybkości reakcji dobrze widoczne są reakcje następcze, w których limonen ulega izomeryzacji do terpinenów oraz terpinolenu. Badania te pozwoliły również na wyznaczenie rzędu badanej reakcji izomeryzacji oraz stałej szybkości reakcji, która wynosiła 8,19 h⁻¹. Szczegółowy opis wyników został opublikowany w czasopiśmie naukowym *Microporous and Mesoporous Materials* 2021, 324, [65].

Ostatnią grupą katalizatorów badanych w tej pracy w procesie izomeryzacji α -pinenu były komercyjne, granulowane węgle aktywne DT0 modyfikowane roztworami kwasów HCl (35-38%) oraz HNO₃ (65%). Węgłe te produkowane są z węgla kamiennego w procesie aktywacji parowo-gazowej i charakteryzują się wysoko rozwiniętą powierzchnią właściwą (1085 m²/g). W pierwszym etapie przygotowania katalizatorów usunięto pył poprzez przemywanie materiału wodą dejonizowaną. Następnie, oczyszczony węgiel modyfikowany był roztworami kwasów HCl (35-38%), HNO₃ (65%) oraz dwustopniowo: najpierw HCl, a następnie HNO₃ w temperaturze wrzenia kwasu przez 2 godziny. Gotowe materiały węglowe

w dalszej kolejności przesączano oraz suszono. Tak przygotowane próbki zostały scharakteryzowane z wykorzystaniem następujących metod instrumentalnych: XRF, UV-Vis, FTIR, SEM, XRD i XPS. Właściwości powierzchni tych materiałów określone zostały za pomocą badań adsorpcji/desorpcji azotu w temperaturze -196°C . Przemycie roztworem kwasu HNO_3 pozwoliło na zwiększenie zawartości grup $-\text{COOH}$ oraz $-\text{C-OH}$ na powierzchni węgla aktywnego (Tabela 1.).

Tabela 2. Zawartość grup funkcyjnych wyrażona jako stężenie atomowe

Grupa funkcyjna	DT0	DT0_HCl	DT0_HNO ₃	DT0_HCl_HNO ₃
C-OH	12,6	12,3	13,7	14,2
C=O	7,1	7,5	7,8	7,8
COOH	2,6	2,1	6,4	6,3
Keto-enolowa	4,1	2,8	0,0	0,0

Grupy te są centrami kwasowymi biorącymi udział w reakcji, a ich zwiększona zawartość poprawiła właściwości katalityczne otrzymanego materiału. Wykorzystanie roztworu kwasu HCl pozwoliło na zwiększenie powierzchni właściwej BET materiału do $1267 \text{ m}^2/\text{g}$, co wiązało się z wypłukaniem zanieczyszczeń z porów, natomiast wykorzystanie kwasu HNO_3 częściowo utleniło węgiel, co wiązało się z obniżeniem powierzchni właściwej BET do $532 \text{ m}^2/\text{g}$. Szczegółowa charakterystyka otrzymanych materiałów została opublikowana w czasopiśmie naukowym *Materials* 2021, 14, 7811, [66]

W pierwszej kolejności przeprowadzono badania mające na celu zbadanie wpływu przeprowadzonej modyfikacji węgla aktywnego DT0 na aktywność katalityczną otrzymanych, modyfikowanych próbek węglowych w procesie izomeryzacji α -pinenu. Warunki prowadzenia izomeryzacji α -pinenu były następujące: temperatura 160°C , zawartość katalizatora 5% wag. w stosunku do α -pinenu i czas reakcji 3 godz. Podczas badań najbardziej aktywny okazał się materiał DT0 modyfikowany dwoma kwasami. Dla tego materiału konwersja α -pinenu wyniosła 100% mol, natomiast selektywności przemiany do kamfenu i limonenu wynosiły odpowiednio 41 oraz 13% mol. Ponadto z wysoką selektywnością tworzyły się również α -terpinen (13% mol), terpinolen (11% mol) oraz γ -terpinen (6% mol).

W kolejnym etapie badań sprawdzono w różnych temperaturach (145 , 160 , 175°C) wpływ czasu reakcji na wartości konwersji α -pinenu oraz selektywności powstających produktów z wykorzystaniem węgla aktywnego przemycanego mieszaniną HCl oraz HNO_3 . Całkowitą konwersję substratu uzyskano w dwóch temperaturach: 160 oraz 175°C . W temperaturze 160°C blisko 100% konwersję uzyskano po czasie 3 godzin, natomiast w temperaturze wyższej (175°C) wymagany czas był o godzinę krótszy. Porównując selektywności produktów można

zauważyć, że selektywność przemiany do limonenu obniża się wraz ze wzrostem temperatury oraz wraz z wydłużaniem czasu prowadzenia reakcji. Wynika to z reakcji następczych, w których limonen ulega izomeryzacji do terpinolenu, α - oraz γ -terpinenu, a następnie produkty te ulegają odwodornieniu do p-cymenu.

Na podstawie przeprowadzonych badań wyznaczono również stałe szybkości reakcji w różnych temperaturach prowadzenia reakcji oraz energię aktywacji reakcji izomeryzacji α -pinenu z wykorzystaniem węgla aktywnego modyfikowanego dwoma kwasami. Szczegółowy opis wyników został opublikowany w czasopiśmie naukowym Materials 2021, 14, 7811, [66]

4. Wnioski

Podstawowym celem niniejszej rozprawy doktorskiej było poszukiwanie nowych, heterogenicznych katalizatorów mogących znaleźć zastosowanie w reakcji izomeryzacji α -pinenu. Najważniejsze wnioski wynikające z badań przeprowadzonych w ramach tej rozprawy doktorskiej są następujące:

- Materiał Ti-SBA-15 jest aktywny w procesie izomeryzacji α -pinenu i wykazuje znacznie wyższą aktywność od TiO_2 stosowanego przemysłowo.
- Ilość tytanu wbudowanego w strukturę krzemionki SBA-15 znacznie wpływa na aktywność tego katalizatora w procesie izomeryzacji α -pinenu. Zbyt duża ilość źródła tytanu, dodana w trakcie syntezy katalizatora, zmniejsza aktywność katalityczną tego materiału - spowodowane jest to powstaniem TiO_2 , który osadza się w porach.
- Katalizatory Ti-MCM-41, ze względu na swoją morfologię (większa ilość wprowadzonego tytanu, wyższa powierzchnia właściwa), wykazały wyższą aktywność w procesie izomeryzacji α -pinenu niż katalizatory Ti-SBA-15. Ich zastosowanie znacznie zmniejszyło ilość wymaganego w procesie izomeryzacji katalizatora, od 15% wag. dla Ti-SBA-15 do 7,5% wag. dla Ti-MCM-41. Zastosowanie katalizatora Ti-MCM-41 pozwoliło również na obniżenie temperatury prowadzenia izomeryzacji ze 180 do 160°C. Dodatkowo, uzyskano wyższą selektywność przemiany do kamfenu oraz limonenu w porównaniu z procesem izomeryzacji biegnącym z wykorzystaniem katalizatorów Ti-SBA-15.
- W trakcie syntezy materiałów Ti-MCM-41 nie zaobserwowano powstawania TiO_2 .
- Katalizatory TS-1 są nieaktywne w procesie izomeryzacji α -pinenu i nieoczekiwanie ich zastosowanie prowadzi do utleniania α -pinenu tlenem z powietrza.
- Naturalne glinokrzemiany okazały się bardzo aktywnymi katalizatorami dla procesu izomeryzacji α -pinenu, a ich zastosowanie pozwala na uzyskanie wyższej selektywności przemiany do kamfenu oraz limonenu niż miało to miejsce w przypadku procesów izomeryzacji α -pinenu prowadzonych w obecności katalizatorów tytanowo-silikatowych.
- Modyfikacja klinoptylolitu przez przemywanie roztworami kwasu siarkowego prowadzi do otrzymania modyfikowanych klinoptylolitów, charakteryzujących się znacznie większą aktywnością w procesie izomeryzacji α -pinenu niż naturalny klinoptylolit. Zastosowanie najlepszego z otrzymanych materiałów (klinoptylolit przemywany 0,1M roztworem H_2SO_4) pozwoliło obniżyć temperaturę prowadzenia izomeryzacji do 70°C, przy 100% konwersji α -pinenu już po czasie 4 minut i przy jednoczesnym zachowaniu wysokich selektywności przemiany do kamfenu (50% mol) oraz limonenu (30% mol).

- Modyfikacja klinoptylolitu przez przemywanie roztworami kwasu siarkowego jest łatwa do przeprowadzenia, skalowalna i nie wymaga skomplikowanego sprzętu w porównaniu do metody syntezy katalizatorów tytanowo-silikatowych.
- Najbardziej aktywnym materiałem okazał się klinoptylolit modyfikowany przez przemywanie roztworem wodnym kwasu siarkowego o stężeniu 0,1M. Zwiększenie aktywności klinoptylolitu przemytego roztworem wodnym kwasu jest składową wielu czynników. Duże znaczenie ma zwiększenie powierzchni właściwej poprzez otwarcie porów oraz zwiększenie ilości centrów aktywnych, jednak, zbyt duże stężenie kwasu powoduje zniszczenie struktury krystalicznej oraz wypłukanie jonów Al^{3+} , K^+ , Mg^{2+} , Ca^{2+} i Fe^{2+} .
- Reakcja izomeryzacji α -pinenu w obecności klinoptylolitu przemytego roztworem wodnym kwasu siarkowego o stężeniu 0,1M jest silnie egzotermiczna i zachodzi gwałtownie.
- Naturalne glinokrzemiany są ekologiczną alternatywą dla syntetycznych katalizatorów tytanowo-silikatowych. Nie zawierają szkodliwych substancji, są łatwe do usunięcia z mieszaniny poreakcyjnej.
- Izomeryzacja α -pinenu w największym stopniu zgodna jest z kinetyką reakcji pierwszego rzędu.
- Zaobserwowane reakcje następcze pozwalają wnioskować, że klinoptylolit modyfikowany przez przemywanie roztworem kwasu siarkowego z powodzeniem może być zastosowany jako katalizator izomeryzacji limonenu.
- Granulowany węgiel aktywny DT0 modyfikowany wodnymi roztworami kwasów (HNO_3 i HCl) jest aktywny w procesie izomeryzacji α -pinenu,
- Modyfikacja węgla aktywnego wodnym roztworem kwasu HNO_3 powoduje utlenienie się węgla, co wpływa na znaczne zmniejszenie powierzchni właściwej katalizatora,
- Najbardziej aktywny w procesie izomeryzacji α -pinenu okazał się węgiel aktywny DT0, modyfikowany dwustopniowo: najpierw wodnym roztworem kwasu HCl , a następnie wodnym roztworem HNO_3 . Duży wpływ na aktywność katalityczną modyfikowanych węgli ma obecność grup $-COOH$ oraz $-C-OH$ na powierzchni materiału, grupy te stanowią centra kwasowe i biorą udział w reakcji izomeryzacji alfa-pinenu.
- Modyfikowane węgle aktywne również są alternatywą dla syntetycznych katalizatorów tytanowo-silikatowych. Ich produkcja jest tania i nie wymaga wykorzystania szkodliwych substancji.

- Dodatkowym atutem wykorzystania węgla aktywnych jako katalizatorów izomeryzacji α -pinenu, jest możliwość ich łatwej modyfikacji, np. poprzez impregnację solami różnych metali. Takie działanie może prowadzić do zwiększenia ich aktywności w badanej reakcji.

5. Literatura

1. Allenspach, M.; Steuer, C. α -Pinene: A never-ending story. *Phytochemistry* **2021**, *190*, 112857, doi:10.1016/j.phytochem.2021.112857.
2. Salehi, B.; Upadhyay, S.; Orhan, I.E.; Jugran, A.K.; Jayaweera, S.L.D.; Dias, D.A.; Sharopov, F.; Taheri, Y.; Martins, N.; Baghalpour, N.; et al. Therapeutic potential of α - and β -pinene: a miracle gift of nature. *Biomolecules* **2019**, *9*, 1–34, doi:10.3390/biom9110738.
3. Saldanha, E.; Pai, R.J.; George, T.; D'Souza, S.; Adnan, M.; Pais, M.; Naik, T.; D'Souza, R.C.C.; D'Cunha, R.; Shrinath Baliga, M. Health effects of various dietary agents and phytochemicals (Therapy of acute pancreatitis). In *Therapeutic, Probiotic, and Unconventional Foods*; Elsevier, **2018**; 303–314, ISBN 9780128146262.
4. Berger, R.G. *Flavours and fragrances: Chemistry, bioprocessing and sustainability*; Springer Berlin Heidelberg: Berlin, Heidelberg, **2007**; Vol. 44; ISBN 9783540493389.
5. Ponomarev, D.; Mettee, H. Camphor and its industrial synthesis. *Chem. Educ. J.* **2016**, *18*, 1–4.
6. Findik, S.; Gündüz, G. Isomerization of α -pinene to camphene. *J. Am. Oil Chem. Soc.* **1997**, *74*, 1145–1151, doi:10.1007/s11746-997-0038-8.
7. Severino, A.; Vital, J.; Lobo, L.S. Isomerization of α -pinene over TiO₂: Kinetics and catalyst optimization. In *Stud. Surf. Scien. Catal.*; **1993**, Vol. 78, 685–692.
8. Trukhin, A.; Kruchkov, F.; Hansen, L.K.; Kallenborn, R.; Kiprianova, A.; Nikiforov, V. Toxaphene chemistry: Separation and characterisation of selected enantiomers of the Polychloropinene mixtures. *Chemosphere* **2007**, *67*, 1695–1700, doi:10.1016/j.chemosphere.2006.05.082.
9. Gusevskaya, E. V. Reactions of terpenes catalyzed by heteropoly compounds: valorization of biorenewables. *ChemCatChem* **2014**, *6*, 1506–1515, doi:10.1002/cctc.201400052.
10. Quintans-Júnior, L.; Moreira, J.C.F.; Pasquali, M.A.B.; Rabie, S.M.S.; Pires, A.S.; Schröder, R.; Rabelo, T.K.; Santos, J.P.A.; Lima, P.S.S.; Cavalcanti, S.C.H.; et al. Antinociceptive activity and redox profile of the monoterpenes (+)-camphene, p-cymene, and geranyl acetate in experimental models. *ISRN Toxicol.* **2013**, *2013*, 1–11, doi:10.1155/2013/459530.
11. Girola, N.; Figueiredo, C.R.; Farias, C.F.; Azevedo, R.A.; Ferreira, A.K.; Teixeira, S.F.; Capello, T.M.; Martins, E.G.A.; Matsuo, A.L.; Travassos, L.R.; et al. Camphene isolated

- from essential oil of *Piper cernuum* (Piperaceae) induces intrinsic apoptosis in melanoma cells and displays antitumor activity in vivo. *Biochem. Biophys. Res. Commun.* **2015**, *467*, 928–934, doi:10.1016/j.bbrc.2015.10.041.
12. Marei, G.; Rabea, E.; Badawy, M. In vitro antimicrobial and antioxidant activities of monoterpenes against some food-borne pathogens. *J. Plant Prot. Pathol.* **2019**, *10*, 87–94, doi:10.21608/jppp.2019.40594.
 13. Marei, G.I.K.; Abdel Rasoul, M.A.; Abdelgaleil, S.A.M. Comparative antifungal activities and biochemical effects of monoterpenes on plant pathogenic fungi. *Pestic. Biochem. Physiol.* **2012**, *103*, 56–61, doi:10.1016/j.pestbp.2012.03.004.
 14. Hachlafi, N. EL; Aanniz, T.; Menyiy, N. El; Baaboua, A. El; Omari, N. El; Balahbib, A.; Shariati, M.A.; Zengin, G.; Fikri-Benbrahim, K.; Bouyahya, A. In vitro and in vivo biological investigations of camphene and its mechanism insights: A Review. *Food Rev. Int.* **2021**, 1–28, doi:10.1080/87559129.2021.1936007.
 15. Santana, H.S.R.; de Carvalho, F.O.; Silva, E.R.; Santos, N.G.L.; Shanmugam, S.; Santos, D.N.; Wisniewski, J.O.; Junior, J.S.C.; Nunes, P.S.; Araujo, A.A.S.; et al. Anti-inflammatory activity of limonene in the prevention and control of injuries in the respiratory system: a systematic review. *Curr. Pharm. Des.* **2020**, *26*, 2182–2191, doi:10.2174/1381612826666200320130443.
 16. Król, S.K.; Skalicka-Woźniak, K.; Kandefler-Szerszeń, M.; Stepulak, A. The biological and pharmacological activity of essential oils in the treatment and prevention of infectious diseases. *Postepy Hig. Med. Dosw.* **2013**, *67*, 1000–1007, doi:10.5604/17322693.1067687.
 17. Aggarwal, K.K.; Khanuja, S.P.S.; Ahmad, A.; Santha Kumar, T.R.; Gupta, V.K.; Kumar, S. Antimicrobial activity profiles of the two enantiomers of limonene and carvone isolated from the oils of *mentha spicata* and *anethum sowa*. *Flavour Fragr. J.* **2002**, *17*, 59–63, doi:10.1002/ffj.1040.
 18. Espina, L.; Gelaw, T.K.; de Lamo-Castellví, S.; Pagán, R.; García-Gonzalo, D. Mechanism of bacterial inactivation by (+)-limonene and its potential use in food preservation combined processes. *PLoS One* **2013**, *8*, e56769, doi:10.1371/journal.pone.0056769.
 19. Igimi, H.; Hisatsugu, T.; Nishimura, M. The use of d-limonene preparation as a dissolving agent of gallstones. *Am. J. Dig. Dis.* **1976**, *21*, 926–939, doi:10.1007/BF01071903.

20. Vieira, A.J.; Beserra, F.P.; Souza, M.C.; Totti, B.M.; Rozza, A.L. Limonene: Aroma of innovation in health and disease. *Chem. Biol. Interact.* **2018**, *283*, 97–106, doi:10.1016/j.cbi.2018.02.007.
21. Rothenberger, O.S.; Krasnoff, S.B.; Rollins, R.B. Conversion of (+)-limonene to (-)-carvone: An organic laboratory sequence of local interest. *J. Chem. Educ.* **1980**, *57*, 741, doi:10.1021/ed057p741.
22. Arrieta, M.P.; López, J.; Ferrándiz, S.; Peltzer, M.A. Characterization of PLA-limonene blends for food packaging applications. *Polym. Test.* **2013**, *32*, 760–768, doi:10.1016/j.polymertesting.2013.03.016.
23. *The Chemistry of Fragrances*; Pybus, D., Sell, C.,; Royal Society of Chemistry: Cambridge, **2007**, ISBN 978-0-85404-824-3.
24. Ebmeyer, F. Theoretical investigations towards an understanding of the α -pinene/camphene rearrangement. *J. Mol. Struct.* **2002**, *582*, 251–255, doi:10.1016/S0166-1280(01)00784-9.
25. Allahverdiev, A.I.; Gündüz, G.; Murzin, D.Y. Kinetics of α -pinene isomerization. *Ind. Eng. Chem. Res.* **1998**, *37*, 2373–2377, doi:10.1021/ie970573t.
26. Rabee, A.I.M.; Durndell, L.J.; Fouad, N.E.; Frattini, L.; Isaacs, M.A.; Lee, A.F.; Mekhemer, G.A.H.; Santos, V.C. do.; Wilson, K.; Zaki, M.I. Citrate-mediated sol–gel synthesis of Al-substituted sulfated zirconia catalysts for α -pinene isomerization. *Mol. Catal.* **2018**, *458*, 206–212, doi:10.1016/j.mcat.2017.10.029.
27. Tzompantzi, F.; Valverde, M.; Pérez, A.; Rico, J.L.; Mantilla, A.; Gómez, R. Synthesis of camphene by α -pinene isomerization using W_2O_3 - Al_2O_3 catalysts. *Top. Catal.* **2010**, *53*, 1176–1178, doi:10.1007/s11244-010-9557-x.
28. Yadav, M.K.; Chudasama, C.D.; Jasra, R. V. Isomerisation of α -pinene using modified montmorillonite clays. *J. Mol. Catal. A Chem.* **2004**, *216*, 51–59, doi:10.1016/j.molcata.2004.02.004.
29. Sidorenko, A.Y.; Aho, A.; Ganbaatar, J.; Batsuren, D.; Utenkova, D.B.; Sen'kov, G.M.; Wärnå, J.; Murzin, D.Y.; Agabekov, V.E. Catalytic isomerization of α -pinene and 3-carene in the presence of modified layered aluminosilicates. *Mol. Catal.* **2017**, *443*, 193–202, doi:10.1016/j.mcat.2017.10.014.
30. Wang, X.; Chen, L.; Huang, D.; Yue, J.; Luo, Z.; Zeng, T. The modification, characterization of H-mordenite and their catalytic activity in isomerization of α -pinene. *Catal. Letters* **2018**, *148*, 3492–3501, doi:10.1007/s10562-018-2547-5.

31. Tian, F.; Wu, Y.; Shen, Q.; Li, X.; Chen, Y.; Meng, C. Effect of Si/Al ratio on mesopore formation for zeolite beta via NaOH treatment and the catalytic performance in α -pinene isomerization and benzylation of naphthalene. *Micropor. Mesopor. Mater.* **2013**, *173*, 129–138, doi:10.1016/j.micromeso.2013.02.021.
32. Wang, J.; Hua, W.; Yue, Y.; Gao, Z. MSU-S mesoporous materials: An efficient catalyst for isomerization of α -pinene. *Bioresour. Technol.* **2010**, *101*, 7224–7230, doi:10.1016/j.biortech.2010.04.075.
33. Zou, J.J.; Chang, N.; Zhang, X.; Wang, L. Isomerization and dimerization of pinene using Al-incorporated MCM-41 mesoporous materials. *ChemCatChem* **2012**, *4*, 1289–1297, doi:10.1002/cctc.201200106.
34. Liu, Y.; Li, L.; Xie, C.X. Acidic functionalized ionic liquids as catalyst for the isomerization of α -pinene to camphene. *Res. Chem. Intermed.* **2016**, *42*, 559–569, doi:10.1007/s11164-015-2041-2.
35. Rocha, K.A. d. S.; Robles-Dutenhefner, P.A.; Kozhevnikov, I. V.; Gusevskaya, E. V. Phosphotungstic heteropoly acid as efficient heterogeneous catalyst for solvent-free isomerization of α -pinene and longifolene. *Appl. Catal. A Gen.* **2009**, *352*, 188–192, doi:10.1016/j.apcata.2008.10.005.
36. Launay, F.; Jarry, B.; Bonardet, J.L. Catalytic activity of mesoporous Ga-SBA-15 materials in α -pinene isomerisation: Similarities and differences with Al-SBA-15 analogues. *Appl. Catal. A Gen.* **2009**, *368*, 132–138, doi:10.1016/j.apcata.2009.08.022.
37. Wróblewska, A.; Miądlicki, P.; Makuch, E. The isomerization of α -pinene over the Ti-SBA-15 catalyst—the influence of catalyst content and temperature. *React. Kinet. Mech. Catal.* **2016**, *119*, 641–654, doi:10.1007/s11144-016-1059-9.
38. Wróblewska, A.; Miądlicki, P.; Sreńscek-Nazzal, J.; Sadłowski, M.; Koren, Z.C.; Michalkiewicz, B. Alpha-pinene isomerization over Ti-SBA-15 catalysts obtained by the direct method: The influence of titanium content, temperature, catalyst amount and reaction time. *Micropor. Mesopor. Mater.* **2018**, *258*, 72–82, doi:10.1016/j.micromeso.2017.09.007.
39. Wróblewska, A.; Miądlicki, P.; Tołpa, J.; Sreńscek-Nazzal, J.; Koren, Z.C.; Michalkiewicz, B. Influence of the titanium content in the Ti-MCM-41 catalyst on the course of the α -pinene isomerization process. *Catalysts* **2019**, *9*, doi:10.3390/catal9050396.
40. Zielińska, B.; Wróblewska, A.; Maślana, K.; Miądlicki, P.; Kielbasa, K.;

- Rozmysłowska-Wojciechowska, A.; Petrus, M.; Woźniak, J.; Jastrzębska, A.M.; Michalkiewicz, B.; et al. High catalytic performance of 2D $Ti_3C_2T_x$ MXene in α -pinene isomerization to camphene. *Appl. Catal. A Gen.* **2020**, *604*, doi:10.1016/j.apcata.2020.117765.
41. Dzedzicka, A.; Sulikowski, B.; Ruggiero-Mikołajczyk, M. Catalytic and physicochemical properties of modified natural clinoptilolite. *Catal. Today* **2016**, *259*, 50–58, doi:10.1016/j.cattod.2015.04.039.
 42. Akgül, M.; Özyağci, B.; Karabakan, A. Evaluation of Fe- and Cr-containing clinoptilolite catalysts for the production of camphene from α -pinene. *J. Ind. Eng. Chem.* **2013**, *19*, 240–249, doi:10.1016/j.jiec.2012.07.024.
 43. Akpolat, O.; Gündüz, G.; Ozkan, F.; Beşün, N. Isomerization of α -pinene over calcined natural zeolites. *Appl. Catal. A Gen.* **2004**, *265*, 11–22, doi:10.1016/j.apcata.2003.12.055.
 44. Ünveren, E.; Günüz, G.; Cakicioğlu-Özkan, F. Isomerization of alpha-pinene over acid treated natural zeolite. *Chem. Eng. Commun.* **2005**, *192*, 386–404, doi:10.1080/00986440590477773.
 45. Akgül, M.; Özyağcı, B.; Karabakan, A. Evaluation of Fe- and Cr-containing clinoptilolite catalysts for the production of camphene from α -pinene. *J. Ind. Eng. Chem.* **2013**, *19*, 240–249, doi:10.1016/j.jiec.2012.07.024.
 46. Kamińska, A.; Miądlicki, P.; Kiełbasa, K.; Kujbida, M.; Sreńscek-Nazzal, J.; Wróbel, R.J.; Wróblewska, A. Activated carbons obtained from orange peels, coffee grounds, and sunflower husks—comparison of physicochemical properties and activity in the alpha-pinene isomerization process. *Materials*. **2021**, *14*, 7448, doi:10.3390/ma14237448.
 47. Simakova, I.L.; Solkina, Y.S.; Moroz, B.L.; Simakova, O.A.; Reshetnikov, S.I.; Prosvirin, I.P.; Bukhtiyarov, V.I.; Parmon, V.N.; Murzin, D.Y. Selective vapour-phase α -pinene isomerization to camphene over gold-on-alumina catalyst. *Appl. Catal. A Gen.* **2010**, *385*, 136–143, doi:10.1016/j.apcata.2010.07.002.
 48. Xiang, J.; Luo, Z. Study on the pinene isomerization catalyzed by TiM. *Chinese J. Chem. Eng.* **2018**, 2537–2541, doi:10.1016/j.cjche.2018.02.005.
 49. Chimal-Valencia, O.; Robau-Sánchez, A.; Collins-Martínez, V.; Aguilar-Elguézabal, A. Ion exchange resins as catalyst for the isomerization of α -pinene to camphene. *Bioresour. Technol.* **2004**, *93*, 119–123, doi:10.1016/j.biortech.2003.10.016.
 50. Li, Y.; Wang, C.; Chen, H.; Hua, W.; Yue, Y.; Gao, Z. Isomerization of α -pinene over porous phosphate heterostructure materials: Effects of porosity and acidity. *Catal.*

- Letters* **2009**, *131*, 560–565, doi:10.1007/s10562-009-9969-z.
51. Liang, J.; Liang, Z.; Zou, R.; Zhao, Y. Heterogeneous catalysis in zeolites, mesoporous silica, and metal–organic frameworks. *Adv. Mater.* **2017**, *29*, doi:10.1002/adma.201701139.
 52. Kresge, C.T.; Vartuli, J.C.; Roth, W.J.; Leonowicz, M.E. The discovery of ExxonMobil's M41S family of mesoporous molecular sieves. *Stud. Surf. Sci. Catal.*, **2004**, 53–72. doi:10.1016/s0167-2991(04)80193-9.
 53. Zhao, D.; Wan, Y.; Zhou, W. *Ordered Mesoporous Materials*; Wiley-VCH Verlag GmbH & Co. KGaA: Weinheim, Germany, **2013**; ISBN 9783527647866.
 54. Wróblewska, A.; Miądlicki, P.; Makuch, E. The isomerization of α -pinene over the Ti-SBA-15 catalyst—the influence of catalyst content and temperature. *React. Kinet. Mech. Catal.* **2016**, *119*, 641–654, doi:10.1007/s11144-016-1059-9.
 55. Wróblewska, A.; Miądlicki, P.; Sreńscek-Nazzal, J.; Sadłowski, M.; Koren, Z.C.; Michalkiewicz, B. Alpha-pinene isomerization over Ti-SBA-15 catalysts obtained by the direct method: The influence of titanium content, temperature, catalyst amount and reaction time. *Micropor. Mesopor. Mater.* **2018**, *258*, 72–82, doi:10.1016/j.micromeso.2017.09.007.
 56. Grün, M.; Unger, K.K.; Matsumoto, A.; Tsutsumi, K. Novel pathways for the preparation of mesoporous MCM-41 materials: control of porosity and morphology. *Micropor. Mesopor. Mater.* **1999**, *27*, 207–216, doi:10.1016/S1387-1811(98)00255-8.
 57. Wróblewska, A.; Miądlicki, P.; Tołpa, J.; Sreńscek-Nazzal, J.; Koren, Z.C.; Michalkiewicz, B. Influence of the titanium content in the Ti-MCM-41 catalyst on the course of the α -pinene isomerization process. *Catalysts* **2019**, *9*, 396, doi:10.3390/catal9050396.
 58. Murray, H. *Applied Clay Mineralogy. Occurrences, processing and application of kaolins, bentonite, palygorskitesepiolite, and common clays*; Elsevier B.V.: Oxford, **2007**; ISBN 9780444517012.
 59. Meunier, A. *Clays*; Springer Berlin Heidelberg, Berlin, Heidelberg, **2005**; ISBN 3-540-21667-7.
 60. Hamedani, N.F.; Ghazvini, M.; Sheikholeslami-Farahani, F.; Jamnani, M.T.B. KF/clinoptilolite nanoparticles as a heterogeneous catalyst for green synthesis of pyrido[2,1-a]isoquinolines using four-component reaction of alkyl bromides. *Comb. Chem. High Throughput Screen.* **2020**, *22*, 728–739,

doi:10.2174/1386207323666191213143417.

61. Takabatake, M.; Motokura, K. Montmorillonite-based heterogeneous catalysts for efficient organic reactions. *Nano Express* **2022**, *3*, 014004, doi:10.1088/2632-959X/ac5ac3.
62. Bonacci, S.; Iriti, G.; Mancuso, S.; Novelli, P.; Paonessa, R.; Tallarico, S.; Nardi, M. Montmorillonite K10: An efficient organo-heterogeneous catalyst for synthesis of benzimidazole derivatives. *Catalysts* **2020**, *10*, doi:10.3390/catal10080845.
63. Bharadwaj, S.K.; Boruah, P.K.; Gogoi, P.K. Phosphoric acid modified montmorillonite clay: A new heterogeneous catalyst for nitration of arenes. *Catal. Commun.* **2014**, *57*, 124–128, doi:10.1016/j.catcom.2014.08.019.
64. Solkina, Y.S.; Reshetnikov, S.I.; Estrada, M.; Simakov, A.; Murzin, D.Y.; Simakova, I.L. Evaluation of gold on alumina catalyst deactivation dynamics during α -pinene isomerization. *Chem. Eng. J.* **2011**, *176–177*, 42–48, doi:10.1016/j.cej.2011.03.106.
65. Miądlicki, P.; Wróblewska, A.; Kiełbasa, K.; Koren, Z.C.; Michalkiewicz, B. Sulfuric acid modified clinoptilolite as a solid green catalyst for solvent-free α -pinene isomerization process. *Micropor. Mesopor. Mater.* **2021**, *324*, doi:10.1016/j.micromeso.2021.111266.
66. Sreńscek-Nazzal, J.; Kamińska, A.; Miądlicki, P.; Wróblewska, A.; Kiełbasa, K.; Wróbel, R.J.; Serafin, J.; Michalkiewicz, B. Activated carbon modification towards efficient catalyst for highvalue-added products synthesis from alpha-pinene. *Materials*, **2021**, *14*, 7811, doi:10.3390/ma14247811.

**Kopie cyklu publikacji stanowiących osiągnięcia naukowe, o których mowa
w art. 13 ust. 2 ustawy**

The isomerization of α -pinene over the Ti-SBA-15 catalyst—the influence of catalyst content and temperature

Agnieszka Wróblewska¹ · Piotr Miądlicki¹ ·
Edyta Makuch¹

Received: 23 May 2016 / Accepted: 28 July 2016 / Published online: 4 August 2016
© Akadémiai Kiadó, Budapest, Hungary 2016

Abstract The Ti-SBA-15 catalyst, which was prepared according to the literature by the hydrothermal method, was used in the isomerization of α -pinene to: camphene and limonene. In this work, the influence of: Ti-SBA-15 catalyst content (5–15 wt%), temperature (80–140 °C), and reaction time (5–48 h) was studied. The most beneficial conditions were determined on the basis of the following functions: the conversion of α -pinene, and the selectivities of camphene and limonene. The most beneficial conditions were taken as: the temperature of 140 °C, the reaction time 48 h and the amount of the catalyst 15 wt%. Under these conditions, the conversion of α -pinene amounted to 60 mol%, and the selectivities of camphene and limonene amounted to 51 and 19 mol%, respectively.

Keywords α -Pinene · Ti-SBA-15 catalyst · Isomerization · Camphene · Limonene · Turpentine

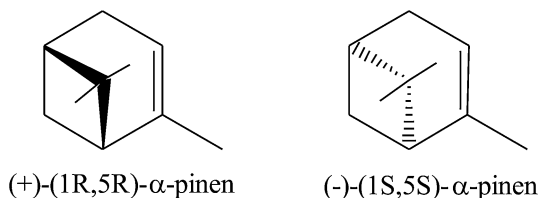
Introduction

Monoterpenes and their analogues—terpenoids, have taste and fragrant properties, and are characterized by a diverse biological and chemical activity. Terpenes, on account of their low price and the simplicity of obtaining them, are applied in many branches of industry and are an ecological alternative to petroleum derivatives. During the last years, great attention has been directed to the utilization of terpenes in fine chemicals production. Terpenes with a great industrial importance are: α -pinene and β -pinene. α -Pinene has two enantiomers: (+)- α -pinene and (–)- α -pinene (Fig. 1).

✉ Agnieszka Wróblewska
Agnieszka.wroblewska@zut.edu.pl

¹ Institute of Organic Chemical Technology, West Pomeranian University of Technology, Pułaskiego 10, PL 70-322 Szczecin, Poland

Fig. 1 The enantiomers of α -pinene



(-)- α -Pinene is obtained from pines growing in Europe, while (+)- α -pinene is commonly present in pines growing in South America. The racemic mixture of those two enantiomers is present in some plant oils, for example in the eucalyptus and orange oils. Moreover, α -pinene can be separated from turpentine by a vacuum rectification method as a 95 % concentrate.

The isomerization of natural terpenes is a very important industrial process, in which very valuable semi-products for perfume industry, food industry and detergents production can be obtained. On the industrial scale, the isomerization of α -pinene is conducted in the presence of TiO_2 as the catalyst, at the temperature of 100 °C and at the atmospheric pressure. The sum of yields of camphene, limonene and tricyclenes in this process amounts to 75–80 %. Nowadays, on account of a low reaction rate of this industrial process, a great interest is observed in search of new catalysts which could show higher activity and better selectivities of limonene and camphene [1–6].

The isomerization of α -pinene was also carried out over the Al-SBA-15 and Ga-SBA-15 catalysts. B. Jarry et al. obtained catalysts with SBA-15 structure, which contained Ga and Al atoms. These catalysts were synthesized by two methods: the direct synthesis method and the grafting method. In the first method, Ga and Al were directly incorporated into the SBA-15 structure, while in the second method, the metal atoms were located only on the surface of the mesoporous SBA-15 material. In the direct method, the following samples of Ga-SBA-15 materials were obtained: Ga-Sulf (hydrated gallium sulfate and tetraethoxysilane were used as the source of Ga and Si, Si/Ga = 17) and Ga Acac (gallium acetylacetonate and tetramethoxysilane were used as the source of Ga and Si, Si/Ga = 23). By the grafting method, the samples of Ga-SBA-15 catalysts named: Ga-Nit ($\text{Ga}(\text{NO}_3)_3$ in ethanol was used, Si/Ga = 35) and Ga-Cl (GaCl_3 in chloroform was used, Si/Ga = 140) were obtained. In the method of the direct synthesis of Al-SBA-15 material, $\text{Al}_2(\text{SO}_4)_3 \cdot 18\text{H}_2\text{O}$ was used as the source of Al (Al-Sulf, Si/Ga = 16). In the grafting method $\text{Al}(\text{O}-i\text{Pr})_3$ in dry hexane was used and this catalyst was named Al-OiPr (Si/Ga = 15). The isomerization was carried out at the temperature of 80 °C during 1 or 3 h (for Ga-Cl) and for the content of the catalyst in the reaction mixture amounted to 6.4 wt%. The results were presented in the form of the content of the appropriate products and α -pinene in the post reaction mixtures. Moreover, the conversion of α -pinene was possible to calculate. The authors observed that the pure SBA-15 material was unreactive. The material having the lowest Ga content showed an incomplete conversion of α -pinene within 1 h (Ga-Cl). The studies also presented that the nature of gallium precursors has an influence on the process of α -pinene isomerization, because as Ga-Sulph and Ga-Acac, samples that had a similar Ga

loading, showed strong differences in α -pinene conversion. For the Ga-Sulf, catalyst the content of the appropriate compounds in the post-reaction mixture was as follows: α -pinene 43.6 %, camphene 21.4 %, α -terpinene 3.7 %, limonene 18.3 % and terpinolene 4.1 % (conversion of α -pinene above 56 %). For Ga-Acac catalyst the content of the appropriate compounds in the post-reaction mixtures was as follows: α -pinene 12.6 %, camphene 25.5 %, α -terpinene 12.1 %, limonene 20.0 % and terpinolene 8.6 % (conversion of α -pinene above 87 %). Moreover, the isomerization over catalysts with the highest Ga content was characterized by significant amounts of polymeric products. The main products in the isomerization process were camphene and limonene (these compounds represents 70 % of all products formed in this process), and the by-products were: α -terpinene and terpinolene. The most active was the Al-OiPr sample of the Al-SBA-15 catalyst. Over this catalyst above 91 % of α -pinene was converted, but the degree of polymerization the obtained products over this catalyst was very high (40 %—polymeric products), and higher than that observed for Ga containing catalysts [7].

Other catalysts used in the process of α -pinene isomerization, which were based on the SBA-15 structure, were PW/SBA-15 catalysts. Chunhua Wu et al. obtained these catalysts by the modification of the SBA-15 structure with phosphotungstic acid ($\text{H}_3\text{PW}_{12}\text{O}_{40}$). The obtained catalysts had different content of the inbuilt heteropolyacid (from 20 to 60 %). The studies were carried out for temperatures in the range of 110–40 °C, reaction time 1–3 h, content catalyst 1–3 % and for heteropolyacid content in the catalyst 20–60 %. The main functions describing the isomerization process were: the conversion of α -pinene and the selectivity of camphene—this compound was found as the main product of this process. The examinations showed the effect of reaction temperature on the catalytic activity of the PW/SBA-15 catalyst—during raising of temperature the conversion of α -pinene and the selectivity of camphene increased and for the temperature 130 °C these functions attained to peak, next they went down. During the prolongation the reaction time, the conversion of α -pinene and the selectivity of camphene increased and achieved the maximum value for 2 h, next they decreased slightly. With increasing the content of the catalyst, these functions raised to the content of the catalyst amounted to 2 %, and next the conversion of α -pinene was practically unchanged, but the selectivity of camphene went down. Moreover, the increasing the amount of the loaded phosphotungstic acid on the SBA-15 material caused the increase of these two main functions to the 40 % PW content and next they kept relatively stable values. For the catalyst contained 40 wt% of heteropolyacid, after the reaction time of 2 h and at the temperature 130 °C, the conversion of α -pinene reached 95 mol% and the main product was camphene, which was formed with the selectivity of 49 mol% [8].

S. Ajaikumar et al. carried out the isomerization of α -pinene over the Au–M–TiO₂/Si-SBA-15 catalysts—bimetallic catalysts, where on the SBA-15 matrix, first TiO₂ was deposited (by the grafting method) and next ions of Au and other metal, such as: Cu, Co, Ni or Zn were deposited on this material. The ratio of Au ions to the ions of the other metal amounted to 1:1. The isomerization of α -pinene over AuNi–TiO₂/SBA-15 was carried out in the hydrogen atmosphere, at the temperature of 250–325 °C and for the reaction time 1–6 h. The course of this process was

described by the conversion of α -pinene and the selectivities of tricyclenes, camphene, *p*-menthene, *p*-cymene, β -phellandrene, but the main product of this process was *p*-cymene and the next product which was formed with high selectivities was *p*-menthene. The examination showed that the reaction time 1 h was enough to obtain almost 100 % conversion of α -pinene, independent of the studied temperature. At the most beneficial temperature (300 °C) and for the reaction time 1 h, the conversion of α -pinene was 100 %, and the selectivities of *p*-cymene and *p*-menthene amounted to 63 and 10 %, respectively (camphene selectivity was 1 %). Prolongation of the reaction time to 6 h caused the increase in the selectivity of camphene to 3 %, *p*-menthene to 14 % and simultaneously the decrease in the selectivity of *p*-cymene to 54 %. The isomerization of α -pinene at the temperature of 300 °C, within 1–6 h and at hydrogen atmosphere was also carried out over pure TiO₂, Si-SBA-15 and TiO₂/SBA-15 materials. Over TiO₂, Si-SBA-15 materials the conversions of α -pinene were low and amounted to 12–8 % (the reaction time changed from 1 to 6 h) and 22–11 % (the reaction time changed from 1 to 6 h), respectively. Over TiO₂, the main product was limonene, its selectivity changed from 47 to 54 % and the second detected product was camphene—its selectivity changed from 12 to 0 %. The main part of the formed products made polymeric products, their selectivity changed from 40 to 47 %. Over Si-SBA-15 also the main product was limonene, its selectivity amounted to about 50 %, the second detected product was camphene (selectivity 2–3 %) and the next detected products were terpinolene and tricyclene (these compounds are only detected for the reaction time 1 h and the selectivity of these compounds amounted to 5 and 3 %, respectively). The selectivity in the direction of polymeric products changed from 27 to 43 %. Over the TiO₂/SBA-15 material (isomerization at hydrogen atmosphere), the conversion of α -pinene amounted to 99 %, limonene was not formed, camphene selectivity was very low (2–3 %) and the main products were: *p*-cymene and *p*-menthene (selectivities 45–38 and 11–21 %, respectively). The selectivity of polymeric products was also high and amounted to 39–24 % [9].

The isomerization of α -pinene in the presence of catalysts having acid centers has been studied by many research groups. The main products of this reaction are: limonene, camphene, terpinenes, terpinolene, tricyclene, bornylene and fenchene [10–16]. The mechanism of the formation of these compounds is presented in Fig. 2.

As shown in Fig. 2, the isomerization of α -pinene is a very complicated reaction on account of the formation of many various carbocations which are created depending on the used catalyst. According to Ebmerer's work, the first stage relies on the protonation of the double bond with the formation of pinanyl cation (I or II). Cation (I) is found to be 13–20 kcal/mol more stable than cation (II). The obtained pinanyl cation can react by the two different reaction paths. The first of them relies on Wegner–Meerwein rearrangement with opening of the four-membered ring. The product of this transformation is isobornyl cation (III), which next undergoes transformation to camphyl cation (IV). By the deprotonation of camphyl cation, camphene is formed. Despite the fact that camphene is one of the main products of α -pinene isomerization, the isobornyl cation (III) might undergo other transformations, for example it can be deprotonated to bornylene. In the an other

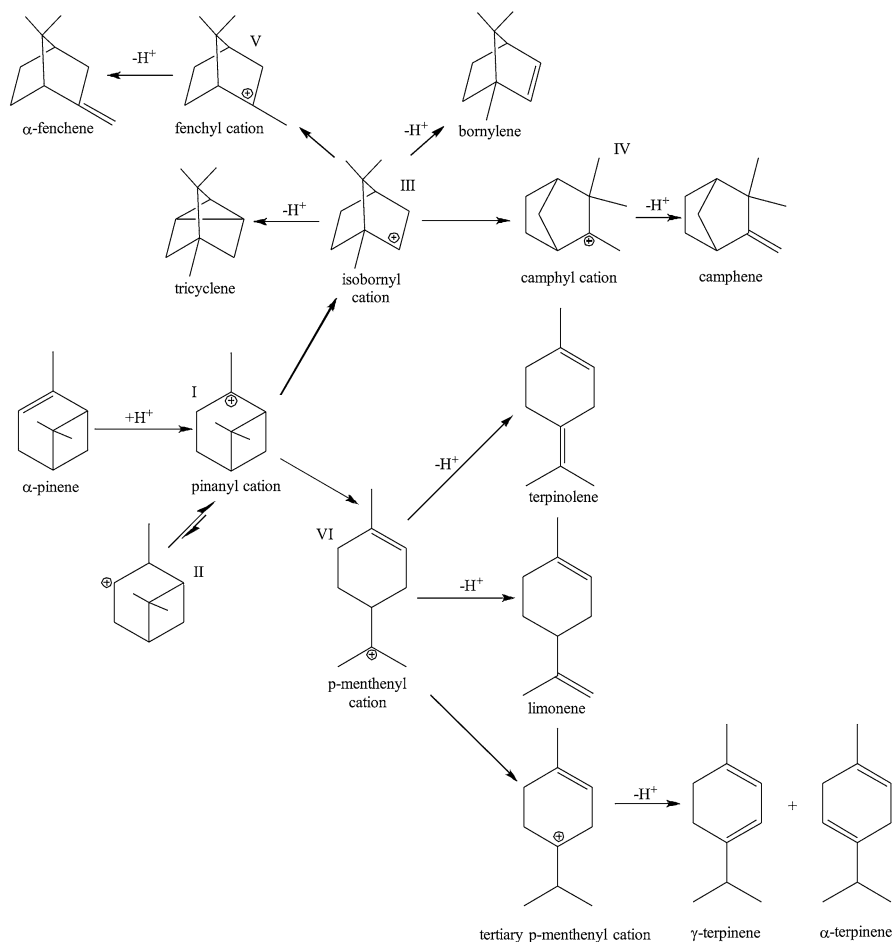


Fig. 2 The mechanism of α -pinene isomerization

transformation, isobornyl cation (III) reacts via the 1,2-shift of a methyl group to fenchyl cation (V), which can be deprotonated to α -fenchene. In the third transformation, isobornyl cation (III) might form tricyclene—this compound is formed through 1,3-deprotonation and creation of the cyclopropane ring in the tricyclic environment. The second path of the transformation of pinanyl cation (I or II) relies on the opening of the four-membered carbonic cyclic ring and formation of *p*-menthenyl cation (VI), which might undergo transformations to limonene, terpinolene and terpinenes.

The aim of this work was the preliminary study on the possibility of the application of the Ti-SBA-15 catalyst in the process of α -pinene isomerization. The utilization of this catalyst in this process has not been described in the literature yet. The aim of this work was also the determination of the best technological parameters (content of the Ti-SBA-15 catalyst, temperature, and reaction time) for

the isomerization of α -pinene over the Ti-SBA catalyst. The tested parameters were changed in the following ranges: Ti-SBA-15 content from 5 to 15 wt%, temperature from 80 to 140 °C, and reaction time from 5 to 48 h. As the most expected products of this process were taken camphene and limonene—products with the taste and fragrant properties and having a lot of applications not only in the perfume and food industry but also in medicine and polymer industry. For the description of the course of α -pinene isomerization the following functions were taken into account: the conversion of α -pinene, the selectivity of camphene, the selectivity of limonene and the sum of selectivities of other products (the all selectivities were calculated in relation to α -pinene consumed).

Experimental

The synthesis of the Ti-SBA-15 catalyst

The Ti-SBA-15 catalyst was synthesized by the method of Berube et al. [17]. The following raw materials were used in the synthesis of the Ti-SBA-15 catalyst: Pluronic P123 (Aldrich, MW = 5800) as the structure-directing agent, tetraethylortosilicalite (TEOS 98 %, Aldrich) as a silicon source and tetraisopropyl orthotitanate (TiPOT >98 %, Merc) as a titanium precursor. The molar ratio of Si/Ti in the gel before crystallization was 40:1. The Ti content in this catalyst was 2.46 wt%, the specific surface area amounted to 622 m²/g, the size of the pores achieved 5.0 nm and the particles of this catalyst had a shape of the rods with the width of about 3–4 μ m and the length of 15 μ m, and were composed with smaller particles with the width of 0.54 μ m and the length of 0.76 μ m. The detailed characteristic of the obtained Ti-SBA-15 catalyst was presented in our previous articles [18, 19].

The method of the isomerization of α -pinene over the Ti-SBA-15 catalyst

The studies on the influence of temperature, content of Ti-SBA-15 catalyst and reaction time on the course of α -pinene isomerization were carried out in the glass reactor with the capacity of 25 cm³, equipped with the reflux condenser and the magnetic stirrer with the heating function. 5 g of α -pinene (98 %, Aldrich) and the appropriate amount of the Ti-SBA-15 catalyst were introduced into the glass reactor. The glass reactor was next immersed into the oil bath and the stirring was started (400 rpm). The values of the process parameters were as follows: catalyst content 5, 10 and 15 wt%, the temperature 80, 100, 120 and 140 °C, and reaction time 5–48 h (the samples for GC analyses were taken after reaction time: 5, 24, and 48 h). After the isomerization process, the catalyst was separated from the post-reaction mixtures with help of a centrifuge.

The identification products by the gas chromatography method

The qualitative and quantitative analyses of the post-reaction mixtures were made by a gas chromatography method (GC). The parameters of the separation were as follows: helium pressure 25 kPa, the temperature of the sample chamber 200 °C, the detector temperature 240 °C, the thermostat temperature raised according to the following program: isothermally 60 °C for 1 min, the increase of temperature with the rate of 15 °C/min to 200 °C, isothermally 200 °C for 3 min, next cooling to 60 °C. During the analyses, the sensitivity was 10, and the volume of injected samples amounted to 4 μ l. For GC analyses FOCUS apparatus was used. It was equipped with the flame-ionization detector (FID), the capillary column RTX-WAX type (0.53 mm \times 30 m \times 1.0 μ m, filled with polyethylene glycol) and autosampler. The samples for GC analyses were prepared in this way: first, the catalyst was separated from the post-reaction mixture with help of the centrifuge, next, 0.250 g of the obtained solution was diluted with 0.750 g of acetone. The quantitative analyses were made with help of the external standard method. For α -pinene and for products analytical curves in the range from 1 to 33 wt% were prepared (curves were composed from eight measured points).

After the GC analyses, a mass balance for each synthesis was made and the main function describing the process were calculated: the conversion of α -pinene, the selectivity of camphene, the selectivity of limonene, and the sum of selectivities of other products (the all selectivities were calculated in relation to α -pinene consumed).

Results and discussion

Our studies were directed to camphene and limonene obtaining as the main products, thus the changes of the selectivities of these two compounds were mainly observed during the changes of Ti-SBA-15 catalyst content, temperature and reaction time. Also, the conversion of α -pinene was taken into consideration. The results obtained for the first Ti-SBA-15 catalyst content (5 wt%) are presented in Table 1 and in Figs. 3 and 4.

Table 1 shows that at chosen temperatures, the prolongation of the reaction time caused the increase in the values of the conversion of α -pinene, it is especially visible for the highest studied temperature (140 °C), at which the increase from 11 to 31 mol% was observed.

Fig. 3 presents that the highest selectivity of camphene—59 mol%, was observed for the highest studied temperature (140 °C) and for the shortest reaction time (5 min). The prolongation of the reaction time to 24 and 48 h, caused a slight decrease in the values of this function to 44 and 45 mol%, respectively. At the temperature of 120 °C, the selectivity of camphene changed slightly and amounted to about 42–47 mol%. At the temperature of 100 °C, the decrease in the values of this function from 54 to 44 mol% was observed. Only at the temperature of 80 °C the increase in the values of the selectivity of camphene was observed, because this function of the process raised from 38 to 52 mol%.

Table 1 The influence of reaction time and temperature on the α -pinene conversion

Amount of the Ti-SBA-15 (wt%)	5															
Temperature (°C)	80				100				120				140			
Reaction time (h)	5	24	48	5	24	48	5	24	48	5	24	48	5	24	48	
Conversion of α -pinene (mol%)	4	8	10	8	11	14	8	11	17	11	24	31	11	24	31	
Amount of the Ti-SBA-15 (wt%)	10															
Temperature (°C)	80				100				120				140			
Reaction time (h)	5	24	48	5	24	48	5	24	48	5	24	48	5	24	48	
Conversion of α -pinene (mol%)	9	11	13	10	13	17	10	15	23	13	28	35	13	28	35	
Amount of the Ti-SBA-15 (wt%)	15															
Temperature (°C)	80				100				120				140			
Reaction time (h)	5	24	48	5	24	48	5	24	48	5	24	48	5	24	48	
Conversion of α -pinene (mol%)	13	23	26	22	27	31	28	40	48	27	48	60	27	48	60	

Amounts of the Ti-SBA-15 catalyst: 0.25 g (5 wt% in relation to the mass of α -pinene), 0.5 g (10 wt% in relation to the mass of α -pinene) and 0.75 g (15 wt% in relation to the mass of α -pinene)

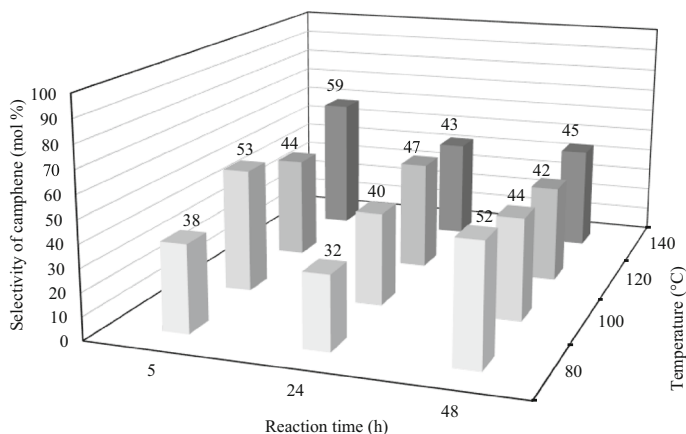
**Fig. 3** The influence of reaction time and temperature on the selectivity of camphene. Amount of the catalyst 0.25 g (5 wt% in relation to the mass of α -pinene)

Fig. 4 shows that at the temperature of 80 °C for the shortest reaction time the selectivity of limonene amounted to 0 mol% and the increase in the reaction time caused the increase in the values of this function to ten (reaction time 24 h) and 7 mol% (reaction time 48 h), respectively. The comparison showed that very similar values were observed for the temperatures: 100 and 120 °C, for which the selectivity of limonene was very low and amounted to 4–6 mol%. The highest

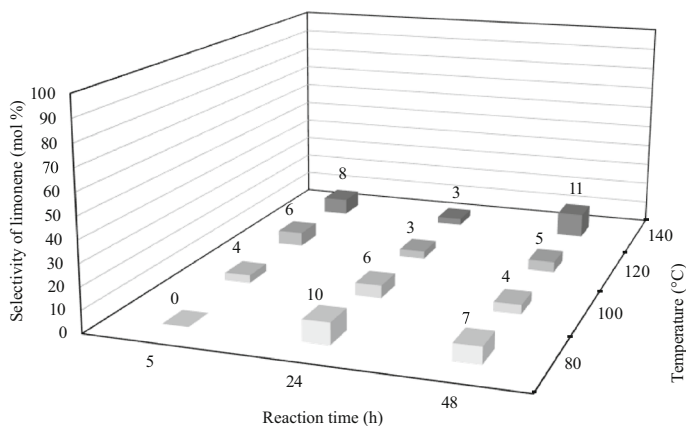


Fig. 4 The influence of reaction time and temperature on the selectivity of limonene. Amount of the catalyst 0.25 g (5 wt% in relation to the mass of α -pinene)

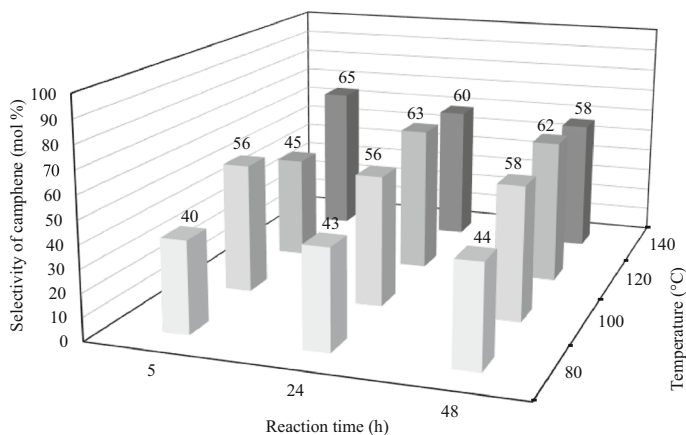


Fig. 5 The influence of reaction time and temperature on the selectivity of camphene. Amount of the catalyst 0.5 g (10 wt% in relation to the mass of α -pinene)

selectivity of limonene was obtained for the temperature of 140 °C and for the reaction time of 48 h—11 mol%.

The results obtained for the Ti-SBA-15 catalyst content amounted to 10 wt% are presented in Table 1 and in Figs. 5 and 6.

Table 1 shows that for all studied temperatures, the conversion of α -pinene raised during the increase of temperature: for the temperature of 80 °C from 9 to 13 mol%, for the temperature of 100 °C from 10 to 17 mol%, for the temperature of 120 °C from 10 to 23 mol% and for the temperature of 140 °C from 13 to 35 mol%. It shows that the most beneficial from the point of view of α -pinene conversion are the highest temperatures, especially 140 °C.

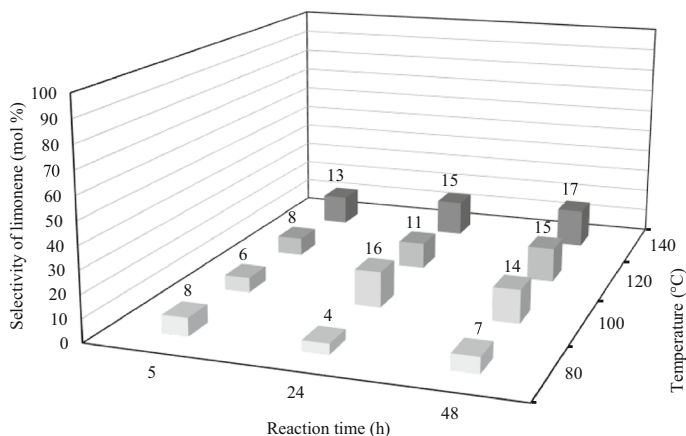


Fig. 6 The influence of reaction time and temperature on the selectivity of limonene. Amount of the catalyst 0.5 g (10 wt% in relation to the mass of α -pinene)

It results from Fig. 5 that at the temperatures of 80 and 100 °C the prolongation of the reaction time practically did not change the selectivity of camphene, which amounted to 40–44 and 56–58 mol%, respectively. For the temperature of 120 °C it was observed a greater increase in values of the selectivity of camphene, which rose from 45 to 62 mol%. The highest values of the selectivity of this compound were achieved at the temperature of 140 °C because this function took the following values: 65 mol% (reaction time 5 h), 60 mol% (reaction time 24 h), and 58 mol% (reaction time 48 h).

Fig. 6 presents that in general, the increase in values of temperature caused the increase in the values of the selectivity of limonene. For temperature of 80 °C the selectivity of limonene changed from 8 to 7 mol%, for temperature 100 °C from 7 to 14 mol%, for temperature 120 °C from 8 to 15 mol% and for temperature 140 °C from 13 to 17 mol%.

The results obtained for the Ti-SBA-15 catalyst content amounted to 15 wt% are presented in Table 1 and on Figs. 7 and 8.

Table 1 shows that the increase of temperature caused the considerable increase in the values of α -pinene conversion. For the temperature of 80 °C, this function rose from 13 mol% (reaction time 5 h) to 26 mol% (reaction time 48 h), for the temperature 100 °C, from 22 mol% (reaction time 5 h) to 31 mol% (reaction time 48 h), for the temperature of 120 °C, from 28 mol% (reaction time 5 h) to 48 mol% (reaction time 48 h) and for the temperature of 140 °C, from 27 mol% (reaction time 5 h) to 60 mol% (reaction time 48 h).

It results from Fig. 7 that the highest selectivity of camphene was obtained for the highest studied temperature (140 °C) and for all studied at this temperature and reaction times, it was similar and amounted to about 51 mol%. For the temperatures of 80 and 100 °C, the decrease in values of this function during the prolongation of the reaction time was observed. Only for the temperature of 120 °C was there a visible increase in the values of camphene selectivity, from 36 to 44 mol%.

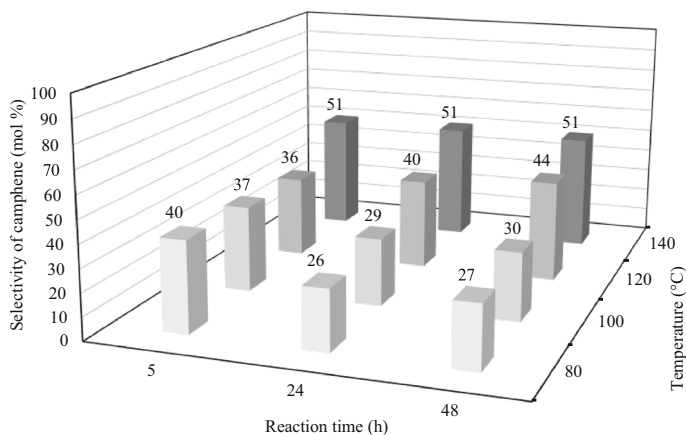


Fig. 7 The influence of reaction time and temperature on the selectivity of camphene. Amount of the catalyst 0.75 g (15 wt% in relation to the mass of α -pinene)

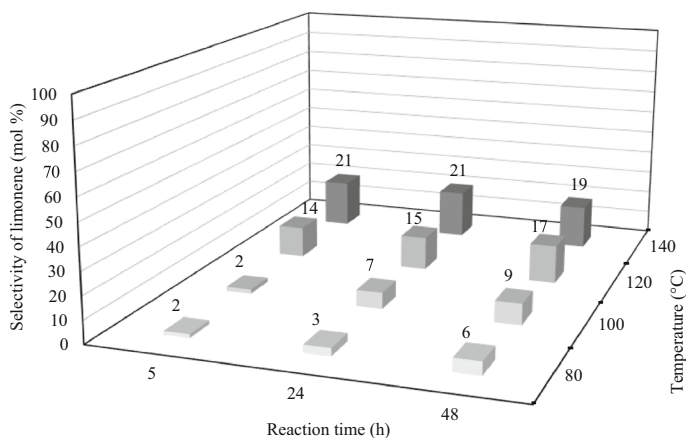


Fig. 8 The influence of reaction time and temperature on the selectivity of limonene. Amount of the catalyst 0.75 g (15 wt% in relation to the mass of α -pinene)

Fig. 8 shows that the highest selectivities of limonene can be obtained for the highest studied temperatures (120 and 140 °C). The values of this function amounted to 14–17 and 21–19 % mol, respectively. It also shows that the values of selectivity of limonene are practically independent of the reaction time. It is the most visible for the temperature of 140 °C. For the temperatures of 80 and 100 °C, the values of limonene selectivity were very low and changed from 2 to 6 mol% and from 2 to 9 mol%, respectively.

The studies presented in this work allowed to choose the most beneficial conditions of α -pinene isomerization: the temperature of 140 °C, the reaction time

48 h and the amount of the catalyst 15 wt%. Under these conditions, the conversion of α -pinene amounted to 60 mol%, and the selectivities of camphene and limonene had the following values: 51 and 19 mol%. Thus, the sum of selectivities of these two compounds amounted to about 70 mol%. It shows that the selectivity of other products was 30 mol%. On the basis of the repeated GC and GC/MS analyses, we established that to the other products present in this post-reaction mixture belong: γ -terpinene (2 mol%), α -terpinene (2 mol%), terpinolene 6 mol% and polymeric products 20 mol%. The presented selectivity of polymeric compounds is considerable lower than presented in work of Jarry et al. [7] and Ajaikumar et al. [9].

The comparison of the results presented in our manuscript for the temperature 80 °C, the reaction time 5 h and the amount of the catalyst 5 wt% with the data presented in the work of Jarry et al. [7] shows that over Ga-Sulph and Ga-Acac catalysts (catalysts obtained by the direct synthesis method the same as the Ti-SBA-15 catalyst used in our work) and under similar conditions (temperature 80 °C, reaction time 1 or 3 h and amount of the catalyst 6.4 wt%) in the post-reaction mixture was detected not only camphene but also limonene. In our work after the reaction time 5 h, only camphene was detected (selectivity about 38 mol%) but prolongation of the reaction time to 24 h and next to 48 h allowed us to obtain limonene as the product of isomerization (selectivity 7–10 mol%) at selectivity of camphene 37 and 52 mol%, respectively. The comparison the conversions of α -pinene showed that at these similar conditions this function was considerably higher for Ga-Sulph and Ga-Acac catalysts (56 and 87 %) than for the Ti-SBA-15 material (4 mol%). It could show that at the compared conditions, catalysts with SBA-15 structure which contain Ga and Al atoms are better catalysts for these reactions. However, our studies also show that for Ti-SBA-15 material at the highest content of the catalyst (15 wt%), at the highest temperature (140 °C) and for the reaction time of 48 h, it is possible to achieve high values of α -pinene conversion—60 mol%, at simultaneously high selectivities of camphene and limonene: 51 and 19 mol%, respectively. These results are good results and are comparable with the results presented in literature [7].

The comparison the results presented in our work (obtained for the temperatures 80–140 °C, the content of the catalyst 5 wt% and the reaction time 5 h) with the data at the most beneficial conditions presented by Wy et al. [8] showed that over the Ti-SBA-15 catalyst the conversions of α -pinene was considerable lower (11 mol% at 140 °C), but the selectivity of camphene was higher—59 mol% (140 °C). In our work at this temperature, the formation of limonene was also detected (selectivity of 8 mol%). Taking into account the process of the separation of the products from the post reaction mixture, obtaining higher selectivities of the most desired products is beneficial because it decreases the cost of the processes of the separation of products and the utilization of the by-products.

The comparison of the results presented by us with the data presented by Ajaikumar et al. [9] is difficult, mainly because the conditions of the isomerization. Ajaikumar et al. showed the results of the isomerization which was conducted at hydrogen atmosphere (our studies were performed at air atmosphere), at considerably higher temperature (250–325 °C) and only reaction time was close: it amounted to 1–6 h. This changing of the conditions caused that Ajaikumar et al.

obtained completely different products of the isomerization reaction—*p*-cymene and *p*-menthene, at almost complete conversion of α -pinene. Under the same conditions, studies were also performed over TiO₂, Si-SBA-15 and TiO₂/SBA-15 (this catalyst was not obtained by the direct method by the grafting method). Over the two first materials, the main products were limonene and camphene, but at low conversion of α -pinene—11–22 % depending on the used material. Over TiO₂/SBA-15 material the main products were *p*-cymene and *p*-menthene at the conversion of α -pinene 99 %.

Taking into account these results, we will obtain the Ti-SBA-15 catalyst by the method of grafting and with the utilization of various sources of Ti in the future. This can help to obtain catalysts with higher content of Ti and probably more active in the process of isomerization of α -pinene.

Conclusions

The studies showed that the Ti-SBA-15 catalyst is the effective catalyst for the process of α -pinene isomerization. In the presence of this catalyst it is possible to obtain high selectivities of camphene (to 65 mol%) at moderate conversions of α -pinene (to 60 mol%). Moreover, as the second very useful product, limonene can be obtained, but its selectivity is considerably lower than camphene (to 21 mol%). From the tested parameters, the detailed studies allowed to select the most beneficial conditions, which are as follows: the temperature of 140 °C, the reaction time 48 h and the amount of the catalyst 15 wt%. Under these conditions, the conversion of α -pinene amounted to 60 mol%, and the selectivities of camphene and limonene amounted to 51 and 19 mol%, respectively. Thus, the sum of selectivities of these two compounds is very high and amounted to about 70 mol%. Such high sum of selectivities of these compounds shows that this process can be interesting from the industrial point of view and taking into account the applications of camphene and limonene, this process should be still studied and developed. Moreover, such high sum of selectivities camphene and limonene at the most beneficial conditions allows to decrease the cost of the processes of the separation these products from the post-reaction mixture and the utilization of by-products. We think that the moderate conversion of α -pinene is a minor problem because α -pinene can be easy separated from the product and sent back to the isomerization process. The prolongation of the reaction time can be probably a worse solution taking into account the possibility of the polymerization the products at such high temperature (at the most beneficial conditions established in this work the selectivity of polymeric products amounted to 20 mol%).

The comparison our results with the results presented in the literature [7–9] showed that the obtaining of Ti-SBA-15 catalysts by the method of grafting and with the utilization of various sources of Ti can be one of the ways of the improving the efficiency of Ti-SBA-15 catalyst in the process of the isomerization of α -pinene. In the future, we would like to work on this problem.

References

1. Kołodziejczyk A (2003) Naturalne związki organiczne. PWN, Warszawa, pp 492–512
2. Sheldon RA, van Bekkum H (2001) Fine chemicals through heterogeneous catalysis. Wiley, Weinheim, pp 242–246
3. Bauer K, Garbe D, Surburg H (2001) Common fragrance and flavor materials. Wiley, Weinheim, pp 51–52
4. Corma A, Iborra S, Velty A (2007) Chemical routes for the transformation of biomass into chemicals. *Chem Rev* 107:2472–2479
5. Coppen JJW (1995) Flavours and fragrances of plant origin. Food and Agriculture Organization of the United Nation, Rome, pp 65–79
6. Lewicka L, Beldowicz M, Kąkol B, Kulig-Adamiak A, Obukowicz B (2005) Terpentyna balsamiczna i siarczanowa jako surowiec do otrzymywania syntetyków zapachowych. *Przem Chem* 84:242–246
7. Jarry B, Launay F, Nogier JP, Bonardet JL (2007) Comparative study of the catalytic activity of Al-SBA-15 and Ga-SBA-15 materials in α -pinene isomerization and oxidative cleavage of epoxide. *Stud Surf Scien Catal* 165:791–794
8. Wu C, Liu H, Zhuang C, Du G (2014) Study on mesoporous PW/SBA-15 for isomerization of α -pinene. *Appl Mech Mater* 483:134–137
9. Ajaikumar S, Goltes M, Larsson W, Shchukarev A, Kordas K, Leino AR, Mikolla JP (2013) Effective dispersion of Au and Au-M (M=Co, Ni, Cu and Zn) bimetallic nanoparticles over TiO₂ grafted SBA-15: their catalytic activity on dehydroisomerization of α -pinene. *Micropor Mesopor Mater* 173:99–111
10. Allahverdiev AI, Gunduz G, Murzin DY (1998) Kinetics of α -pinene isomerization. *Ind Eng Chem Res* 37:2373–2377
11. Severino A, Vital J, Lobo LS (1993) Isomerization of α -pinene over TiO₂: kinetics and catalyst optimization. *Stud Surf Scien Catal* 78:685–693
12. Rachwalik R, Olejniczak Z, Jiao J, Huang J, Hunger M, Sulikowski B (2007) Isomerization of α -pinene over dealuminated ferrite-type zeolites. *J Catal* 252:161–170
13. Launay F, Jarry B, Bonardet JL (2009) Catalytic activity of mesoporous Ga-SBA-15 materials in α -pinene isomerization: similarities and differences with Al-SBA-15 analogues. *Appl Catal A: General* 368:132–138
14. Agabekov VE, Sen'kov GM, Sidorenko AYU, Tuyen ND, Tuan VA (2011) New α -pinene isomerization catalysts. *Catal Ind* 3:319–330
15. Weitman M, Major DY (2011) Challenges posed to bornyl diphosphate synthase: diverging reaction mechanisms in monoterpenes. *J Am Chem Soc* 132:6349–6360
16. Ebmeyer F (2002) Theoretical investigations towards and understanding of the α -pinene/camphene rearrangement. *J Mol Struct* 582:251–255
17. Berube F, Khadhraoui A, Janicke MT, Kleitz F, Kaliaguine S (2010) Optimizing silica synthesis for the preparation of mesoporous Ti-SBA-15 epoxidation catalysts. *Ind Eng Chem Res* 49:6977–6985
18. Wróblewska A, Makuch E (2012) The utilization of Ti-SBA-15 catalyst in the epoxidation of allylic compounds. *Reac Kinet Mech Cat* 105:451–469
19. Wróblewska A (2014) The epoxidation of limonene over the ts-1 and Ti-SBA-15 catalysts. *Molecules* 19:19907–19922



Contents lists available at ScienceDirect

Microporous and Mesoporous Materials

journal homepage: www.elsevier.com/locate/micromeso

Alpha-pinene isomerization over Ti-SBA-15 catalysts obtained by the direct method: The influence of titanium content, temperature, catalyst amount and reaction time



Agnieszka Wróblewska^{a,*}, Piotr Miądlicki^{a,**}, Joanna Sreńscek-Nazzal^b,
Marcin Sadłowski^b, Zvi C. Koren^c, Beata Michalkiewicz^b

^a West Pomeranian University of Technology Szczecin, Faculty of Chemical Technology and Engineering, Institute of Organic Chemical Technology, Pulaskiego 10, 70-322 Szczecin, Poland

^b West Pomeranian University of Technology Szczecin, Faculty of Chemical Technology and Engineering, Institute of Inorganic Technology and Environment Engineering, Pulaskiego 10, 70-322 Szczecin, Poland

^c Department of Chemical Engineering, Shenkar College of Engineering, Design and Art, 12 Anna Frank St., Ramat Gan 52526 Israel

ARTICLE INFO

Article history:

Received 7 July 2017

Received in revised form

5 September 2017

Accepted 10 September 2017

Available online 12 September 2017

Keywords:

Ti-SBA-15

Isomerization

Alpha-pinene

Limonene

Camphene

ABSTRACT

This work presents the studies on the isomerization of alpha-pinene in the presence of Ti-SBA-15 catalysts with different titanium contents: 0.75, 0.90, 1.10, and 3.10 wt%, as established by the EDX method, and 0.60, 0.76, 1.08, and 2.53 wt%, as measured by the ICP-AES method. These catalysts were prepared by the hydrothermal method and were characterized by the followed instrumental techniques: XRD, UV-Vis, FT-IR, SEM, ICP-AES, EDX, TEM, and AFM. Additionally, textural parameters were determined by N₂ adsorption/desorption. Preliminary studies showed that the most active catalyst was the material prepared from the crystallization gel with the molar ratio of Si:Ti = 20:1. This catalyst was further used for the detailed studies on α -pinene isomerization according to the following parameters: temperature range of 20–200 °C, 0.5–20 wt% catalyst content, and reaction times from 15 min to 24 h. The optimal conditions for α -pinene isomerization were determined on the basis of its conversion and the selectivity of the produced camphene. This study also showed that the process of α -pinene isomerization is complex because subsequent reactions occurred during the process.

© 2017 Elsevier Inc. All rights reserved.

1. Introduction

Mobil company researchers, using surfactants as templates, produced a series of mesoporous materials from the M41S family: MCM-41 with hexagonal structure, MCM-48 with cubic structure, and MCM-51 with layered structure [1]. This discovery was groundbreaking for organic reactions that are catalyzed by zeolites, because when zeolites are used as catalysts, the particles size of the organic compounds involved in the reactions cannot exceed 10 Å. The obtained mesoporous materials, with pores of 2–50 nm, were instrumental in breaking this barrier and enabled reactions with larger, often branched organic molecules [2]. The only disadvantage

connected with the use of these materials was their inferior hydrothermal properties [3]. A breakthrough in the improvement of these properties was the discovery of a material called SBA-15, which was obtained in 1998 by Zhao et al. SBA-15 is a hexagonal material with a narrow pore size distribution of 5–15 nm, a wall thickness of 3.1–6.4 nm and a small crystallite size. The main advantage of this material is its high surface to pore volume ratio and also its uniform structure. Additionally, a characteristic of this material is that the mesoporous channels are connected by microporous channels. It has better hydrothermal properties and a greater resistance to acids in comparison with older materials from this group, *i.e.*, MCM-41 [4].

One of the modifications of the SBA-15 material is the incorporation of titanium atoms into the silica structure. There are numerous theories regarding how titanium is coordinated in the silica lattice – Fig. 1. One of them assumes that titanium occurs in the form of hydrated titanyl groups that are adjacent to the Si-OH groups (a), another indicates the presence of Ti=O groups (b), or

* Corresponding author.

** Corresponding author.

E-mail addresses: Agnieszka.Wroblewska@zut.edu.pl (A. Wróblewska), Piotr.Miadlicki@zut.edu.pl (P. Miądlicki).

that Ti^{+4} is bounded in the silica structure in the same manner as Si^{+4} (c) [5]. Some researchers suggest the formation of titanium dimers (d, e) on the surface of the catalyst. More complex structures have also been proposed and these depend on the amount of titanium incorporated in the mesoporous silica structure and on the processing conditions [6–9].

The direct synthesis of the Ti-SBA-15 material is carried out in a similar way as SBA-15, and the titanium source is introduced directly to the crystallization gel. The precursor of titanium is usually tetraisopropyl orthotitanate (TiPOT) or other organic derivatives of titanium [10]. The Ti-SBA-15 obtained in this way shows excellent catalytic properties and can be used as a slightly acidic catalyst in the selective oxidation or isomerization of large and branched organic molecules [11]. The SBA-15 material can also be modified by the grafting method by putting titanium atoms only on the surface of the catalyst, and for this purpose TiPOT as the titanium source can also be used [12]. The Ti-SBA-15 materials are much more environmentally friendly than standard homogeneous catalysts whose regeneration causes the creation of many non-environmentally friendly compounds [13].

The isomerization of α -pinene on an industrial scale is carried out using TiO_2 as the catalyst at 140 °C and for about 48 h. The main products of this reaction are camphene and limonene, and the total selectivity of these compounds is 70% [14]. In order to shorten the reaction time and increase the selectivity of products, various studies were performed using the following catalysts: Al-SBA-15, Ga-SBA-15 [15], PW/SBA-15 [16], Ga-MCM-41 [17], $\text{SO}_4/\text{ZrO}_4/\text{HMS}$ [18], $\text{AlCl}_3/\text{SiO}_2$, ferrite-type zeolites [19], acid treated natural zeolites [20], TCA/Y-zeolite [21], heat-treated natural zeolites [22], natural clays [23], heteropoly acids [24], and Fe-doped sulfated zirconia [25]. Our previous preliminary studies have shown that Ti-SBA-15 is also an active catalyst in the α -pinene isomerization process and that the main products in this process are, as stated above, camphene and limonene [26].

Camphene is a very valuable product in the organic chemical industry and it is used in the syntheses of many chemicals, for example during the chlorination reaction many compounds are formed with the name of toxaphene, which is widely used as an insecticide [27]. Camphene is also used for the production of synthetic camphor, which is an important fragrance [28]. Reaction of camphene with guaiacol leads to valuable cyclohexanol products [29]. Camphene obtained from the essential oil *Piper cernuum* possesses anti-cancer properties [30]. Limonene, which is the second main product of the α -pinene isomerization process, is also widely used in the chemical, fragrance and food industries. The mixture of limonene in the presence of α -pinene and 1,8-cineole shows a therapeutic activity similar to commonly used antibiotics and mucolytic drugs [31]. Disproportionation reaction of limonene produces a mixture of p-cymene and p-menthane [32]. One of the most important reactions using limonene as a raw material is the

conversion of (+)-limonene to (-)-carvone (carvone is used as a peppermint flavour) [33]. The application of limonene as an additive for plastics that will have contact with food, such as, polyethylene, low density polyethylene, high density polyethylene, polystyrene, and polylactic acid (PLA), was also studied [34]. Camphene, limonene, and all other compounds formed in smaller selectivities in the process of α -pinene isomerization are commercially important fragrances widely used in the perfume, food and organic industries [35].

The alpha-pinene isomerization mechanism is very complicated due to the formation of many products that depend on the type of catalyst used. α -pinene can isomerize according to two pathways. In the first (Path A) bicyclic products are formed, namely: camphene, fenchene, bornylene, and tricyclene. The second path (Path B) leads to the formation of monocyclic products, such as: limonene, terpinolene, isoterpinolene, terpinenes, phellandrene and, in the subsequent reaction, p-cymene. The mechanisms of these reactions have been described in our earlier work [26]. In this work we present the mechanisms in a simplified form (Fig. 2).

In the set of mechanisms in Fig. 2, our preliminary studies [26] and applications of the products of α -pinene isomerization show that this process can be developed in the direction of increasing the selectivity of specific products by selecting the appropriate processing conditions and by using catalysts having various Ti contents. The first purpose of this work was to investigate the effect of titanium content in the Ti-SBA-15 catalysts on the course of the α -pinene isomerization process by mainly focusing on the selectivities of relevant products and on the conversion of α -pinene. Such studies have not been previously presented in the literature. It was particularly interesting to check whether all the titanium introduced into the crystallization gel could be incorporated into the silica structure and whether anatase, a mineral form of titanium dioxide, would be detected in samples of catalysts obtained with higher titanium content in the crystallization gel. In addition, it was very interesting to examine, for the first time, how the presence of anatase in the Ti-SBA-15 catalysts can have an influence on the α -pinene isomerization process. In these studies we used Ti-SBA-15 catalysts that were synthesised in a different way from that used in our previous work [26]. The main difference was in the higher content of water, which would improve the crystallization conditions and consequently affect the higher activity of the resulting catalyst. First, the obtained Ti-SBA-15 catalysts were characterized using appropriate instrumental methods. Next, a series of studies on α -pinene isomerization was conducted to select the most active catalyst. Subsequent studies were conducted only over the selected catalyst. The aims of these investigations were to study the effect of temperature, catalyst content and reaction time on the course of isomerization of α -pinene in order to determine the most favourable conditions for this process.

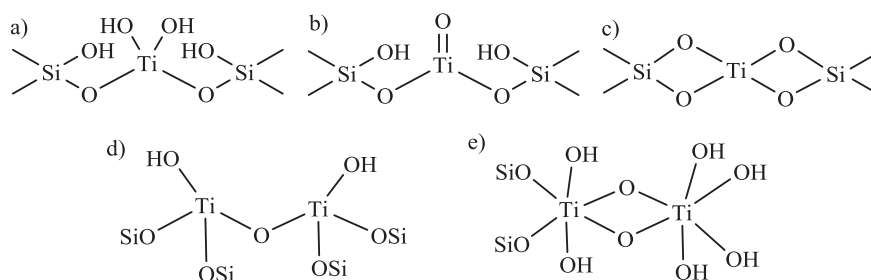


Fig. 1. The bonding modes of titanium to the silica.

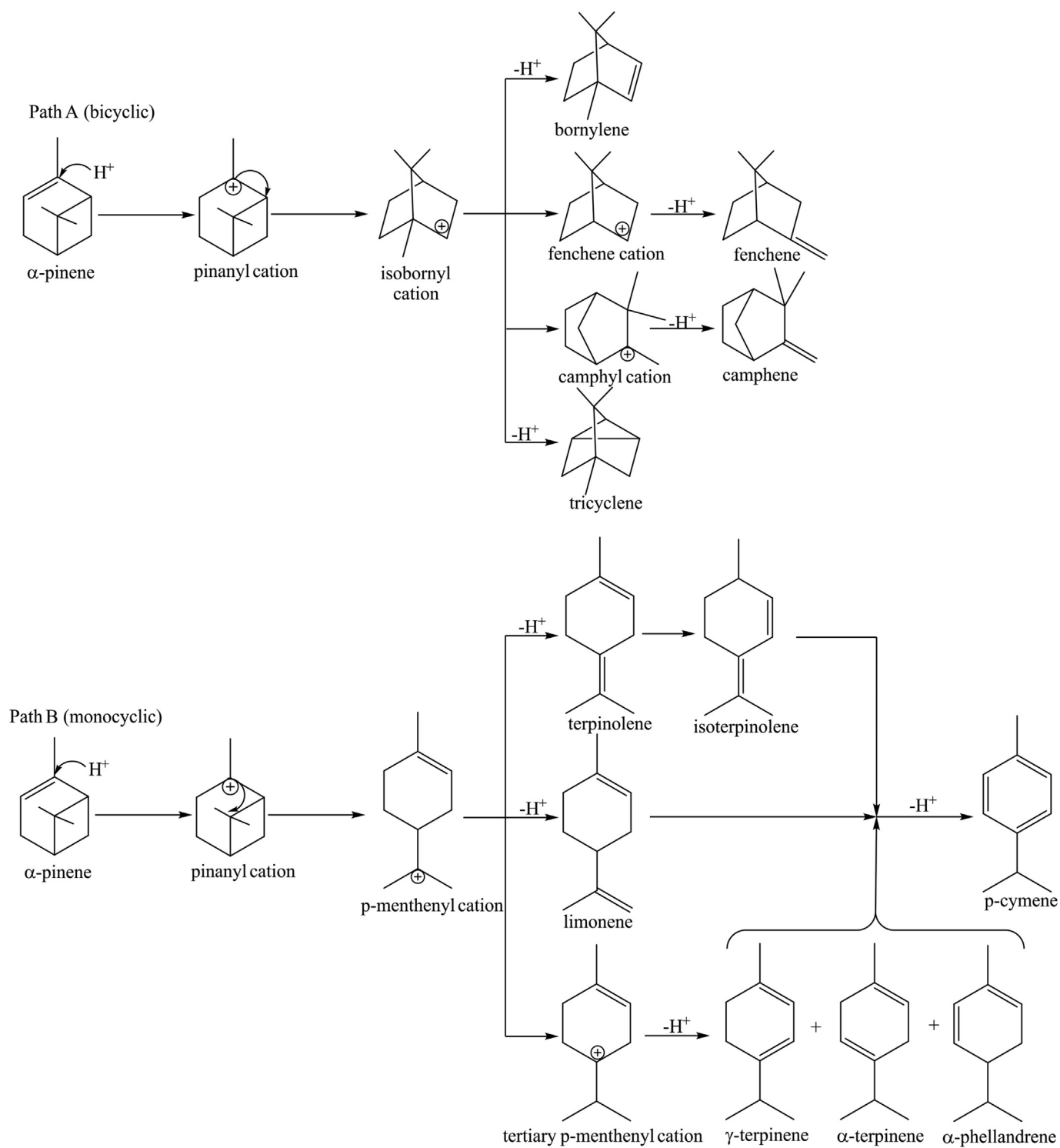


Fig. 2. The simplified mechanisms of the α -pinene isomerization process.

2. Experimental

2.1. Synthesis of the Ti-SBA-15 catalysts

Ti-SBA-15 catalysts with different molar ratios of Si:Ti in the crystallization gel (40:1, 30:1, 20:1 and 10:1) were obtained by the hydrothermal method [10]. During the syntheses the following raw materials were used: Pluronic P123 as a template (Aldrich,

MW = 5800), tetraethyl o-silicate as a silicon source (TEOS, 98% Aldrich), tetraisopropyl o-titanate as a titanium source (TiPOT, 97%, Aldrich), hydrochloric acid (HCl 35–38%, Chempur), and deionized water. In a standard method 18 g of template (biodegradable, triblock copolymer of ethylene oxide and propylene oxide, Pluronic P123) was dissolved at the temperature of 35 °C in a mixture of 376 g water and 10.5 mL HCl (37 wt% aqueous solution). Then, a mixture of 39.0 g of TEOS and TiPOT was rapidly added to this

solution (1.30 g TiPOT for the catalyst with the molar ratio Si:Ti = 40:1, 1.80 g TiPOT for the catalyst with the molar ratio Si:Ti = 30:1, 2.66 g TiPOT for the catalyst with the molar ratio Si:Ti = 20:1, and 5.31 g TiPOT for the catalyst with the molar ratio Si:Ti = 10:1). The resulting mixture was vigorously stirred and maintained at the temperature of 35 °C for 24 h, then the obtained crystallization gel was put into an autoclave, where it was maintained without stirring for a further 24 h at 35 °C. The resulting precipitate was filtered off, washed with deionized water and methanol on a filter and then dried at 100 °C for 24 h and calcined for 5 h at 550 °C. In this way Ti-SBA-15 materials in the form of a white powder and having different titanium contents were obtained.

2.2. Characteristics of the obtained catalysts

The X-ray diffraction (XRD) pattern of the catalysts were recorded by a PANalytical Empyrean X-ray diffractometer using Cu K α ($\lambda = 0.154$ nm) as the radiation source in the 2θ range 0.1–3° with a step size of 0.013, and in the 2θ range 10–35° with a step size of 0.05.

The average crystallite size of TiO₂ was obtained using the Scherrer equation after correcting for instrumental broadening [36]:

$$L = \frac{K\lambda}{B \cos \theta}$$

where L is the apparent crystallite size, K is the Scherrer constant (usually equal to 0.89), B is the full width at half-maximum of the lines (after correcting for instrumental broadening) in the 2θ scan, and λ is the X-ray wavelength. We used the line at 2θ 23°.

Textural properties were determined on the basis of nitrogen sorption at –196 °C (QUADRASORB evoTM Gas Sorption Surface Area and Pore Size Analyzer). Before sorption measurements all samples were outgassed at 250 °C for at least 20 h. The specific surface area was calculated on the basis of the Brunauer–Emmett–Teller (S_{BET}) equation and the multi-point method. The relative pressure range was selected on the basis of the linear section of the BET plot, i.e., in the relative pressure range (0.05–0.2). Pore volume distribution, micropore volume V_{micro} , and the mean pore diameter (d_m) were calculated by the DTF method. The total pore volume (V_{tot}) was obtained from the nitrogen volume adsorbed at a relative pressure of 0.98. The lattice parameters (a_0) were calculated for a 2D hexagonal system by the formula: $a_0 = 2d_{100}/\sqrt{3}$, where d_{100} is the interplanar spacing corresponding to the (100) Bragg reflection. The wall thickness (W_t) was calculated by subtracting the mean pore diameter (d_m) from the lattice parameter (a_0).

Scanning electron microscope (SEM) micrographs were obtained using an ultra-high resolution field emission scanning electron microscope (Hitachi UHR FE-SEM SU8020, Tokyo, Japan) equipped with the secondary electron (SE) detectors and an energy dispersive X-ray detector (EDX). On the basis of EDX measurements and ICP-AES spectrometry (Optima 5300 DV, Perkin-Elmer) the quantitative content of titanium in the catalysts was determined.

For ICP-AES analysis, samples were dissolved by applying a four step procedure utilizing H₂SO₄, HF, HNO₃ and H₃PO₄ in sequence. The mixtures were treated by acids in a microwave oven (Milestone MLS 1200 Mega) with the power 150–650 W (20 min for each step).

Transmission electron microscopy (TEM) pictures were made using TEM-FEI Tecnai F20 microscope operating at 200 kV.

The surface morphology of the samples was also studied by atomic force microscopy (AFM) with a Bruker NanoScope V SPM (Scanning Probe Microscope) working in MultiMode.

The incorporation of titanium in the structure of silica was characterized by UV-Vis (SPECORD M40) examinations in the wavelength range from 200 to 600 nm. In addition, FT-IR spectra were made (Thermo Nicolet 380 apparatus) in the range of wavenumbers from 400 to 4000 cm^{–1}.

2.3. Catalytic tests in α -pinene isomerization

Studies on the effect of titanium content in Ti-SBA-15 catalysts on the α -pinene isomerization process and determination of the most beneficial conditions using the most active Ti-SBA-15 catalyst were carried out in a glass reactor with the capacity of 25 cm³, equipped with a reflux condenser and magnetic stirrer with heating function. For the isomerization test, 4 g of α -pinene (98%, Aldrich) and a suitable amount of catalyst were put into the reactor which was then placed in an oil bath. The intensity of stirring was constant and amounted to 400 rpm. In the first stage of the studies the activities of the catalysts obtained with different molar ratios of Si:Ti in the crystallization gel (10:1, 20:1, 30:1, 40:1) were tested. The reaction was studied in the range of 1–48 h at 140 °C with 10 wt% catalyst content. In the next step, the most active catalyst was used to determine the most favourable reaction conditions. For this purpose, the studies on the influence of various technological parameters were conducted: temperatures (in the range of 20–200 °C), catalyst content (in the range of 0.5–20 wt%), and reaction time (from 15 min to 24 h).

For quantitative and qualitative analyses, the post-reaction mixture was centrifuged and dissolved in acetone in a 1:3 wt ratio. The qualitative analyses were performed by the GC-MS method using a ThermoQuest apparatus equipped with a Voyager detector and a DB-5 column (filled with phenylmethylsiloxanes, 30 m \times 0.25 mm \times 0.5 μ m). The parameters of analyses were as follows: helium flow of 1 mL/min, the temperature of the sample chamber 200 °C, the temperature of the detector 250 °C, the temperature of the furnace - isothermally for 2.5 min at 50 °C, then increase at the rate of 10 °C/min to 300 °C. Quantitative analyses were performed with a Thermo Electron FOCUS chromatograph equipped with a FID detector and a TR-FAME column (filled with cyanopropylphenyl, 30 m \times 0.25 mm \times 0.25 μ m). The parameters of the analyses were as follows: helium flow of 0.7 mL/min, sample chamber temperature of 200 °C, detector temperature of 250 °C, temperature of the furnace - isothermally for 7 min at 60 °C followed by the rate of 15 °C/min to 240 °C. In order to determine the composition of the post-reaction mixtures the method of an external standard was used. For establishing the amounts of products and of the unreacted substrate, calibration curves were made for eight measurement points within a concentration range of 0–33 wt%. The mass balances for the syntheses allowed the calculations of the following functions that describe the process: the conversion of α -pinene and the selectivities of relevant products (camphene, limonene, α -terpinene, γ -terpinene, terpinolene, α -phellandrene, p-cymene, and campholenic aldehyde). The selectivities of other products of isomerization, which included small amounts of tricyclene, fenchene, polymer compounds and oxidation products, were also calculated.

3. Results and discussion

3.1. Characteristics of the catalysts

UV–vis spectroscopy is a very useful method to investigate the coordination states of the Ti species in the SBA-15 structure. The

bands at 210–230, and 240–260 nm wavelengths are the evidence for the presence of tetrahedral and octahedral coordinated Ti species, respectively [37], whereas the absorption band for anatase is present at about 330–350 nm [38]. The UV-Vis spectra of the Ti-SBA-15 materials show a characteristic absorption peak at about 210 nm, which confirms the presence of titanium in tetrahedral coordination in the silica structure - Fig. 3. In addition, the bands in the range of 225–260 nm and at about 290 nm are also visible, and these bands can be assigned to titanium in the octahedral coordination. The change in the coordination number of titanium may be due to the absorption of water molecules by titanium ions incorporated into the silica structure, which mainly occurs on the surface of the catalyst, or with formation of titanium dimers shown in Fig. 1. In addition, for three Ti-SBA-15 catalysts with the molar Si:Ti ratios of 40:1, 30:1, 20:1, small inflection points at around 330 nm can be noted. In the case of the last catalyst (with the molar ratio of 10:1) this band is more visible, which is indicative of the presence of TiO₂ in the form of anatase. The presence of anatase can influence the activity of the produced material.

In the IR spectra of the obtained Ti-SBA-15 catalysts the following main bands are observed: 1625–1650, 1000–1300, 960, 800, and 460 cm⁻¹ (Fig. 4). The band in the range of 1625–1650 cm⁻¹ is assigned to bending vibrations of the -OH groups derived from water molecules adsorbed on the surface of the material. Bands for the wavelengths of 440 and 800 cm⁻¹ are attributed to bending deformations of Si-O-Si groups, where the angle between the bonds changes, and to the symmetrical valence vibrations associated with changes to the lengths of the bonds. The band in the range of 1000–1300 cm⁻¹ is attributed to the presence of Si-O-Si bonds related to the formation of silica. For the Ti-SBA-15 material the most characteristic band is at 960 cm⁻¹, which is associated with the isomorphous substitution of Si by Ti ions. It is attributed to the stresses of the polar Si-O-Ti bonds or the presence of the titanil group Ti=O, and it confirms the incorporation of titanium into the silica structure.

Ti contents estimated by EDX and ICP are presented in Table 1. The results of the ICP and the averaged EDX measurements were in good agreement with each other. It should be noted that EDX gives information about element concentration on the surface (depth of

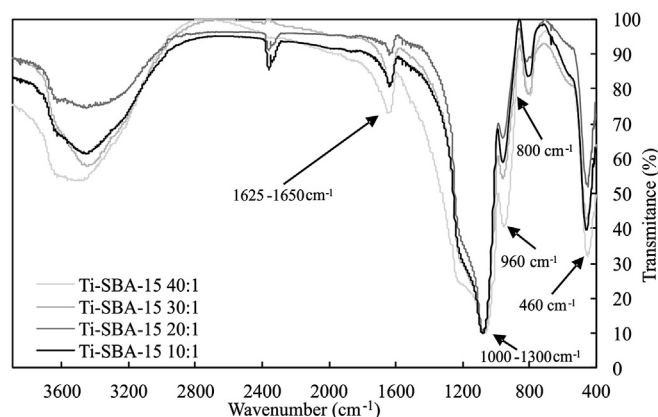


Fig. 4. IR spectra of Ti-SBA-15 catalysts with the varying molar ratios of silicon to titanium in the crystallization gel.

about 1 μm), whereas the ICP method shows an averaged analysis for the sample.

Fig. 5 shows nitrogen sorption isotherms for Ti-SBA-15 samples. The estimated textural parameters such as specific surface area, total pore volume, micropore volume, and mean pore diameter are compiled in Table 1. It was found on the basis of Fig. 5 that all the isotherms are Type IV according to the IUPAC classification and exhibited a H1/H2 hysteresis loop [39]. Because of a sharp inflection, capillary condensation within uniform pores can be assumed. The similar position of the adsorption branch inflection of every isotherm suggests that all Ti-SBA-15 have similar pore sizes. The pore size distribution curves obtained by means of the DFT method and shown in Fig. 6 confirm the similarity of the pore sizes. The average size of the pores was in the range of 5.29–5.36 nm (Table 1). A very narrow pore size distribution (from 4.5 to 6 nm) was obtained for all of the Ti-SBA-5 samples. The values of specific surface areas, total pore volumes, micropore volumes were also similar for these catalysts (Table 1). These results indicate that all the Ti-SBA-15 samples crystallized without any significant changes in textural parameters despite possessing differing contents of Ti. Moreover, no pore blocking due to the formation of TiO₂ clusters on the surface occurred.

The low-angle XRD patterns are shown in Fig. 7. All materials showed a well-resolved peak at the 2θ value of about 1° indexed as (100) indicating that they possess periodic structures. This peak is typical for the SBA-15 structure but the reflections of (110) and (200) were not observed, which means that the incorporation of titanium partly destroyed the ordered structure of the SBA-15 material. The position of the (100) diffraction peak gradually shifted to a higher angle with increasing Si content. The crystal radii for tetrahedrally coordinated Si⁴⁺ and Ti⁴⁺ are equal to 0.04 nm and 0.056 nm, respectively [40]. The higher the number of Ti⁴⁺ species incorporated in the SBA-15 framework, the higher the d-spacing value. The 2θ and d-spacing values are listed in Table 2. On the basis of d-spacing values of the (100) reflections, lattice parameters (a₀) and wall thickness (W_t) were calculated (Table 2). As expected, according to Besançon et al. [41] and Zhang et al. [42], the lattice spacing increased when the Ti content was increased. The wall thickness increased as well.

Fig. 8 shows the high-angle XRD patterns of the Ti-SBA-15 samples. Each pattern exhibits a broad peak at ca. 23° typical of amorphous silica. Contrary to the UV-Vis results, peaks corresponding to anatase at about 2θ ≈ 25° were absent. Anatase particles could be too small to result in Bragg diffraction. On the basis of the 23° line the apparent crystallite size of TiO₂ was estimated

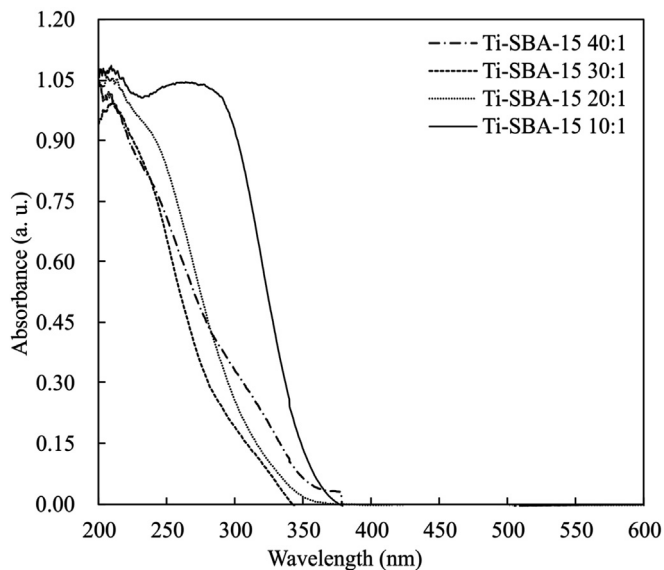


Fig. 3. UV-Vis spectra of Ti-SBA-15 catalysts with the varying molar ratios of silicon to titanium in the crystallization gel.

Table 1

Textural parameters and titanium content for the studied Ti-SBA-15 catalysts with the varying molar ratios of silicon to titanium in the crystallization gel; the maximum measured pore diameters are given in parentheses.

Samples (Ti-SBA-15)	S_{BET} (m^2/g)	V_{tot} (cm^3/g)	V_{micro} (cm^3/g)	d_{m} (nm)	Ti content obtained by EDX (wt %)	Ti content obtained by ICP (wt%)
40:1	757	0.639 (190 nm)	0.093	5.29	0.75	0.60
30:1	771	0.631 (185 nm)	0.121	5.36	0.90	0.76
20:1	766	0.625 (182 nm)	0.121	5.36	1.10	1.08
10:1	731	0.585 (174 nm)	0.091	5.32	3.10	2.53

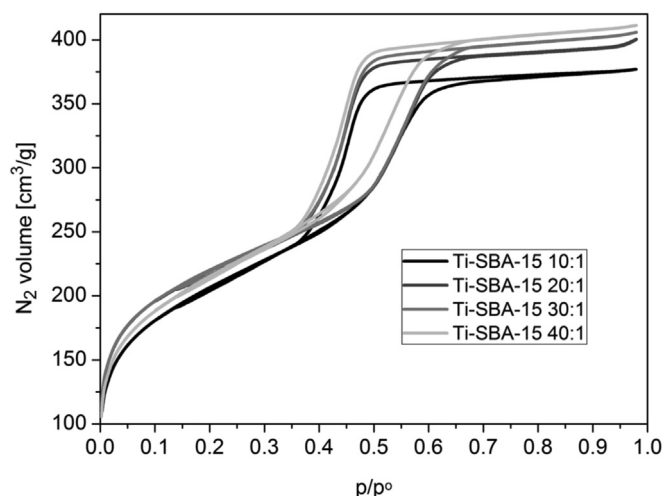


Fig. 5. N_2 adsorption–desorption isotherms of Ti-SBA-15 catalysts with different molar ratios of silicon to titanium in the crystallization gel.

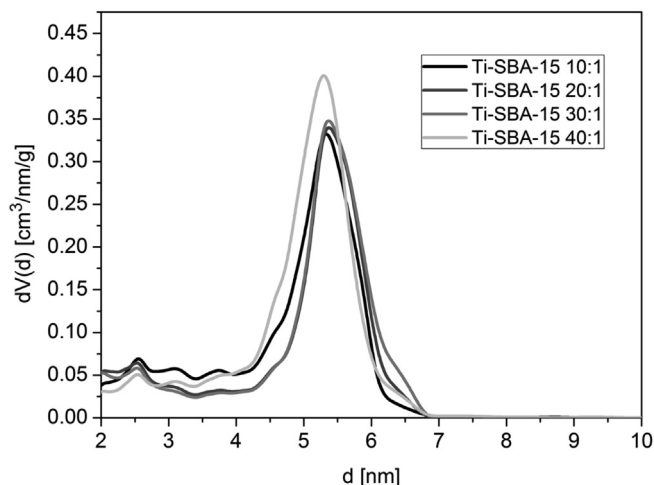


Fig. 6. Pore-size distribution for Ti-SBA-15 catalysts with different molar ratios of silicon to titanium in the crystallization gel.

using the Scherrer equation, and was equal to 1.10 ± 0.05 nm for all the samples. This is indicative of a high degree of TiO_2 dispersion on the SBA-15 surface.

The SEM pictures (Fig. 9a–d) showed a worm-like structure for the Ti-SBA-15 catalysts. The well-formed, oval shaped particles, which are reminiscent of rice grains, are joined together and form long fibrous macrostructures with a relative particle size of several micrometres. This morphology is typical for SBA-15 materials [43].

Transmission electron micrographs confirm the 2D hexagonal pore arrangement (Fig. 10a–d) and the long-range mesoporous

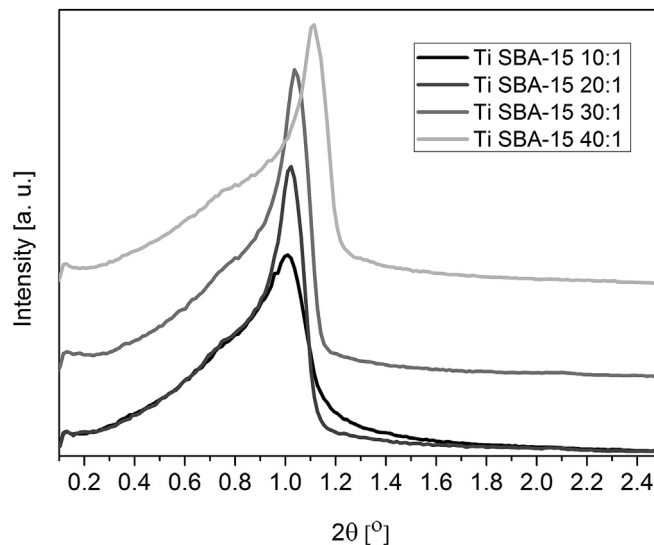


Fig. 7. Low-angle X-ray diffraction data for Ti-SBA-15 samples with different molar ratios of silicon to titanium in the crystallization gel.

Table 2

Structural parameters for Ti-SBA-15 catalysts with the varying molar ratios of silicon to titanium in the crystallization gel.

Samples (Ti-SBA-15)	2θ ($^\circ$)	d (nm)	a_0 (nm)	W_t (nm)
40:1	1.110	7.95	9.18	3.89
30:1	1.038	8.5	9.81	4.45
20:1	1.016	8.69	10.03	4.67
10:1	1.006	8.77	10.13	4.81

architecture (Fig. 10c). The samples exhibited structures typical to that of the SBA-15 material. No noticeable nanoparticles were observed for all Ti-SBA-15 samples. The anatase particles were probably placed on the inner surface of the SBA-15 material.

Fig. 11a–d shows Ti-SBA-15 surface profiles obtained by the AFM method. The average roughness of Ti-SBA samples was quite high and increased with Ti content. The average roughness was equal to 210, 179, 149, and 67 for Si:Ti molar ratios of 10:1, 20:1, 30:1, and 40:1, respectively.

3.2. Catalytic activity

The first step of our studies involved the determination of the activities of the produced catalysts with different titanium contents in the process of the isomerization of α -pinene. The activity was evaluated on the basis of the conversion of α -pinene and the selectivities of the appropriate products. Taking into account the preliminary results described in our previous article [26], the following parameters were chosen for the studies on the activities of the catalysts: temperature of 140 $^\circ\text{C}$, catalyst content of 10 wt%

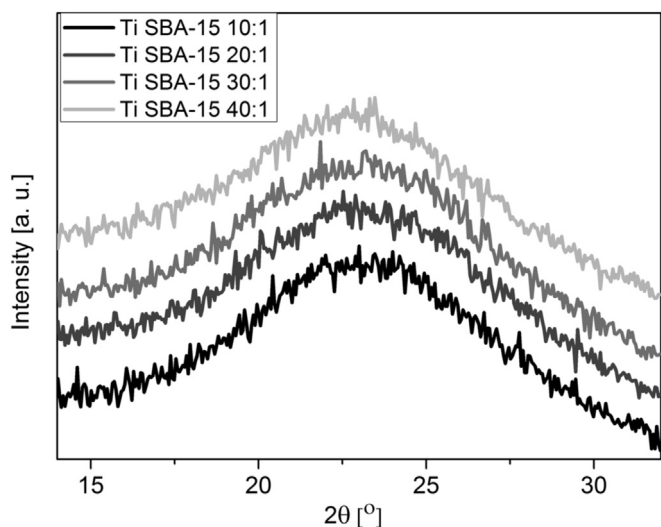


Fig. 8. High-angle X-ray diffraction data for Ti-SBA-15 samples with different molar ratios of silicon to titanium in the crystallization gel.

(in relation to α -pinene), and reaction time from 1 to 48 h. The catalyst with the highest activity was used for further research on the determination of the most favourable reaction conditions for the isomerization of α -pinene. Fig. 12 shows that the highest

conversion of α -pinene (42.63 mol%) was obtained for the reaction time of 24 h and over the catalyst with the molar ratio of Si:Ti in the crystallization gel equal to 20:1. In the case of the catalyst with the Si:Ti molar ratio of 10:1 in the crystallization gel, the conversion of α -pinene was lower and this could be caused by the presence of large amounts of TiO_2 formed during the synthesis, which can block the channels of the Ti-SBA-15 catalyst.

The selectivities of the relevant products from all the catalysts were similar. In the examined process, mainly camphene and limonene were formed, and, in somewhat lesser amounts, α -terpinene, γ -terpinene, terpinolene, p-cymene, α -phellandrene, and campholenic aldehyde. In the reaction mixtures small amounts of the following products were also detected: tricyclene, fenchene, bornylene, products of oxidation and heavy polymeric products (these products have been marked as other products in Table 3). The values of α -pinene conversion and selectivities of appropriate products after the reaction time of 24 h are presented in Table 3.

The results show that in comparison with the industrially used TiO_2 [14], Ti-SBA-15 catalysts produce lower selectivities of camphene and limonene, while at the same time produce higher selectivities of the other products, mainly α -pinene, γ -terpinene, p-cymene and α -phellandrene, but in a shorter time (24 h). Prolongation of the reaction time to 48 h (reaction time used in the industrial process) increased the selectivity of heavy polymeric products. This phenomenon is probably connected with the difference in structure of TiO_2 and Ti-SBA-15 catalysts (presence of channels with active centres inside the structure of Ti-SBA-15

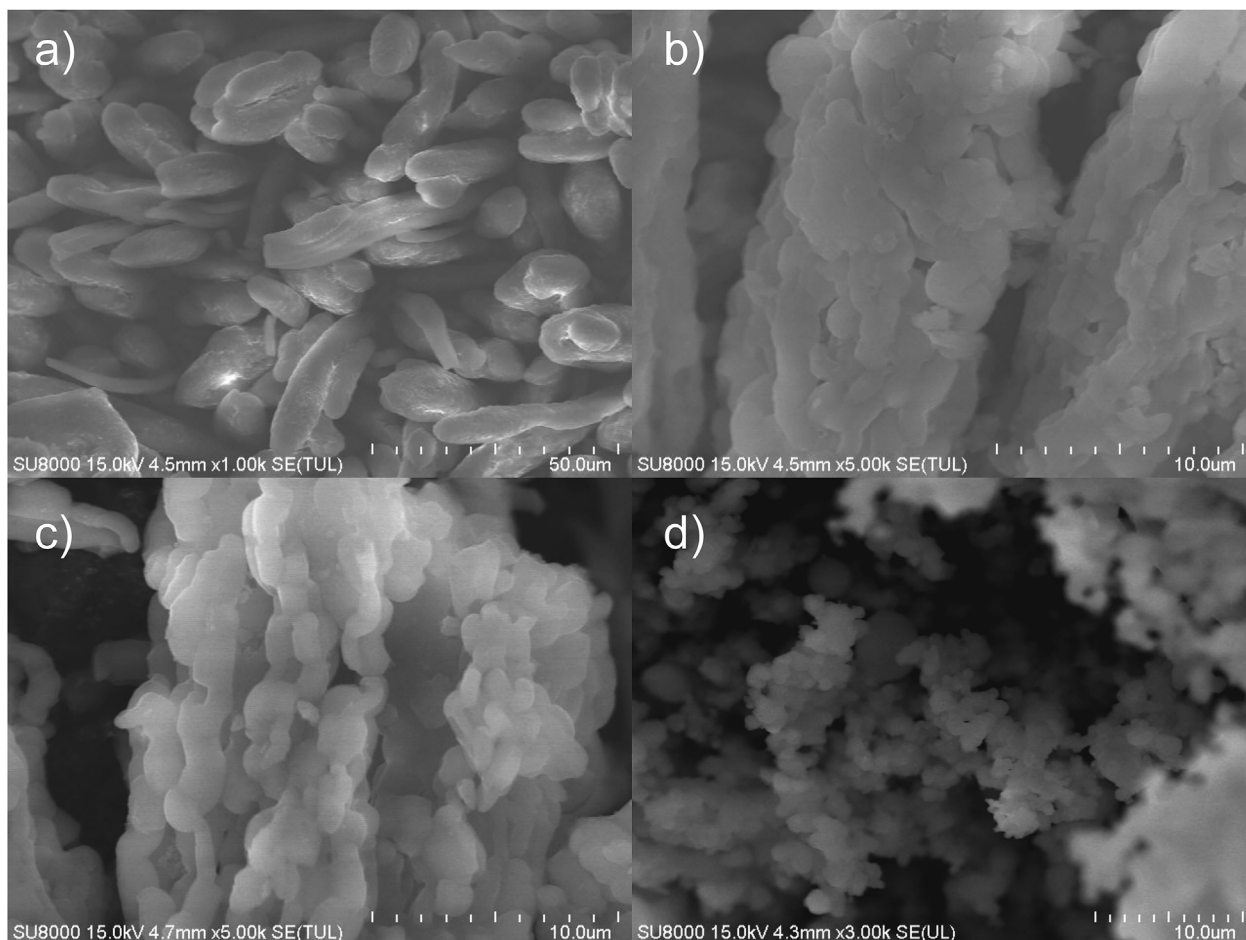


Fig. 9. SEM micrographs of Ti-SBA-15 catalysts with the varying molar ratios of silicon to titanium in the crystallization gel: a) 10:1, b) 20:1, c) 30:1, d) 40:1.

catalysts). It is probable that in the first step of the isomerization process over Ti-SBA-15 catalysts, the light, and preferable, products are formed. Increasing the reaction time causes these products, which are present in the pores, to undergo subsequent reactions (mainly polymerization). Heavy polymeric products undergo transformation to tars and block the pores, which in consequence causes a decrease in the activity of the catalysts. On the other hand, when we take into account the durability of the Ti-SBA-15 catalysts and easiness of their regeneration [44], their utilization in the process of α -pinene isomerization is justified. The phenomenon of blocking of pores by tar products is known in the case of porous catalysts, e.g. zeolites. One of the signs of product polymerisation is the darkening of the reaction mixture (mixtures of light and transparent compounds become brown) and also a significant increase in the density of these mixtures is observed. In the case of our reaction mixtures, both the colour changes in the reaction mixtures and the increased density of these mixtures were observed.

Another advantage connected with the utilization of Ti-SBA-15 catalysts is the shortening of the reaction time by half in comparison with the standard industrial process. Table 3 also shows that the 10:1 M ratio Ti-SBA-15 catalyst, which has anatase in its pores (as noted above), was less active than the Ti-SBA-15 catalyst obtained with the crystallization gel having Si:Ti molar ratio of 20:1, but more active than the first two Ti-SBA-15 catalysts presented in Table 3 (40:1 and 30:1 M ratios). This phenomenon shows that anatase not only blocks pores and causes the reduction in the values of conversion of α -pinene at the same selectivities of appropriate products, but anatase probably also takes part in the isomerization process. Thus, the presence of anatase in pores can be beneficial when we synthesize Ti-SBA-15 catalysts at the molar

ratio of silicon to titanium in the crystallization gel higher than 20:1.

The second stage of the studies focused on the determination of the most favourable conditions for conducting the isomerization reaction over the most active catalyst. Taking into account previous results of the research (Table 3), the Ti-SBA-15 catalyst with the titanium content of 1.10 wt% (equivalent to the molar ratio of silicon to titanium in the crystallization gel of 20:1) was chosen for the next steps in our studies. Towards this end, the following parameters were tested: temperature in the range of 20–200 °C, catalyst content 0.5–20 wt% in relation to α -pinene, and reaction time from 15 min to 24 h. This stage was mainly performed to increase the α -pinene conversion and the selectivities of the desired products (limonene and camphene).

Fig. 13 shows the effect of temperature in the range of 20–200 °C on the isomerization of α -pinene in the presence of the 20:1 Ti-SBA-15 catalyst. The reaction was carried out for 7 h in the presence of 10 wt%. As the temperature increased, the conversion of pinene increased to a maximum (60.03 mol%) at 180 °C and then decreased to 54.61 mol% at 200 °C. This decrease may be caused by the very rapid boiling of the reaction mixture.

The main reaction products were camphene and limonene, which formed with similar selectivities in the whole range of temperatures that were investigated (Fig. 14). At 180 °C, where the highest conversion of α -pinene was achieved, camphene was formed with the selectivity of 30.30 mol%, while limonene was produced at 34.54 mol%. Other products that were formed with much lower selectivity were (in units of mol%): α -terpinene (4.76), γ -terpinene (4.25), terpinolene (7.62), p-cymene (1.97), α -phellandrene (3.56), and campholenic aldehyde (0.23). Furthermore, with a total selectivity of 12.76 mol%, fenchene, tricyclene and

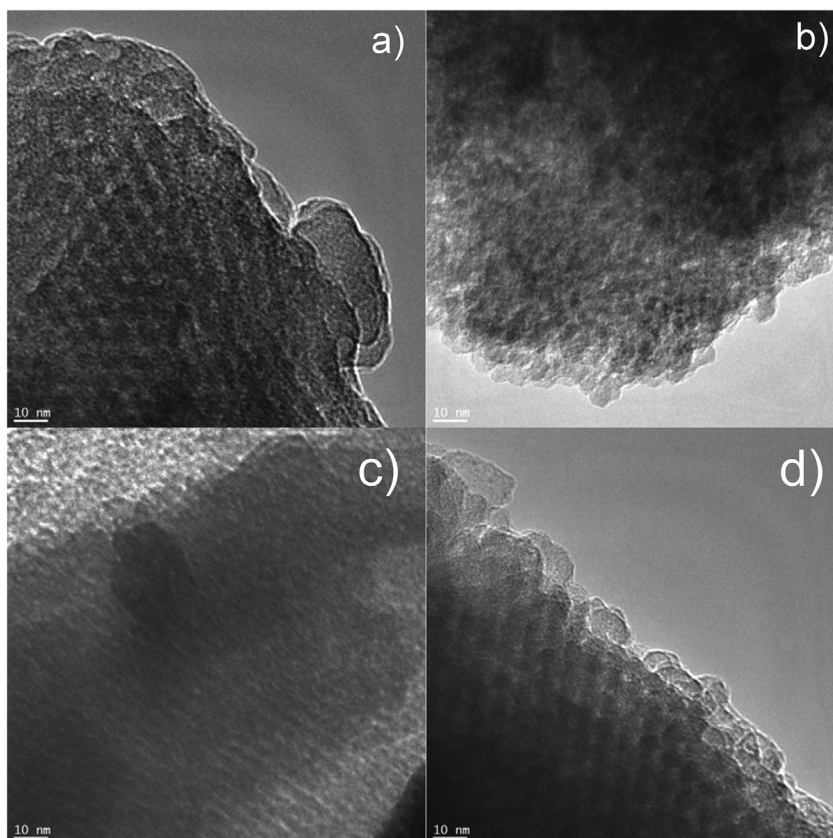


Fig. 10. TEM micrograph of Ti-SBA-15 catalysts with the varying molar ratios of silicon to titanium in the crystallization gel: a) 10:1, b) 20:1, c) 30:1, d) 40:1.

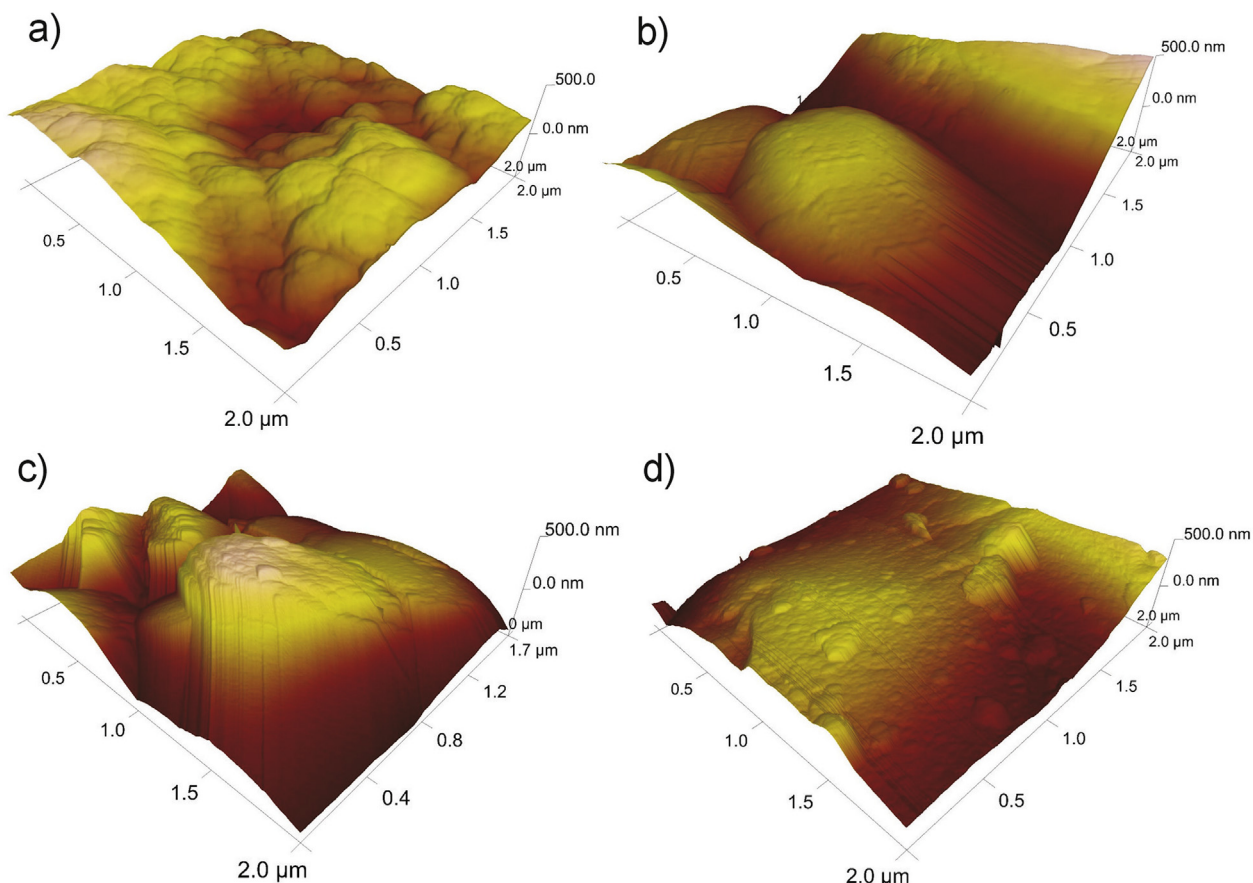


Fig. 11. 3D AFM images of Ti-SBA-15 catalysts with the varying molar ratios of silicon to titanium in the crystallization gel: a) 10:1, b) 20:1, c) 30:1, d) 40:1.

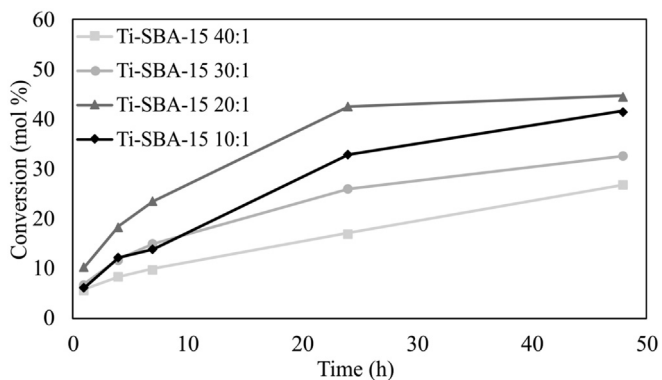


Fig. 12. The influence of titanium content on the α -pinene conversion with the varying molar ratios of silicon to titanium in the crystallization gel.

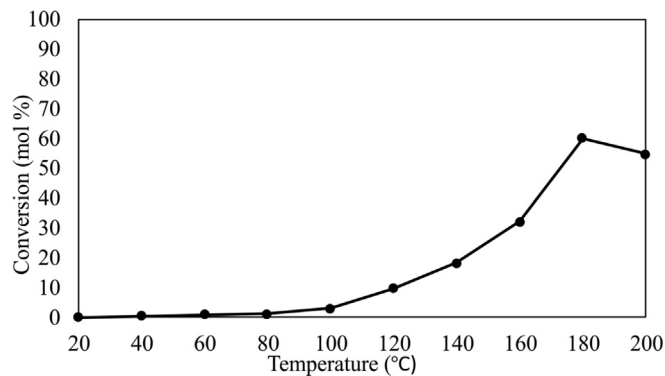


Fig. 13. The influence of temperature on the α -pinene conversion over Ti-SBA-15 (20:1) after 7 h.

Table 3
The influence of titanium content on the α -pinene conversion and selectivity of products after 24 h with the varying molar ratios of silicon to titanium in the crystallization gel.

Samples Ti-SBA-15	Conversion (mol %)	Selectivity (mol%)								
		α -pinene	camphene	limonene	α -terpinene	γ -terpinene	terpinolene	p-cymene	α -phellandrene	campholenic aldehyde
40:1	17.04	22.72	27.24	1.91	2.83	6.64	6.97	2.02	3.65	26.01
30:1	25.99	22.01	32.72	1.39	2.78	5.39	5.26	2.25	2.36	25.84
20:1	42.63	24.40	36.99	1.91	3.21	6.40	4.11	2.34	1.09	19.55
10:1	33.00	24.06	34.99	1.29	2.94	5.74	3.17	2.40	1.50	23.91

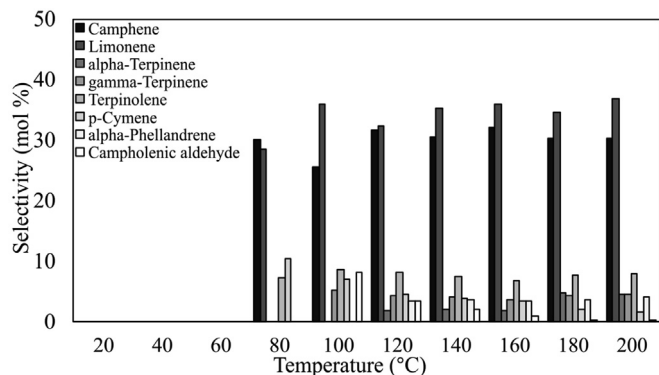


Fig. 14. The influence of temperature on the products selectivity over Ti-SBA-15 catalyst (20:1) after 7 h.

polymeric products are also formed. It can be noted that higher levels of campholenic aldehyde are produced at lower temperatures (100 and 120 °C). This demonstrates a greater contribution from the undesired oxidation reactions of α -pinene with oxygen from the air.

Another studied parameter was the catalyst content in relation to α -pinene. For this purpose, a series of tests was carried out at 180 °C, at which the highest conversion of α -pinene was achieved. The tested range of catalyst content was changed from 0.5 to 20 wt %. As the catalyst content increased, the conversion of α -pinene increased to a maximum of 95.12 mol% for the catalyst content of 15 wt%. The increase in the catalyst content to 20 wt% did not lead to an increase in conversion of α -pinene, but it caused the formation of polymeric products with higher selectivity (Fig. 15).

As the catalyst content increased, the selectivities of α -terpinene, γ -terpinene and terpinolene increased with simultaneous lowering in limonene selectivity (Fig. 16). This is a positive direction of transformations because α -terpinene, γ -terpinene and terpinolene are products with much higher market value. Camphene was formed throughout the whole tested range of catalyst content with the selectivity of about 30 mol%. For the catalyst content of 15 wt%, which proved to be optimal given a high conversion of α -pinene after 7 h (95.12 mol%), the selectivities of the appropriate products were as follows (in units of mol%): camphene (27.38), limonene (26.44), α -terpinene (6.88), γ -terpinene (16.16), terpinolene (8.66), p-cymene (2.82), α -phellandrene (1.92), campholenic aldehyde (0.06), and other products (9.68). The selectivities of the appropriate products in the whole range of studied catalyst contents are presented in Fig. 16.

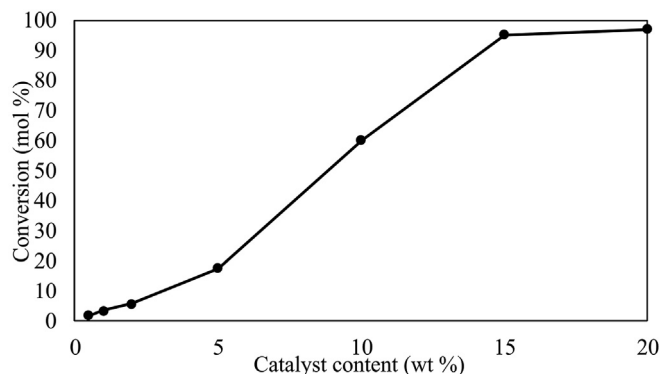


Fig. 15. The influence of catalyst content on the α -pinene conversion over Ti-SBA-15 catalyst (20:1) after 7 h at 180 °C.

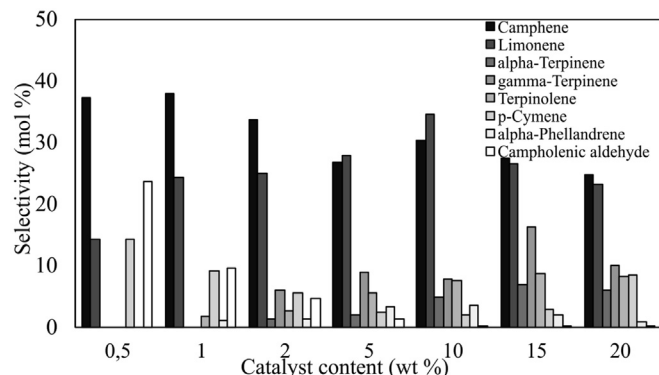


Fig. 16. The influence of catalyst content on the products selectivity over Ti-SBA-15 catalyst (20:1) after 7 h at 180 °C.

The studies on the influence of reaction time were conducted using a larger scale (taking into account the size of the apparatus). In this case, 20 g of α -pinene was mixed with 3 g of Ti-SBA-15 catalyst and samples were analysed in the range of the reaction time from 15 min to 24 h. At the studied conditions α -pinene conversion was almost total after the reaction time amounted to 6 h (97.97 mol%) – Fig. 17. After this time the following selectivities of the appropriate products were observed (in units of mol%): camphene (25.93), limonene (23.51), and γ -terpinene (18.74). Moreover, the formations of α -terpinene (8.04 mol%), terpinolene (12.90), p-cymene (4.66) and α -phellandrene (2.05) were also observed. Lengthening the reaction time (more than 6 h) leads to follow-up reactions in which limonene and other monocyclic terpenes isomerize to p-cymene, as can be seen in Fig. 18. This shows that the Ti-SBA-15 catalyst is also suitable for performing the isomerization of other natural compounds such as limonene.

4. Conclusions

Direct syntheses of titanium-substituted SBA-15 materials (up to molar ratio Si/Ti = 10), were performed without any loss in textural properties. Only XRD measurements showed some insignificant destruction of the ordered structure of the SBA-15 material.

The current studies show that a Ti-SBA-15 catalyst is effective in the α -pinene isomerization process. Its use enables the achievement of almost 100 mol% conversion of α -pinene after the reaction time of 6 h. This is a much shorter reaction time compared to industrial processes in which TiO₂ is used; in the presence of TiO₂ as the catalyst, such a high conversion is obtained after about 48 h

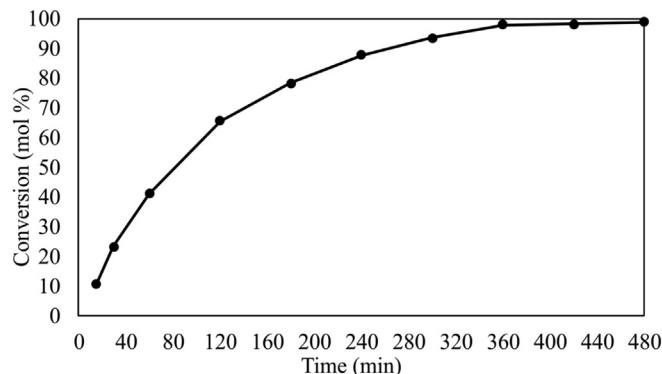


Fig. 17. The influence of time on the α -pinene conversion over Ti-SBA-15 catalyst (20:1) at 180 °C and 15 wt% of catalyst.

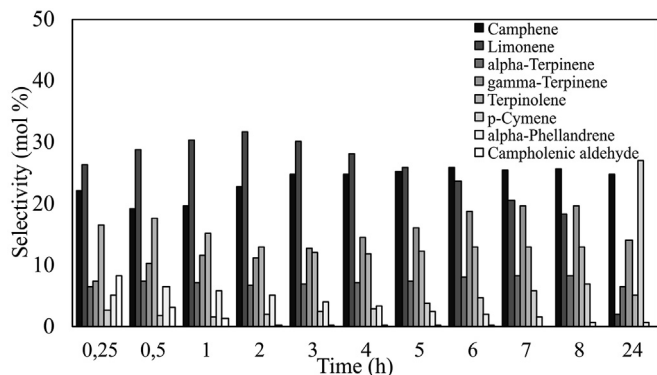


Fig. 18. The influence of time on the products selectivity over Ti-SBA-15 (20:1) at 180 °C and 15 wt% of catalyst.

[14]. The additional advantage associated with the use of a Ti-SBA-15 catalyst is connected with the formation of a number of useful intermediates with considerable selectivities for the perfumery industry. It was shown that titanium incorporated in the silica structure significantly enhances the activity of the Ti-SBA-15 catalyst in the isomerization process, but too much titanium added to the crystallization gel results in the formation of TiO₂, which causes a decrease in the catalytic activity. This may be due to the fact that the precipitated TiO₂ blocks the channels and pores of the catalyst. This study has shown that the best titanium content in the Ti-SBA-15 catalyst is 1.1 wt% (molar ratio of silicon to titanium in the crystallization gel of 20:1). In addition, the second stage of the current research allowed us to choose the most favourable reaction conditions for the α -pinene isomerization process, which was at a temperature of 180 °C, reaction time of 6 h, and catalyst content of 15 wt%. It is interesting and worth pointing out that the considerable elongation of the reaction time results in follow-up reactions in which monocyclic terpenes are isomerized to p-cymene.

The results of the most beneficial conditions of α -pinene isomerization showed that the Ti-SBA-15 catalyst can be used in future industrial processes because it gives better results than the TiO₂ catalyst and at milder conditions.



References

- [1] B. Su, C. Sanchez, X. Yang, in: D. Zhao, Y. Wan, W. Zhou (Eds.), *Hierarchically Structured Porous Materials*, Wiley-VCH, 2012, pp. 58–61.
- [2] F.D. Renzo, F. Fajula, *Stud. Surf. Sci. Catal.* 157 (2005) 1–12.
- [3] O.A. Anunziata, A.R. Beltramone, M.L. Martínez, L.L. Belon, *J. Colloid Interface Sci.* 315/1 (2007) 184–190.
- [4] D. Zhao, Y. Wan, W. Zhou, *Ordered Mesoporous Materials*, Wiley-VCH, 2014, pp. 5–25.
- [5] A. Wróblewska, E. Milchert, *Przem. Chem.* 84 (10) (2005) 723–727.

- [6] L. Marchese, E. Gianotti, V. Dellarocca, T. Maschmeyer, F. Rey, S. Docuccia, J.M. Thomas, *Phys. Chem. Chem. Phys.* 1 (1999) 585–592.
- [7] J.M. Fraile, J.L. Garcia, J.A. Mayoral, E. Vispe, *J. Catal.* 204 (1) (2001) 146–156.
- [8] E. Gianotti, C. Bisio, L. Marchese, M. Guidotti, N. Ravasio, R. Psaro, S. Coluccia, *J. Phys. Chem.C* 111 (3) (2007) 5083–5089.
- [9] H.L. Xie, Y.X. Fan, C.H. Zhou, Z.X. Du, E.Z. Min, Z.H. Ge, X.N. Lia, *Chem. Biochem. Eng. Q.* 22 (1) (2008) 25–39.
- [10] F. Berube, F. Kleitz, S. Kaliaguine, *J. Phys. Chem. C* 112 (37) (2008) 14403–14411.
- [11] M. Walasek, A. Wróblewska, *Pol. J. Chem. Technol.* 18 (4) (2016) 9–14.
- [12] F. Berube, B. Nohair, F. Kleitz, S. Kaliaguine, *Chem. Mater.* 22 (6) (2010) 1988–2000.
- [13] G. Du, S. Lim, M. Pinault, C. Wang, F. Fang, L. Pfeiffer, G.L. Haller, *J. Catal.* 253 (1) (2008) 74–90.
- [14] E. Gastao, Du Pont, US 2551795 A, 8 May 1951, 1951.
- [15] F. Launay, B. Jarry, J.L. Bonardet, *Appl. Catal. A* 10 (4) (2009) 1208–1217.
- [16] C. Wu, H. Liu, C. Zhuang, G. Du, *App. Mech. Matter* 483 (2014) 134–137.
- [17] R. Luque, J.M. Campelo, T.D. Conesa, D. Luna, J.M. Marinad, A.A. Romero, *Microporous Mesoporous Mater.* 103 (1) (2007) 333–340.
- [18] M.A. Ecomier, A.F. Lee, K. Wilson, *Microporous Mesoporous Mater.* 80 (1–3) (2005) 305–310.
- [19] R. Rachwalik, Z. Olejniczak, J. Jiao, J. Huang, M. Hunger, B. Sulikowski, *J. Catal.* 252 (2) (2007) 161–170.
- [20] E. Unveren, G. Gunduz, F. Cakicioglu-ozkan, *Chem. Eng. Comm.* 192 (3) (2005) 386–404.
- [21] N. Wijayati, H.D. Pranowo, Jumina, Triyono, *Indo. J. Chem.* 11 (3) (2001) 234–237.
- [22] O. Akpolat, G. Gunduz, F. Ozkan, N. Besug, *Appl. Catal. A* 265 (1) (2005) 11–22.
- [23] G. Gynduz, D.Y. Murzin, *React. Kinet. Catal. Lett.* 75 (2) (2002) 231–237.
- [24] B. Atalay, G. Gunduz, *Chem. Eng. J.* 168 (3) (2011) 1311–1318.
- [25] L. Jianfeng, Z. Jie, M. Changxi, Y. Yinghong, H. Weiming, G. Zi, *Chin. J. Chem.* 29 (2011) 1095–1100.
- [26] A. Wróblewska, P. Miądlicki, E. Makuch, *Reac. Kinet. Mech. Cat.* 119 (2) (2016) 641–654.
- [27] M. Coelhan, M. Maurer, *J. Agric. Food Chem.* 53 (26) (2005) 10105–10112.
- [28] C. Glaser (1907) Maryland. US875062 A, 31 Dec 1907.
- [29] L.I.U. Bin-Tang, Y.U. Jin-Quan, F.E.N.G. Ai-Qun, Z.H.O.U. Ping, X.I.A.O. Shu-De, *Chin. J. Org. Chem.* 15 (3) (1995) 318–322.
- [30] N. Girola, C.R. Figueiredo, C.F. Farias, R.A. Azevedo, A.K. Ferreira, S.F. Teixeira, T.M. Capello, E.G.A. Martins, A.L. Matsuo, L.R.J.H.G. Lago, *Biochem. Biophys. Res. Commun.* 467 (4) (2015) 928–934.
- [31] S.K. Król, K. Skalicka-Woźniak, M. Kandefer-Szerszeń, A. Stepulak, *Postepy Hig. Med. Dośw.* 67 (2013) 1000–1007.
- [32] M.A. Martin-Luengoa, M. Yatesb, M.J. Martinez Domingo, B. Casala, M. Iglesiasa, M. Estebana, E. Ruiz-Hitzky, *Appl. Catal. B* 81 (3–4) (2008) 218–224.
- [33] E.E. Royals, S.E. Horne Jr., *J. Am. Chem. Soc.* 73 (1951) 5856–5857.
- [34] M.P. Arrieta, J. López, S. Ferrándiz, M.A. Peltzer, *Pol. Test.* 32 (4) (2013) 760–768.
- [35] D. Pybus, C. Sell, *The Chemistry of Fragrances*, The Royal Society of Chemistry, 1999, pp. 24–51.
- [36] J. Sreńscek-Nazzal, W. Kamińska, B. Michalkiewicz, Z.C. Koren, *Ind. Crop. Prod.* 47 (2013) 153–159.
- [37] C.F. Geobaldo, S. Bordiga, A. Zecchina, E. Giamello, *Catal. Lett.* 16 (1–2) (1992) 109–115.
- [38] F. Chiker, J.P. Nogier, F. Launay, J.L. Bonardet, *Appl. Catal. A Gen.* 243 (2) (2003) 309–321.
- [39] K.S.W. Sing, D.H. Everett, R.A.W. Haul, L. Moscou, R.A. Pierotti, J. Rouquerol, T. Siemienińska, *Pure. Appl. Chem.* 57 (1985) 603–619.
- [40] R.D. Shannon, *Acta. Cryst.* 32 (1976) 751–767.
- [41] M. Besançon, L. Michelin, L.J.L. Vidal, K. Assaker, M. Bonne, B. Lebeau, J.-L. Blin, *New J. Chem.* 40 (2016) 4386.
- [42] H. Zhang, C. Tang, Y. Lv, F. Gao, L. Dong, *J. Porous. Mater.* 21 (2014) 63–70.
- [43] S. Rasalingam, R. Peng, R.T. Koodali, *J. Nanomater* 2014 (2014) 1–42.
- [44] A. Wróblewska, E. Makuch, *J. Adv. Oxid. Technol.* 17 (1) (2014) 44–52.

Article

Influence of the Titanium Content in the Ti-MCM-41 Catalyst on the Course of the α -Pinene Isomerization Process

Agnieszka Wróblewska ^{1,*}, Piotr Miądlicki ^{1,*}, Jadwiga Tołpa ¹, Joanna Sreńscek-Nazzal ¹, Zvi C. Koren ² and Beata Michalkiewicz ¹

¹ Institute of Organic Chemical Technology, Faculty of Chemical Technology and Engineering, West Pomeranian University of Technology Szczecin, Pulaskiego 10, 70-322 Szczecin, Poland; jadwigatolpaa@gmail.com (J.T.); Joanna.Sreńscek@zut.edu.pl (J.S.-N.); Beata.Michalkiewicz@zut.edu.pl (B.M.)

² Department of Chemical Engineering, Shenkar College of Engineering, Design and Art, 12 Anna Frank St., Ramat Gan 52526, Israel; zvi@shenkar.ac.il

* Correspondence: agnieszka.wroblewska@zut.edu.pl (A.W.); piotr.miadlicki@zut.edu.pl (P.M.)

Received: 5 April 2019; Accepted: 22 April 2019; Published: 27 April 2019



Abstract: Titanium-containing mesoporous silica catalysts with different Ti contents were prepared by the sol–gel method, whereby the molar ratios of silicon to titanium in the crystallization gel amounted to, respectively, 40:1, 30:1, 20:1 and 10:1. The produced Ti-MCM-41 materials were characterized by the following instrumental methods: XRD, UV-Vis, FT-IR, SEM, and XRF. Textural parameters were also determined for these materials by means of the N₂ adsorption/desorption method. The activities of these catalysts were investigated in the α -pinene isomerization process. The most active catalyst was found to be the material with the molar ratio of Si:Ti equal to 10:1, which contained 12.09 wt% Ti. This catalyst was used in the extended studies on the α -pinene isomerization process, and the most favorable conditions for this reaction were found to be temperature of 160 °C, reaction time of 7 h, with the catalyst composition of 7.5 wt% relative to α -pinene. These studies showed that the most active catalyst, at the best reaction conditions, allowed for the attainment of 100% conversion of α -pinene over a period of 7 h. After this time the selectivities (in mol%) of the main products were as follows: camphene (35.45) and limonene (21.32). Moreover, other products with lower selectivities were formed: γ -terpinene (4.38), α -terpinene (8.12), terpinolene (11.16), p-cymene (6.61), and α -phellandrene (1.58).

Keywords: Ti-MCM-41; isomerization; α -pinene; camphene; limonene; natural compounds; green chemistry

1. Introduction

Porous materials [1] have found applications in many fields, e.g., in catalysis [2], nanotechnology [3], medicine [4], in processes of liquid and gaseous sewage treatment [5], and in separation of mixture components [6]. Until the 1990s, the most commonly used materials in these fields were molecular sieves, especially zeolites. However, one of the few disadvantages of zeolites is their small pore diameter. The need to solve this problem prompted researchers to look for materials with a regular structure, such as zeolites, but with a larger pore diameter [7].

A breakthrough in this field occurred in 1990, when two independent research teams produced mesoporous silica with a strictly defined internal structure. Yanagisawa et al., using layered kanemite and surfactants, obtained mesoporous silica FSM-16 (folding sheet materials using C16 surfactant), which had excellent structural features [8].

The second method of producing mesoporous silica, known as MCM-41 (Mobil Composition of Matter No. 41), was presented by scientists from Mobil Oil [9]. The MCM-41 belongs to the M41S family and is one of the most-researched mesoporous materials. It is characterized by a hexagonal arrangement of cylindrical pores with a narrow diameter distribution and a large inner surface [10]. Despite the fact that the structure of the walls of the MCM-41 material is amorphous, it has a crystalline arrangement, which results from its ordered and periodically repeated structure [11]. This material is obtained by combining the sol-gel method with the method of templating, which allows for the production of materials with ordered, uniform pores. This process involves the use of surfactants or block polymers, which under appropriate conditions, form micelles on which polycondensation of silica monomers occurs. After completing the sol-gel process, the matrix is removed in the extraction or calcination process and a material with regular pores is obtained, the size of which corresponds to the size of the removed template [12]. The great advantage of the MCM-41 material is the easiness of its modification. One of these methods is based on the incorporation of titanium atoms into the silica structure, already at the stage of gel synthesis. For this purpose, a sufficient amount of the Ti-containing compound is added to the crystallization gel [13]. The Ti-MCM-41 materials produced in this way have found many applications as catalysts for reactions involving various organic compounds [14–16]. Mesoporous silica materials can also be modified by the grafting method. In this method, metal atoms are placed on the surface of the mesoporous material. Using both direct and grafting methods, MCM-41 materials containing the following metals were successfully synthesized: Mo [17], Ni [18], Co [19], Ga [20], Zr [21], Cu [22], Pd [23] or Fe [24]. In addition, studies were conducted on the conditions for obtaining the siliceous structure of MCM-41 (including Ti-MCM-41), so that the obtained material was characterized by greater stability in water at elevated temperatures and an ability to inhibit the phenomenon of metal leaching (Ti leaching in the case of Ti-MCM-41 catalysts) [25,26].

Alpha-pinene is a natural terpene found in the oils of coniferous trees, especially the pine, from which the compound's name is derived. Currently, the isomerization of α -pinene on an industrial scale is performed on TiO_2 modified with sulfuric acid at 140 °C. The main products of this reaction are bicyclic products, including camphene, bornylene, tricyclene, α -fenchene (formed with a total selectivity of 70 mol%), and monocyclic products, including limonene, α - and γ -terpinene, terpinolene, cymene and α -phellandrene [27]. These products are shown in Figure 1.

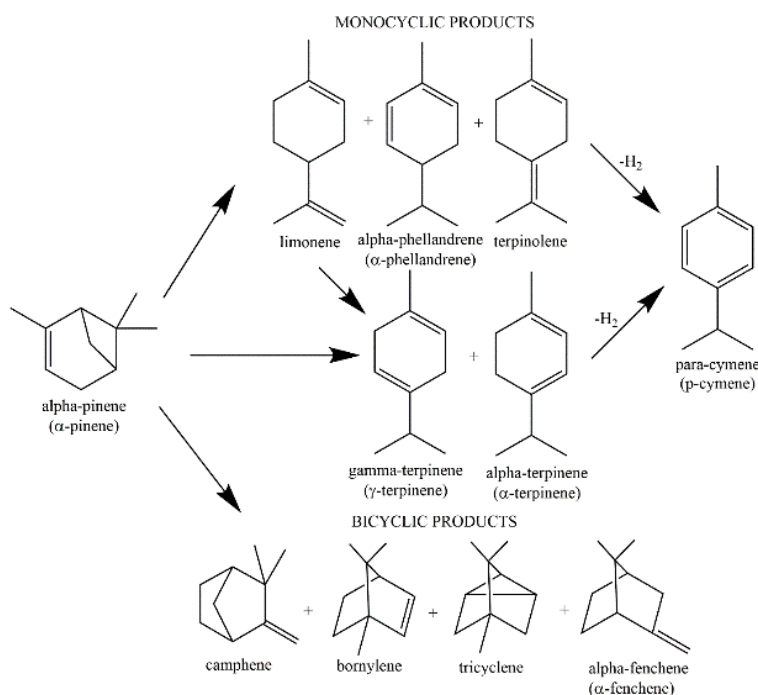


Figure 1. Main products of α -pinene isomerization process and paths of their formation.

The goal of the α -pinene isomerization process is to produce camphene with the highest selectivity. Camphene is an added value product due to its wide use and price. An interesting historical aspect is that in the middle of the 19th century, a related product—camphine (a mixture of turpentine dissolved in oil with some camphor)—was used as fuel for lamps [28], but due to its explosiveness and quick burning, its use was abandoned. Currently, camphene is mainly used as an intermediate in light organic synthesis, *inter alia*, in the production of toxaphene (an insecticide) [29]. In addition, in the reaction of camphene with acetic acid, isobornyl acetate is formed, which is an intermediate in the production of synthetic camphor [30]. Camphene is also used in the production of terpenecyclohexanols, which are an alternative to sandal oil and are widely used in the perfumery industry [31]. Camphene is also used as a fragrant and flavor substance. The mixture of camphene with pinene and cineole has medicinal properties and is used for kidney and hepatobiliary disorders [32]. Moreover, N. Girola et al. confirmed the anticancer properties of camphene [33].

In order to lower the temperature of α -pinene isomerization and to achieve the highest selectivity of transformation to the desired product, camphene, new catalysts for carrying out the α -pinene isomerization are sought. Chunhua Wu et al. applied the SBA-15 catalyst modified with phosphotungstic acid for the isomerization of α -pinene [34]. The reaction was performed at 130 °C for 2 h, after which the conversion of α -pinene was about 95%, while the camphene selectivity was about 48.5 mol%. J. Wu et al. examined Al-MCM-41 catalysts with different SiO₂ to Al₂O₃ ratios in the α -pinene isomerization process. The most active catalyst among the tested materials was the one with a molar ratio of 20:1 [35]. The reaction was accomplished at 160 °C, and the main products were camphene and limonene. Another team researching the isomerization of α -pinene using mesoporous catalysts is F. Launay et al. [36]. They applied the Ga/SBA-15 catalyst obtained by various methods (direct method and post-synthesis grafting method). At 80 °C, after 1 h, using the catalyst obtained by the direct method, they received camphene with a yield of 28%. G. Nie et al. used the MCM-41 catalyst modified by the wet impregnation method with tungstophosphoric acid [37]. They achieved the highest selectivity of transformation to camphene (40.6 mol%) and limonene (11.2 mol%), with 100% conversion of α -pinene, at 160 °C after 3 h.

In our previous work [38,39], we presented the isomerization of α -pinene over Ti-SBA-15 catalysts with different titanium contents. On the basis of the conducted tests, it was shown that the optimal titanium content in the Ti-SBA-15 catalyst is 1.1 wt% with the molar ratio of silicon to titanium in the crystallization gel of 20:1. In addition, the second stage of the research allowed for the selection of the most favorable conditions for the α -pinene isomerization process: temperature = 180 °C, catalyst content = 15 wt%, and reaction time = 6 h. The selectivities (in mol%) of the products were as follows: camphene 25.93, limonene 23.51, and γ -terpinene 18.74. Moreover, the formations (and selectivities) of the following products were also determined: α -terpinene (8.04), terpinolene (12.90), p-cymene (4.66), and α -phellandrene (2.05). During the research, it was noticed that a significant extension of the reaction time lead to subsequent reactions in which monocyclic terpenes are dehydrogenated to p-cymene [38,39].

Other micro- and mesoporous materials used as catalysts in the α -pinene isomerization process are: TCA/Y zeolite [40], desilicated ZSM-5, ZSM-12, MCM-22, and ZSM-12/MCM-41 [41], zeolite BETA [42], and SO₄/ZrO₂/HMS [43]. In addition, research was conducted on the use of natural materials (clinoptilolite, sepiolite, and montmorillonite) in the α -pinene isomerization process [44–48].

As shown above, mesoporous silicate catalysts, particularly those containing titanium, may be active catalysts in the α -pinene isomerization process, e.g., the Ti-SBA-15 catalyst. The Ti-MCM-41 catalyst, as compared with the Ti-SBA-15 material, is obtained in a simpler way (without the autoclaving step) and from cheaper raw materials, hence its synthesis is associated with the consumption of less energy and at the same time is more economical. Therefore, it was decided to determine whether the Ti-MCM-41 catalyst could also be used in the isomerization process of α -pinene. The purpose of this work was to investigate the effect of titanium content in the Ti-MCM-41 catalysts on the course of the α -pinene isomerization process. A series of studies on the α -pinene isomerization process

was conducted to select the most active catalyst. Subsequently, the influence of temperature, catalyst content, and reaction time were studied over the selected, best, catalyst. Our aim at this stage of tests was to determine the most favorable conditions for α -pinene isomerization over the Ti-MCM-41 catalyst. This was accomplished by quantitatively characterizing the main functions describing this process: selectivities of the appropriate products (mainly camphene) and the conversion of α -pinene. The Ti-MCM-41 materials were first characterized using the following instrumental methods: XRD, UV-Vis, FT-IR, SEM, and XRF. Also textural parameters were determined for these materials with the help of the N_2 adsorption/desorption method.

2. Results and Discussion

2.1. Characteristics of Catalysts

The relative titanium content in the Ti-MCM-41 catalysts was determined using the XRF method. The amount of Ti depends on the molar ratio of silicon to titanium in the crystallization gel. Thus the following compositions of Ti (in units of wt%) for the respective Si:Ti ratios were obtained: 3.12 for the 40:1 ratio; 4.51 for 30:1, 5.58 for 20:1, and 12.09 for 10:1.

Low-angle X-ray diffraction studies allowed for the confirmation that the MCM-41 structure for all tested materials was indeed obtained. Diffraction patterns presented in Figure 2 show one very intense peak corresponding to reflex (100), and in the case of the catalyst with the 40:1 Si:Ti molar ratio in the crystallization gel, two small peaks corresponding to reflexes (110) and (200). These data are consistent with the literature and confirm the hexagonal nature of the mesoporous silica with the MCM-41 structure. The maximum of the reflex (100) shifted to the higher 2θ as the Ti content increased. This indicates that interplanar d_{100} spacing decreased because of the incorporation of Ti atoms, instead of Si atoms, into the MCM-structure. Because of the difference between the ionic radii of Ti^{4+} (0.068 nm) and Si^{4+} (0.041 nm), the substitution of Ti cations for Si ones distorts the tetrahedral coordination geometry around the Ti. The incorporation of Ti into the structure disordered the hexagonal arrangement in the Ti-MCM-41 materials, which increases with the amount of Ti. Moreover the intensity of the reflex (100) decreased with Ti content. This phenomenon has been previously reported [49]. These authors postulated that a lamellar phase is formed, which would cross-link and subsequently form the hexagonal phase.

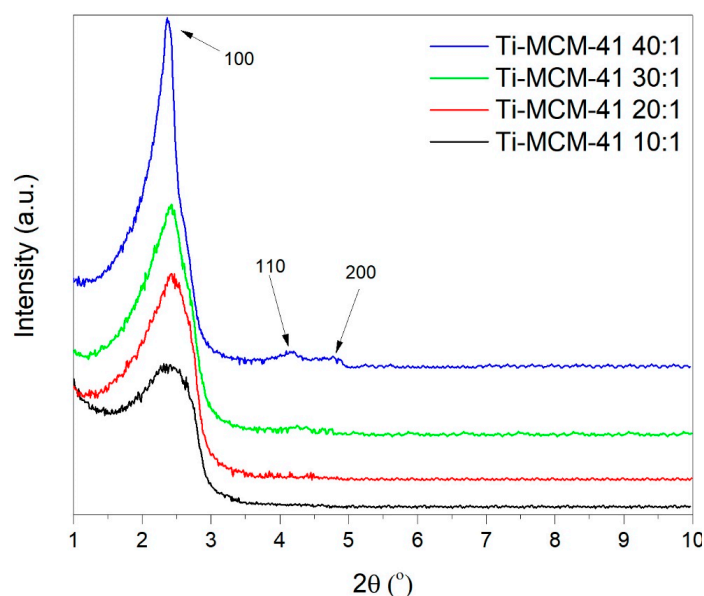


Figure 2. Low-angle X-ray diffraction patterns for Ti-MCM-41 samples with different molar ratios of Si:Ti in the crystallization gel (respectively, 40:1, 30:1, 20:1, and 10:1).

Figure 3 shows the high-angle XRD patterns of the Ti-MCM-41 materials. Each pattern exhibits a broad peak at 2θ from 15 to 30° , which is typical for amorphous silica [50]. The peak corresponding to the anatase form of TiO_2 at $2\theta \approx 25^\circ$ was absent for all studied Ti-MCM-41 materials. This is in line with the results obtained by the UV-VIS method, which did not confirm the presence of anatase in the Ti-MCM-41 materials, as mentioned below.

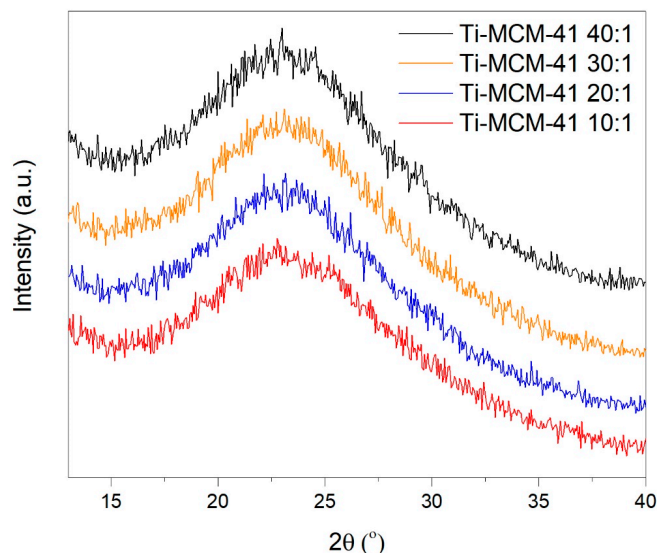


Figure 3. High-angle X-ray diffraction data for Ti-MCM-41 samples with different molar ratios of Si:Ti in the crystallization gel (respectively, 40:1, 30:1, 20:1, and 10:1).

In the UV-Vis spectrum of Ti-MCM-41 materials (Figure 4), a characteristic absorption band centered at the 215 nm wavelength is present, which confirms the coordinative inclusion of titanium (in the form of Ti^{+4}) in the silica structure. The band in the range of 225–260 nm is responsible for the occurrence of titanium in the form of dimers (Ti-O-Ti) on the surface of the catalyst [51]. In addition, in these spectra there is an absorption band at a wavelength of about 295 nm, which is derived from titanium having the coordination number of 5 or 6. The change in the coordination number of titanium can result from the coordination of water molecules by titanium included in the silica structure, which mainly occurs on the surface of the catalyst. The lack of a peak at 330–350 nm indicates the absence of TiO_2 in the form of anatase in the studied Ti-MCM-41 materials [52].

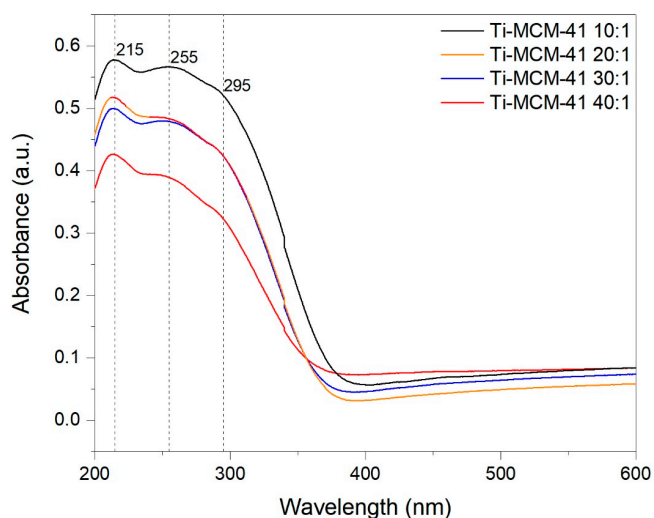


Figure 4. UV/Vis spectra of the Ti-MCM-41 catalysts with different molar ratios of Si:Ti in the crystallization gel (respectively, 40:1, 30:1, 20:1, and 10:1).

In the IR spectrum of Ti-MCM-41 materials (Figure 5), the following main absorption bands can be observed: 440, 800, 960, 1000–1300, 1625–1650, 2350, and 3500 cm^{-1} . The band in the range of 1625–1650 cm^{-1} is attributed to the bending vibrations of the –OH groups, coming from the water molecules adsorbed on the surface of the material. The bands at the 440 and 800 cm^{-1} wavenumbers are attributed to the bending deformation vibrations of the Si–O–Si groups, which cause a change in the angle between the bonds, and symmetrical valence vibrations, which cause changes in the lengths of the bonds. The band in the range of 1000–1300 cm^{-1} is attributed to the presence of Si–O–Si bonds, which exist in the siliceous structure and are characteristic for it. The 960 cm^{-1} band present in the materials is associated with the isomorphous substitution of Si by Ti ions and it is attributed to the stresses of the Si–O–Ti polar bonds or the presence of the titanyl group, $>\text{Ti}=\text{O}$. This band confirms the inclusion of titanium in the structure of silica [53]. It can be seen that as the titanium content increases, the intensity of this band increases. In addition, the 960 cm^{-1} band is attributed to the stretching vibrations of the Si–OH groups that are on the surface of the material [54]. The 3500 cm^{-1} band is associated with the presence of hydroxyl groups on the surface of the catalysts, while the band at 2350 cm^{-1} indicates the presence of carbon dioxide in the materials. The obtained spectra are in accordance with literature data [55].

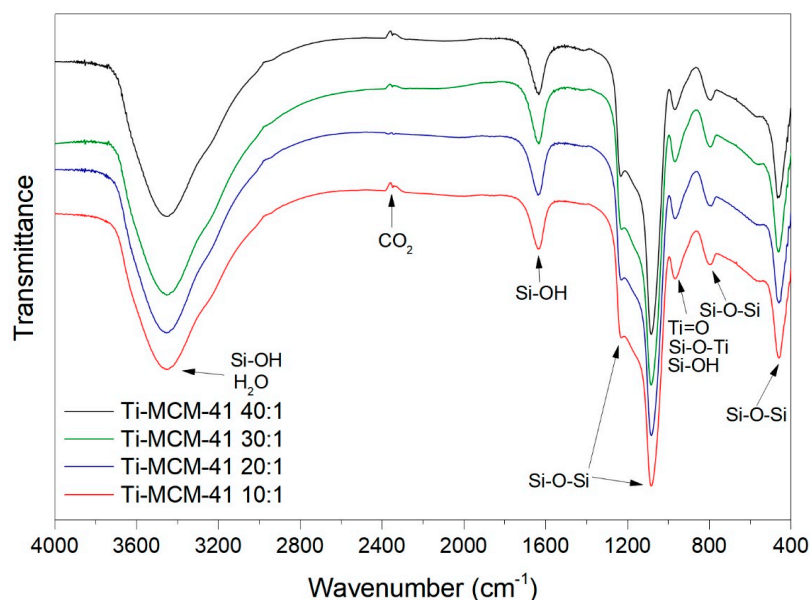


Figure 5. FT-IR spectra of Ti-MCM-41 catalysts with different molar ratios of Si:Ti in the crystallization gel (respectively, 40:1, 30:1, 20:1, and 10:1).

In the SEM photographs of the Ti-MCM-41 materials (Figure 6), well-formed spherical particles, with sizes in the range of 0.2–1 μm , can be observed. These can combine into larger structures, which is typical for this type of material.

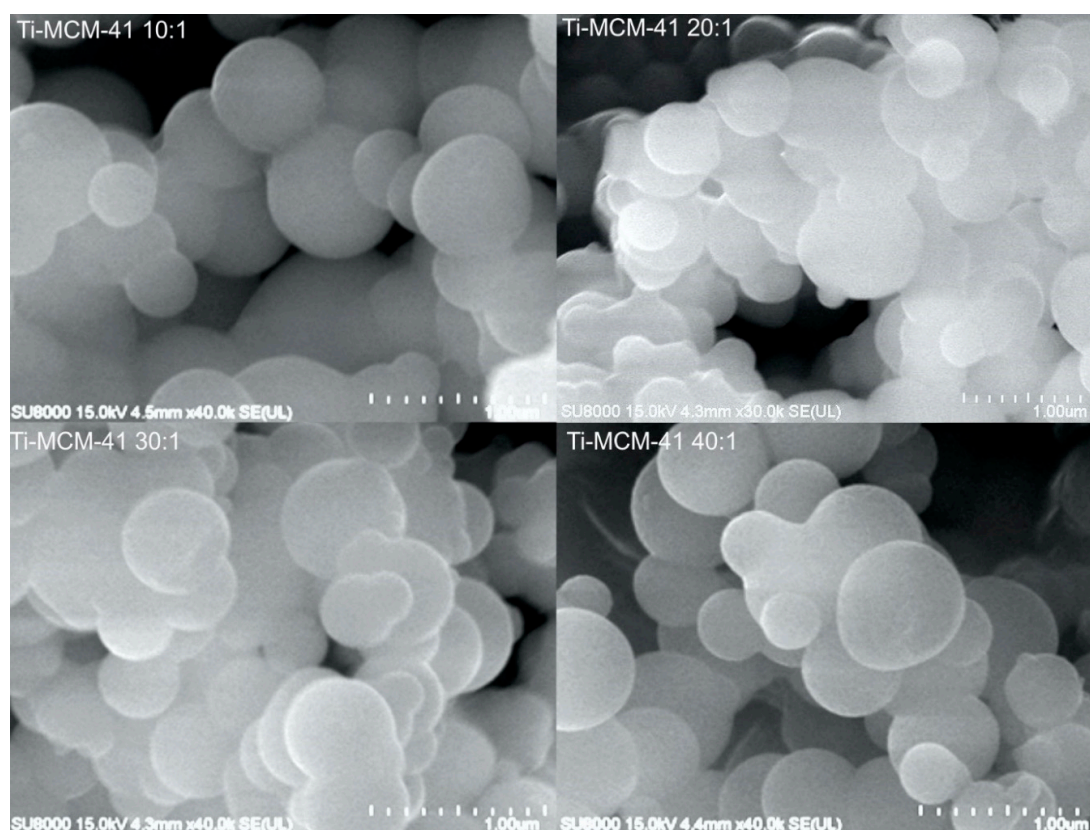


Figure 6. SEM pictures of Ti-MCM-41 catalysts with different molar ratios of Si:Ti in the crystallization gel (respectively, 40:1, 30:1, 20:1, and 10:1).

Table 1 shows the specific surface area, S_{BET} , and the pore volume V_p of the catalysts. A slight decrease in the specific surface area of the materials along with the increase in the titanium content indicates small changes in the structure of the catalysts. In addition, similar V_p values suggest that pores are similar in size and are not blocked by TiO_2 molecules.

Table 1. Textural parameters for the Ti-MCM-41 catalysts with different molar ratios of Si:Ti in the crystallization gel (respectively, 40:1, 30:1, 20:1, and 10:1).

Material	S_{BET} (m^2/g)	V_p (cm^3/g)
Ti-MCM-41 10:1	902	0.839
Ti-MCM-41 20:1	1014	0.839
Ti-MCM-41 30:1	1071	0.826
Ti-MCM-41 40:1	1063	0.840

All synthesized Ti-MCM-41 materials exhibit a type IV isotherm with H1 hysteresis loops at intermediate relative pressures (Figure 7). This indicates well-shaped pores with a hexagonal shape. Similarly shaped isotherms also indicate similar pore sizes [56]. Thus, the similar position of the adsorption branch inflection of every isotherm suggests that all Ti-MCM-41 materials have similar pore sizes. The specific surface area for high Si content (Si:Ti 40:1 and 30:1) are nearly the same. However, further decreasing the Si content (Si:Ti 20:1 and 10:1) decreased the value of the specific surface area. The analysis of the pore size distribution curves obtained by means of the DFT method (Figure 8) showed that the pores of all the samples exhibited similar pore diameters (3–4.2 nm). The average pore diameter calculated by DFT was equal to 3.53 nm for all Ti-MCM-41 catalysts. Only the pore volume decreased with increasing Ti content. As was mentioned above, Ti was incorporated into the MCM-41 structure, and this inclusion invariably distorts the geometry around Ti from an ideal

tetrahedral coordination. The XRD patterns give evidence that the destruction was dramatic especially for materials with the higher Ti content. On the basis of the investigations performed by all the methods, one can conclude that the pores were not partially blocked but some of them were closed. The contribution of closed pores strongly depended on the Ti content in the structure.

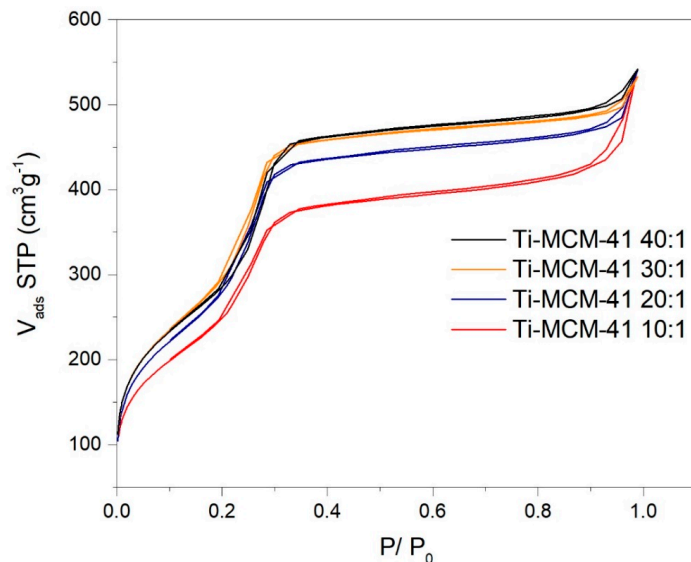


Figure 7. N₂ adsorption–desorption isotherms of Ti-MCM-41 catalysts with different molar ratios of Si:Ti in the crystallization gel (respectively, 40:1, 30:1, 20:1, and 10:1).

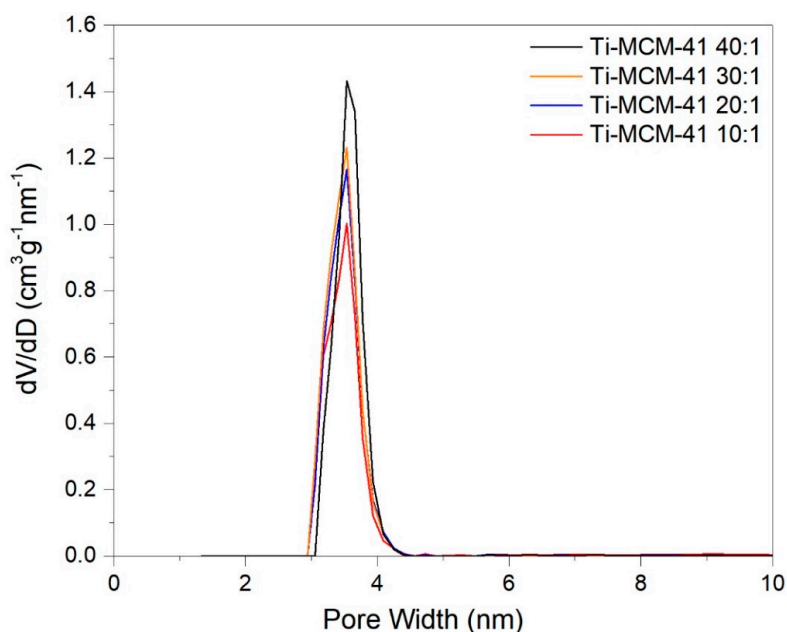


Figure 8. Pore-size distribution for Ti-MCM-41 catalysts with different molar ratios of Si:Ti in the crystallization gel.

2.2. Studies on the Catalytic Activity of Ti-MCM-41 Materials

In the first stage of the research, the effect of the molar ratio of silicon to titanium in the crystallization gel (and of the resulting Ti composition) on the activity of the corresponding Ti-MCM-41 material was examined. The parameters of the α -pinene isomerization process were as follows: temperature 160 °C, catalyst content 7.5 wt% in relation to α -pinene, and reaction time 6 h. These parameters have been selected based on the results of our previous studies using Ti-SBA-15 catalysts [39].

The most active Ti-MCM-41 catalyst was used for further research to determine the most favorable conditions for the isomerization of α -pinene (the second stage of our research).

Figure 9 relates to the first stage of testing and shows that the highest conversion of α -pinene (97.08 mol%) was achieved after 6 h for the catalyst designated “Ti-MCM-41 10:1”. The remaining catalysts showed significantly lower activity, which shows that increasing the amount of titanium introduced in the structure of silica significantly increases the catalytic activity of the materials. The shape of the curve representing the function of conversion of α -pinene can be approximated by a volcano-dependence presented by Frattini et al. [57]. In this work, similar volcano-dependency between W loading and catalyst activity was presented. For the highest Ti content, the highest conversion of α -pinene is achieved, 97.08 mol%. For three other Si/Ti molar ratios, this conversion function is considerably lower, and amounted to 49.48 mol% (Si/Ti = 20:1), 45.29 mol% (Si/Ti = 30:1) and 39.19 mol% (Si/Ti = 40:1). Higher levels of titanium in the crystallization gel (molar ratio Si:Ti < 10) could no longer be beneficial due to the possibility of anatase formation which would decrease the catalyst activity by blocking the pores. In addition, the number of closed pores could be increased, which would reduce the specific surface area of the catalyst; this tendency is noticeable in Table 1.

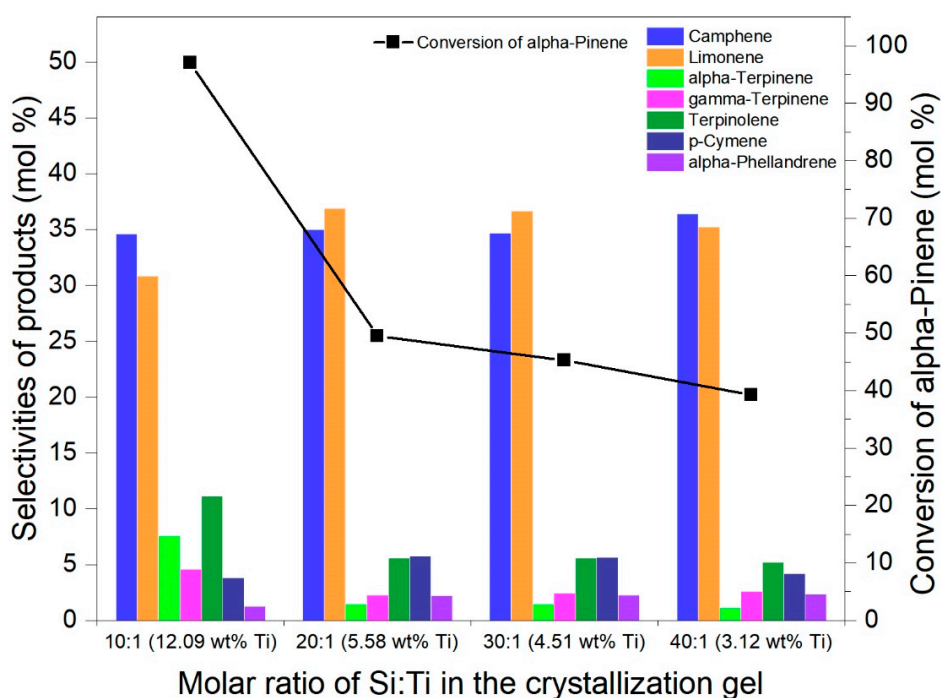


Figure 9. The influence of the molar ratio of Si:Ti in the crystallization gel on the conversion of α -pinene and on the selectivities of the appropriate products (temperature 160 °C, catalyst content 7.5 wt%, and reaction time 6 h).

The selectivities of the products were similar for the four tested Ti-MCM-41 catalysts. Among the products, the highest selectivities were achieved for camphene (35 mol%) and limonene (37 mol%). In the case of the Ti-MCM-41 10:1 catalyst, the lower selectivity of limonene results from the subsequent reaction— isomerization of the resulting limonene to terpinenes, terpinolene, and p-cymene.

The second stage of the studies consisted in determining the most favorable conditions for the isomerization of α -pinene over the most active Ti-MCM-41 catalyst. Taking into consideration the results from the first phase of the tests, the Ti-MCM-41 10:1 catalyst containing 12.09 wt% Ti was chosen for the second stage of tests. The influence of the following parameters was investigated: temperature 80–180 °C, catalyst content 2.5–15 wt% in relation to α -pinene, and reaction time from 15 min to 24 h.

Figure 10 shows the effect of temperature in the range of 80–180 °C on the isomerization of α -pinene in the presence of the Ti-MCM-41 10:1 catalyst. The reaction was carried out for 7 h in

the presence of 7.5 wt% of the catalyst. With increasing temperature, the conversion of α -pinene increased to a maximum (100 mol%) for a temperature of 160 °C—below this temperature this function of the isomerization process showed considerably lower values (80 °C–0.10 mol%, 100 °C–6.80 mol%, 120 °C–20.50 mol%, and 140 °C–63.90 mol%). Low values of α -pinene conversion at lower temperatures are most likely associated with limitations in diffusion to the pores of the catalyst. In addition, some pores are unavailable due to the fact that they have been closed. The isomerization reaction probably occurs only in the active titanium centers found on the surface of the catalyst. The increase in temperature causes the molecules of the organic compound to penetrate into the pores more easily and the isomerization reaction can also occur in the active titanium centers present in the catalyst pores. The main reaction products were camphene and limonene, which were formed with similar selectivities throughout the range of temperatures tested (80–160 °C). At 180 °C, the low selectivity of limonene indicates that it has been isomerized to terpinolene, terpinenes, and p-cymene.

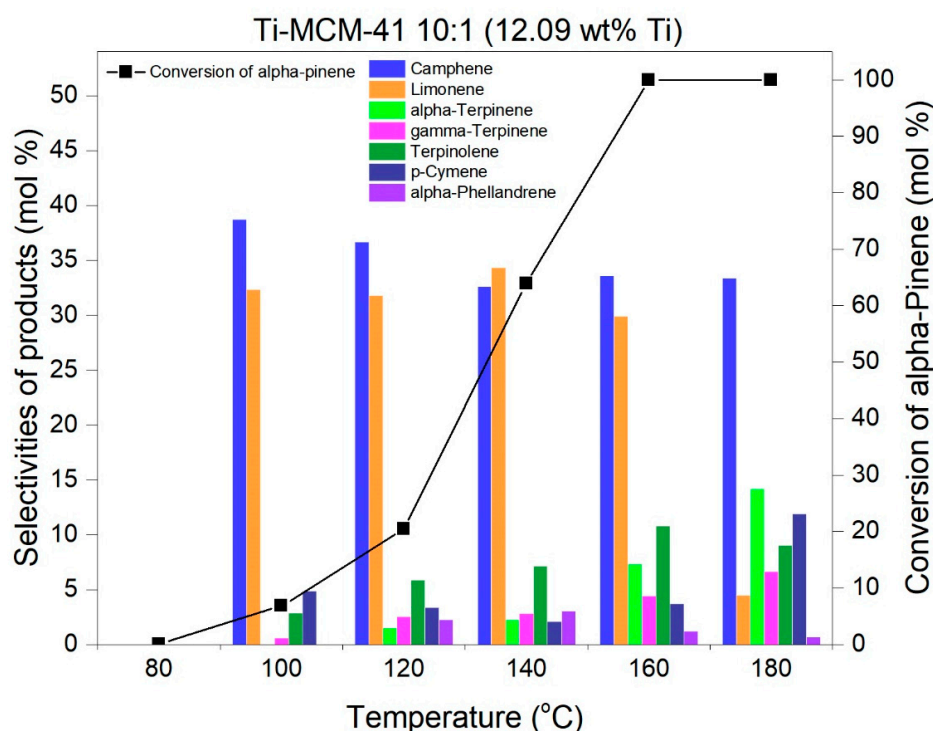


Figure 10. The influence of temperature on the conversion of α -pinene and on the product selectivity over Ti-MCM-41 10:1 (catalyst content 7.5 wt% relative to α -pinene, reaction time 7 h).

The next examined parameter was the content of the catalyst involved in the reaction (Figure 11). For this purpose, a series of tests was performed at 160 °C. The tested range of catalyst content ranged from 2.5 to 12.5 wt% relative to α -pinene. With increasing catalyst content, the conversion of α -pinene increased to 100 mol% at the catalyst content of 7.5 wt%—for lower catalyst contents, the number of active titanium sites is insufficient to allow for all of the α -pinene to be consumed. Raising the catalyst content to values above 7.5 wt% did not significantly increase the selectivity of camphene, but contributed to the subsequent reaction, which is the isomerization of limonene.

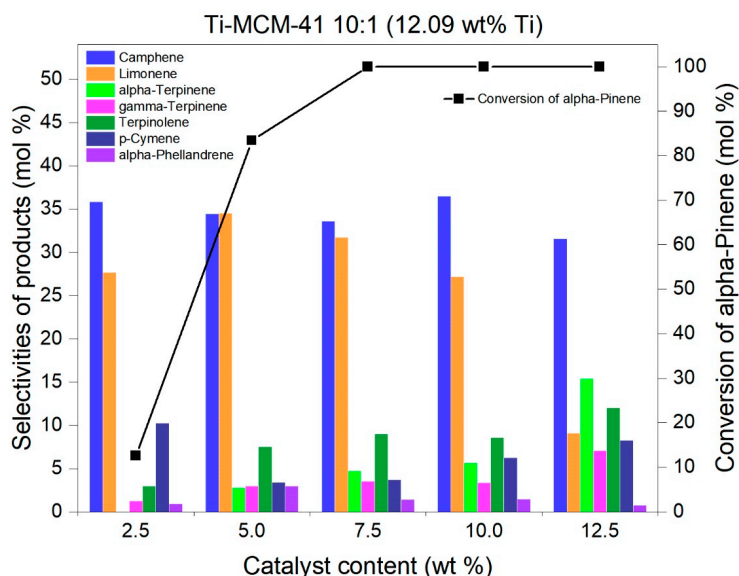


Figure 11. The influence of the Ti-MCM-41 10:1 catalyst content on the α -pinene conversion and on the product selectivity (temperature 160 °C, reaction time 6 h).

Studies on the effect of reaction time on the course of isomerization of α -pinene were carried out using a larger amount of reaction mixture. In this case, 20 g of α -pinene was mixed with 1.5 g of the Ti-MCM-41 10:1 catalyst, and the samples of the reaction mixture for GC analyses were taken in the range of 15 min to 24 h. In the studied conditions, α -pinene almost completely reacted after 7 h (conversion of α -pinene equal to 97.97 mol%), as depicted in Figure 12. After this time, the main products formed with the highest selectivity are: camphene (35.45 mol%) and limonene (21.32 mol%). Moreover, other minor products (with their calculated selectivities in mol%) were produced: γ -terpinene (4.38), α -terpinene (8.12), terpinolene (11.16), p-cymene (6.61), and α -phellandrene (1.58). After 24 h, it can be noted that in the reaction mixture, limonene, which reacted mainly to form α -terpinene and p-cymene, was significantly reduced.

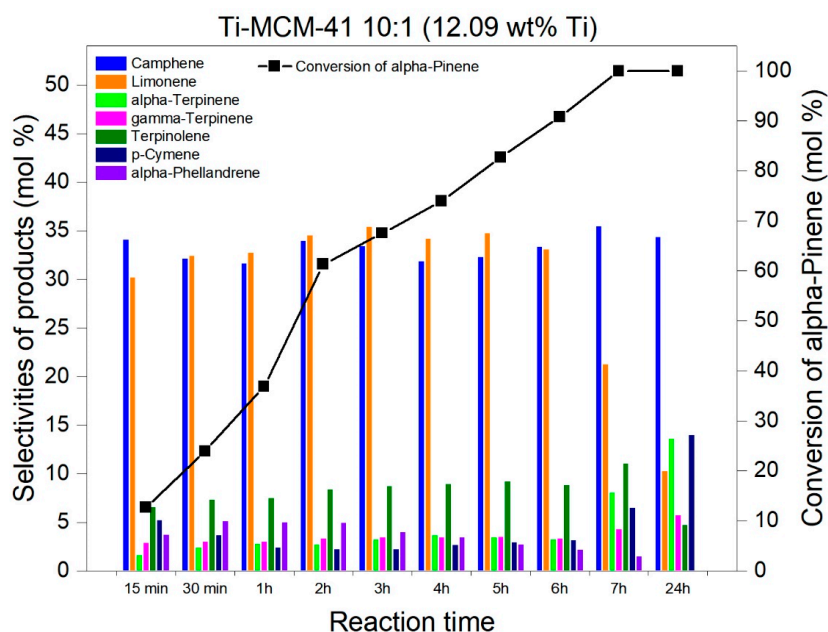


Figure 12. The influence of the reaction time on the conversion of α -pinene and on the product selectivity (temperature 160 °C, 7.5 wt% Ti-MCM-41 10:1 catalyst content relative to α -pinene).

3. Materials and Methods

3.1. Synthesis of Ti-MCM-41 Catalysts

Ti-MCM-41 catalysts with different molar ratios of silicon to titanium in the crystallization gel (40:1, 30:1, 20:1, and 10:1) were obtained by the method described by M. Grun et al. [58]. The samples of the Ti-MCM-41 catalysts produced in this manner are named respectively: “Ti-MCM-41 40:1”, “Ti-MCM-41 30:1”, “Ti-MCM-41 20:1”, and “Ti-MCM-41 10:1”. In the standard synthesis, 17.71 g of cetyltrimethylammonium bromide (99%, Fluka, Poznań, Poland) is dissolved in 324.1 g of deionized water and poured into a glass reactor equipped with a mechanical stirrer. Next, 132.02 g of ammonia (25% aqueous solution, POCh, Gliwice, Poland) is added to the previously prepared solution. In the next step, 422.1 g anhydrous ethanol (analytical grade, POCh, Gliwice, Poland) is added to the resulting mixture. The contents of the reactor are mixed for 15 min, and then a solution containing 33.11 g of tetraethyl orthosilicate, TEOS (98%, Aldrich, Poznań, Poland), is added dropwise. Following that, depending on the catalyst prepared, the appropriate amount of tetrabutyl orthotitanate, TBOT (99%, Fluka, Poland), is added to obtain the following molar ratios of Si/Ti: for 10:1, 5.421 g; for 20:1, 2.708 g; for 30:1, 1.755 g; and for 40:1, 1.354 g. The resulting crystallization gel is then stirred for 2 h and then left for 16 h without stirring at ambient temperature. After this time, the catalyst is filtered, washed with deionized water, and dried at 100 °C for 24 h and then calcined at 550 °C.

3.2. Characteristics of the Ti-MCM-41 Catalysts

The Ti content in each catalyst was calculated using an energy dispersive X-ray fluorescence (EDXRF) spectrometer (Epsilon 3, PANalytical, Almelo, The Netherlands).

For the produced catalysts, XRD analysis was performed in order to determine whether an MCM-41 structure was obtained for all tested materials. The X-ray diffraction (XRD) patterns of the catalysts were recorded by a X-ray diffractometer (Empyrean, PANalytical, Almelo, the Netherlands) using Cu K ($\lambda = 0.154$ nm) as the radiation source in the 2θ range $0.1\text{--}10^\circ$ with a step size of 0.013, and in the 2θ range $10\text{--}40^\circ$ with a step size of 0.05.

Textural properties were determined on the basis of nitrogen sorption at -196 °C (QUADRASORB evo Gas Sorption Surface Area and Pore Size Analyzer, Quantachrome Instruments, Boynton Beach, FL, USA). Prior to the sorption measurements all samples were outgassed at 250 °C for at least 20 h. The specific surface area was calculated on the basis of the Brunauer–Emmett–Teller (BET) equation and multi-point method. The relative pressure range was selected on the basis of the linear section of the BET plot, i.e., in the relative pressure range 0.05–0.2. Pore volume distribution, micropore volume V_{micro} , and the mean pore diameter (d_m) were calculated by the density functional theory (DFT) method. The total pore volume (V_{tot}) was obtained from the nitrogen volume adsorbed at a relative pressure of 0.98.

The scanning electron microscope (SEM) micrographs were obtained using ultra-high resolution field emission scanning electron microscope (UHR FE-SEM Hitachi SU8020, Tokyo, Japan) equipped with the secondary electron (SE) detectors and an energy dispersive X-ray detector (EDX).

The incorporation of titanium in the structure of silica was characterized by UV-Vis (V-650, Jasco, Tokyo, Japan) examinations in the wavelength range from 200 to 600 nm. Also, FT-IR spectra were obtained (Nicolet 380, Thermo Fisher Scientific, Waltham, MA, USA) in the range of wavenumbers from 400 to 4000 cm^{-1} .

3.3. Isomerization of α -Pinene

Studies on the influence of titanium content in the Ti-MCM-41 catalysts on the α -pinene isomerization process and the determination of the best conditions for the most active catalyst were carried out in a 25 cm^3 glass reactor equipped with a reflux condenser and magnetic stirrer with a heating function. For studies on the isomerization, 4 g of α -pinene (98%, Aldrich, Poland) and the appropriate amount of catalyst were weighed into the reactor, which was then placed in an oil bath. The mixing speed was constant at 400 rpm.

In the first stage of the research, the activities of the Ti-MCM-41 catalysts with different molar ratios of silicon to titanium in the crystallization gel (10:1, 20:1, 30:1, 40:1) were investigated. The reaction temperature was 160 °C, the amount of catalyst amounted to 7.5 wt% relative to α -pinene, and the reaction time was 6 h. In the next stage, the most active catalyst was used to determine the most favorable conditions for the α -pinene isomerization. For this purpose the influence of the following parameters was studied: temperature in the range of 80–180 °C, catalyst content in the range of 2.5–12.5 wt%, reaction time from 15 min to 24 h. During the studies on the influence of reaction time, the amount of the reaction mixture was increased five-fold, and samples were taken at specific intervals.

The procedure for performing the qualitative and quantitative analyses of the post-reaction mixtures using the GC method was presented in our previous work [38]. The most active catalyst and the best conditions of the α -pinene isomerization process were determined on the basis of the mass balances according to which the main functions characterizing the process were determined: the conversion of α -pinene and selectivities of the main product camphene, as well as others (limonene, α -terpinene, γ -terpinene, terpinolene, α -phellandrene, and *p*-cymene). Selectivities were also determined for the remaining isomerization products that were formed in small amounts: tricyclene, α -fenchene, bornylene, polymer compounds, and oxidation products.

4. Conclusions

The studies show that Ti-MCM-41 catalysts are active in the α -pinene isomerization process, and that the increase in titanium content introduced into the silica structure significantly increases Ti-MCM-41 catalyst activity in this process. On the basis of the tests carried out, it was shown that the most active catalyst was the one with a Si:Ti molar ratio of 10:1 in the crystallization gel, which contains 12.09 wt% Ti. In addition, the most favorable conditions for the isomerization of α -pinene were: temperature 160 °C, reaction time 7 h, and catalyst content of 7.5 wt% relative to α -pinene. It has also been shown that a significant increase in the reaction time leads to subsequent reactions in which monocyclic terpenes are transformed to *p*-cymene. The use of the optimal Ti-MCM-41 10:1 catalyst can yield 100% conversion of α -pinene, and, with the relatively high product selectivities, many useful intermediates (camphene, limonene, γ -terpinene, α -terpinene, terpinolene, *p*-cymene, and α -phellandrene) for various industries can also be formed in this process.

The Ti-MCM-41 catalysts, due to their morphology (higher amount of introduced titanium, higher specific surface area), showed better activity in the α -pinene isomerization process than Ti-SBA-15 catalysts. Their use significantly reduced the amount of catalyst used for 100 mol% substrate conversion, from 15 wt% for Ti-SBA-15 [39] to 7.5 wt% for Ti-MCM-41. The use of the Ti-MCM-41 catalyst also allowed for the reduction of the reaction temperature from 180 to 160 °C. In addition, the selectivities of the main products changed because camphene and limonene were produced with a total selectivity of more than 70 mol%. An additional advantage of using the Ti-MCM-41 catalyst in this process, in comparison with the Ti-SBA-15 catalyst, is that the Ti-MCM-41 catalyst is obtained in a simpler way and from cheaper raw materials, hence it is an economical heterogeneous catalyst.

A comparison of our results with the results presented in the literature [34–37] shows that similar results can be obtained over the Ti-MCM-41 catalyst as over SBA-15 and MCM-41 catalysts modified by the impregnation with phosphotungstic acid. Unfortunately, these catalysts are more expensive considering their synthesis and subsequently also the possibility of their regeneration. Similar results were also obtained over Al-MCM-41 and Ga/SBA-15 catalysts. However, these two catalysts may not be active in another process in which titanium silicates are used, namely in the epoxidation process, and this is our second direction of research on the possibilities of obtaining useful products from α -pinene.

The process described in the current study has industrial applications and should be developed. In the future, research on the influence of different solvents and their concentration on the α -pinene isomerization process should be performed. In this work we show a variant of this process without the use of a solvent, which is more ecological one. Further studies on the isomerization process should also be performed in the autoclave, which will most likely lead to lowering the temperature of this

process by conducting isomerization under autogenous pressure. We are also planning to prepare MCM-41 materials impregnated with various sources of titanium, perhaps they will be more active than the Ti-MCM-41 materials obtained by the direct method.

Author Contributions: A.W. prepared the conception of isomerization of α -pinene over selected titanium silicate catalysts. She had substantial contributions in the interpretation of research results. She critically corrected the preliminary version of this manuscript, including introduction, discussion of the results and conclusions. She translated the manuscript into English. P.M. prepared Ti-MCM-41 catalysts and performed α -pinene isomerization reactions in the laboratory. He prepared the GC analyses and took part in the calculations of the main functions describing the studied process and in the interpretation of data for the work. He prepared the first, preliminary version of this manuscript. J.T. took part in the calculations of the main functions describing the studied process on the basis of GC analyses and in the interpretation of data. J.S.-N. performed nitrogen adsorption at 77 K. Z.C.K. was involved in the discussions about the results, in the interpretation of the data, and in preparing the final version of the manuscript. B.M. made SEM pictures and was involved in discussions about results.

Conflicts of Interest: The authors declare no conflicts of interest.

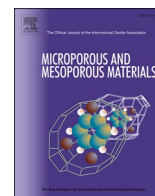
References

1. Petkovich, N.; Stein, A. Colloidal Crystal Templating Approaches to Materials with Hierarchical Porosity. In *Hierarchically Structured Porous Materials*; Su, B., Sanchez, C., Yang, X., Zhao, X., Wan, Y., Zhou, W., Eds.; Wiley-VCH: Weinheim, Germany, 2012; pp. 58–61.
2. Mihai, G.D.; Meynen, V.; Beyers, E.; Mertens, M.; Bilba, N.; Cool, P.; Vansant, E.F. Synthesis, structural characterization and photocatalytic activity of Ti-MCM-41 mesoporous molecular sieves. *J. Porous Mater.* **2009**, *16*, 109–118. [[CrossRef](#)]
3. Douroumis, D.; Onyesom, I.; Maniruzzaman, M.; Mitchell, J. Mesoporous silica nanoparticles in nanotechnology. *Crit. Rev. Biotechnol.* **2013**, *33*, 229–245. [[CrossRef](#)]
4. Peruzynska, M.; Szelag, S.; Trzeciak, K.; Kurzawski, M.; Cendrowski, K.; Barylak, M. *In vitro* and *in vivo* evaluation of sandwich-like mesoporous silica nanoflakes as promising anticancer drug delivery system. *Int. J. Pharm.* **2016**, *506*, 458–468. [[CrossRef](#)]
5. Badaničová, M.; Zeleňák, V. Organo-modified mesoporous silica for sorption of carbon dioxide. *Monatshefte Chem.* **2010**, *141*, 677–684. [[CrossRef](#)]
6. Brady, R.; Woonton, B.; Gee, M.; O'Connor, A. Hierarchical mesoporous silica materials for separation of functional food ingredients—A review. *Innov. Food Sci. Emerg. Technol.* **2008**, *9*, 243–248. [[CrossRef](#)]
7. Garcia-Martinez, J.; Li, K. *Mesoporous Zeolites: Preparation, Characterization and Applications*; Wiley-VCH: Weinheim, Germany, 2015; pp. 1–7.
8. Miądlicki, P.; Wróblewska, A.; Kochmańska, A.; Jędrzejewski, R.; Sreńscek-Nazzal, J. Syntetyczny kanemit jako prekursor mezoporowatych materiałów krzemionkowych. *Prz. Geol.* **2005**, *58*, 787.
9. Melo, R.A.A.; Giotto, M.V.; Rocha, J.; Urquieta-González, E.A. MCM-41 Ordered Mesoporous Molecular Sieves Synthesis and Characterization. *Mater. Res.* **1991**, *2*, 173–179. [[CrossRef](#)]
10. Schwarz, J.A.; Contescu, C.I.; Putyera, K. *Dekker Encyclopedia of Nanoscience and Nanotechnology*; Taylor & Francis Group: New York, NY, USA, 2004; pp. 1797–1811.
11. Salemi Golezani, A.; Sharifi Fateh, A.; Ahmad Mehrabi, H. Synthesis and characterization of silica mesoporous material produced by hydrothermal continues pH adjusting path way. *Prog. Nat. Sci. Mater. Int.* **2016**, *26*, 411–414. [[CrossRef](#)]
12. Barczak, M.; Dąbrowski, A. Mostkowane polisilsekwiksany: Synteza, struktura i właściwości adsorpcyjne. *Wiad. Chem.* **2008**, *62*, 977–998.
13. Wang, S.; Ma, C.; Shi, Y.; Ma, X. Ti incorporation in MCM-41 mesoporous molecular sieves using hydrothermal synthesis. *Front. Chem. Sci. Eng.* **2014**, *8*, 95–103. [[CrossRef](#)]
14. Berlini, C.; Guidotti, M.; Moretti, G.; Psaro, R.; Ravasio, N. Catalytic epoxidation of unsaturated alcohols on Ti-MCM-41. *Catal. Today* **2000**, *60*, 219–225. [[CrossRef](#)]
15. Silvestre-Alberó, J.; Domine, M.E.; Jordá, J.L.; Navarro, M.T.; Rey, F.; Rodríguez-Reinoso, F.; Corma, A. Spectroscopic, calorimetric, and catalytic evidences of hydrophobicity on Ti-MCM-41 silylated materials for olefin epoxidations. *Appl. Catal. A Gen.* **2015**, *507*, 14–25. [[CrossRef](#)]

16. Fadhli, M.; Khedher, I.; Fraile, J.M. Modified Ti/MCM-41 catalysts for enantioselective epoxidation of styrene. *J. Mol. Catal. A Chem.* **2016**, *420*, 282–289. [[CrossRef](#)]
17. Bigi, F.; Piscopo, C.G.; Predieri, G.; Sartori, G.; Scotti, R.; Zaroni, R.; Maggi, R. Molybdenum-MCM-41 silica as heterogeneous catalyst for olefin epoxidation. *J. Mol. Catal. A Chem.* **2014**, *386*, 108–113. [[CrossRef](#)]
18. Shu, Y.; Shao, Y.; Wei, X.; Wang, X.; Sun, Q.; Zhang, Q.; Li, L. Synthesis and characterization of Ni-MCM-41 for methyl blue adsorption. *Microporous Mesoporous Mater.* **2015**, *214*, 88–94. [[CrossRef](#)]
19. Xin, H.; Ke, T. Preparation and adsorption denitrogenation from model fuel or diesel oil of heteroatoms mesoporous molecular sieve Co-MCM-41. *Energy Source Part A.* **2016**, *38*, 2560–2567. [[CrossRef](#)]
20. Collard, X.; Li, L.; Lueangchaichaweng, W.; Bertrand, A.; Aprile, C.; Pescarmona, P.P. Ga-MCM-41 nanoparticles: Synthesis and application of versatile heterogeneous catalysts. *Catal. Today.* **2014**, *235*, 184–192. [[CrossRef](#)]
21. Olyaei, A. Rapid and Efficient One-Pot Green Synthesis of 12-Aryl-8,9,10,12-tetrahydrobenzo[a]xanthene-11-ones Using Zr-MCM-41 Catalyst. *Synth. Commun.* **2015**, *45*, 94–104. [[CrossRef](#)]
22. Deshmane, V.G.; Abrokwah, R.Y.; Kuila, D. Synthesis of stable Cu-MCM-41 nanocatalysts for H₂ production with high selectivity via steam reforming of methanol. *Int. J. Hydrogen Energy* **2015**, *40*, 10439–10452. [[CrossRef](#)]
23. Fu, X.; Liu, Y.; Yao, W.; Wu, Z. One-step synthesis of bimetallic Pt-Pd/MCM-41 mesoporous materials with superior catalytic performance for toluene oxidation. *Catal. Commun.* **2016**, *83*, 22–26. [[CrossRef](#)]
24. Lan, B.; Huang, R.; Li, L.; Yan, H.; Liao, G.; Wang, X.; Zhang, Q. Catalytic ozonation of p-chlorobenzoic acid in aqueous solution using Fe-MCM-41 as catalyst. *Chem. Eng. J.* **2013**, *219*, 346–354. [[CrossRef](#)]
25. Sanaeishoar, H.; Sabbaghan, M.; Mohave, F. Synthesis and characterization of micro-mesoporous MCM-41 using various ionic liquids as co-templates. *Microporous Mesoporous Mater.* **2015**, *217*, 219–224. [[CrossRef](#)]
26. Guncheva, M.; Dimitrov, M.; Ossowicz, P.; Janus, E. Tetraalkylammonium acetates and tetraalkylammonium tetrafluoroborates as new templates for room-temperature synthesis of mesoporous silica spheres. *J. Porous Mater.* **2018**, *25*, 935–943. [[CrossRef](#)]
27. Agabekov, E.; Sen'kov, G.M.; Sidorenko, A.Y.; Tuyen, N.D.; Tuan, V.A. New α -pinene isomerization catalysts. *Catal. Ind.* **2011**, *3*, 319–330. [[CrossRef](#)]
28. Tarbell, I.M. *The History of the Standard Oil Company*; Cosmico: New York, NY, USA, 2010; p. 274.
29. Kapp, T.; Kammann, U.; Vobach, M.; Vetter, W. Synthesis of low and high chlorinated toxaphene and comparison of their toxicity by zebrafish (*Danio rerio*) embryo test. *Environ. Toxicol. Chem.* **2006**, *25*, 2884–2889. [[CrossRef](#)] [[PubMed](#)]
30. Ponomarev, D.; Mettee, H. Camphor and its Industrial Synthesis. *Chem. Educ. J.* **2016**, *18*, 1–4.
31. Bin-Tang, L.; Jin-Quan, Y.; Ai-Qun, F.; Ping, Z.; Shu-De, X. Study on selective alkylation of guaiacol with camphene over H-Mordenite. *Chin. J. Org. Chem.* **1995**, *15*, 318–322.
32. Kim, D.H.; Goh, H.J.; Lee, H.W.; Kim, K.S.; Kim, Y.T.; Moon, H.S.; Lee, S.W.; Park, S.Y. The Effect of Terpene Combination on Ureter Calculus Expulsion after Extracorporeal Shock Wave Lithotripsy. *Korean J. Urol.* **2014**, *55*, 36–40. [[CrossRef](#)]
33. Girola, N.; Figueiredo, C.R.; Farias, C.F.; Azevedo, R.A.; Ferreira, A.K.; Teixeira, S.F.; Capello, T.M.; Martins, E.G.; Matsuo, A.L.; Travassos, L.R.; Lago, J.H. Camphene isolated from essential oil of *Piper cernuum* (Piperaceae) induces intrinsic apoptosis in melanoma cells and displays antitumor activity *in vivo*. *Biochem. Biophys. Res. Commun.* **2015**, *467*, 928–934. [[CrossRef](#)]
34. Wu, C.H.; Liu, H.Q.; Zhuang, C.F.; Ben, G. Study on Mesoporous PW/SBA-15 for Isomerization of α -Pinene. *Appl. Mech. Mater.* **2013**, *483*, 134–137. [[CrossRef](#)]
35. Zou, J.; Chang, N.; Zhang, X.; Wang, L. Isomerization and Dimerization of Pinene using Al-Incorporated MCM-41 Mesoporous Materials. *ChemCatChem* **2012**, *4*, 1289–1297. [[CrossRef](#)]
36. Launay, F.; Jarry, B.; Bonardet, J.L. Catalytic activity of mesoporous Ga-SBA-15 materials in α -pinene isomerisation: Similarities and differences with Al-SBA-15 analogues. *Appl. Catal. A* **2009**, *368*, 132–138. [[CrossRef](#)]
37. Nie, G.; Zou, J.; Feng, R.; Zhang, X.; Wang, L. HPW/MCM-41 catalyzed isomerization and dimerization of pure pinene and crude turpentine. *Catal. Today* **2014**, *234*, 271–277. [[CrossRef](#)]
38. Wróblewska, A.; Miądlicki, P.; Makuch, E. The isomerization of α -pinene over the Ti-SBA-15 catalyst—The influence of catalyst content and temperature. *React. Kinet. Mech. Catal.* **2016**, *119*, 641–654. [[CrossRef](#)]

39. Wróblewska, A.; Miądlicki, P.; Sreńscek-Nazzal, J.; Sadłowski, M.; Koren, Z.C.; Michalkiewicz, B. Alpha-pinene isomerization over Ti-SBA-15 catalysts obtained by the direct method: The influence of titanium content, temperature, catalyst amount and reaction time. *Microporous Mesoporous Mater.* **2018**, *258*, 72–82. [[CrossRef](#)]
40. Wijayati, N.; Pranowo, H.D.; Jumina, J.; Triyono, T. Synthesis of terpineol from α -pinene catalyzed by TCA/Y-zeolite. *Indones. J. Chem.* **2011**, *11*, 234–237. [[CrossRef](#)]
41. Mokrzycki, L.; Sulikowski, B.; Olejniczak, Z. Properties of Desilicated ZSM-5, ZSM-12, MCM-22 and ZSM-12/MCM-41 Derivatives in Isomerization of α -Pinene. *Catal. Lett.* **2009**, *127*, 296–303. [[CrossRef](#)]
42. Tian, F.; Wu, Y.; Shen, Q.; Li, X.; Chen, Y.; Meng, C. Effect of Si/Al ratio on mesopore formation for zeolite beta via NaOH treatment and the catalytic performance in α -pinene isomerization and benzylation of naphthalene. *Microporous Mesoporous Mater.* **2013**, *173*, 129–138. [[CrossRef](#)]
43. Ecmier, M.A.; Lee, A.F.; Wilson, K. High activity, templated mesoporous $\text{SO}_4/\text{ZrO}_2/\text{HMS}$ catalysts with controlled acid site density for α -pinene isomerization. *Microporous Mesoporous Mater.* **2005**, *80*, 129–138. [[CrossRef](#)]
44. Ünveren, E.; Gündüz, G.; Cakicioğlu-Özkan, F. Isomerization of Alpha-pinene Over Acid Treated Natural Zeolite. *Chem. Eng. Commun.* **2005**, *192*, 386–404. [[CrossRef](#)]
45. Gündüz, G.; Murzin, D.Y. Influence of catalyst pretreatment on alpha-pinene isomerization over natural clays. *React. Kinet. Mech. Catal.* **2002**, *75*, 231–237. [[CrossRef](#)]
46. Akpolat, O.; Gündüz, G.; Ozkan, F.; Beşün, N. Isomerization of α -pinene over calcined natural zeolites. *Appl. Catal. A* **2004**, *265*, 11–22. [[CrossRef](#)]
47. Yadav, M.K.; Chudasama, C.; Jasra, R. Isomerisation of α -pinene using modified montmorillonite clays. *J. Mol. Catal. A Chem.* **2004**, *216*, 51–59. [[CrossRef](#)]
48. Atalay, B.; Gündüz, G. Isomerization of α -pinene over H3PW12O40 catalysts supported on natural zeolite. *Chem. Eng. J.* **2011**, *168*, 1311–1318. [[CrossRef](#)]
49. Luan, Z.; He, H.; Zhou, W.; Klinowski, J. Transformation of lamellar silicate into the mesoporous molecular sieve MCM-41. *Chem. Soc., Faraday Trans.* **1998**, *94*, 979–983. [[CrossRef](#)]
50. Zakaria, M.B.; Elmorsi, M.A.; Ebeid, E. Corrosion Protection of Aluminum Metal Using MCM-41 Films Supported by Silver Nanoparticles and Distyrylpyrazine Photopolymer. *Adv. Sci. Eng. Med.* **2015**, *7*, 423–428. [[CrossRef](#)]
51. Hu, Y.; Martra, G.; Zhang, J.; Higashimoto, S.; Coluccia, S.; Anpo, M. Characterization of the Local Structures of Ti-MCM-41 and Their Photocatalytic Reactivity for the Decomposition of NO into N_2 and O_2 . *J. Phys. Chem. B* **2006**, *110*, 1680–1685. [[CrossRef](#)]
52. Balu, A.M.; Hidalgo, J.M.; Campelo, J.M.; Luna, D.; Luque, R.; Marinas, J.M.; Romero, A.A. Microwave oxidation of alkenes and alcohols using highly active and stable mesoporous organotitanium silicates. *J. Mol. Catal. A Chem.* **2008**, *293*, 17–24. [[CrossRef](#)]
53. Han, Y.; Kim, H.; Park, J.; Lee, S.; Kim, J. Influence of Ti doping level on hydrogen adsorption of mesoporous Ti-SBA-15 materials prepared by direct synthesis. *Int. J. Hydrogen Energy.* **2012**, *37*, 14240–14247. [[CrossRef](#)]
54. Azimov, F.; Markova, I.; Stefanova, V.; Sharipov, K. Synthesis and characterization of SBA-15 and Ti-SBA-15 nanoporous materials for DME catalysts. *J. Univ. Chem. Technol. Metall.* **2012**, *47*, 333–340.
55. Angeles-Beltrán, D.; Negrón-Silva, G.; Lomas-Romero, L.; Iglesias-Arteaga, M.A.; Santos-Aires, F.J.C. Titanium-modified MCM-41 Prepared by Ultrasound and by Hydrothermal Treatment, Catalysts for Acetylation Reactions. *J. Mex. Chem. Soc.* **2008**, *52*, 175–180.
56. Atchudan, R.; Perumal, S.; Edison, T.N.J.I.; Lee, Y.R. Highly graphitic carbon nanosheets synthesized over tailored mesoporous molecular sieves using acetylene by chemical vapor deposition method. *RSC Adv.* **2015**, *5*, 93364–93373. [[CrossRef](#)]
57. Frattini, L.; Isaacs, M.A.; Parlett, C.M.A.; Wilson, K.; Kyriakou, G.; Lee, A.F. Support enhanced α -pinene isomerization over HPW/SBA-15. *Appl. Catal. B Environ.* **2017**, *200*, 10–18. [[CrossRef](#)]
58. Grün, M.; Unger, K.K.; Matsumoto, A.; Tsutsumi, K. Novel pathways for the preparation of mesoporous MCM-41 materials: Control of porosity and morphology. *Microporous Mesoporous Mater.* **1999**, *27*, 207–216. [[CrossRef](#)]





Sulfuric acid modified clinoptilolite as a solid green catalyst for solvent-free α -pinene isomerization process

Piotr Miądlicki^{a,*}, Agnieszka Wróblewska^{a,*}, Karolina Kiełbasa^a, Zvi C. Koren^b,
Beata Michalkiewicz^a

^a West Pomeranian University of Technology in Szczecin, Faculty of Chemical Technology and Engineering, Department of Catalytic and Sorbent Materials Engineering, Pułaskiego 10, PL, 70-322 Szczecin, Poland

^b The Edelstein Center, Department of Chemical Engineering, Shenkar College of Engineering, Design and Art, 12 Anna Frank St., Ramat Gan, 52526, Israel

ARTICLE INFO

Keywords:

Isomerization
 α -Pinene
Camphene
Limonene
Natural compounds
Green chemistry
Clinoptilolite
Zeolites
High value-added chemicals

ABSTRACT

The isomerization of α -pinene – a renewable bioresource – was investigated as a relatively simple method for the syntheses of camphene and limonene, industrially important products. The catalytic activity of H_2SO_4 -modified clinoptilolite was evaluated without any solvent and the results show its applicability as a novel, green, reusable and promising catalyst in organic syntheses. The method is cost-effective and energy efficient because of the use of relatively low temperatures: at 30 °C and after 1 h, conversion was equal to 18%. In addition, this process has a short-time performance: 100% conversion after only 4 min at 70 °C. Camphene and limonene were the products that were formed with the highest selectivities of 50% and 30%, respectively. Clinoptilolite modified by H_2SO_4 solutions (0.01–2 M) as a catalyst for α -pinene isomerization has not been described up to now. The catalyst samples were characterized using various instrumental methods (XRD, FT-IR, UV–Vis, SEM, and XRF). The nitrogen sorption method was used to determine the textural parameters, and the acid-sites concentration was established with the help of the titration method. The mixtures of compounds were analyzed via gas chromatography (GC). The comprehensive kinetic modeling of α -pinene isomerization over the most active catalyst (clinoptilolite modified by 0.1 M H_2SO_4 solution) was performed. The first order kinetics of α -pinene conversion was found, and the value of the reaction rate constant at 70 °C was equal to 8.19 h⁻¹. It was concluded that the high activity of the prepared modified clinoptilolite in α -pinene isomerization is a multifaceted function of textural properties, crystallinity, chemical composition, and acid-sites concentration.

1. Introduction

The conversion of biomass into high value-added chemicals has attracted much attention in recent decades due to its feasibility and immense commercial prospects. For several decades, scientists have been conducting research on effective syntheses of high value-added chemicals from biomass [1]. Biomass is a low-cost and abundant resource, however it requires environmentally friendly and cost-effective methods of conversion to useful products [2].

Pinenes, especially α -pinene, have been attracting research interests as renewable bioresources for the production of resin precursors, pharmaceutical intermediates, and high density fuel and additives [3]. α -Pinene is mainly extracted from resin tapping processes and also from cellulose production and wood-pulp papermaking. It is available in

significant quantities and relatively inexpensive to isolate, and a beneficial way of α -pinene utilization is in its isomerization. The products which are formed during α -pinene isomerization can be divided into two groups: bicyclic products (camphene and tricyclene) and products that have one ring (terpinolene, α - and γ -terpinene, limonene, and *p*-cymene). Fig. 1 presents the main and secondary products of the α -pinene isomerization process.

Among these products, camphene and limonene are particularly important [4]. Camphene is used as a raw material in light organic syntheses, for example, as the toxaphene insecticide [5], and in the synthesis of camphor. Camphene reacts with acetic acid in the presence of a strongly acidic catalyst to produce isobornyl acetate, which is an intermediate for the production of camphor [6]. Camphene also has medical and anticancer properties [7,8]. Another use of camphene is as a

* Corresponding author.

** Corresponding author.

E-mail addresses: Piotr.miadlicki@zut.edu.pl (P. Miądlicki), Agnieszka.Wroblewska@zut.edu.pl (A. Wróblewska).

<https://doi.org/10.1016/j.micromeso.2021.111266>

Received 13 April 2021; Received in revised form 18 June 2021; Accepted 25 June 2021

Available online 30 June 2021

1387-1811/© 2021 The Authors. Published by Elsevier Inc. This is an open access article under the CC BY license (<http://creativecommons.org/licenses/by/4.0/>).

fragrant and flavor additive and in the production of cleaning agents, e. g., toilet scented cubes, which are designed to mask unpleasant odors.

Limonene, which is the second main product of the α -pinene isomerization process, is also widely used. One of the most important reactions using limonene as a raw material is the transformation of (+)-limonene to (–)-carvone, which is used as a peppermint flavor [9]. Limonene has also found applications as a fumigant and repellent [10, 11], and can be a substitute for toxic solvents used in extraction methods [12]. The application of limonene as an additive for plastics, such as, low- and high-density polyethylene, polystyrene, and polylactic acid (PLA), which will be in contact with foods, was also studied [13].

The conversion of α -pinene was investigated several decades ago using homogeneous catalysts [14,15]; however, this process is environmentally unfriendly. Heterogeneous catalysis is more attractive due to its industrial and economic importance. Heterogeneous catalysts received substantial attention owing to their higher selectivity, faster reaction rates, easy work-up procedures, simple filtration, environmentally friendly materials, recoverability of these porous materials, cost-reductions, and they do not generate effluents [16]. An additional advantage of the solution proposed in this work (apart from the use of a heterogeneous catalyst) is that the isomerization process is performed without any solvent. This lowers the processing costs associated with the separation of products and organic raw materials from the solvent. It is also safe for the environment as there are no solvent vapors released to the atmosphere.

Among the porous materials used as heterogeneous catalysts, zeolites of natural origin, modified zeolites of natural origin, synthetic zeolites and zeolite-like materials are of great interest. These materials, however, have wider applications than just catalysis. There are reports in the literature on the use of these materials as sulfate-selective electrodes based on a modified carbon paste electrode with surfactant modified zeolites [17] zeolitic carbon paste electrode for indirect determination

of Cr(VI) in aqueous [18], and Sn(IV)-clinoptilolite carbon paste electrode for the determination of Hg(II) [19]. Surfactant-modified zeolites are also effective sorbents for different types of anionic and organic contaminants (for example for the removal of Pb(II) from aqueous solutions) [20], and moreover, these materials are used as host systems for medical applications (for example, delivering of cephalexin). Many applications of zeolites and zeolite-like materials are due to their properties, such as, high cation exchange capacity, size, shape, and charge selectivity [20,21].

Various solid catalysts (especially zeolites and zeolite-like materials) were applied for the α -pinene isomerization, and these include: sulfated zirconia [22], W_2O_3/Al_2O_3 [23], acid-modified illite [24], calcined H-mordenite [25], zeolite beta [26], MSU-S mesoporous molecular sieves [27], Al-MCM-41 [3], ionic liquids [28], phosphotungstic heteropoly acids [29], Ti-SBA-15 [30,31], Ti-MCM-41 [32], and exfoliated- Ti_3C_2 [33]. Additionally, modified clinoptilolites [4,34–36] were described as active catalysts used in this reaction. Table 1 shows more details regarding these catalytic materials.

However, the goal is still to produce new catalysts that possess high activity, i. e., showing large conversions at a low temperature and after a short period of time. For these reasons, we decided to utilize modified clinoptilolite as the catalyst, and its structure is presented in Fig. 2.

Clinoptilolite is one the most abundant and inexpensive natural zeolites [37]. We have chosen this mineral because it is a green heterogeneous reusable natural catalyst that can be active without any solvent. Sulfuric acid solutions from 0.01 to 2 M were used for the modification of natural clinoptilolite, and the choice of this acid as a modifier was based on the H_2SO_4/TiO_2 industrial catalyst system [38].

Clinoptilolite is a silica-rich member of the heulandite family of zeolites with a unit cell composition of $(Na,K)_6(Al_6Si_{30}O_{72}) \cdot 20H_2O$. It has a monoclinic framework consisting of a ten membered ring (pore size: $7.5 \times 3.1 \text{ \AA}$) and two eight membered rings ($4.6 \times 3.6 \text{ \AA}$, $4.7 \times 2.8 \text{ \AA}$) [39,

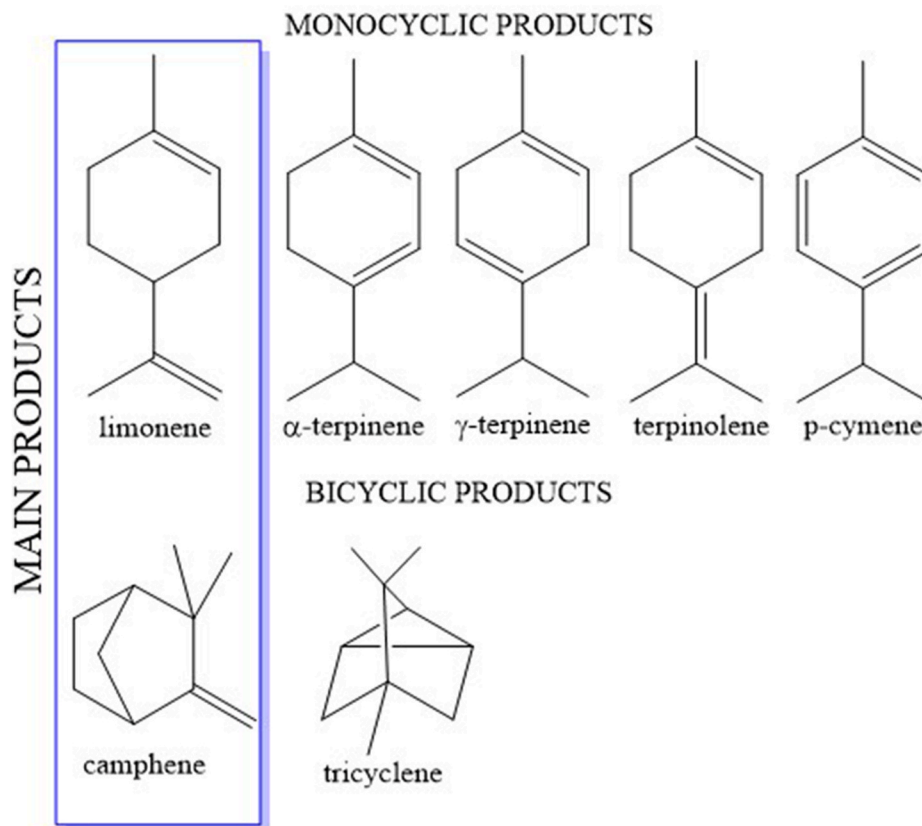


Fig. 1. Main and secondary products of α -pinene isomerization.

Table 1
The most active catalysts for α -pinene isomerization.

Catalyst	Temperature [°C]	Time [h]	Conversion [%]	Selectivity of camphene [%]	Selectivity of limonene [%]	Ref.
SO ₄ /Al _x ZrO ₂	85	6	32	–	–	[22]
W ₂ O ₃ -Al ₂ O ₃	150	2	73	55	–	[23]
Acid-modified illite	140	6	100	54	24	[24]
Calcinated H-Mordenite	130	4	98.5	–	–	[25]
Zeolite beta	70	0.5	91.4	43.9	35.3	[26]
MSU-S mesoporous molecular sieve	70	4	97	48	31.4	[27]
Al-MCM-41	160	2 min	98	30	30	[3]
[HSO ₃ -(CH ₂) ₃ -NEt ₃]Cl-ZnCl ₂	140	4	97.6	64.8	–	[28]
Silica-supported H ₃ PW ₁₂ O ₄₀	60	1	98	31	17	[29]
Ti-SBA-15	180	6	98	23.9	23.5	[30,31]
Ti-MCM-41	160	7	98	35.4	21.3	[32]
Exfoliated-Ti ₃ C ₂	160	6	98.4	59.3	23	[33]
HCl-modified clinoptilolite from Slovakia	90	3	41	57	32	[34]
Fe-loaded clinoptilolite	155	8	93.7	65.6	4.4	[4]
Heat-treated natural clinoptilolite	155	3	100	39	25	[35]
HCl-modified clinoptilolite	155	2	100	35	15	[36]
H ₂ SO ₄ -modified clinoptilolite from Turkey	70	4 min	100	55	29	This article
H ₂ SO ₄ -modified clinoptilolite from Turkey	30	1	18	46	19	This article

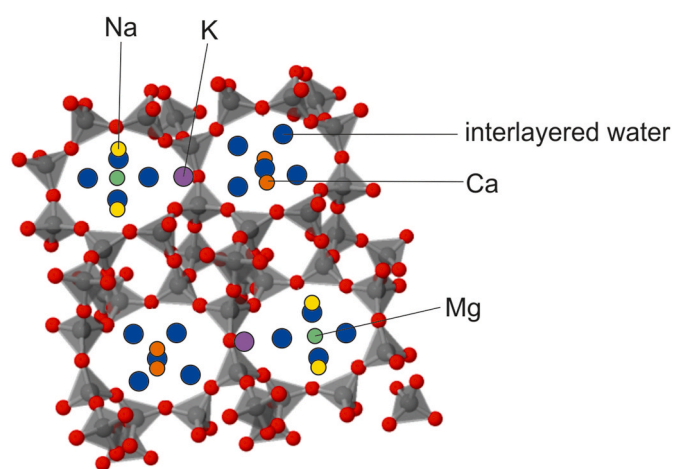


Fig. 2. Structure of clinoptilolite.

40). Its Si/Al ratio is greater than 4 (it can be, e.g., 4.84 [39]) while for typical heulandite materials this ratio is lower than 4. Clinoptilolite materials are mostly enriched with potassium and sodium, typically occurring as microscopic crystals normally 2–20 μm in size, and commonly intimately admixed with other fine-grained minerals. The mineral usually contains 4 to 7 cations per unit cell [41]. Clinoptilolite is a natural zeolite, which is present in large amounts (millions of tons) in volcanic tuffs and in alkaline-lake deposits [42].

Clinoptilolite has many applications. It is used as a sorbent for purifying water [43–46] and gases [47,48], for obtaining sensitive carbon paste electrodes for the voltammetric determination of some heavy metal cations [49], for obtaining materials showing photocatalytic activity [50], and it is also used as a cheap animal feed additive that improves the growth and conditions of animals [51,52]. In recent years, interest in the use of natural zeolites as catalysts in chemical reactions has increased significantly. Such materials often require certain modifications to improve their activity, and, once modified, they can be an inexpensive and ecological alternative to synthetic zeolites frequently used as heterogeneous catalysts.

In this work, we investigated the isomerization of α -pinene (produced from biomass) to appropriate products, not only camphene and limonene but also to other isomeric compounds by means of the heterogeneous, solid green modified clinoptilolite catalyst. The novel method presented here is cost-effective and energy efficient because of the use of low temperatures and short-time performance. According to the best of our knowledge, such catalytic activity in the isomerization of

α -pinene using low temperatures and short durations have not been described up to now. Further, the clinoptilolite modified by H₂SO₄ for α -pinene isomerization process is described for the first time in this work. Additional advantages of the method discussed is that it produces a reasonable yield, and that these catalysts can be recycled with a very easy workup.

2. Experimental

2.1. Modifications of clinoptilolite

Clinoptilolite (50 μm average particle size) with purity of about 85–90% was obtained from Rota Mining Corporation (Turkey). Samples of clinoptilolite were modified with appropriate solutions of sulfuric acid (POCH, 95%) with various concentrations (0.01–2 M) for 4 h at 80 °C. For the modification, 10 cm³ of the appropriate acid solution was used for 1 g of zeolite sample. The obtained aqueous suspension was mixed via a mechanical stirrer at the mixing speed of 500 rpm. Then, the modified clinoptilolite sample was filtered off and washed on the filter with distilled water until no SO₄²⁻ ions could be detected in the filtrate, and dried at 100 °C for 24 h. A natural, unmodified clinoptilolite was labeled as CLIN. The names of the modified clinoptilolite samples were given based on the acid concentration used: for example, clinoptilolite modified with 0.01 M solution of H₂SO₄ was denoted as CLIN 0.01.

2.2. Characteristics of the pristine and modified clinoptilolite samples

The SEM (scanning electron microscope) pictures were taken utilizing the SU8020 ultra-high-resolution field emission SEM (UHR FE-SEM) from Hitachi (Tokyo, Japan). Samples were applied to carbon adhesive tape.

X-ray diffraction (XRD) analyses were performed to determine the structures of the modified clinoptilolite samples. The XRD patterns were recorded by an Empyrean PANalytical (Malvern, United Kingdom) X-ray diffractometer with the Cu lamp used as the radiation source in the 2 θ range 5–40° with a step size of 0.026.

The elemental compositions of the samples were evaluated by means of an EDXRF (energy dispersive X-ray fluorescence) Epsilon 3 PANalytical (Malvern, United Kingdom) B-V. spectrometer.

The method of nitrogen sorption at 77 K was performed with the QUADRASORB evo Gas Sorption Surface Area and Pore Size Analyzer in order to determine the textural properties of the catalysts. The Brunauer–Emmett–Teller (BET) method was applied for the calculation of the specific surface area. The total pore volume (TPV) was estimated utilizing the volume of N₂ adsorption at p/p₀ \approx 1. The density functional theory (DFT) method was utilized to calculate the micropore volume

(MPV) and pore size distribution (PSD).

The acid-sites concentration was determined using the titration method described by Vilcoq et al. [53]. Accordingly, 20 mg of material were added to 10 cm³ of 0.01 M solution of NaOH. The solution was shaken at room temperature for 4 h. The material was then filtered off and the pH of a filtrate was determined by a titration with 0.01 M solution of HCl in the presence of phenolphthalein as an indicator. The acid-sites concentration, *N_s*, was established taking into account the following formula:

$$N_s = \frac{([OH^-]_0 - [OH^-]_{4h}) * V}{m}$$

where, [OH⁻] = the hydroxide group molar concentration determined by the titration (mol/dm³), V = the volume of NaOH solution added to zeolite sample, and m = the mass of zeolite sample

For each catalyst, FT-IR spectra were obtained with the Thermo Nicolet 380 (Waltham, United States) spectrometer with ATR unit for wavenumbers from 400 to 4000 cm⁻¹. Also, UV-Vis spectra were obtained for the wavelength range from 190 to 900 nm using the Jasco 650 (Pfungstadt, Germany) spectrometer with a horizontal integrating sphere (PIV-756).

2.3. Catalytic tests

Catalytic studies in the α-pinene isomerization were performed in a 25-cm³ glass reactor in which the reflux condenser was mounted and a magnetic stirrer was placed. First, 7 g of α-pinene (98%, Aldrich) and the applicable amount of clinoptilolite were weighed directly inside the reactor. Next, the reactor was placed in an oil bath and the mixing was started at a speed of 400 rpm.

In the first phase of the investigations, the activities of pristine clinoptilolite and the clinoptilolite catalysts modified with appropriate sulfuric acid solutions were examined. The experimental conditions were a temperature of 70 °C, content of the catalyst of 7.5 wt% in relation to the mass of α-pinene (α-pinene mass 7 g), and reaction time of 1 h. These parameters were chosen on the basis of our preliminary tests. For this purpose, the temperature was selected so that after 1 h the α-pinene conversion did not reach 100% and, thus, it was possible to compare the activities of the tested catalysts. Next, the best modified clinoptilolite was utilized to establish the most favorable conditions for the studied isomerization reaction. Therefore the experimental parameters were varied accordingly: temperature 30–80 °C, catalyst amount 2.5–12.5 wt%, and time of reaction from 30 to 600 s. For the trials based on the effect of the time on the isomerization, the amount of the reaction mixture (α-pinene plus catalyst) was increased four-fold (α-pinene mass 28 g), and samples of this mixture were taken at appropriate time intervals (every 30 s) for the gas chromatographic (GC) analyses. The method describing the GC determinations was presented in detail in our earlier work [31]. In order to perform the quantitative analysis, the reaction mixture was centrifuged and dissolved in acetone in a weight ratio of 1:10. The quantitative analysis was performed with a Thermo Electron FOCUS chromatograph equipped with an FID detector and a ZB-1701 column (30 m × 0.53 mm × 1 μm). The operating parameters of the chromatograph were as follows: helium flow 1.5 mL/min, injector temperature 250 °C, detector temperature 250 °C, furnace temperature isothermally for 2 min at 50 °C, increase at a rate of 4 °C/min to 80 °C, then rising at 20 °C/min to 240 °C. To determine the composition of post-reaction mixtures, the method of internal normalization was used.

The most active sample of clinoptilolite catalyst and the most favorable conditions that can be used in the α-pinene isomerization were established by taking into account mass balances. For these calculations, the main functions needed for characterizing the isomerization process were determined. These functions include α-pinene conversion (*C_{α-pinene}*), selectivities (*S_{product}*) of the main products of the transformation of this terpene compound (camphene and limonene), as well as other

products (*p*-cymene, α-terpinene, γ-terpinene, tricyclene, and terpinolene). Selectivities were also calculated for α-fenchene, bornylene, and polymer and oxidation products, and the sum of the selectivities of these products was labeled as “Others” in the figures, but they were characterized by low values. The main functions describing the process were calculated in the following way:

$$C_{\alpha\text{-pinene}} = \frac{\text{number of moles of } \alpha\text{-pinene reacted}}{\text{number of moles of } \alpha\text{-pinene introduced into the reaction}} * 100\%$$

$$S_{\text{product}} = \frac{\text{number of moles of appropriate product}}{\text{number of moles of } \alpha\text{-pinene reacted}} * 100\%$$

3. Results and discussion

3.1. Characterizations of clinoptilolite samples

The scanning electron microscopy images, before (CLIN) and after acid treatment, are presented in Fig. 3.

Similar elongated irregular shapes are presented in all the images, and the morphology was not affected by the H₂SO₄ treatment. These observations were also described by other authors for clinoptilolite [54] and mordenite [55] treated by HCl.

The XRD patterns of the pristine and modified clinoptilolite are showed in Fig. 4. The XRD plots showed characteristic peaks of clinoptilolite, according to JCPDS card 25–1349, in pristine and acid-treated samples (2θ = 9.85°, 11.19°, 13.09°, 16.92°, 17.31°, 19.09°, 20.42°, 22.48°, 22.75°, 25.06°, 26.05°, 28.02°, 28.58°, 29.07°, 30.12°, 31.97°, 32.77°). Four peaks (2θ = 20.86°, 26.6°, 36.55°, 39.45°) according to JCPDS card 85–0930 were assigned to quartz, which is an impurity present in natural clinoptilolite. The pristine CLIN XRD spectra were very similar to those presented by other authors [56,57].

The XRD data of pristine CLIN and those of JCPDS card 25–1349 are shown in Table 2. The obtained and reference d-space values (*d_{exp}* and *d_{ref}* respectively) were compared and the relative error was calculated using the equation:

$$RF[\%] = \left| \frac{d_{\text{ref}} - d_{\text{exp}}}{d_{\text{ref}}} \right| \cdot 100\%$$

The d space values presented in Table 2 were very similar to those obtained by Nezamzadeh-Ejhieh and Moenirad [56]. Four signals were not identified in pristine CLIN but their intensities were lower than 26%. The relative intensities of pristine CLIN (*I_{exp}*) and reference (*I_{ref}*) were also compared. It was found that the signal intensities of pristine CLIN and reference samples are well correlated.

The concentrations of sulfuric acid solutions up to 0.1 M did not have an effect on the clinoptilolite structure. The intensity of the peaks of CLIN 0.01 and CLIN 0.1 samples are the same as pristine CLIN. Treating clinoptilolite with solution concentrations of 0.5 M and higher destroys the clinoptilolite crystal structure. It is clearly seen in the XRD patterns of Fig. 4 that intensities of clinoptilolite peaks decrease gradually with acid concentration from 0.5 M. The relative crystallinity of the clinoptilolite phase decreased with an acid concentration above 0.1 M, which can be attributed to dealumination of the structure. The higher the pH of the solution the greater dealumination occurs. The changes of the XRD patterns are especially seen for peaks around 23°. The lowering of the Al concentration was confirmed by the EDXRF analysis (Table 2). Quartz is inert in relation to sulfuric acid, therefore, the intensity of the quartz peaks in the XRD patterns for all samples are similar.

Crystallite sizes were calculated by using the Scherrer and Williamson-Hall equations. In the Scherrer equation [58],

$$D = \frac{k\lambda}{\beta \cos\theta}$$

D is the crystallite size (nm), k is a constant – shape factor (common value is equal to 0.9), λ is the wavelength of the x-ray radiation (for Cu

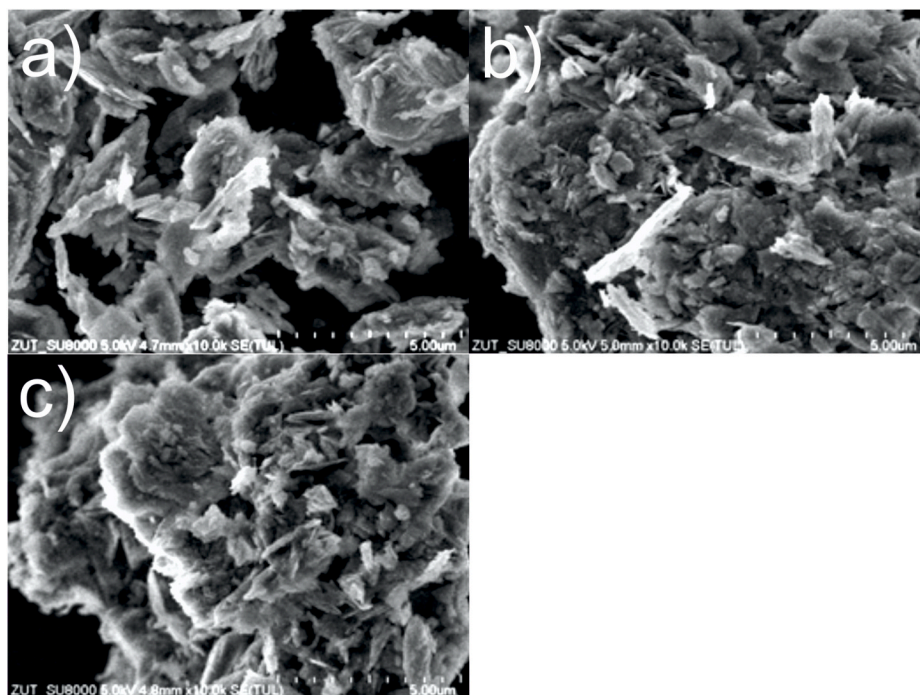


Fig. 3. SEM images a) CLIN, b) CLIN 0.5, c) CLIN 2.

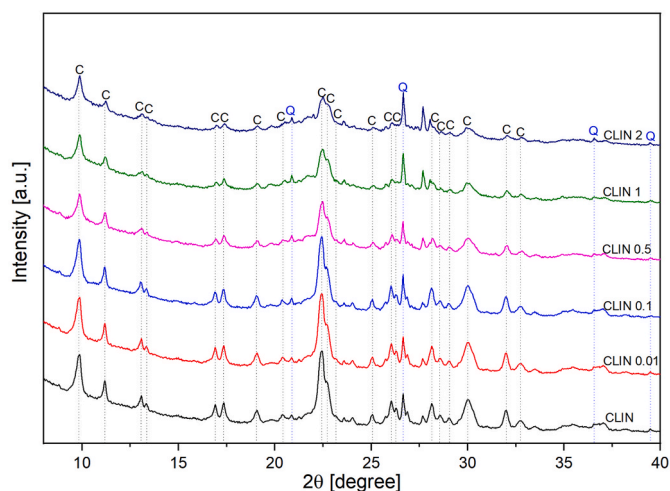


Fig. 4. XRD patterns of clinoptilolite samples.

$K_{\alpha} = 0.1541$ nm), β is the corrected full width at half maximum (FWHM) of broad peaks and θ is the diffraction angle. In the Williamson-Hall equation [59],

$$\beta \cos \theta = \frac{k\lambda}{D} + \eta \sin \theta$$

η is equal to 4ϵ , and ϵ represents microstrain. The corrected FWHM, β , was calculated by subtracting the squares of the instrumental correction (β_m) from the measured FWHM (β_i) [60]:

$$\beta = \sqrt{\beta_m^2 - \beta_i^2}$$

The Scherrer equation is a common method for determining the mean size of crystallites or single crystals but it takes into account broadening of peaks only because of the particle size and cannot be applied for materials with microstrain. The Williamson-Hall equation evaluates simultaneous effects of the size broadening ($k\lambda/D$ – the

Table 2

XRD data of pristine CLIN and JCPDS card 25-1349.

d_{exp} [Å]	d_{ref} [Å]	RE [%]	I_{exp} [%]	I_{ref} [%]
8.976	8.99	0.16%	100	85
7.904	7.91		27	40
6.764	6.76	0.06%	13	15
	6.64			10
	5.93			5
5.239	5.23	0.17%	13	15
5.124	5.12	0.08%	15	30
4.649	4.65	0.02%	14	30
4.35	4.346	0.09%	8	10
3.956	3.971	0.38%	72	100
3.909	3.91	0.03%	46	70
	3.835			10
3.554	3.549	0.14%	11	20
3.42	3.418	0.06%	20	45
	3.383			25
3.184	3.165	0.60%	21	40
3.124	3.122	0.06%	14	25
3.072	3.074	0.07%	9	20
2.967	2.976	0.30%	32	65
2.799	2.794	0.18%	16	40
2.733	2.733	0.00%	9	25

Scherrer equation) and the strain broadening ($\eta \sin(\theta)$). When the strain in the sample reaches 0, the Williamson-Hall formula gives the Scherrer equation [58].

When the Scherrer method was applied, the plot of $\cos(\theta)/K\lambda$ versus $1/\beta$ is produced, and the crystallite size was equal to the slope of the best-fitting line. Williamson-Hall plots, namely $\beta \cos(\theta)$ versus $\sin(\theta)$, were also constructed. The crystallite size was calculated on the basis of the intercept value of the linear plot: $D = k\lambda/\text{intercept}$, and the strain is equal to the slope of the line. The Williamson-Hall plots are presented in Fig. 5, and the results obtained using Scherrer and Williamson-Hall are presented in Table 3.

Table 3 shows the differences between crystallite sizes calculated by the Scherrer and Williamson-Hall methods. The crystallite sizes determined from the Scherrer equation were in the range of 57.5–47.1 nm, and from the Williamson-Hall equation were in the range of 56.8–37.7

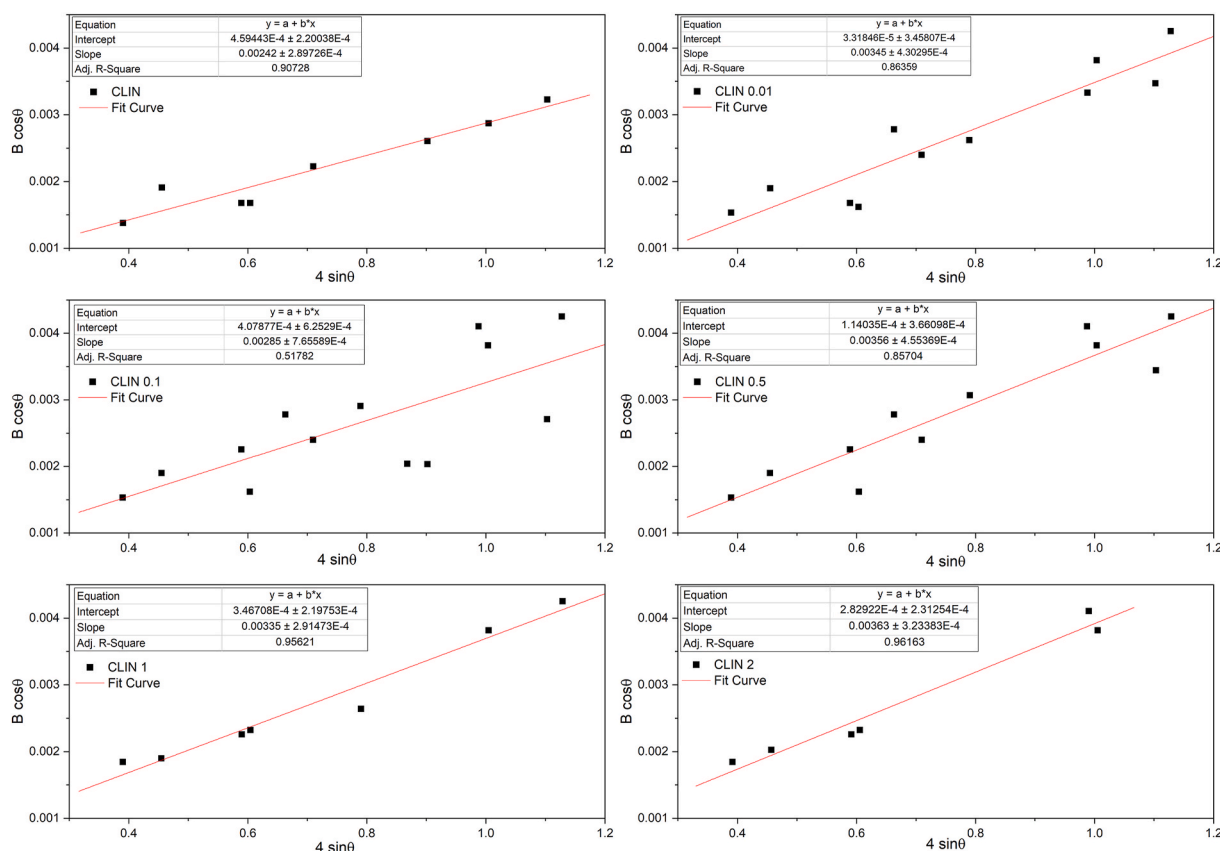


Fig. 5. The Williamson-Hall plots applied for the estimation of the crystallite size of the samples.

Table 3

Sizes of the clinoptilolite sample crystallites calculated by the Scherrer (D_s) and Williamson-Hall (D_{W-H}) methods and microstrain (ϵ).

	D_s [nm]	D_{W-H} [nm]	$\epsilon \cdot 10^3$
CLIN	57.5	56.8	0.46
CLIN 0.01	54.2	53.5	0.03
CLIN 0.1	53.4	48.1	0.41
CLIN 0.5	51.5	45.6	0.11
CLIN 1	49.3	40.9	0.35
CLIN 2	47.1	37.7	0.28

nm. The difference was effected by internal strain not considered in the Scherrer equation. We have observed a positive slope for all the samples, which reveals the tensile strain possibility (Fig. 5). The tensile strain is due to the grain contact coherency and boundary stresses, stacking faults, and triple junction [61]. It was also found that the XRD peaks were getting wider with H_2SO_4 concentration and with the crystallite size becoming smaller.

The results of the elemental analysis via EDXRF are listed in Table 4, and these results are similar to those obtained by other authors [56,57]. We did not identify Na and Ti, but it is a common phenomenon that the same zeolites differ in chemical composition. The reason is the ability to

Table 4

Compositions (in wt%) of clinoptilolite samples as measured via EDXRF.

	Si	Al	K	Mg	Ca	Fe
CLIN	31.86	5.32	2.46	0.36	3.80	2.00
CLIN 0.01	32.53	5.38	2.68	0.34	3.48	2.07
CLIN 0.1	31.38	4.72	2.38	0.28	2.63	1.97
CLIN 0.5	36.09	3.38	2.20	0.13	1.09	1.45
CLIN 1	35.53	2.91	1.73	0.10	0.54	1.09
CLIN 2	37.42	2.69	1.28	0.09	0.37	0.87

exchange the cations.

When zeolite is reacted with an acidic solution, exchange of H^+ ion with exchangeable cations in zeolite (K^+ , Mg^{2+} , Ca^{2+} , Fe^{2+}) occurs and Al removal can transpire. The lowering of aluminum and cation concentrations was quite small for acid concentrations up to 0.1 M. Sulfuric acid did not have an effect on the silicon content. The similar effect is also reported in the publications of other authors [18,62].

Fig. 6 presents N_2 adsorption-desorption isotherms at 77 K.

All the isotherms exhibited Type II isotherm with H3 type hysteresis according to the IUPAC classification [63]. The shape of the isotherm

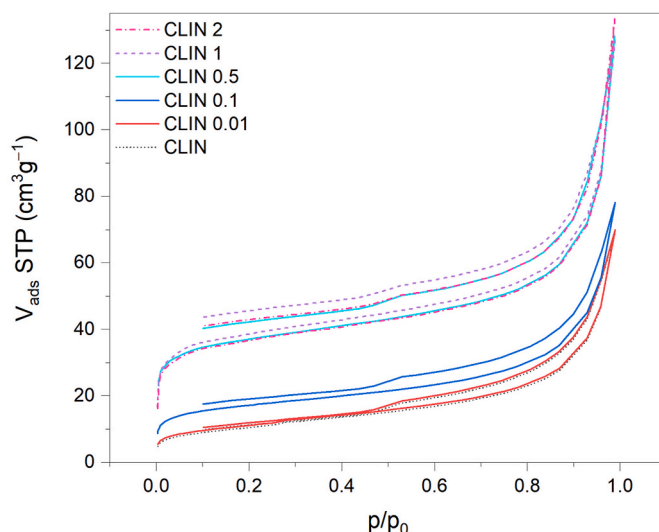


Fig. 6. N_2 adsorption-desorption isotherms of clinoptilolite samples.

indicated unrestricted monolayer-multilayer adsorption and presence of mesopores and macropores. The shape remains the same after acid treatment. The shift in position towards higher y-axis values indicates an increase of pore volume, and the highest increase was observed for CLIN 0.5, CLIN 1, and CLIN 2.

The surface areas, pore volumes (total TPV and micropore MPV), and total acid-sites concentrations of the unmodified and acid-treated clinoptilolite samples are given in Table 5. Additionally Fig. 7 presents the dependence of acid-sites concentration vs. BET plot, and the pore size distributions (PSD) are presented in Fig. 8.

Acid-sites concentration vs. BET plot is presented in Fig. 7. It is clearly seen that there is an exponential relationship between these parameters. The exceptions were the values obtained for CLIN 2. The purpose is that the clinoptilolite structure of CLIN2 was seriously damaged, which is seen on the basis of XRD data (Fig. 4.).

The acid treatment of pristine clinoptilolite with solutions of H_2SO_4 increase the surface area and pore volume of the modified samples. The increase in surface area and pore volume after hydrothermal treatment is caused by the dissolution of the material that blocked the pores. Acid washing of natural zeolites may remove impurities that block pores, progressively eliminating cations, and can increase porosity. On the other hand, too high of an acid concentration (above 1 M) destroys the crystal structure of clinoptilolite, which is associated with a slightly reduced BET surface and volume of pores.

The acid-base titrations of the heterogeneous zeolite catalysts provide evidence for the existence of acid-sites in these materials. A significant increase of acid-sites concentration was observed up to the 0.5 M acid-modified clinoptilolite. A further increase in the acid concentration did not cause a significant increase of acidity of the samples.

The FTIR spectra of the clinoptilolite samples are shown in Fig. 9. The characteristic band at 1628 cm^{-1} and the wide double band between 2900 and 3750 cm^{-1} are attributed to the existence of adsorbed water. Specifically, the broad bands at 3376 and 3622 cm^{-1} can be assigned to the O–H stretching vibration mode of adsorbed water in the zeolite (water molecules associated with Na and Ca in the channels and cages of zeolite structure), intermolecular hydrogen bonding, and Si–OH–Al bridges. The usual bending vibration of H_2O is observed at 1628 cm^{-1} [64–66]. The band at 441 cm^{-1} (bending vibration of O–T–O, where T = Al, Si) is characteristic of the pore opening. The weak band detected at 602 cm^{-1} is assigned to bending vibrations between tetrahedra, particularly to double ring vibrations.

The strongest band at 1016 cm^{-1} is assigned to the asymmetric stretching vibrations of the internal TO_4 tetrahedra. This is the main zeolitic vibration related to Si–O–Si, which can be covered by the stretching vibration of Al–O–Si and Al–O. The position of this band is governed by the Al/Si ratio and is considered to be indicative of the number of Al atoms per formula unit. Very small shifts were observed for CLIN 0.01 (1020 cm^{-1}) and CLIN 0.1 (1022 cm^{-1}). For samples treated with sulfuric acid concentrations higher than 0.1 M, the shift was considerably higher and the band was detected at 1040 cm^{-1} . The shifting to the higher wavenumber (and frequency) of this band is associated with an increase in the ratio of Si/Al in the zeolite framework after the acid modification [66,67].

The band at 790 cm^{-1} belongs to Si–O–Si bonds [66,68]. The more

Table 5
Surface properties of the clinoptilolite samples.

	BET [m^2/g]	TPV [cm^3/g]	MPV [cm^3/g]	Acid-sites concentration [mmol/g]
CLIN	36	0.090	0.002	0.18
CLIN 0.01	40	0.109	0.003	0.28
CLIN 0.1	63	0.121	0.010	0.54
CLIN 0.5	138	0.199	0.035	0.98
CLIN 1	145	0.196	0.035	0.99
CLIN 2	136	0.207	0.033	1.04

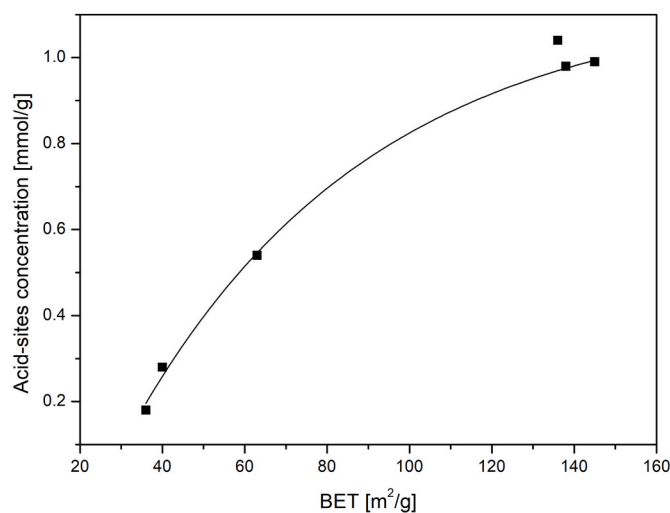


Fig. 7. Acid-sites concentration vs. BET plot.

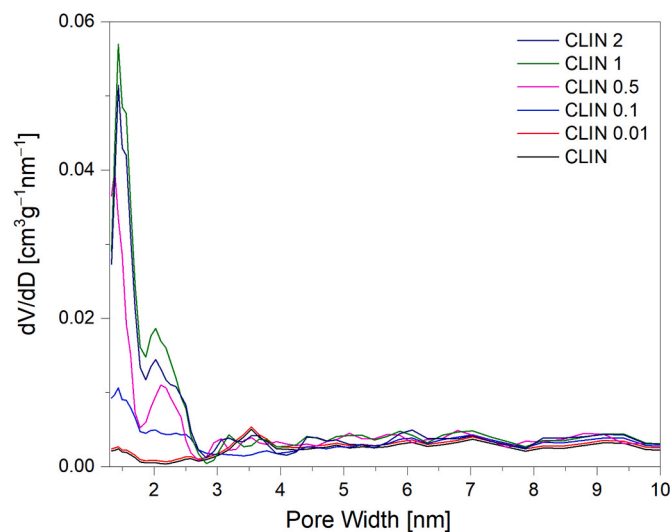


Fig. 8. Pore size distributions of clinoptilolite samples.

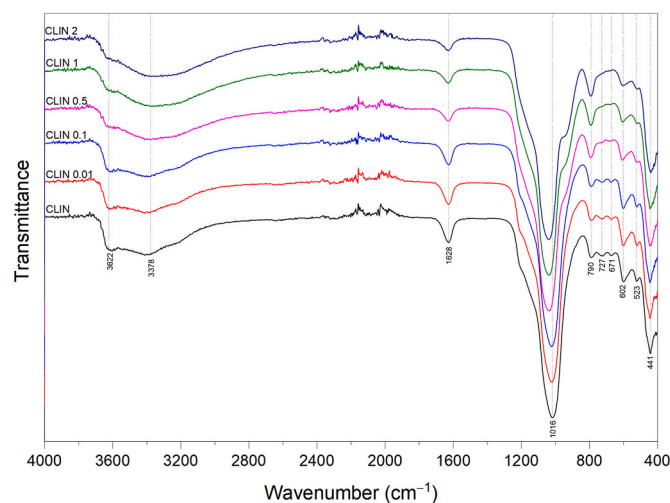


Fig. 9. FTIR spectra of the clinoptilolite samples.

intensive peaks were observed for clinoptilolite treated with acid

concentrations stronger than 0.1 M. It confirms the considerable increase of the Si/Al ratio for the CLIN 0.5, CLIN 1, and CLIN 2 samples.

The bands at 727, 671, 602 and 523 cm^{-1} are assigned to extra-framework cations in the clinoptilolite matrix [64]. These bands were present in the spectra of clinoptilolite treated by 0.01 and 0.1 M acid. The extra-framework cations were completely removed by sulfuric acid with concentration of 0.5 M and higher. The conclusions deduced from the FTIR spectra are consistent with the XRD patterns.

The UV-Vis spectra (Fig. 10) indicate an increase in light absorbance in the 200–900 nm range for 0.01 and 0.1 M acid-modified samples. It is related to the removal of impurities causing the pores to be relatively empty. A further increase in acid concentration causes a significant leaching of certain elements (Al, K, Mg, Ca, Fe), which is associated with a significant reduction in light absorption in the tested range. For all studied samples of clinoptilolite, we can observe one absorption maximum at 249 nm [66]. As the concentration of the acid used for modification of clinoptilolite increases, the intensity of this band decreases and this band shifts to higher wavelength values. There is also a weak absorption band at 272 nm, which disappears as the concentration of acid used for the modification of clinoptilolite increases. There is also an intense absorption band at 302 nm, which shifts towards lower wavelength values as the concentration of the acid used to modify clinoptilolite increases. In the case of three consecutive bands (369, 407 and 496 nm), no shifts of the absorption bands are observed.

3.2. Activities of the clinoptilolite samples

The first series of tests that we performed on the activities of the clinoptilolite samples was to determine the influence of the sulfuric acid concentration on the activity of the clinoptilolite materials. The parameters for the α -pinene isomerization were as follows: temperature 70 °C, catalyst amount 7.5 wt%, and 1 h reaction time. Fig. 11 shows that the best conversion of α -pinene (88 mol%) was achieved after 1 h, and it was obtained for the CLIN 0.1 catalyst. This result can be due to the increase in the specific surface area brought about by the opening of the pores and removal of impurities that was caused by the acid modification. In addition, this procedure allows for an increase in the quantity of acid centers that are active sites in the isomerization process. However, not only do the number of acid centers or the specific surface area determine the activity of the catalyst, a very important factor is the remaining intact structure of clinoptilolite. Treating clinoptilolite with 0.01 M H_2SO_4 caused a slight increase in the textural parameters (surface area, pore and micropore volumes), but did not have an effect on

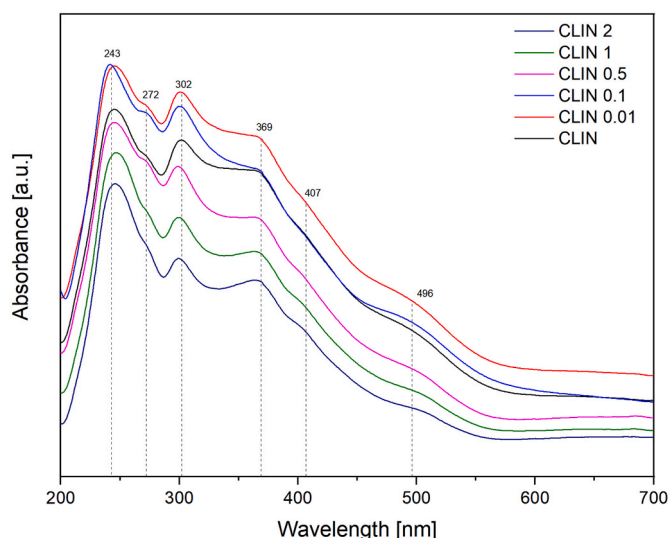


Fig. 10. UV-Vis spectra of clinoptilolite samples.

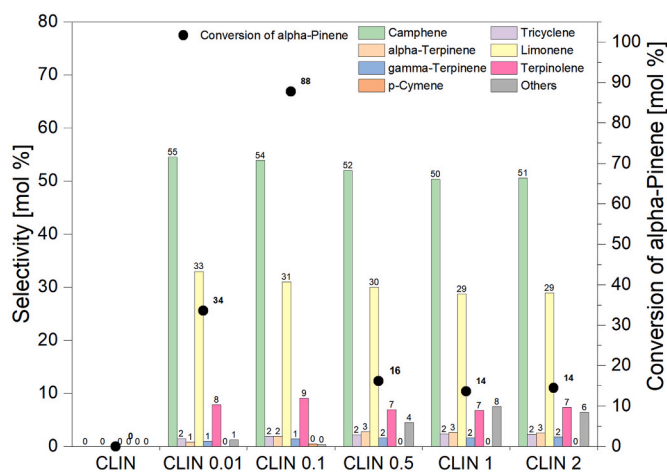


Fig. 11. Activities of modified and unmodified clinoptilolite in α -pinene isomerization (temperature 70 °C, catalyst content 7.5 wt%, and time of 1 h).

the structure. These insignificant changes led to α -pinene conversion of 34% at 70 °C after 1 h. The modification by 0.1 M H_2SO_4 significantly increased the textural parameters, whereas the crystallinity of clinoptilolite still remained intact. A very active catalyst was obtained, and the conversion was equal to 88%. Treatment with an acid concentration higher than 0.1 M initiated damage of the clinoptilolite structure, and despite the high values of textural parameters and acid-sites concentration, the activity of modified clinoptilolite was lowered. The changes in elemental composition of the materials should also be taken into account, as too high a concentration of acid used in the modification can cause leaching of elements, especially the dealumination of the structure of modified samples of clinoptilolite.

Dziedzicka et al. [34] described clinoptilolite modified by HCl solutions and high temperature. They showed that modified clinoptilolites having surface area of about 40 and 60 m^2/g were the most active in α -pinene isomerization, but they were not able to explain why. The lowest temperature at which the reactions were performed by Dziedzicka et al. [34] was equal to 75 °C. After 1 h the conversion of α -pinene was lower than 10% whereas in our investigations over CLIN 0.1 at 70 °C, after 1 h the α -pinene conversion was 88%. The selectivities to camphene and limonene were similar as those that were previously described [34].

It is noticeable from Fig. 11 that as the sulfuric acid concentration used for the clinoptilolite modification increased, selectivity of camphene and limonene slightly decreased (selectivity of the first compound from 55 to 51 mol% and selectivity of the second compound from 33 to 29 mol%). This small decrease can be connected to the change in composition of the catalytic materials, and especially with the change in the amount of the following cationic elements: Al^{3+} , K^+ , Mg^{2+} , Ca^{2+} , Fe^{2+} . The selectivities of the remaining products are similar for all active catalysts and are accordingly (in mol%): tricyclene (1.5–2.5), α -terpinene (1–2), γ -terpinene (1–2), and terpinolene (7–9). The most active CLIN 0.1 catalyst – the catalyst showing the highest α -pinene conversion after 1 h – was used for the next step of our activity tests.

Fig. 12 presents the dependence of conversion of α -pinene on the acid sites concentration.

The results of catalytic tests presented in Fig. 12 are consistent with the results of instrumental tests of modified clinoptilolite samples. The most active sample of clinoptilolite is CLIN 0.1. The samples washed with acid solutions of higher concentration proved to be less active due to the more degraded structure and the reduced amount of aluminum. At the same time, however, they were more active than the unmodified clinoptilolite sample.

The goal of the second stage of research on the activity of modified

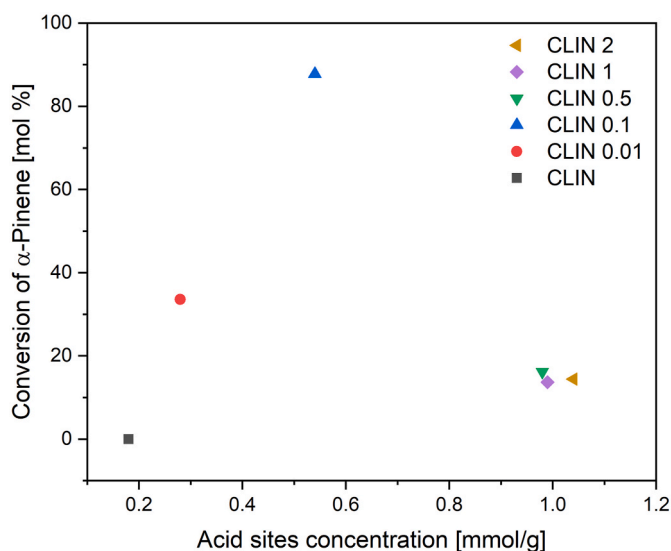


Fig. 12. Dependence of conversion of alpha-pinene on the acid sites concentration in α -pinene isomerization (temperature 70 °C, catalyst content 7.5 wt%, and time of 1 h).

clinoptilolite samples in the α -pinene isomerization was to determine the effect of temperature. The reaction was performed for 1 h with 7.5 wt% of CLIN 0.1 catalyst and in the temperature range of 30–80 °C. The results of these studies are presented in Fig. 13.

Fig. 13 shows that increasing the temperature, increases the α -pinene conversion to 99.44 mol% for 80 °C. The main products, which were created with similar selectivities – in the whole range of tested temperatures (30–80 °C) – were camphene (53–55 mol%) and limonene (29–31 mol%). At 80 °C, the slightly higher selectivity of terpinolene (from 8 to 11 mol%) and lower selectivity of camphene (from 55 to 49 mol%) and limonene (from 31 to 29 mol%), indicate that follow-up reactions, such as, isomerization and dimerization of limonene and camphene to other products, were occurring. The temperature of 70 °C was found to be optimal as this produced the high values for the conversion of α -pinene (89 mol%) and selectivity of camphene (54 mol %).

The next tested parameter was the catalyst content (Fig. 14). For this investigation, a series of studies was performed at 70 °C, and the catalyst

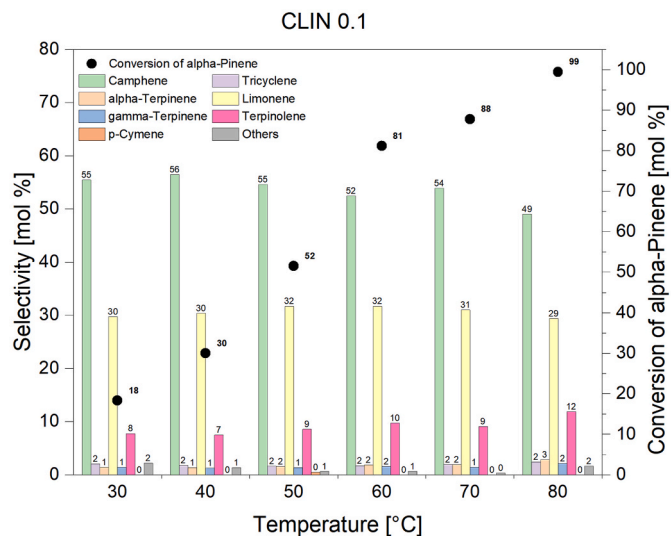


Fig. 13. The effect of process temperature on the course of α -pinene conversion and on the products selectivities over CLIN 0.1 catalyst (catalyst content 7.5 wt %, time of 1 h).

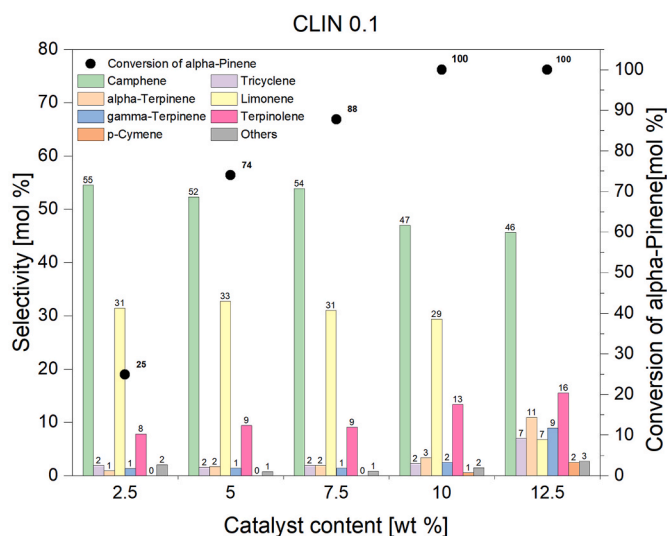


Fig. 14. The effect of the CLIN 0.1 catalyst amount on α -pinene conversion and products selectivities (temperature 70 °C, time 1 h).

content was varied from 2.5 to 12.5 wt%. It is apparent from Fig. 11 that increasing the catalyst amount, increases the conversion of α -pinene to 100 mol% with the catalyst contents of 10 and 12.5 wt%. Moreover, the increase in the CLIN 0.1 material content to above 7.5 wt% did not cause an essential increase in the values of the camphene selectivity but led to the isomerization of limonene in which the following products were formed: α - and γ -terpinene, terpinolene, and *p*-cymene. Studies on the impact of temperature and the content of catalyst indicate that the reaction can be controlled using these parameters, i.e., using a higher temperature can reduce the amount of catalyst required for the reaction or vice versa. The amount of catalyst selected for the next stage was 10 wt%.

The effect of the time of reaction on the isomerization process was studied using an increased quantity of the mixture of α -pinene and catalyst because samples for GC analyses were taken during the course of the reaction. Thus, the organic raw material (α -pinene, 20 g) was mixed with 2 g of clinoptilolite, which was named “CLIN 0.1 catalyst”. Reaction samples were taken for the time of the reaction from 30 to 600 s for the GC analyses. At the studied parameters (Fig. 15), α -pinene reacted completely (conversion of α -pinene was 100 mol%) after 210 s. That α -pinene reacts completely after 210 min can be due to, in part, the highly exothermic reaction, and that we used a larger amount of the

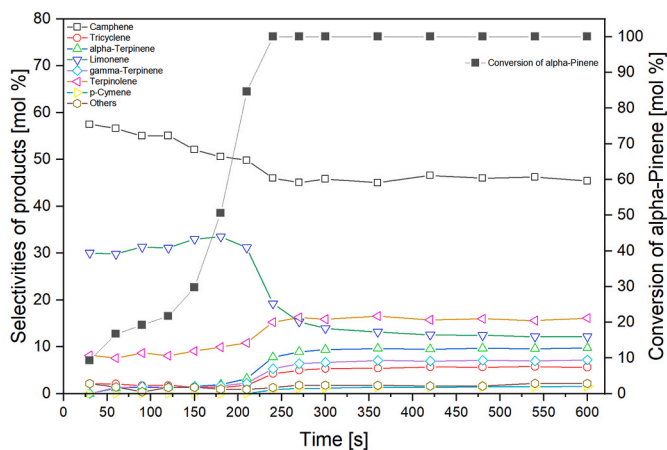


Fig. 15. The effect of time of the isomerization on the values of α -pinene conversion and products selectivity (temperature 70 °C, 10 wt% CLIN 0.1 catalyst amount).

mixture of α -pinene and catalyst. For the 100 mol% α -pinene conversion, the products which achieved the highest values of selectivities (in mol%) were: camphene (50) and limonene (31). The other products that were formed after 210 s were: tricyclene (2), γ -terpinene (2), α -terpinene (3), and terpinolene (11).

From Fig. 15 it is also noticeable that after the reaction time of 240 s, the isomerization of limonene to γ -terpinene begins in the post-reaction mixture (change in selectivity from 2 to 7 mol%), α -terpinene (from 3 to 10 mol%), terpinolene (from 11 to 16 mol%) and *p*-cymene (from 0 to 2 mol%). With the progress of the reaction, the selectivity of camphene decreases from 57 to 45 mol%. This is due to subsequent reactions in which camphene isomerizes to tricyclene.

Fig. 15 also shows that the selectivities of the transformations to all products depend on the reaction time, but only in the range from 30 to 270 s. This relationship is no longer observed for longer reaction times. The dependence of the selectivities of transformations of all products on the conversion of α -pinene is also observed in the same range of reaction times.

3.3. Kinetic studies

The comprehensive kinetic modeling of α -pinene isomerization over clinoptilolite (modified with 0.1 M H₂SO₄ – CLIN 0.1) was performed for several orders, using the following equations:

$$\frac{dC_{\alpha\text{-pinene}}}{dt} = kC_{\alpha\text{-pinene}} \text{ differential rate law for first order} \quad (1)$$

$$\frac{C_A^{1-n} - C_{A_0}^{1-n}}{n-1} = kt \text{ integral rate law for orders different from one} \quad (2)$$

where $C_{\alpha\text{-pinene}}$ is α -pinene concentration, t is reaction time, and k is the reaction rate constant.

The highest regression coefficient ($R^2 = 0.9677$) was obtained for the first-order reaction. This reaction order matches our previous results achieved for α -pinene isomerization over Ti₃C₂ and ex-Ti₃C₂ [33], and similar results were also reported by other authors, namely, Ünveren et al. [36] and Allahverdiev et al. [69].

The calculated value of the reaction rate constant at 70 °C equals 8.19 h⁻¹. This value is more than an order of magnitude higher than reaction rate coefficients calculated for Ti₃C₂ and ex-Ti₃C₂, equal to 0.22 and 0.65 h⁻¹, respectively. It confirms that α -pinene isomerization over clinoptilolite is an exceptionally faster reaction.

The reaction network of the proposed mechanism of α -pinene isomerization over clinoptilolite is given in Fig. 16. Furthermore, the advanced arrangement of α -pinene isomerization was introduced and

presented in Table 6.

A precise reaction mechanism is an essential element of reliable predictive modeling. The proposed reaction mechanism was described by eight reaction paths – columns counted from N (1) to N (8). Chemical equations of the fundamental and intermediate steps, including reactants and surface species, were placed in 17 rows.

In Table 6, unity is synonymous with the occurrence of the sequence of elementary reactions, which must run from reactants to products. For example, 1 (marked by bold and underlined digit at the intersection of 3rd row and 5th column) means that α -pinene leads to terpinolene only when it is supported by an irreversible formation of Z(α -pinene)₂ from Z(α -pinene). Zero indicates that a reaction equation described in a row is not interconnected with a product placed in a column. For example, 0 (marked by bold and underlined digit at the intersection of 10th row and 1st column) means that this is impossible to lead to tricyclene from Z(α -pinene)₂ or (α + γ -terpinene) because both paths are not connected. Unity with minus corresponds to reaction wherein an intermediate product is consumed to final product in one step. For example, -1

Table 6
Reaction mechanism for α -pinene isomerization.

No.	Steps	N (1)	N (2)	N (3)	N (4)	N (5)	N (6)	N (7)	N (8)
1	Z + A \rightleftharpoons Z(A)	1	1	1	1	1	0	0	0
2	Z(A) \rightleftharpoons Z(A) ₁	1	1	0	0	0	0	0	0
3	Z(A) \rightleftharpoons Z(A) ₂	0	0	1	1	<u>1</u>	0	0	0
4	Z(A) ₁ \rightleftharpoons Z(B)	1	0	0	0	0	0	0	0
5	Z(A) ₁ \rightleftharpoons Z(C)	0	1	0	0	0	0	0	0
6	Z(B) \rightleftharpoons Z + B	1	0	0	0	0	0	0	0
7	Z(C) \rightleftharpoons Z + C	0	1	0	0	0	0	0	0
8	Z(A) ₂ \rightleftharpoons Z(D)	0	0	1	0	0	0	0	0
9	Z(D) \rightleftharpoons Z + D	0	0	1	0	0	-1	0	0
10	Z(A) ₂ \rightleftharpoons Z(E)	<u>0</u>	0	0	1	0	0	0	0
11	Z(E) \rightleftharpoons Z + (E)	0	0	0	1	0	0	-1	0
12	Z(A) ₂ \rightleftharpoons Z(F)	0	0	0	0	1	0	0	0
13	Z(F) \rightleftharpoons Z + F	0	0	0	0	1	0	0	<u>-1</u>
14	Z(D) \rightleftharpoons Z(G)	0	0	0	0	1	0	0	0
15	Z(E) \rightleftharpoons Z(G)	0	0	0	0	0	0	1	0
16	Z(F) \rightleftharpoons Z(G)	0	0	0	0	0	0	0	1
17	Z(G) \rightleftharpoons G	0	0	0	0	0	0	0	1

Note: N(1) α -pinene = tricyclene, N(2) α -pinene = camphene, N(3) α -pinene = limonene, N(4) α -pinene = α + γ -terpinene, N(5) α -pinene = terpinolene, N(6) limonene = *p*-cymene, N(7) α + γ -terpinene = *p*-cymene, N(8) terpinolene = *p*-cymene; Z denotes surface sites.

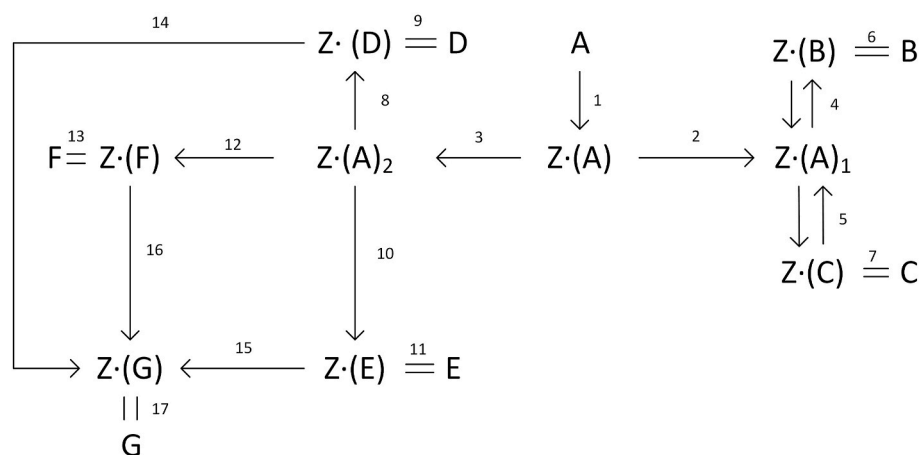


Fig. 16. Reaction network of the mechanism of α -pinene isomerization. Note: A - α -pinene, B - tricyclene, C - camphene, D - limonene, E - α + γ -terpinene, F - terpinolene, G - *p*-cymene.

(marked by bold and underlined digit at the intersection of 13th row and 8th column) means that *p*-cymene as final product is formed in one step from terpinolene (intermediate product).

For the analysis of the detailed kinetic modeling, several differential equations (2)–(5) were tested by rearranging the kinetic equations for selectivity:

$$-\frac{dC_B}{dC_A} = f_1 + f_2 \frac{C_C}{C_A} - f_3 \frac{C_B}{C_A} \quad (3)$$

$$-\frac{dC_C}{dC_A} = f_4 - f_2 \frac{C_C}{C_A} + f_3 \frac{C_B}{C_A} \quad (4)$$

$$-\frac{dC_D}{dC_A} = f_5 - f_6 \frac{C_D}{C_A} \quad (5)$$

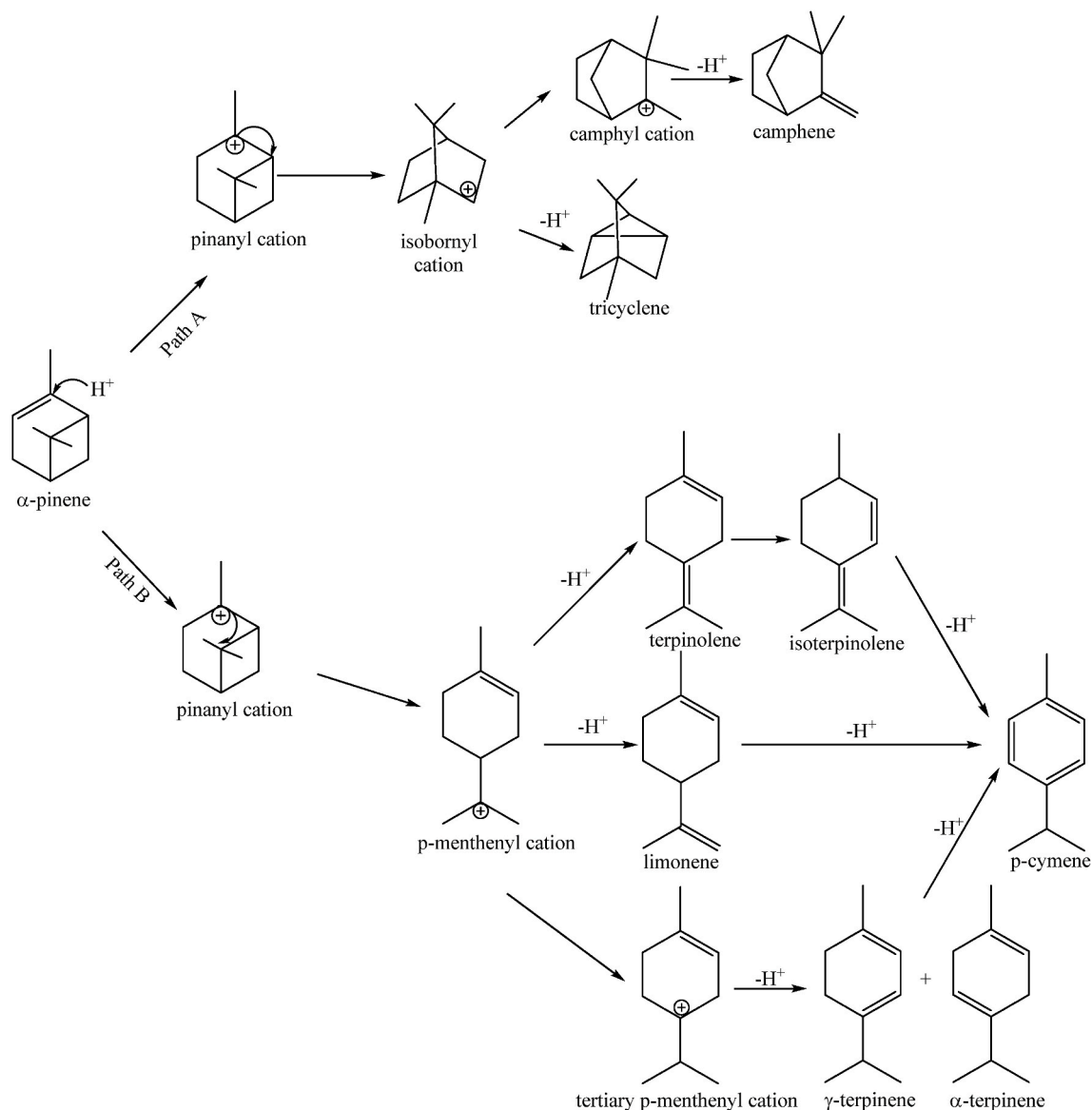
$$-\frac{dC_G}{dC_A} = f_7 \frac{C_D}{C_A} + f_8 \frac{C_E}{C_A} + f_9 \frac{C_F}{C_A} \quad (6)$$

For undermentioned modeling one assumption was made: the rates leading to camphene and tricyclene ($1 \rightarrow 2 \rightarrow 5 \rightarrow 7$); ($1 \rightarrow 2 \rightarrow 4 \rightarrow 6$) as

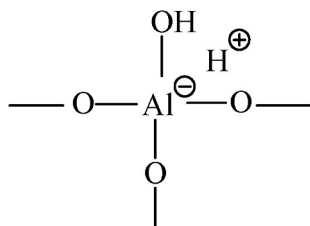
well *p*-cymene ($3 \rightarrow 8 \rightarrow 11 \rightarrow 14$); ($3 \rightarrow 9 \rightarrow 12 \rightarrow 14$) ($3 \rightarrow 10 \rightarrow 13 \rightarrow 14$) are not interrelated.

The values of the dimensionless parameters in equations (2)–(5) were obtained for α -pinene isomerization over clinoptilolite and are compiled in Table 7 with their standard errors.

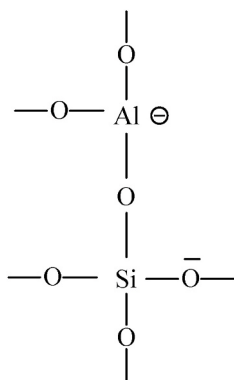
The proposed model and mechanism fit the experimental data. Obviously, calculated empirical dimensionless parameters for α -pinene isomerization over clinoptilolite achieved significantly different values from those obtained over Ti_3C_2 and ex- Ti_3C_2 . Moreover, the quantity of these parameters is reduced in comparison with earlier studies. In our two previous publications presenting the isomerization of α -pinene over the Ti-SBA-15 catalyst and the isomerization of limonene over clinoptilolite, we presented the basis of the mechanism of the isomerization of α -pinene and limonene, including the use of clinoptilolite as the catalyst [31,70]. The α -pinene isomerization is characterized by two pathways. In the first (Path A) bicyclic products can be formed (camphene and tricyclene) and the second path (Path B) leads to the formation of monocyclic products, such as limonene, terpinolene, terpinenes, and, in the subsequent reaction, *p*-cymene [31]:



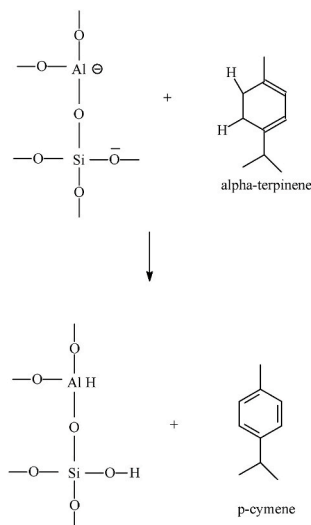
In both pathways, a main role is played by a proton derived from a strongly acidic site (Brønsted acidic site of aluminum):



This proton attaches to the double bond in the α -pinene molecule, and this initiates a cycle of transformations of the resulting carbocation, as a result of which, after the elimination of the proton, we can obtain camphene, tricyclene, limonene, terpinolene and terpinenes. The *p*-cymene formation may be based on transformations of limonene, terpinolene and terpinenes with the help of a proton derived from the Brønsted acidic site or on the direct dehydrogenation of α -terpinene at the Lewis acid site of aluminum presented below [70]:



The manner of dehydrogenation of α -terpinene at the Lewis acid site of aluminum can be presented in the following way [70]:



4. Conclusions

Conversion of α -pinene obtained from biomass into the high value-added substances, camphene and limonene, is an important area of study. Development of green heterogeneous catalysts with high activity at low temperature is essential for resource-efficiency optimization and

Table 7
Statistical parameters.

Dimensionless parameter	Estimated value	Standard error (\pm)
f_1	0.01	0.0038
f_2	0.08	0.0017
f_3	0.08	0.0039
f_4	0.43	0.0283
f_5	0.59	0.0307
f_6	0.32	0.0171
f_7	0.03	0.0082
f_8	0.03	0.0079
f_9	0.03	0.0071

energy saving. This study demonstrates the efficacy of clinoptilolite modified by 0.1 M H_2SO_4 as the green catalyst. CLIN 0.1 is cheap to produce, ecological and very active in α -pinene isomerization. CLIN 0.1 was active even at the low temperature of 30 °C, and after 1 h, 18% conversion was achieved. At 70 °C, after just 4 min, 100% conversion was attained. After the reaction, the catalyst does not contain harmful substances and is easy to dispose of. Moreover, the clinoptilolite modification process does not require complicated and expensive equipment and is easy to perform on a large scale.

The main products and their selectivities (in mol%) were as follows: camphene (about 50%) and limonene (about 31%). Other equally valuable products include: tricyclene (2%), γ -terpinene (2%), α -terpinene (3%), and terpinolene (11%). The isomerization of α -pinene over CLIN 0.1 at 70 °C followed first-order kinetics. A comparison of the presented results (temperature of 70 °C) with our previous results obtained for Ti_3C_2 [33] and the results of Dziejzicka et al. [34] obtained for the best catalyst, clinoptilolite modified with HCl solution, revealed the overwhelming efficiency of our new modified catalyst. The calculated value of the reaction rate constant ($8.19 h^{-1}$ for temperature 70 °C) of our modified catalyst is over 10 times higher in respect to exfoliated Ti_3C_2 ($0.65 h^{-1}$) and over 60 times higher than for clinoptilolite modified by HCl solutions ($0.13 h^{-1}$). Table 1 also shows that in our studied it was possible to obtain 100% mol conversion of α -pinene with respective selectivities of transformation to camphene and limonene of 55 and 29 mol%, and during a very short reaction time of 4 min. Comparable values of conversion of α -pinene and selectivities of these two products were obtained for exfoliated- Ti_3C_2 and $[HSO_3-(CH_2)_3-NEt_3]Cl-ZnCl_2$ catalysts but in considerable longer reaction time 6 and 4 h, respectively.

Finally, we concluded that the activity of modified clinoptilolite in α -pinene isomerization is a multi-parameter function of textural properties, crystallinity, chemical composition, and acid-sites concentration.

CRediT authorship contribution statement

Piotr Miądlicki: Investigation, Formal analysis, Data curation, Writing – original draft. **Agnieszka Wróblewska:** Conceptualization, Supervision, Writing – original draft, Writing – review & editing. **Karolina Kielbasa:** Investigation, Writing – original draft. **Zvi C. Koren:** Writing – original draft, Writing – review & editing. **Beata Michalkiewicz:** Investigation, Writing – original draft, Writing – review & editing.

Declaration of competing interest

The authors declare that they have no known competing financial interests or personal relationships that could have appeared to influence the work reported in this paper.

Acknowledgments

We would like to thank Erdem Ayzazoğlu, Rota Mining Corporation, Turkey, for the clinoptilolite samples.

- ammonium surfactant and dithizone for the voltammetric determination of Sn(II), *J. Colloid Interface Sci.* 501 (2017) 321–329, <https://doi.org/10.1016/j.jcis.2017.04.068>.
- [50] H. Derikvand, A. Nezamzadeh-Ejehieh, Comprehensive study on enhanced photocatalytic activity of heterojunction ZnS-NiS/zeolite nanoparticles: experimental design based on response surface methodology (RSM), impedance spectroscopy and GC-MASS studies, *J. Colloid Interface Sci.* 490 (2017) 652–664, <https://doi.org/10.1016/j.jcis.2016.11.105>.
- [51] L. Jarosz, D. Stępień-Pyśniak, Z. Gradzki, M. Kapica, A. Gacek, The effect of feed supplementation with zakarpacki zeolite (clinoptilolite) on percentages of T and B lymphocytes and cytokine concentrations in poultry, *Poultry Sci.* 96 (2017) 1–7, <https://doi.org/10.3382/ps/pex030>.
- [52] H. Valpotic, D. Gračner, R. Turk, D. Đuričić, S. Vince, I. Folnožić, M. Lojkić, I.Ž. Žaja, L. Bedrica, N. Mačesić, I. Getz, T. Dobranić, M. Samardžija, Zeolite clinoptilolite nanoporous feed additive for animals of veterinary importance: potentials and limitations, *Period. Biol.* 119 (2017) 159–172, <https://doi.org/10.18054/pb.v119i3.5434>.
- [53] L. Vilcoq, V. Spinola, P. Moniz, L.C. Duarte, F. Carvalheiro, C. Fernandes, P. Castilho, Acid-modified clays as green catalysts for the hydrolysis of hemicellulosic oligosaccharides, *Catal. Sci. Technol.* 5 (2015) 4072–4080, <https://doi.org/10.1039/c5cy00195a>.
- [54] M. Abatal, A.V.C. Quiroz, M.T. Olguín, A.R. Vázquez-Olmos, J. Vargas, F. Anguebes-Franseschi, G. Giacomani-Vallejos, Sorption of Pb(II) from aqueous solutions by acid-modified clinoptilolite-rich tuffs with different Si/Al ratios, *Appl. Sci.* 9 (2019), <https://doi.org/10.3390/app9122415>.
- [55] K. Elaiopoulos, T. Perraki, E. Grigoropoulou, Monitoring the effect of hydrothermal treatments on the structure of a natural zeolite through a combined XRD, FTIR, XRF, SEM and N₂-porosimetry analysis, *Microporous Mesoporous Mater.* 134 (2010) 29–43, <https://doi.org/10.1016/j.micromeso.2010.05.004>.
- [56] A. Nezamzadeh-Ejehieh, S. Moenirad, Heterogeneous photocatalytic degradation of furfural using NiS-clinoptilolite zeolite, *Desalination* 273 (2011) 248–257, <https://doi.org/10.1016/j.desal.2010.12.031>.
- [57] A. Nezamzadeh-Ejehieh, K. Shirvani, CdS loaded an Iranian clinoptilolite as a heterogeneous catalyst in photodegradation of p -aminophenol, *J. Chem.* 2013 (2013) 1–11, <https://doi.org/10.1155/2013/541736>.
- [58] N. Pourshirband, A. Nezamzadeh-Ejehieh, S. Nezamoddin Mirsattari, The coupled AgI/BiOI catalyst: synthesis, brief characterization, and study of the kinetic of the EBT photodegradation, *Chem. Phys. Lett.* 761 (2020) 138090, <https://doi.org/10.1016/j.cplett.2020.138090>.
- [59] T. Tamiji, A. Nezamzadeh-Ejehieh, Electrocatalytic behavior of AgBr NPs as modifier of carbon past electrode in the presence of methanol and ethanol in aqueous solution: a kinetic study, *J. Taiwan Inst. Chem. Eng.* 104 (2019) 130–138, <https://doi.org/10.1016/j.jtice.2019.08.021>.
- [60] G.T. Anand, L.J. Kennedy, J.J. Vijaya, K. Kaviyaranan, M. Sukumar, Structural, optical and magnetic characterization of Zn_{1-x}Ni_xAl₂O₄ (0 ≤ x ≤ 5) spinel nanostructures synthesized by microwave combustion technique, *Ceram. Int.* 41 (2015) 603–615, <https://doi.org/10.1016/j.ceramint.2014.08.109>.
- [61] A. Norouzi, A. Nezamzadeh-Ejehieh, Preparation, characterization, and investigation of the catalytic property of α-Fe₂O₃-ZnO nanoparticles in the photodegradation and mineralization of methylene blue, *Chem. Phys. Lett.* 752 (2020) 137587, <https://doi.org/10.1016/j.cplett.2020.137587>.
- [62] S. Sharifian, A. Nezamzadeh-Ejehieh, Modification of carbon paste electrode with Fe (III)-clinoptilolite nano-particles for simultaneous voltammetric determination of acetaminophen and ascorbic acid, *Mater. Sci. Eng. C* 58 (2016) 510–520, <https://doi.org/10.1016/j.msec.2015.08.071>.
- [63] K. Sing, Reporting physisorption data for gas/solid systems with special reference to the determination of surface area and porosity, *Pure Appl. Chem.* 57 (1985) 603–619, <https://doi.org/10.1351/pac198557040603>.
- [64] D. Ruiz-Serrano, M. Flores-Acosta, E. Conde-Barajas, D. Ramírez-Rosales, J. M. Yáñez-Limón, R. Ramírez-Bon, Study by XPS of different conditioning processes to improve the cation exchange in clinoptilolite, *J. Mol. Struct.* 980 (2010) 149–155, <https://doi.org/10.1016/j.molstruc.2010.07.007>.
- [65] E.P. Favvas, C.G. Tsanaktsidis, A.A. Sapalidis, G.T. Tzilantonis, S.K. Papageorgiou, A.C. Mitropoulos, Clinoptilolite, a natural zeolite material: structural characterization and performance evaluation on its dehydration properties of hydrocarbon-based fuels, *Microporous Mesoporous Mater.* 225 (2016) 385–391, <https://doi.org/10.1016/j.micromeso.2016.01.021>.
- [66] A. Nezamzadeh-Ejehieh, A. Shirzadi, Enhancement of the photocatalytic activity of Ferrous Oxide by doping onto the nano-clinoptilolite particles towards photodegradation of tetracycline, *Chemosphere* 107 (2014) 136–144, <https://doi.org/10.1016/j.chemosphere.2014.02.015>.
- [67] T. Ramishvili, V. Tsitsishvili, R. Chedia, E. Sanaia, V. Gabunia, N. Kokiashvili, Preparation of ultradispersed crystallites of modified natural clinoptilolite with the use of ultrasound and its application as a catalyst in the synthesis of methyl salicylate, *Am. J. Nano Res. Appl.* 5 (2017) 26–32, <https://doi.org/10.11648/j.nano.s.2017050301.17>.
- [68] A. Aghadavoud, K.R.E. Sarae, H.R. Shakur, R. Sayyari, Removal of uranium ions from synthetic wastewater using ZnO/Na-clinoptilolite nanocomposites, *Radiochim. Acta* 104 (2016) 809–819, <https://doi.org/10.1515/ract-2016-2586>.
- [69] A.I. Allahverdiev, S. Irandoust, D.Y. Murzin, Isomerization of α-pinene over clinoptilolite, *J. Catal.* 185 (1999) 352–362, <https://doi.org/10.1006/jcat.1999.2474>.
- [70] M. Retajczyk, A. Wróblewska, A. Szymańska, B. Michalkiewicz, Isomerization of limonene over natural zeolite-clinoptilolite, *Clay Miner.* 54 (2019) 121–129, <https://doi.org/10.1180/clm.2019.18>.

Article

Activated Carbon Modification towards Efficient Catalyst for High Value-Added Products Synthesis from Alpha-Pinene

Joanna Sreńscek-Nazzal ^{1,*}, Adrianna Kamińska ¹, Piotr Miądlicki ¹, Agnieszka Wróblewska ^{1,*},
Karolina Kielbasa ¹, Rafał Jan Wróbel ¹, Jarosław Serafin ² and Beata Michalkiewicz ¹

- ¹ Department of Catalytic and Sorbent Materials Engineering, Faculty of Chemical Technology and Engineering, West Pomeranian University of Technology in Szczecin, Piastów Ave. 42, 71-065 Szczecin, Poland; kaminska.adrianna@zut.edu.pl (A.K.); piotr.miadlicki@zut.edu.pl (P.M.); Karolina.Kielbasa@zut.edu.pl (K.K.); rafal.wrobel@zut.edu.pl (R.J.W.); Beata.Michalkiewicz@zut.edu.pl (B.M.)
- ² Barcelona Research Center in Multiscale Science and Engineering, Department of Chemical Engineering, Institute of Energy Technologies, Technical University of Catalonia, Eduard Maristany 16, 08019 Barcelona, Spain; jaroslaw.serafin@upc.edu
- * Correspondence: jsrenscek@zut.edu.pl (J.S.-N.); Agnieszka.Wroblewska@zut.edu.pl (A.W.)

Abstract: DT0-activated carbons modified with HCl and HNO₃ acids, which were used for the first time in the catalytic process of alpha-pinene isomerization, are presented in this study. The carbon materials DT0, DT0_HCl, DT0_HNO₃, and DT0_HCl_HNO₃ were examined with the following methods: XRF, SEM, EDX, XPS, FT-IR, XRD, and N₂ adsorption at −196 °C. It was shown that DT0_HCl_HNO₃-activated carbon was the most active material in the alpha-pinene isomerization process. Detailed studies of alpha-pinene isomerization were carried out over this carbon by changing the reaction parameters such as time (5–180 min) and temperature (60–175 °C). The 100% conversion of alpha-pinene was achieved at the temperature of 160 °C and catalyst content of 5 wt% after 3 h over the DT0_HCl_HNO₃ catalyst. Camphene and limonene were the main products of the alpha-pinene isomerization reaction.

Keywords: alpha-pinene isomerization; commercial activated carbon; acid treatment



Citation: Sreńscek-Nazzal, J.; Kamińska, A.; Miądlicki, P.; Wróblewska, A.; Kielbasa, K.; Wróbel, R.J.; Serafin, J.; Michalkiewicz, B. Activated Carbon Modification towards Efficient Catalyst for High Value-Added Products Synthesis from Alpha-Pinene. *Materials* **2021**, *14*, 7811. <https://doi.org/10.3390/ma14247811>

Academic Editor: Antonio Gil Bravo

Received: 8 November 2021

Accepted: 15 December 2021

Published: 17 December 2021

Publisher's Note: MDPI stays neutral with regard to jurisdictional claims in published maps and institutional affiliations.



Copyright: © 2021 by the authors. Licensee MDPI, Basel, Switzerland. This article is an open access article distributed under the terms and conditions of the Creative Commons Attribution (CC BY) license (<https://creativecommons.org/licenses/by/4.0/>).

1. Introduction

In recent years, there has been a growing interest in commercial, porous, activated carbons as materials that can be used in many fields of research. Due to the developed specific surface and porosity, activated carbons belong to the group of materials of various applications and constantly growing practical importance.

Currently, activated carbons (AC) are obtained from raw materials rich in elemental carbon, which include waste materials from industry and agriculture or alternative materials. Materials that belong to the first group and are used on an industrial scale include coconut shell [1] and nutshell [2].

Another group are alternative materials that are used in the production of commercial activated carbons. This group includes, among others: charcoal [3], peat [4–6] anthracite [7–9] wood [10–12], and municipal solid waste [13]. The content of elemental carbon in agricultural and industrial waste is lower than in the alternative materials [14]; therefore, the efficiency of the production of activated carbons from waste materials is lower than in the case of AC production from alternative materials [15].

Activated carbons are characterized by a well-developed porous structure and a large specific surface area as well as varying surface chemistry. The chemical properties of carbonaceous materials are attributed to the presence of various functional groups and heteroatoms (oxygen, nitrogen, hydrogen, sulfur, potassium, sodium, aluminum, and phosphorus) [16]. The presence of these atoms in the structure of activated carbons may result from their introduction into the carbon matrix during precursor activation/post-

synthesis modification or may result from the content of these elements in the raw material used [17,18].

Modification is a promising and effective way to increase the functionality of carbonaceous materials, which can then be used in many fields [19,20]. In order to improve the chemical properties, the surface modification of activated carbons is used. Surface modification can be divided into thermal modification [21] and chemical modification [22]. In addition, there are reports in the literature on the biological modification of activated carbons (using bacteria) [23,24].

Chemical modification, in turn, is divided into liquid and gas modification [25]. The most widely studied compounds used for liquid modification are nitric acid [26], sulfuric acid [27,28] phosphoric acid [28,29], hydrochloric acid [30], and hydrogen peroxide [31].

The modification of activated carbons with acids allows for the oxidation of their surface and an increase in the hydrophilicity of the surface of the carbonaceous material. In addition, during acid treatment, non-organic and ash residues are removed from the material. This process also increases the acidic properties of the activated carbons that have been treated with the acid [32].

In the work presented by Aggarwal et al., granulated activated carbon was subjected to a liquid-phase oxidation process in the presence of nitric acid, ammonium persulfate, and hydrogen peroxide. Modification with these compounds increased the number of oxygen groups on the surface of the tested materials and thus allowed for the increase of the functionality of the granulated activated carbons [33].

Another team used HNO_3 to modify activated carbons. It was reported that the oxygen functional groups that were mainly formed were carboxylic acid, phenolic, lactone, and quinol groups. The presented results clearly indicated the relationship between the presence of oxygen functional groups and the activity of active carbons in the tested process. It was concluded that, along with the increase in the number of functional groups on the surface of activated carbon, its sorption capacity increased [34].

In the work presented by the team of Strelko [35], commercial activated carbon was treated with nitric acid in order to introduce acid functional groups into the material. The acid treatment resulted in a decrease in the surface area and pore volume and at the same time, the modified carbon was characterized by an acid surface (the dominant surface functional groups were carboxyl groups). After the modification, the sample showed cation-exchange activity in a wide pH range; thus, it was more active in the investigated metal adsorption process.

Activated carbon was also modified with HCl and NaOH solutions [36]. The carbonaceous material exposed to HCl and KOH was characterized by the presence of (carboxyl, hydroxyl, and carbonyl) functional groups. Chemical treatment changed the surface of functional groups, surface morphology, and texture of the activated carbon. Modification with HCl and NaOH increased the adsorption selectivity of the tested activated carbon.

Wu et al. [30] used HCl, HNO_3 , and NaOH as compounds to modify the surface of activated carbon. It was noticed that the number of C-O functional groups increased for the carbons subjected to acid modification, while their number decreased after alkaline modification. By means of chemical activation, the modified activated carbon showed a higher adsorption efficiency of organic chemicals.

Xu et al. [37] used HNO_3 in various concentrations to modify the surface of the activated carbon. For activated carbons after modification, an increase in the number of carboxyl groups was observed as compared to the untreated activated carbon. As the concentration of the HNO_3 solution increased (up to 20% of HNO_3 solutions), the amount of functional groups on the AC surface also increased and then decreased (50% of HNO_3 solution). By chemically modifying the surface, this carbon became more efficient in the ion Pb^{2+} adsorption process.

Activated carbons subjected to surface modification with acids have found application in many chemical processes. They have been widely used to adsorb many chemical compounds, including azo dyes [38], acid dyes [39], mercury [40], benzene and

toluene [41], VOC (volatile organic compounds) [42], lead [43], chromium [44], and manganese ions [45]. Modified activated carbons have also been used in electrochemistry as supercapacitors [46–48] and as capacitive and pseudocapacitive energy storage devices in supercapacitors [49]. In catalysis, acid-modified activated carbons have been used as catalysts for acetylation of glycerol [50], in oxidative carbonylation of methanol [51], esterification of fatty acids [52], and the synthesis of N-alkylimidazoles and imidazolium ionic liquids [53].

Alpha-pinene belongs to the group of monoterpenes with the general formula $C_{10}H_{16}$. Taking into account the fact that this compound has a double bond between carbon atoms, it can be transformed into many useful compounds. These compounds can be used in many industries [54].

The main products of alpha-pinene isomerization are camphene and limonene. The first is a bicyclic monoterpene with a pleasant camphor scent. Camphene is characterized by strong aromatic properties, thanks to which it has been used in many industries. In the perfume industry, camphene is used as one of the fragrance components. The use of essential oils based on camphene in the food industry is aimed at improving the smell and deepening the taste of dishes [55]. Additionally, thanks to its fragrance properties, camphene has a repellent effect against various insects [56].

Limonene belongs to single-ring monoterpenes with a characteristic citrus scent. Limonene can be obtained by steam distillation from the peel of citrus fruits [57]. In the food industry, this compound is used as a flavoring additive to improve the taste and aroma of dishes. In the cosmetics industry, limonene is used in the production of cosmetics [58]. Limonene has also been used as a bio-solvent in the household chemistry industry [59] and as a natural and ecological repellent [60].

The isomerization of alpha-pinene on an industrial scale is carried out with TiO_2 acidic catalyst, and the temperature of the process ranges from 150 to 170 °C. One of the disadvantages of this method is the fact that the catalyst must be synthesized “in situ” because it is not commercially available. Moreover, the reaction rate is slow [61], and the selectivity to bicyclic and monocyclic terpenes is insufficient [62].

At present, the aim is to use catalysts that show higher activity and selectivity for the main products of alpha-pinene isomerization. The catalysts that have been used in the alpha-pinene isomerization reaction are zeolites [63], silica [64,65], ion exchange resin [55], H-mordenite molecular sieves [62], $2D Ti_3C_2TxMXene$ [66], zirconium sulfate [67], activated TiO_2 [68], and natural aluminosilicates modified with acid [69].

This paper presents the process of alpha-pinene isomerization over commercial DT0 catalysts modified with hydrochloric and nitric acids. To the best of our knowledge, such catalysts have not been used in the alpha-pinene isomerization up to now. In these studies, we used commercial carbon DT0, which was modified in a different way than in our previous work [70], in which activated carbon (EuroPh and FPV) was modified with plasma. An advantage of the acid-modified DT0 catalyst was that it was obtained with a simple, one-step, low-cost method compared to the expensive activated carbon plasma modification method. Our research aimed to compare the activity of modified DT0 catalysts under specified conditions of alpha-pinene isomerization. The influence of temperature on the rate of alpha-pinene isomerization was investigated for the most active catalyst in the reaction. The catalytic activity was determined by the alpha-pinene conversion values and the selectivity of limonene and camphene. The conducted studies also provided significant information related to the physicochemical characteristics of the DT0 modified carbons.

2. Materials and Methods

2.1. Chemicals and Materials

Commercial activated carbon DT0 with diameter grain 0.5 mm (Grand Activated, Hajnówka, Poland) was selected as the starting material for preparing catalysts for the alpha-pinene isomerization process. Hydrochloric acid (35%–38% p.a., CHEMPUR, Piekary

Śląskie, Poland) and nitric acid (65% p.a., CHEMPUR, Piekary Śląskie, Poland) were used to treat ACs. The acid-treated ACs will be referred to by their name and type of acid used for treatment. Samples with commercial activated carbon treated with HCl will be named DT0_HCl, with HNO₃—DT0_HNO₃, and with both—DT0_HCl_HNO₃.

Modification of ACs with Acids

ACs were treated with hydrochloric and nitric acids. A commercial activated carbon was continuously modified in different ways: first with hydrochloric acid; second with nitric acid; and for the last one, two-step modification was used and, finally, a two-step process (firstly with hydrochloric and then nitric acid) to prepare modified ACs with different acid groups. First, 10 g of activated carbon named DT0 was ultrasonically washed with deionized water to remove small activated carbon powder. The sample was poured into a round bottom flask and placed in a heating mantle (CHEMLAND, Stargard, Poland). Then 100 mL of hydrochloric acid (at an acid to DT0 ratio of 1:1) was added into a round bottom flask, and the obtained mixture was refluxed. AC modification was continued for 2 h. Finally, activated carbon was washed repeatedly with deionized water until pH was constant and dried at 120 °C overnight. The same procedure was used with nitric acid.

2.2. Textural Properties and Chemical Characterization of the Carbons

The textural parameters of the modified ACs were investigated with N₂ adsorption/desorption at −196 °C using an ASAP 2460 instrument (Micrometrics, Norcross, GA, USA). The samples were degassed at 250 °C in a vacuum environment for 14 h before measurements. Experimental adsorption data at a relative pressure (P/P_0) of less than 0.3 were used to calculate surface area values using the standard Brunauer, Emmett, and Teller (BET) equation. The pore size distribution was determined using the density functional theory (DFT) based on nitrogen adsorption data. For the DFT method, the N₂-DFT adsorption slit model was used.

The elemental composition of modified catalysts was examined using the energy dispersive X-ray fluorescence (ED-XRF) (Epsilon 3, PanAnalytical, Almelo, The Netherlands). The measurement was performed in a helium atmosphere using the OMNIAN standardless analysis program.

The morphology of the samples was observed via scanning electron microscopy with cold emission (SU8020, Ultra-High Resolution Field Emission Scanning Electron Microscope; Hitachi Ltd., Hitachi City, Japan). Images were taken with a 5 kV accelerating voltage using a triple detector system. The microscope was additionally equipped with an Energy Dispersive Spectroscopy system (EDS; EDSNSS312, Thermo Fisher Scientific, Waltham, MA, USA), owing to which qualitative analysis could be performed.

FTIR spectra of the modified carbon samples were obtained utilizing a Nicolet 380 ATR-FTIR spectrometer (Thermo Fisher Scientific Inc., Waltham, MA, USA). Before the spectrum of a sample was recorded, the background line obtained was arbitrarily and automatically subtracted. The spectra were recorded in the range of 4000–400 cm^{−1}.

The X-ray photoelectron spectroscopy measurements were performed in a commercial multipurpose (XPS, LEED, UPS, AES) UHV surface analysis system (PREVAC) (PREVAC, Rogów, Poland). The routinely obtained base pressure was in the low 10^{−10} mbar range. The analysis chamber was equipped with a non-monochromatic X-ray photoelectron spectroscopy (XPS, PREVAC, Rogów, Poland) and kinetic electron energy analyzer (SES-2002; Scienta Scientific AB, Uppsala, Sweden). The calibration of the spectrometer was performed using Ag 3d_{5/2} transition. The pulverized samples were thoroughly degassed under vacuum prior to measurement. During XPS measurements, the vacuum was in the low 10^{−9} mbar range. The X-ray Mg K_α ($h\nu = 1253.7$ eV) radiation was applied.

Powder X-ray diffraction was used for the analysis of the AC structure by measuring the intensity of radiation reflected at various angles (X'Pert-PRO, Panalytical, Almelo, The Netherlands). Copper radiation ($K\alpha_1 = 0.154056$ nm) was used. Measurements were performed for the range of 10~100 in 2 θ scale for modified ACs. The performed

diffraction patterns were analyzed by comparing the position and intensity of the reflections on the obtained diffraction patterns with the standard diffraction patterns from the ICDD PDF4+2015 database based on the X'Pert HighScore computer program.

2.3. Alpha-Pinene Isomerization Method

Studies on the activity of DT0 materials in α -pinene isomerization process were carried out in a 10 cm³ glass reactor equipped with a reflux condenser and magnetic stirrer with a heating function. For studies on isomerization, 2 g of α -pinene (98%, Aldrich, Sigma-Aldrich, Burlington, MA, USA) and the appropriate amount of catalyst were weighed into the reactor, which was then placed in an oil bath. The mixing speed was constant at 500 rpm. The effect of the following parameters was examined: temperatures (in the range of 145–175 °C) and reaction time (from 5 to 180 min).

Quantitative analyses were performed with a Thermo Electron FOCUS chromatograph (Waltham, MA, USA) equipped with an FID detector and a ZB-1701 column (30 m \times 0.53 mm \times 1 μ m). The parameters of the analyses were as follows: helium flow of 1 mL/min, sample chamber temperature of 220 °C, detector temperature of 250 °C, the temperature of the furnace—isothermally for 2 min at the temperature of 50 °C followed by growth step of 5 °C/min to 100 °C, and growth with the increment of 10 °C/min to 200 °C. In order to determine the composition of the post-reaction mixtures, the internal normalization was used.

3. Results and Discussion

3.1. Characterization

Figure 1 shows a SEM-EDX image of typical DT0 samples before and after modification.

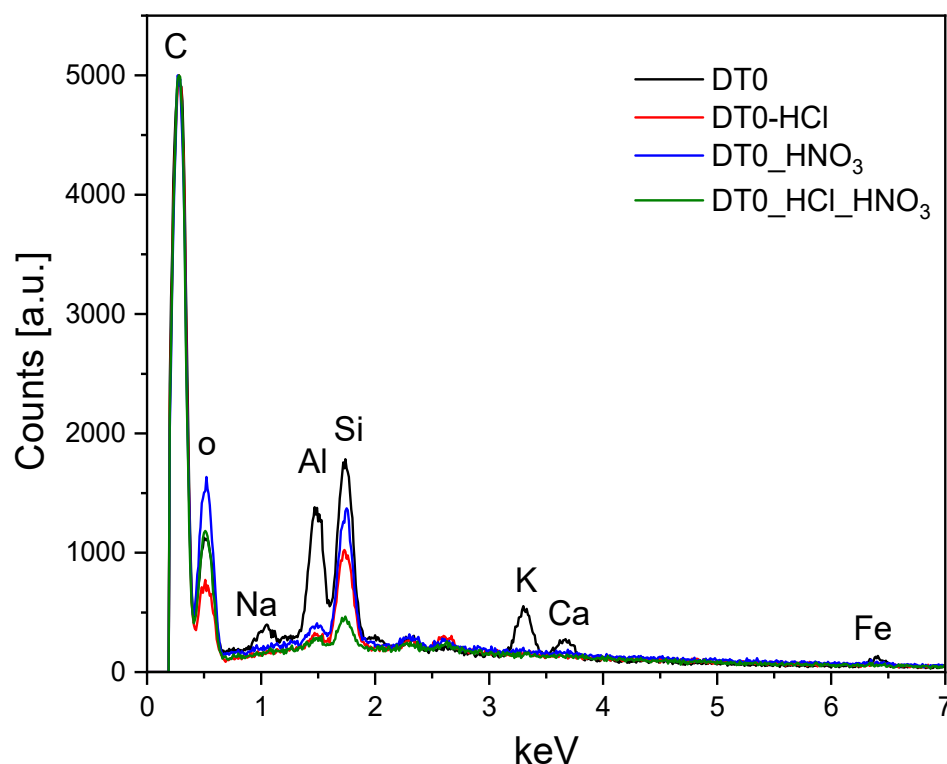


Figure 1. EDX spectra of DT0 samples.

The EDX analysis revealed that the pristine sample contained, besides carbon, the following elements: oxygen, sodium, alumina, silicon, potassium, calcium, and iron. After acid treatment, Na, K, Ca, and Fe were completely removed. Al and Si were partially removed. The quantitative results of EDX measurements are presented in Table 1. The EDX analysis was confirmed by XRF measurements. X-ray fluorescence spectroscopy

(XRF) is a powerful analytical technique that provides both qualitative and quantitative information on a wide variety of sample types including solids, liquids, slurries, and loose powders. Theoretically, it can quantify elements from sodium up to uranium. Practically the detection of small amounts of sodium is difficult. This is the reason that there is no carbon, oxygen, and sodium in Table 2 concerning elemental analysis based on XRF measurements. These elements are listed in Table 1—with the elemental analysis on the basis of EDX measurements. The quantitative results of XRD and XRF results were comparable, and these different techniques allowed us to draw the same conclusions. The elements present in DT0 were completely or partially removed after acid treatment.

Table 1. The elemental analysis based on EDX measurements.

	DT0 [wt%]	DT0_HCl [wt%]	DT0_HNO ₃ [wt%]	DT0_HCl_HNO ₃ [wt%]
C	51	66.1	48.5	62.8
O	33.9	29.9	46.5	34.5
Na	0.9			
Al	3.9	0.3	0.5	0.3
Si	5.1	3.7	4.5	2.4
K	2.9			
Ca	0.8			
Fe	1.5			

Table 2. The elemental analysis based on XRF measurements.

	DT0 [wt%]	DT0_HCl [wt%]	DT0_HNO ₃ [wt%]	DT0_HCl_HNO ₃ [wt%]
Al	2.1			
Si	4.1	2.7	3.1	2.3
K	2.9			
Ca	1.2		0.1	
Fe	1.7	0.3	0.2	0.1

According to XRF measurements, alumina was completely removed after acid treatment. However, EDX investigation show the presence of Al below 1%. Alumina is less soluble in acids than Na, K, Ca, and Fe. It is well known that the solubility of silicon in acids is very low, but we were not able to identify silicon compounds if they were amorphous. Thus, we can say that the silicon and its compounds present in DT0 were very difficult to dissolve in acid, which came as no surprise.

The XPS analysis enables quantitative determination of functional carbon groups [71]. Depending on the kind of bonding and amount of oxygen atoms attached the shift of carbon signals towards higher binding energies can be observed. The C1s signals presented in Figure 2 were carefully deconvoluted to components according to the procedure given elsewhere [72]. Table 3 presents the elemental content of the surface expressed as atomic concentration.

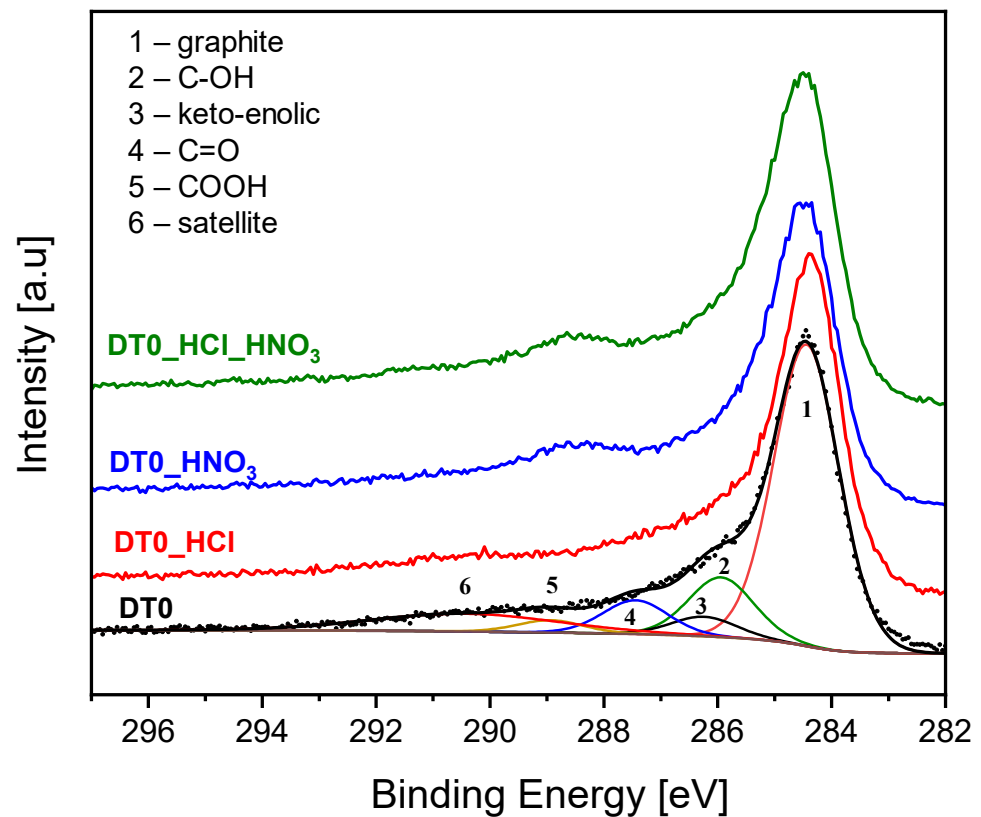


Figure 2. X-ray photoelectron C1s spectra. For the DT0 the components are indicated.

Table 3. The content of C 1s components expressed as atomic concentration.

Assignment	DT0	DT0_HCl	DT0_HNO ₃	DT0_HCl_HNO ₃
C	63.1	63.1	60.5	61.0
C-OH	12.6	12.3	13.7	14.2
keto-enolic	4.1	2.8	0.0	0.0
C=O	7.1	7.5	7.8	7.8
COOH	2.6	2.1	6.4	6.3
satellite	10.7	12.1	11.7	10.8

The tail on the left-hand side of the dominant component is related with the presence of carbon-oxygen species. In DT0_HNO₃ and DT0_HCl_HNO₃ samples a hump at about 289 eV is observed. This can be attributed to a significant increase of COOH groups over the carbon surface. It is clearly the oxidation effect of HNO₃. Table 4 presents surface elemental contents of the samples.

Table 4. Elemental content of the sample surfaces.

	%at			
	C1s	O1s	Si2p	Ca2p
DT0	68.2	26.4	4.8	0.6
DT0_HCl	56.6	32.8	10.3	0.3
DT0_HNO ₃	59.2	34.6	6.1	0.1
DT0_HCl_HNO ₃	59.7	34.2	6.0	0.1

Figure 3 presents the XP spectra of the analyzed samples.

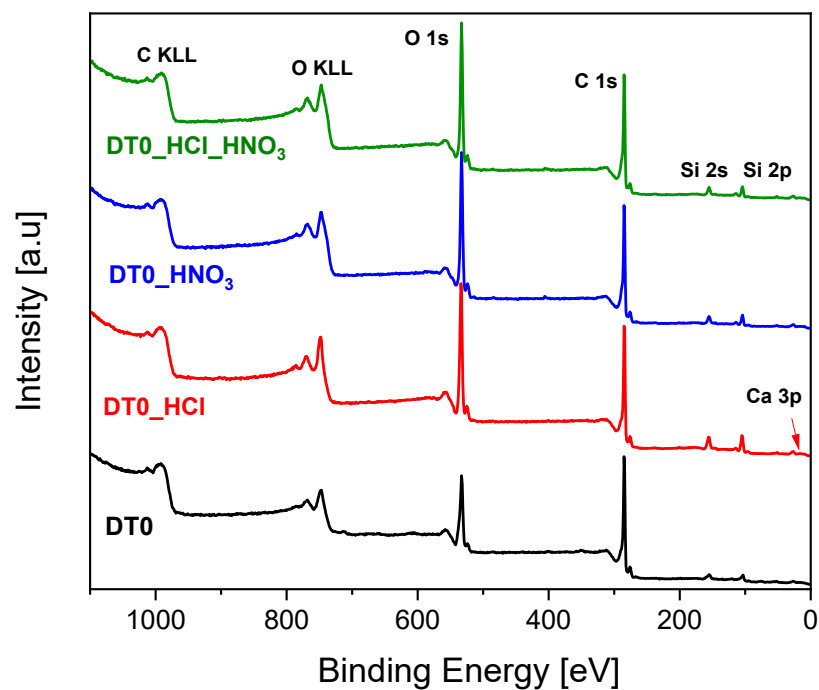


Figure 3. X-ray photoelectron survey spectra.

The content of calcium decreases as a result of acid treatment. The higher content of silicon after acid treatment is most probably the effect of removing the calcium screening effect. In the case of DT0_HCl sample, the increase of oxygen content is observed. This is not the result of oxidation but rather an effect of calcium removal as HCl is not an oxidizing agent. Such effects were observed previously [72].

Figure 4 shows the FTIR spectra of activated carbons.

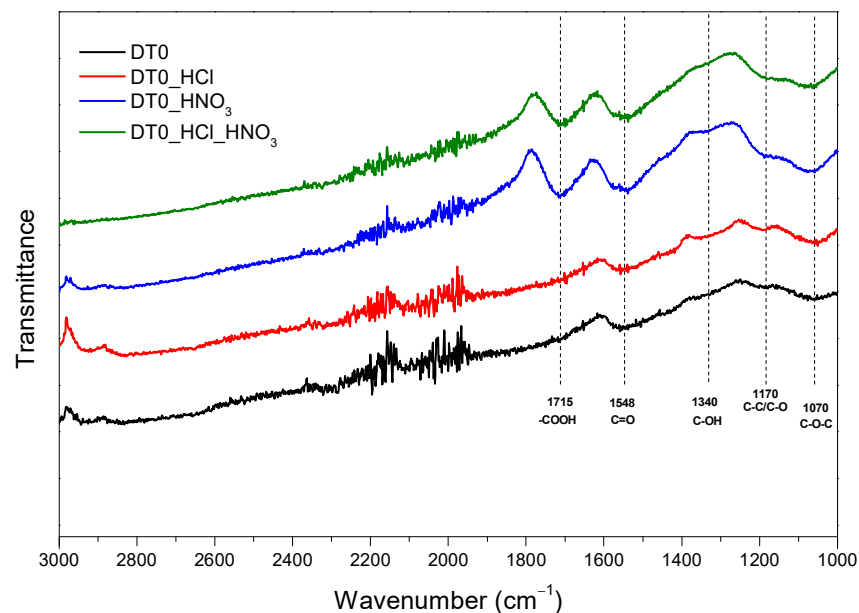


Figure 4. FTIR spectra of DT0, DT0_HCl, DT0_HNO₃, and DT0_HCl_HNO₃.

Figure 4 shows FTIR spectra of DT0 samples. The signal from the carboxylic group (1715 cm^{-1}) was not observed for DT0 and DT0_HCl. Only samples treated with HNO₃ had COOH groups on the surface. Additionally, a weak signal from the hydrophilic group (1340 cm^{-1}) was observed only for the carbons treated with HNO₃. The absorption band appeared at 1548 cm^{-1} corresponding to the C=O stretching vibration [73]. This signal was

present for all the samples, but for samples treated with HNO_3 , it was considerably higher. The presence of $\text{C}=\text{O}$ groups on the surface of DT0 treated with HNO_3 was enhanced. The intensity of signals attributed to functional groups containing oxygen was as follows: $\text{DT0_HCl_HNO}_3 > \text{DT0_HNO}_3 > \text{DT0_HCl} \approx \text{DT0}$. The broad peak located at about 1070 cm^{-1} related to the $\text{C}-\text{O}$ stretching vibration of various functional groups [74] and a very small peak located about 1170 cm^{-1} related to $\text{C}-\text{C}/\text{C}-\text{O}$ [75] were present on the surface of all samples. The FTIR results were consistent with the XPS results.

The acid-treated DT0 carbons were characterized with Raman spectroscopy and are shown in Figure 5.

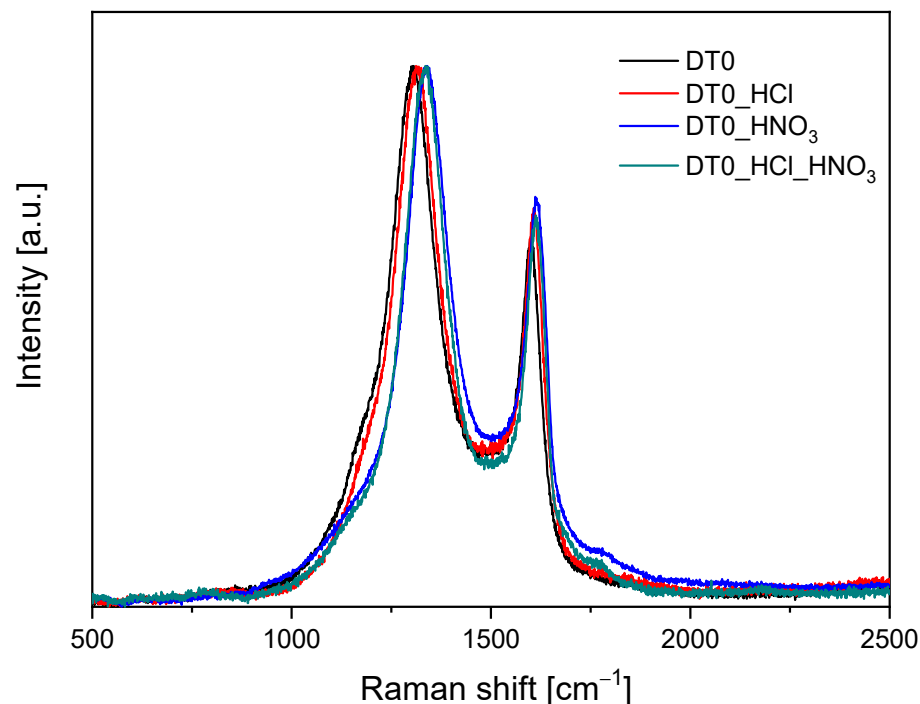


Figure 5. Raman spectra of samples.

The G peak, centered around 1595 cm^{-1} , can be assigned to the ordered carbon structure. G-band arises from the stretching of the $\text{C}-\text{C}$ bond in graphitic materials and is common to all sp^2 carbon systems. In the graphitic disorder of the carbon structure, the band around 1310 cm^{-1} named D was observed. The intensity ratio of the G-band and D-band (I_G/I_D) was used to evaluate the quality of carbon materials. The higher the I_G/I_D value, the lower the graphitic disorder observed [76]. Table 5 shows the determined values of the I_G/I_D ratios.

Table 5. Values of the I_G/I_D ratios of activated carbons modified with HCl and HNO_3 .

Sample	I_G/I_D
DT0	0.65
DT0_HCl	0.70
DT0_HNO ₃	0.71
DT0_HCl_HNO ₃	0.70

The values of I_G/I_D for carbons were in the range of 0.65–0.72 and were similar to the previously reported for activated biocarbons [77]. The highest I_G/I_D ratios were observed in the samples modified with acids in comparison to the unmodified DT0, which correspond to the better ordered structure in modified carbons.

The graphitic structure of DT0 carbons was analyzed with the XRD method. The X-ray diffraction profiles for carbons are shown in Figure 6.

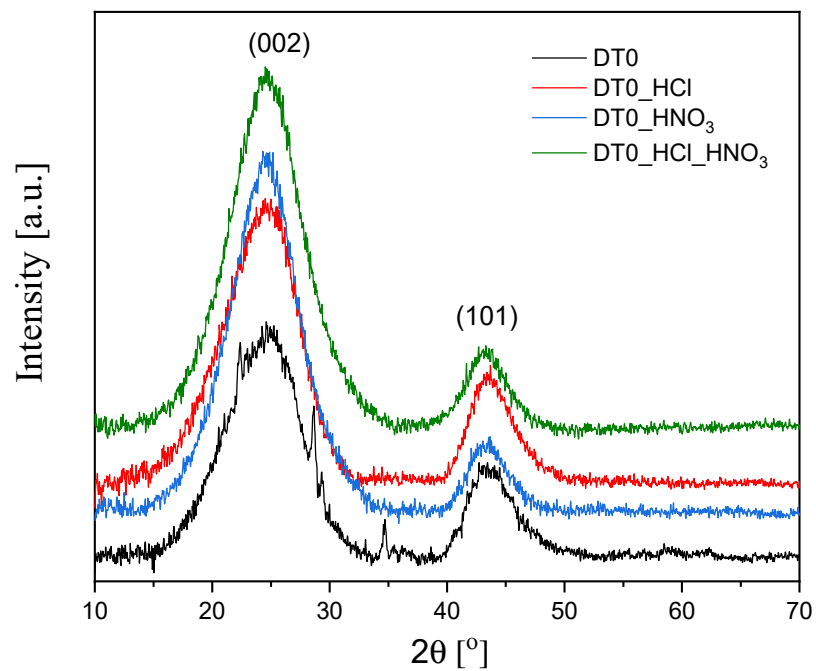


Figure 6. Diffraction patterns of DT0 carbons.

The diffractograms showed broad peaks and the absence of very sharp peaks. This indicates that the carbon was amorphous in nature [78]. The amorphous structure of the DT0 was identified by the peak at $2\theta = 24^\circ$ and peak at $2\theta = 43^\circ$, which referred to the diffraction peaks (002) and (101) [79–81].

The carbon morphology of studied samples at $50,000\times$ magnifications is shown in Figure 7.

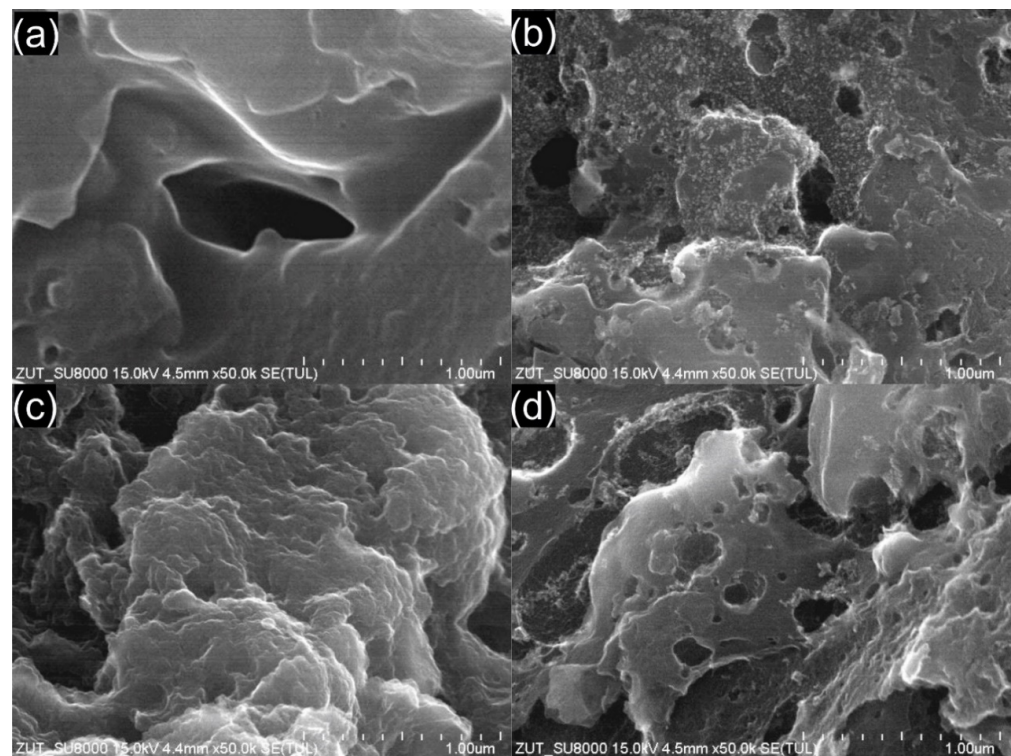


Figure 7. SEM images of activated carbon: (a) DT0, (b) DT0_HCl, (c) DT0_HNO₃, and (d) DT0_HCl_HNO₃.

SEM images of the DT0 carbons showed that the adsorbent had texture with a heterogeneous surface and a variety of randomly distributed holes. The presence of holes of various diameters and irregular shapes was observed in DT0 HCl and DT0_HCl_HNO₃. Contrary to that, a very smooth surface was identified for DT0. Similar shapes were observed for the other commercial activated carbons [82–84].

The proposed methods of DT0 modification with inorganic acids influenced the textural properties. Figure 8 shows the nitrogen adsorption isotherms at $-196\text{ }^{\circ}\text{C}$ of the studied DT0 carbons.

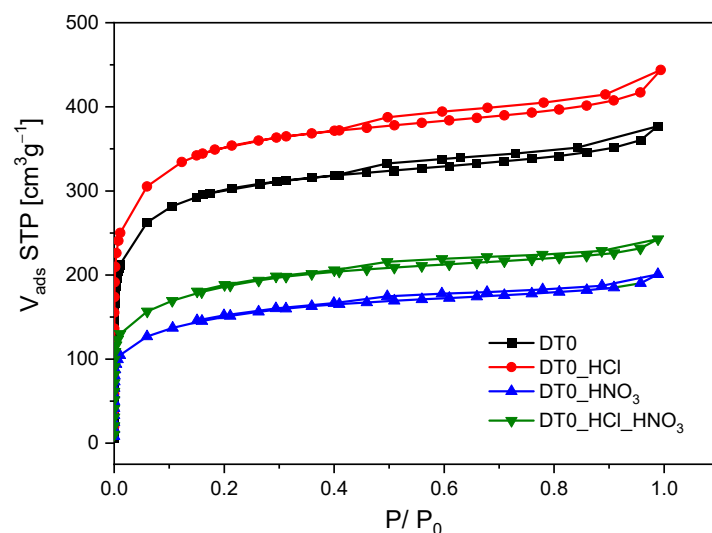


Figure 8. N₂ adsorption–desorption isotherms of DT0 carbons.

The presented isotherms combine type I, which is characteristic of microporous materials, and type IV, which is characteristic of mesoporous materials [85]. Nitrogen adsorption increased very quickly at low P/P_0 values, which is a characteristic feature of microporous materials. The formation of hysteresis loops at relative pressure higher than 0.4 indicated the multilayer adsorption process characterizing mesoporous structures. The hysteresis of catalysts was the type H4 associated with narrow slit pores, including pores in the micropore region. These are typical sorption isotherms for activated carbons [77,86].

Figure 9 shows the pore size distributions for the ACs determined by means of the N₂ adsorption results at $-196\text{ }^{\circ}\text{C}$ using the density functional theory (DFT). Overall, it can be seen that the ACs have mainly micropores with a certain amount of mesopores.

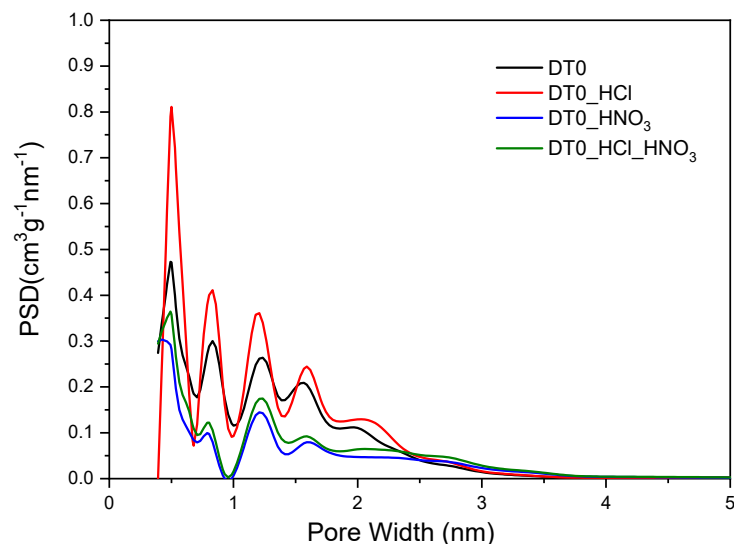


Figure 9. DFT pore size distribution of DT0 carbons.

It was stated that the acid-treated DT0 carbon samples showed significant differences in pore volume size compared to the pristine sample. In the case of DT0 carbon modified with nitric acid and the two-stage treatment with hydrochloric acid and nitric acid, a significant reduction in the pore volume in the range of 0.4–2.5 nm was observed. In contrast, treatment of DT0 with hydrochloric acid significantly increased the pore volume. This is because the treatment of AC with hydrochloric acid removes minerals, which in turn may increase the porosity. The DT0_HCl carbon had the best-developed micropores in the range of 0.4–2 nm. All the DT0 carbons contained mesopores with a size of 2–3.5 nm as well (Figure 9). Table 6 presents the textural parameters of DT0 carbons.

Table 6. Textural parameters of DT0 carbons.

Carbon	S_{BET} [m^2/g]	V_{tot} [cm^3/g]	V_{mic} [cm^3/g]
DT0	1085	0.583	0.349
DT0_HCl	1267	0.687	0.407
DT0_HNO ₃	532	0.311	0.160
DT0_HCl_HNO ₃	651	0.375	0.197

It was found that the treatment of DT0 carbon with HCl, HNO₃, HCl, and HNO₃ acids affected its porous structure to a greater or lesser extent. Treatment with HCl increased the surface area of the starting DT0 carbon from 1085 to 1267 m^2/g and increased the total pore volume from 0.583 to 0.687 cm^3/g . Thus, the increase of textural parameters in DT0_HCl may be caused by removing Na, K, and Ca salts by dissolving them in HCl, which promotes the development of the surface and pore structure.

It was evident from the EDX (Table 1) and XRF (Table 2) measurements that the minerals were dissolved with HCl and HNO₃. Unfortunately, HNO₃ simultaneously oxidized the carbon structure and damaged the micro- and mezopores. That is why only the S_{BET} of DT0_HCl increased (Table 6). The advantage of HNO₃ treatment was the increase of oxygen-containing groups on the surface, especially COOH. The concentration of oxygen on the surface of DT0_HCl_HNO₃ was similar to DT0_HNO₃, but the S_{BET} and V_{tot} were higher than those of DT0_HNO₃ because of the simultaneous action of both acids.

The effect of HNO₃ had the greatest effect on reducing the specific surface area from 1085 to 532 m^2/g , and the total carbon pore volume after modification was the smallest and amounted to 0.311 cm^3/g . A fairly significant reduction in S_{BET} resulted from partial oxidation of carbon by strongly oxidizing nitric acid (V).

A significant reduction in textural parameters was also found in the case of carbon modified with HNO₃ after previous modification with non-oxidizing HCl. With this two-step modification, the S_{BET} of DT0_HCl_HNO₃ decreased from 1085 to 651 cm^3/g and the total pore volume decreased to 0.375 cm^3/g . However, this suggests that the double modification of carbon compared to the treatment of DT0 only with the oxidizing acid HNO₃ had a more favorable effect on the development of porosity of the material. Similar conclusions leading to an increase in the porosity of carbons after their treatment with acids can be found in other studies [72,87]. There are also reports showing a decrease in the specific surface area of the carbons after acid treatment [88,89].

3.2. Alpha-Pinene Isomerization Process

In the first stage of catalytic tests, studies on alpha-pinene isomerization were carried out on DT0 carbon and on DT0_HCl, DT0_HNO₃, and DT0_HCl_HNO₃ carbons. The aim was to determine the most active catalyst for the process of α -pinene isomerization. At this stage, the following conditions were used in the tests: temperature 160 °C, the content of catalyst at 5 wt% (in relation to the amount of alpha-pinene), and reaction time of 3 h. Figure 10 shows the results of isomerization of alpha-pinene obtained in the study.

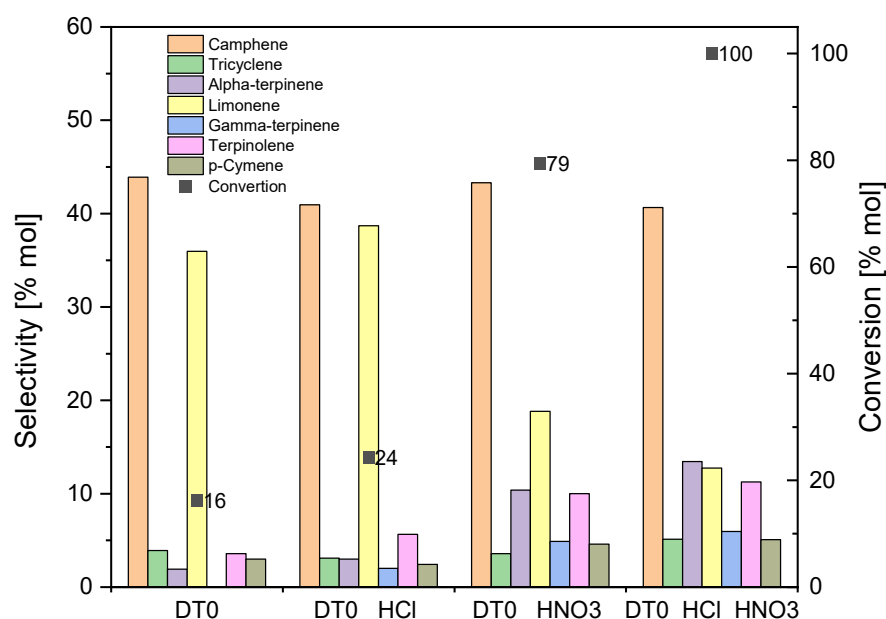


Figure 10. Comparison of the activity of DT0, DT0_HCl, DT0_HNO₃, and DT0_HCl_HNO₃ catalysts in the alpha-pinene isomerization process (applied conditions: temperature 160 °C, reaction time of 3 h, and the content of catalyst at 5 wt%).

Figure 10 shows that the most active catalyst was DT0_HCl_HNO₃. It allows for achieving the maximum conversion of alpha-pinene (100 mol%). The selectivities of the transformation to camphene and limonene on this catalyst were 41 and 13 mol%, respectively. The formation of alpha-terpinene (selectivity 13 mol%), gamma-terpinene (selectivity 6 mol%), terpinolene (selectivity 11 mol%), and p-cymene (selectivity 5 mol%) could also be observed on this porous material. Similar values of transformation selectivity were observed for the DT0_HNO₃ catalyst, while the alpha-pinene conversion for the process carried out on this catalyst was lower by 21 mol%.

The results obtained on the other two catalysts are much worse, as the conversion on them reaches 16 mol% (DT0 catalyst) and 24 mol% (DT0_HCl catalyst). However, in the case of these two catalysts, attention is drawn to the very high selectivity of the transformation to limonene reaching the value of 36 mol% (DT0 catalyst) and 39 mol% (DT0_HCl catalyst), with the selectivity of transformation to camphene similar to that obtained on the previous two catalysts (44 mol% DT0 catalyst and 41 mol% DT0_HCl catalyst). On the other hand, the transformation selectivities to the remaining products are not significant for these two catalysts.

In the catalytic tests presented in this stage of the studies, the synergistic effect of HCl and HNO₃ acids on DT0-activated carbon is also visible. It is visible in the fact that for the DT0_HCl_HNO₃ sample, the selectivity of transformation to terpinolene increased compared to the unmodified DT0 sample and the DT0_HCl and DT0_HNO₃ samples (more than twofold increase). A similar effect was seen with p-cymene, gamma-terpinene, and alpha-terpinene. The synergistic effect of HCl and HNO₃ on the DT0 carbon simultaneously reduced the selectivity of transformation to limonene as compared to the unmodified DT0 sample (by about 20 mol%).

The comparison of the results presented in Table 3 (tests using the XPS method) shows that the DT0_HNO₃ and DT0_HCl_HNO₃ catalysts differ significantly (almost 3 times) from the other two catalysts in the content of carboxyl groups (COOH group). They also have slightly more C-OH groups (DT0 and DT0_HCl with 12.6 and 12.3, and DT0_HNO₃ and DT0_HCl_HNO₃ with 13.7 and 14.2, respectively). It should also be noted that, in the case of DT0_HNO₃ and DT0_HCl_HNO₃ carbon materials, no keto-enolic groups were observed. This increased content of COOH and C-OH groups in the DT0_HNO₃ and DT0_HCl_HNO₃ carbon materials and the lack of keto-enolic groups in them may

be the reason for the greater activity of DT0_HNO₃ and DT0_HCl_HNO₃ in the alpha-pinene isomerization process. It seems more advantageous to wash the DT0 carbon with the aqueous solution containing both nitric acid and hydrochloric acid, and not with the aqueous solution of the nitric acid alone.

Based on the research results presented at this stage, the DT0_HCl_HNO₃ catalyst was considered to be the most active.

The research on the effect of temperature on the course of alpha-pinene isomerization on the DT0_HCl_HNO₃ material is shown in Figure 11. The tests were carried out at the following temperatures: 60, 90, 120, 145, 160, and 175 °C, for 3 h and with catalyst content of 5 wt%.

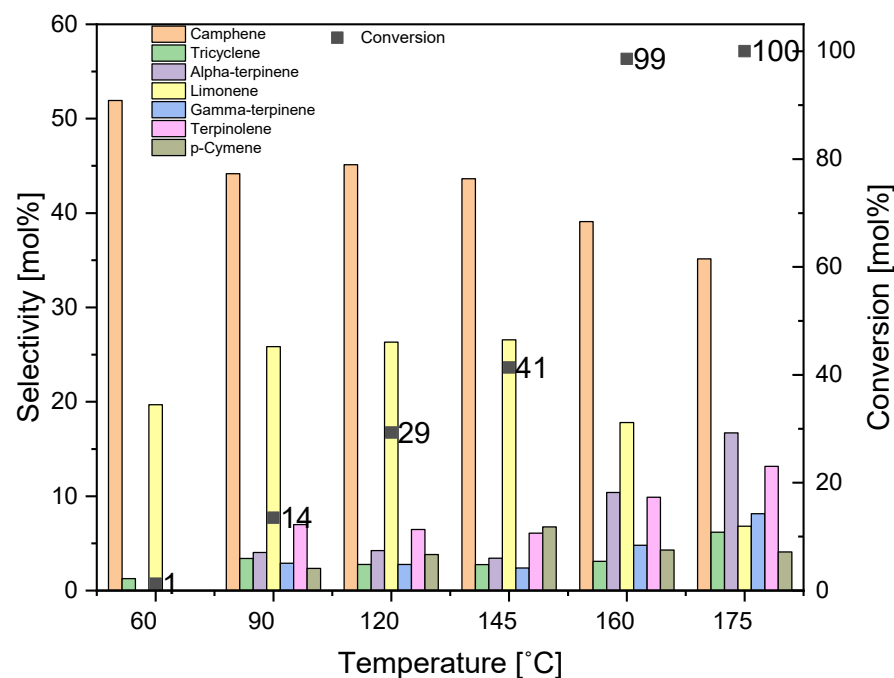


Figure 11. Influence of temperature on alpha-pinene isomerization process for DT0_HCl_HNO₃ catalyst (applied conditions: content of catalyst at 5 wt% and reaction time of 3 h).

The comparison of the results obtained at the two lowest temperatures (60 and 90 °C) shows that these temperatures are too low to carry out the alpha-pinene isomerization process, as the conversion of this raw material is only 1 and 14 mol%. In addition, the process temperature increasing from 60 to 90 °C resulted in a decrease of the selectivity of transformation to camphene (from 52 mol% to 44 mol%). The further increase of temperature to 145 °C did not cause any significant changes in the selectivity of the transformation to camphene. Comparing the results obtained for the two lowest temperatures, it can also be noticed that increase of temperature increases the selectivity of transformation to limonene (from 20 to 26 mol%), terpinolene (from 0 to 7 mol%), alpha-terpinene (from 0 to 4 mol%), gamma-terpinene (0 to 3 mol%), tricyclene (1 to 3 mol%), and p-cymene (0 to 2 mol%). The highest alpha-pinene conversions were obtained by carrying out the isomerization process at temperatures of 120 and 145 °C at 29 and 41 mol%, respectively. The highest alpha-pinene conversions were obtained by carrying out the isomerization process at temperatures of 160 and 175 °C (99 and 100 mol%, respectively). At these temperatures, the highest selectivity of transformation to several products was also obtained: tricyclene—3 and 6 mol%, alpha-terpinene—10 and 17 mol%, gamma-terpinene—5 and 8 mol%, and terpinolene—10 and 13 mol%. The highest selectivity of transformation to limonene was obtained at temperatures of 120 and 145 °C, then its value decreased (to 7 mol%). As the process temperature increased, an increase in the selectivity of the transformation to the dehydrogenation product (p-cymene) was also observed, and at the highest temperatures, it was about 4–7 mol%.

To study the effect of reaction time on alpha-pinene isomerization, three temperatures were selected at which the highest values of alpha-pinene conversion were obtained: 145, 160, and 175 °C. The tests were carried out with DT0_HCl_HNO₃ catalyst in the reaction mixture of 5 wt% and in the range of reaction times from 5 to 180 min. The results are presented in Figures 12–14.

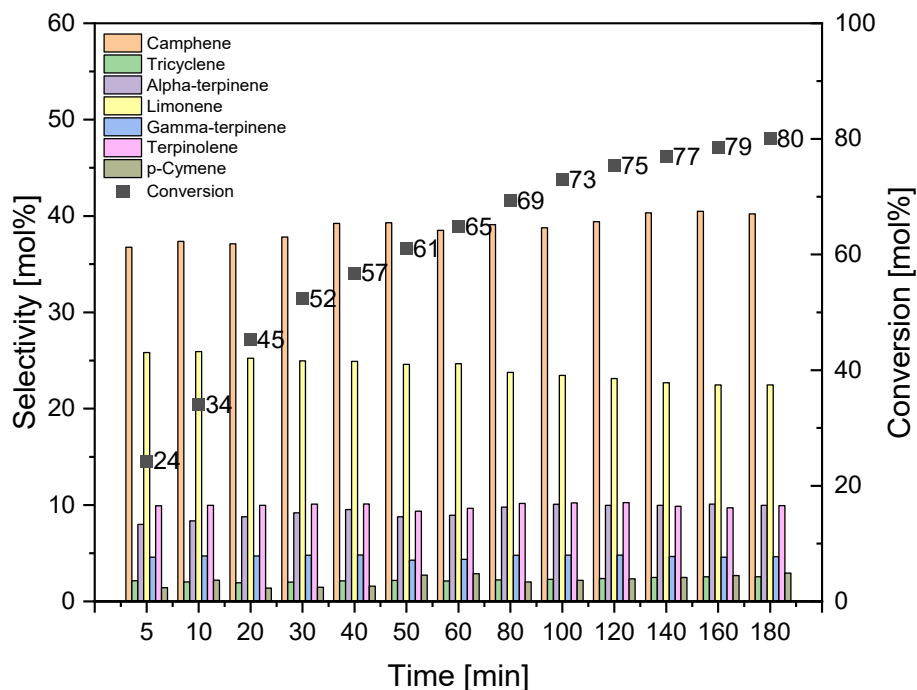


Figure 12. Effect of reaction time on alpha-pinene isomerization on DT0_HCl_NO₃ catalyst at 145 °C (catalyst amount 5 wt%).

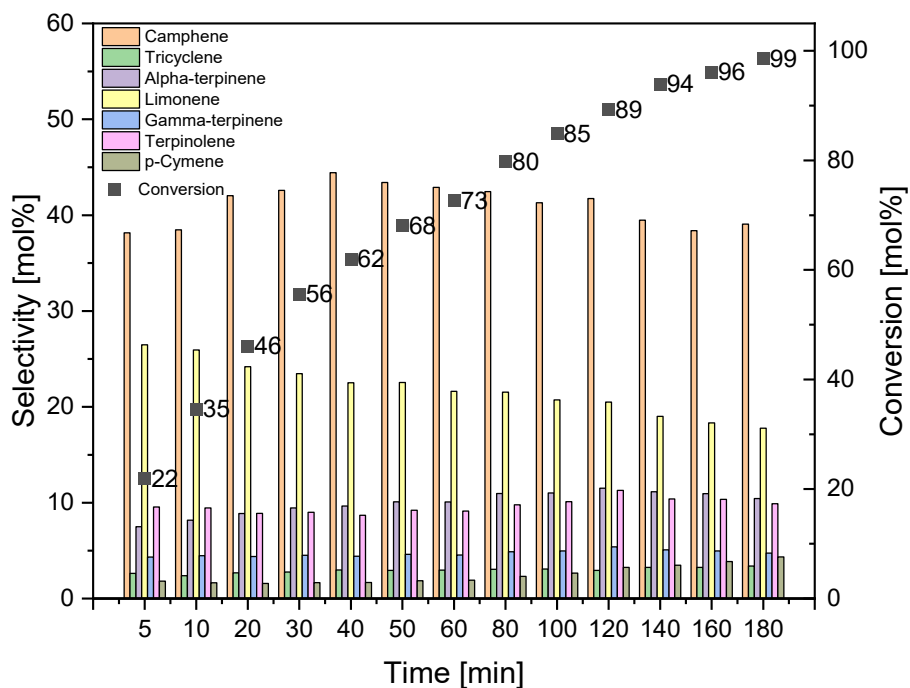


Figure 13. Effect of reaction time on alpha-pinene isomerization on DT0_HCl_NO₃ catalyst at 160 °C (catalyst amount 5 wt%).

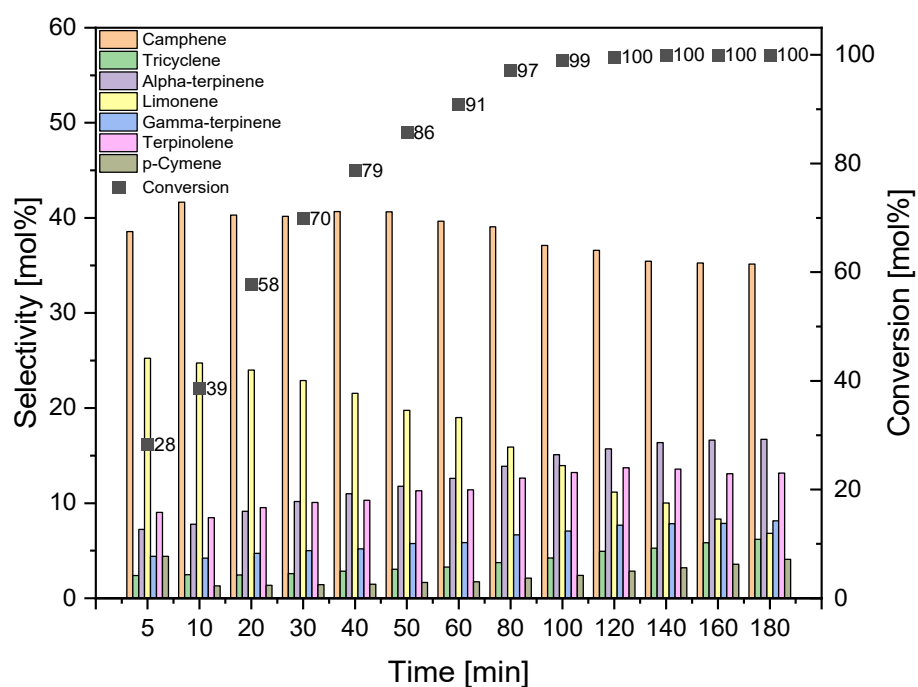


Figure 14. Effect of reaction time on alpha-pinene isomerization on DT0_HCl_NO₃ catalyst at 175 °C (catalyst amount 5 wt%).

A comparison of the results obtained at the three tested temperatures shows that the alpha-pinene conversion of about 100 mol% can be achieved by carrying out isomerization at the two highest temperatures, while for the temperature of 160 °C the time required to achieve such a high conversion is 180 min, and for the temperature of 175 °C the time required is 100 min, which is significantly shorter. The maximum selectivities of the transformation to camphene obtained at the three tested temperatures are similar and amount to 41–44 mol%. The highest selectivity of tricyclene was noted for the process carried out at the temperature of 175 °C and for the reaction time of 160–180 min (6 mol%). At the same temperature of 175 °C and for the same reaction time, the highest selectivity of alpha-terpinene (about 17 mol%), gamma-terpinene (about 8 mol%), terpinolene (about 13 mol%), and p-cymene (4 mol%) was also observed. Figures 12–14 also show that the highest selectivity of camphene (40–44 mol%) can be achieved by carrying out the isomerization process: longer than 40 min (the most advantageous are 40–50 min) at 145 °C, for 40–50 min at 160 °C, or for 10–50 min at 175 °C. The comparison of the results for the selectivity of transformation to limonene shows that the selectivity of this compound decreases with increasing the reaction time and increasing the temperature, and the highest selectivity of the transformation to this compound (about 24–25 mol%) is obtained for short reaction times: for the temperature of 145 °C for a reaction time up to 30 min, for temperatures of 160 °C and 175 °C for a time reaction time not exceeding 10 min.

3.3. Kinetic Studies

The comprehensive kinetic studies of α -pinene isomerization at a temperature of 145 °C, 160 °C, and 175 °C over DT0_HCl_HNO₃ were performed for several orders, using the following equations.

For first order:

$$-\frac{dC_{\alpha\text{-pinene}}}{dt} = kC_{\alpha\text{-pinene}}, \quad (1)$$

For orders different from one:

$$\frac{C_{\alpha\text{-pinene}}^{1-n} - C_{\alpha\text{-pinene}_0}^{1-n}}{n-1} = kt, \quad (2)$$

where $C_{\alpha\text{-pinene}}$ is the α -pinene concentration, t is the reaction time, and k is the reaction rate constant.

Kinetic parameters for the kinetic equations were determined using a parameter estimation software. The highest regression coefficients were obtained for the first-order reaction for α -pinene isomerization in all three reaction temperatures. Therefore, the consumption rate of α -pinene followed the first-order kinetics. This reaction order matches our previous results achieved for instance for α -pinene isomerization over Ti_3C_2 and ex- Ti_3C_2 [66] over clinoptilolite (modified with 0.1 M H_2SO_4 —CLIN 0.1) [63]. Moreover, similar results were also reported by other authors, namely, Ünveren et al. [90] and Alahverdiev et al. [91].

The calculated reaction rate coefficients for the first-order reaction are compiled in Table 7.

Table 7. The α -pinene isomerization kinetic parameters.

Temperature [°C]	k [h ⁻¹]	R ²
145	0.47	0.8875
160	1.22	0.9741
175	2.74	0.9914

The highest value of the reaction rate constant was calculated at 175 °C ($k = 2.74 \text{ h}^{-1}$). This value is nearly six times higher than the calculated constant at 140 °C ($k = 0.47 \text{ h}^{-1}$).

Dependence of these kinetic constants as a function of temperature strongly supports the assumption of the first-order kinetics. Temperature dependence of the first-order kinetic constant obeyed Arrhenius dependence with the global activation energy equal to 91.5 kJ/mol. Calculated activation energy matches results achieved for typical values of activation energy for α -pinene isomerization (for example 80.9 kJ/mol [17]).

4. Conclusions

The modification of activated carbons with acids is very beneficial compared with plasma. The method presented here is considerably cheaper. The plasma oxidized only the outside surface of the grains. The acid treatment oxidized the inside and outside surface and also removed the minerals blocking the pores.

The modification of carbon material DT0 with acid treatment showed that it is more advantageous to wash DT0 carbon with the aqueous solution containing both nitric acid and hydrochloric acid, and not with the aqueous solution of the nitric acid alone. The least preferred method is washing of DT0 carbon with the solution of hydrochloric acid alone. DT0 carbons washed with the aqueous solution of nitric acid with hydrochloric acid and with the aqueous solution of nitric acid alone showed the presence of the increased amount of COOH and C-OH groups, which is most likely the reason for their increased activity in the α -pinene isomerization process compared to pure DT0 carbon and DT0 carbon treated with the aqueous solution of hydrochloric acid. Moreover, the activities of the DT0_HNO₃ and DT0_HCl_HNO₃ carbons may also be influenced by the lack of keto-enolic groups in these samples.

Author Contributions: Conceptualization, B.M., J.S.-N. and A.W.; methodology, B.M., J.S.-N. and A.W.; validation, B.M., A.W. and J.S.-N.; formal analysis, B.M., A.W. and J.S.-N.; investigation, J.S.-N., B.M., A.K., P.M., R.J.W. and J.S.; data curation, J.S.-N., A.W. and B.M.; writing—original draft preparation, B.M., A.W., J.S.-N., R.J.W., A.K., J.S., K.K. and P.M.; writing—review and editing, J.S.-N., B.M., A.W., A.K., P.M., K.K. and J.S.; visualization, J.S.-N., A.K., P.M. and K.K.; supervision, B.M. and A.W. All authors have read and agreed to the published version of the manuscript.

Funding: The APC was funded by Rector of the West Pomeranian University of Technology in Szczecin for PhD students of the Doctoral School, grant number: ZUT/23/2021.

Institutional Review Board Statement: Not applicable.

Informed Consent Statement: Not applicable.

Data Availability Statement: The data presented in this study are available on request from the corresponding author.

Conflicts of Interest: The authors declare no conflict of interest.

References

1. Lutfi, M.; Hanafi; Susilo, B.; Prasetyo, J.; Sandra; Prajogo, U. Characteristics of activated carbon from coconut shell (*Cocos nucifera*) through chemical activation process. *IOP Conf. Ser. Earth Environ. Sci.* **2021**, *733*, 012134. [[CrossRef](#)]
2. Mkungunugwa, T.; Manhokwe, S.; Chawafambira, A.; Shumba, M. Synthesis and Characterisation of Activated Carbon Obtained from Marula (*Sclerocarya birrea*) Nutshell. *J. Chem.* **2021**, *2021*, 5552224. [[CrossRef](#)]
3. Kütahyalı, C.; Eral, M. Selective adsorption of uranium from aqueous solutions using activated carbon prepared from charcoal by chemical activation. *Sep. Purif. Technol.* **2004**, *40*, 109–114. [[CrossRef](#)]
4. Uraki, Y.; Tamai, Y.; Ogawa, M.; Gaman, S.; Tokurad, S. Preparation of activated carbon from peat. *BioResources* **2009**, *4*, 205–213. [[CrossRef](#)]
5. Varil, T.; Bergna, D.; Lahti, R.; Romar, H.; Hu, T.; Lassi, U. Activated carbon production from peat using ZnCl₂: Characterization and applications. *BioResources* **2017**, *12*, 8078–8092. [[CrossRef](#)]
6. Tsubouchi, N.; Nishio, M.; Shinohara, Y.; Bud, J.; Mochizuki, Y. Production of activated carbon from peat by with natural soda ash and effect of nitrogen addition on the development of surface area. *Fuel Process. Technol.* **2018**, *176*, 76–84. [[CrossRef](#)]
7. Boujibar, O.; Ghamouss, F.; Ghosh, A.; Achak, O.; Chafik, T. Activated carbon with exceptionally high surface area and tailored nanoporosity obtained from natural anthracite and its use in supercapacitors. *J. Power Sources* **2019**, *436*, 226882. [[CrossRef](#)]
8. Song, G.; Deng, R.; Yao, Z.; Chen, H.; Romero, C.; Lowe, T.; Driscoll, G.; Kreglow, B.; Schobert, H.; Baltrusaitis, J. Anthracite coal-based activated carbon for elemental Hg adsorption in simulated flue gas: Preparation and evaluation. *Fuel* **2020**, *275*, 117921. [[CrossRef](#)]
9. Jha, D.; Haider, M.B.; Kumar, R.; Byamba-Ochir, N.; Shim, W.G.; Marriyappan Sivagnanam, B.; Moon, H. Enhanced Adsorptive Desulfurization Using Mongolian Anthracite-Based Activated Carbon. *ACS Omega* **2019**, *4*, 20844–20853. [[CrossRef](#)]
10. Hwang, I.-H.; Kobayashi, J.; Kawamoto, K. Characterization of products obtained from pyrolysis and steam gasification of wood waste, RDF, and RPF. *Waste Manag.* **2014**, *34*, 402–410. [[CrossRef](#)] [[PubMed](#)]
11. Foo, K.Y.; Hameed, B.H. Mesoporous activated carbon from wood sawdust by K₂CO₃ activation using microwave heating. *Bioresour. Technol.* **2012**, *111*, 425–432. [[CrossRef](#)]
12. Budianto, A.; Kusdarini, E.; Effendi, S.S.W.; Aziz, M. The Production of Activated Carbon from Indonesian Mangrove Charcoal. *IOP Conf. Ser. Mater. Sci. Eng.* **2019**, *462*, 012006. [[CrossRef](#)]
13. Gopu, C.; Gao, L.; Volpe, M.; Fiori, L.; Goldfarb, J.L. Valorizing municipal solid waste: Waste to energy and activated carbons for water treatment via pyrolysis. *J. Anal. Appl. Pyrolysis* **2018**, *133*, 48–58. [[CrossRef](#)]
14. Yahya, M.A.; Al-Qodah, Z.; Ngah, C.W.Z. Agricultural bio-waste materials as potential sustainable precursors used for activated carbon production: A review. *Renew. Sustain. Energy Rev.* **2015**, *46*, 218–235. [[CrossRef](#)]
15. McDougall, G.J. Physical nature and manufacture of activated carbon. *J. S. Afr. Inst. Min. Metall.* **1991**, *91*, 109–120.
16. Lendzion-Bieluń, Z.; Czekajło, L.; Sibera, D.; Moszyński, D.; Sreńscek-Nazzal, J.; Morawski, A.W.; Wrobel, R.J.; Michalkiewicz, B.; Arabczyk, W.; Narkiewicz, U. Surface characteristics of KOH-treated commercial carbons applied for CO₂ adsorption. *Adsorpt. Sci. Technol.* **2018**, *36*, 478–492. [[CrossRef](#)]
17. Snoeyink, V.L.; Weber, W.J. The surface chemistry of active carbon; a discussion of structure and surface functional groups. *Environ. Sci. Technol.* **1967**, *1*, 228–234. [[CrossRef](#)]
18. El-Sayed, Y.; Bandosz, T.J. Adsorption of valeric acid from aqueous solution onto activated carbons: Role of surface basic sites. *J. Colloid Interface Sci.* **2004**, *273*, 64–72. [[CrossRef](#)]
19. Zóttowska, S.; Bielan, Z.; Zembrzuska, J.; Siwińska-Ciesielczyk, K.; Piasecki, A.; Zielińska-Jurek, A.; Jesionowski, T. Modification of structured bio-carbon derived from spongin-based scaffolds with nickel compounds to produce a functional catalyst for reduction and oxidation reactions: Potential for use in environmental protection. *Sci. Total Environ.* **2021**, *794*, 148692. [[CrossRef](#)]
20. Sulym, I.; Zdarta, J.; Ciesielczyk, F.; Sternik, D.; Derylo-Marczewska, A.; Jesionowski, T. Pristine and Poly(Dimethylsiloxane) Modified Multi-Walled Carbon Nanotubes as Supports for Lipase Immobilization. *Materials* **2021**, *14*, 2874. [[CrossRef](#)]
21. Liu, G.; Li, X.; Campos, L.C. Role of the functional groups in the adsorption of bisphenol A onto activated carbon: Thermal modification and mechanism. *J. Water Supply Res. Technol.-Aqua* **2017**, *66*, 105–115. [[CrossRef](#)]
22. Ania, C.O.; Parra, J.B.; Pis, J.J. Oxygen-Induced Decrease in the Equilibrium Adsorptive Capacities of Activated Carbons. *Adsorpt. Sci. Technol.* **2004**, *22*, 337–351. [[CrossRef](#)]
23. Li, Z.; Dvorak, B.; Li, X. Removing 17β-estradiol from drinking water in a biologically active carbon (BAC) reactor modified from a granular activated carbon (GAC) reactor. *Water Res.* **2012**, *46*, 2828–2836. [[CrossRef](#)] [[PubMed](#)]
24. Li, B.-J.; Hu, J.; Huang, L.-Y.; Lv, Y.; Zuo, J.; Zhang, W.; Ying, W.-C.; Matsumoto, M.R. Removal of MTBE in biological activated carbon adsorbers. *Environ. Prog. Sustain. Energy* **2013**, *32*, 239–248. [[CrossRef](#)]
25. Vinke, P.; van der Eijk, M.; Verbree, M.; Voskamp, A.F.; van Bekkum, H. Modification of the surfaces of a gasactivated carbon and a chemically activated carbon with nitric acid, hypochlorite, and ammonia. *Carbon N. Y.* **1994**, *32*, 675–686. [[CrossRef](#)]

26. Yao, S.; Zhang, J.; Shen, D.; Xiao, R.; Gu, S.; Zhao, M.; Liang, J. Removal of Pb(II) from water by the activated carbon modified by nitric acid under microwave heating. *J. Colloid Interface Sci.* **2016**, *463*, 118–127. [[CrossRef](#)] [[PubMed](#)]
27. Chen, C.; Duan, Y.; Huang, T.; Zhu, M.; Liu, X.; Wei, H. Regeneration Characteristics of Elemental Sulfur-Modified Activated Carbon for Mercury Removal. *Energy Fuels* **2021**, *35*, 9497–9508. [[CrossRef](#)]
28. Eustáquio, H.; Lopes, C.; Da Rocha, R.; Cardoso, B.; Pergher, S. Modification of activated carbon for the adsorption of humic acid. *Adsorpt. Sci. Technol.* **2015**, *33*, 117–126. [[CrossRef](#)]
29. Monser, L.; Ben Amor, M.; Ksibi, M. Purification of wet phosphoric acid using modified activated carbon. *Chem. Eng. Process. Process Intensif.* **1999**, *38*, 267–271. [[CrossRef](#)]
30. Wu, C.; Li, L.; Zhou, H.; Ai, J.; Zhang, H.; Tao, J.; Wang, D.; Zhang, W. Effects of chemical modification on physicochemical properties and adsorption behavior of sludge-based activated carbon. *J. Environ. Sci.* **2021**, *100*, 340–352. [[CrossRef](#)]
31. Takaoka, M.; Yokokawa, H.; Takeda, N. The effect of treatment of activated carbon by H₂O₂ or HNO₃ on the decomposition of pentachlorobenzene. *Appl. Catal. B Environ.* **2007**, *74*, 179–186. [[CrossRef](#)]
32. Shen, W.; Li, Z.; Liu, Y. Surface Chemical Functional Groups Modification of Porous Carbon. *Recent Patents Chem. Eng.* **2008**, *1*, 27–40. [[CrossRef](#)]
33. Aggarwal, D.; Goyal, M.; Bansal, R.C. Adsorption of chromium by activated carbon from aqueous solution. *Carbon N. Y.* **1999**, *37*, 1989–1997. [[CrossRef](#)]
34. Jia, Y.F.; Thomas, K.M. Adsorption of Cadmium Ions on Oxygen Surface Sites in Activated Carbon. *Langmuir* **2000**, *16*, 1114–1122. [[CrossRef](#)]
35. Strelko, V.; Malik, D.J. Characterization and Metal Sorptive Properties of Oxidized Active Carbon. *J. Colloid Interface Sci.* **2002**, *250*, 213–220. [[CrossRef](#)]
36. Tan, I.A.W.; Abdullah, M.O.; Lim, L.L.P.; Yeo, T.H.C. Surface Modification and Characterization of Coconut Shell-Based Activated Carbon Subjected to Acidic and Alkaline Treatments. *J. Appl. Sci. Process Eng.* **2017**, *4*, 186–194. [[CrossRef](#)]
37. XU, T.; LIU, X. Peanut Shell Activated Carbon: Characterization, Surface Modification and Adsorption of Pb²⁺ from Aqueous Solution. *Chin. J. Chem. Eng.* **2008**, *16*, 401–406. [[CrossRef](#)]
38. Patra, C.; Gupta, R.; Bedadeep, D.; Narayanasamy, S. Surface treated acid-activated carbon for adsorption of anionic azo dyes from single and binary adsorptive systems: A detail insight. *Environ. Pollut.* **2020**, *266*, 115102. [[CrossRef](#)]
39. Walker, G.M.; Weatherley, L.R. Adsorption of acid dyes on to granular activated carbon in fixed beds. *Water Res.* **1997**, *31*, 2093–2101. [[CrossRef](#)]
40. ShamsiJazeyi, H.; Kaghazchi, T. Investigation of nitric acid treatment of activated carbon for enhanced aqueous mercury removal. *J. Ind. Eng. Chem.* **2010**, *16*, 852–858. [[CrossRef](#)]
41. Wibowo, N.; Setyadhi, L.; Wibowo, D.; Setiawan, J.; Ismadji, S. Adsorption of benzene and toluene from aqueous solutions onto activated carbon and its acid and heat treated forms: Influence of surface chemistry on adsorption. *J. Hazard. Mater.* **2007**, *146*, 237–242. [[CrossRef](#)]
42. Pak, S.-H.; Jeon, M.-J.; Jeon, Y.-W. Study of sulfuric acid treatment of activated carbon used to enhance mixed VOC removal. *Int. Biodeterior. Biodegrad.* **2016**, *113*, 195–200. [[CrossRef](#)]
43. Singh, C.K.; Sahu, J.N.; Mahalik, K.K.; Mohanty, C.R.; Mohan, B.R.; Meikap, B.C. Studies on the removal of Pb(II) from wastewater by activated carbon developed from Tamarind wood activated with sulphuric acid. *J. Hazard. Mater.* **2008**, *153*, 221–228. [[CrossRef](#)] [[PubMed](#)]
44. Liu, S.X.; Chen, X.; Chen, X.Y.; Liu, Z.F.; Wang, H.L. Activated carbon with excellent chromium(VI) adsorption performance prepared by acid–base surface modification. *J. Hazard. Mater.* **2007**, *141*, 315–319. [[CrossRef](#)]
45. Tran, T.N.; Kim, D.-G.; Ko, S.-O. Adsorption Mechanisms of Manganese (II) Ions onto Acid-treated Activated Carbon. *KSCE J. Civ. Eng.* **2018**, *22*, 3772–3782. [[CrossRef](#)]
46. Hulicova-Jurcakova, D.; Sereych, M.; Lu, G.Q.; Bandosz, T.J. Combined Effect of Nitrogen- and Oxygen-Containing Functional Groups of Microporous Activated Carbon on its Electrochemical Performance in Supercapacitors. *Adv. Funct. Mater.* **2009**, *19*, 438–447. [[CrossRef](#)]
47. Lota, G.; Centeno, T.A.; Frackowiak, E.; Stoeckli, F. Improvement of the structural and chemical properties of a commercial activated carbon for its application in electrochemical capacitors. *Electrochim. Acta* **2008**, *53*, 2210–2216. [[CrossRef](#)]
48. Li, X.; Jiang, Y.; Wang, P.; Mo, Y.; Lai, W.; Li, Z.; Yu, R.; Du, Y.; Zhang, X.; Chen, Y. Effect of the oxygen functional groups of activated carbon on its electrochemical performance for supercapacitors. *New Carbon Mater.* **2020**, *35*, 232–243. [[CrossRef](#)]
49. Venhryn, B.Y.; Stotsko, Z.A.; Grygorchak, I.I.; Bakhmatyuk, B.P.; Mudry, S.I. The effect of ultrasonic and HNO₃ treatment of activated carbon from fruit stones on capacitive and pseudocapacitive energy storage in electrochemical supercapacitors. *Ultrason. Sonochem.* **2013**, *20*, 1302–1307. [[CrossRef](#)]
50. Khayoon, M.S.; Hameed, B.H. Acetylation of glycerol to biofuel additives over sulfated activated carbon catalyst. *Bioresour. Technol.* **2011**, *102*, 9229–9235. [[CrossRef](#)]
51. Zhang, G.; Li, Z.; Zheng, H.; Fu, T.; Ju, Y.; Wang, Y. Influence of the surface oxygenated groups of activated carbon on preparation of a nano Cu/AC catalyst and heterogeneous catalysis in the oxidative carbonylation of methanol. *Appl. Catal. B Environ.* **2015**, *179*, 95–105. [[CrossRef](#)]
52. Kastner, J.R.; Miller, J.; Geller, D.P.; Locklin, J.; Keith, L.H.; Johnson, T. Catalytic esterification of fatty acids using solid acid catalysts generated from biochar and activated carbon. *Catal. Today* **2012**, *190*, 122–132. [[CrossRef](#)]

53. Durán-Valle, C.J.; Madrigal-Martínez, M.; Martínez-Gallego, M.; Fonseca, I.M.; Matos, I.; Botelho do Rego, A.M. Activated carbon as a catalyst for the synthesis of N-alkylimidazoles and imidazolium ionic liquids. *Catal. Today* **2012**, *187*, 108–114. [[CrossRef](#)]
54. Sánchez-Velandia, J.E.; Pájaro, E.; Villa, A.L.; Martínez-O, F. Selective synthesis of camphene from isomerization of α - and β -pinene over heterogeneous catalysts. *Microporous Mesoporous Mater.* **2021**, *324*, 111273. [[CrossRef](#)]
55. Chimal-Valencia, O.; Robau-Sánchez, A.; Collins-Martínez, V.; Aguilar-Elguézabal, A. Ion exchange resins as catalyst for the isomerization of α -pinene to camphene. *Bioresour. Technol.* **2004**, *93*, 119–123. [[CrossRef](#)] [[PubMed](#)]
56. Kapp, T.; Kammann, U.; Vobach, M.; Vetter, W. Synthesis of low and high chlorinated toxaphene and comparison of their toxicity by zebrafish (*Danio rerio*) embryo test. *Environ. Toxicol. Chem.* **2006**, *25*, 2884–2889. [[CrossRef](#)] [[PubMed](#)]
57. Thomas, A.F.; Bessière, Y. Limonene. *Nat. Prod. Rep.* **1989**, *6*, 291–309. [[CrossRef](#)]
58. Schultes, R.E. Common Fragrance and Flavor Materials: Preparation, Properties and Uses. *Econ. Bot.* **1987**, *41*, 493. [[CrossRef](#)]
59. Paggiola, G.; Van Stempvoort, S.; Bustamante, J.; Barbero, J.M.V.; Hunt, A.J.; Clark, J.H. Can bio-based chemicals meet demand? Global and regional case-study around citrus waste-derived limonene as a solvent for cleaning applications. *Biofuels Bioprod. Biorefin.* **2016**, *10*, 686–698. [[CrossRef](#)]
60. Ciriminna, R.; Lomeli-Rodriguez, M.; Demma Carà, P.; Lopez-Sanchez, J.A.; Pagliaro, M. Limonene: A versatile chemical of the bioeconomy. *Chem. Commun.* **2014**, *50*, 15288–15296. [[CrossRef](#)]
61. Solkina, Y.S.; Reshetnikov, S.I.; Estrada, M.; Simakov, A.; Murzin, D.Y.; Simakova, I.L. Evaluation of gold on alumina catalyst deactivation dynamics during α -pinene isomerization. *Chem. Eng. J.* **2011**, *176*, 42–48. [[CrossRef](#)]
62. Liu, Y.; Zheng, D.; Li, B.; Lyu, Y.; Wang, X.; Liu, X.; Li, L.; Yu, S.; Liu, X.; Yan, Z. Isomerization of α -pinene with a hierarchical mor-denite molecular sieve prepared by the microwave assisted alkaline treatment. *Microporous Mesoporous Mater.* **2020**, *299*, 110117. [[CrossRef](#)]
63. Miądlicki, P.; Wróblewska, A.; Kielbasa, K.; Koren, Z.C.; Michalkiewicz, B. Sulfuric acid modified clinoptilolite as a solid green catalyst for solvent-free α -pinene isomerization process. *Microporous Mesoporous Mater.* **2021**, *324*, 111266. [[CrossRef](#)]
64. Frattini, L.; Isaacs, M.A.; Parlett, C.M.A.; Wilson, K.; Kyriakou, G.; Lee, A.F. Support enhanced α -pinene isomerization over HPW/SBA-15. *Appl. Catal. B Environ.* **2017**, *200*, 10–18. [[CrossRef](#)]
65. Wróblewska, A.; Miądlicki, P.; Sreńscek-Nazzal, J.; Sadłowski, M.; Koren, Z.C.; Michalkiewicz, B. Alpha-pinene isomerization over Ti-SBA-15 catalysts obtained by the direct method: The influence of titanium content, temperature, catalyst amount and reaction time. *Microporous Mesoporous Mater.* **2018**, *258*, 72–82. [[CrossRef](#)]
66. Zielińska, B.; Wróblewska, A.; Maślana, K.; Miądlicki, P.; Kielbasa, K.; Rozmysłowska-Wojciechowska, A.; Petrus, M.; Woźniak, J.; Jastrzębska, A.M.; Michalkiewicz, B.; et al. High catalytic performance of 2D Ti₃C₂T_x MXene in α -pinene isomerization to camphene. *Appl. Catal. A Gen.* **2020**, *604*, 117765. [[CrossRef](#)]
67. Comelli, N.A.; Ponzi, E.N.; Ponzi, M.I. α -Pinene isomerization to camphene: Effect of thermal treatment on sulfated zirconia. *Chem. Eng. J.* **2006**, *117*, 93–99. [[CrossRef](#)]
68. Severino, A.; Vital, J.; Lobo, L.S. Isomerization of α -pinene over TiO₂: Kinetics and catalyst optimization. *Stud. Surf. Sci. Catal.* **1993**, *78*, 685–692. [[CrossRef](#)]
69. Sidorenko, A.Y.; Senkov, G.M.; Agabekov, V.E. Effect of acid treatment on the composition and structure of a natural aluminosilicate and on its catalytic properties in α -pinene isomerization. *Catal. Ind.* **2014**, *6*, 94–104. [[CrossRef](#)]
70. Glonek, K.; Wróblewska, A.; Makuch, E.; Ulejczyk, B.; Krawczyk, K.; Wróbel, R.J.; Koren, Z.C.; Michalkiewicz, B. Oxidation of limonene using activated carbon modified in dielectric barrier discharge plasma. *Appl. Surf. Sci.* **2017**, *420*, 873–881. [[CrossRef](#)]
71. Takahagi, T.; Ishitani, A. XPS study on the surface structure of carbon fibers using chemical modification and C1s line shape analysis. *Carbon N. Y.* **1988**, *26*, 389–395. [[CrossRef](#)]
72. Geśkiewicz-Puchalska, A.; Zgrzebnicki, M.; Michalkiewicz, B.; Narkiewicz, U.; Morawski, A.W.; Wrobel, R.J. Improvement of CO₂ uptake of activated carbons by treatment with mineral acids. *Chem. Eng. J.* **2017**, *309*, 159–171. [[CrossRef](#)]
73. Ahmed, M.J. Preparation of activated carbons from date (*Phoenix dactylifera* L.) palm stones and application for wastewater treatments: Review. *Process Saf. Environ. Prot.* **2016**, *102*, 168–182. [[CrossRef](#)]
74. Li, M.; Liu, Y.; Liu, S.; Shu, D.; Zeng, G.; Hu, X.; Tan, X.; Jiang, L.; Yan, Z.; Cai, X. Cu(II)-influenced adsorption of ciprofloxacin from aqueous solutions by magnetic graphene oxide/nitrioltri-acetic acid nanocomposite: Competition and enhancement mechanisms. *Chem. Eng. J.* **2017**, *319*, 219–228. [[CrossRef](#)]
75. Badruddoza, A.Z.M.; Tay, A.S.H.; Tan, P.Y.; Hidajat, K.; Uddin, M.S. Carboxymethyl- β -cyclodextrin conjugated magnetic nanoparticles as nano-adsorbents for removal of copper ions: Synthesis and adsorption studies. *J. Hazard. Mater.* **2011**, *185*, 1177–1186. [[CrossRef](#)] [[PubMed](#)]
76. Reyhani, A.; Nozad Golikand, A.; Mortazavi, S.Z.; Irannejad, L.; Moshfegh, A.Z. The effects of multi-walled carbon nanotubes graphitization treated with different atmospheres and electrolyte temperatures on electrochemical hydrogen storage. *Electrochim. Acta* **2010**, *55*, 4700–4705. [[CrossRef](#)]
77. Serafin, J.; Baca, M.; Biegun, M.; Mijowska, E.; Kalerćzuk, R.J.; Sreńscek-Nazzal, J.; Michalkiewicz, B. Direct conversion of biomass to nanoporous activated biocarbons for high CO₂ adsorption and supercapacitor applications. *Appl. Surf. Sci.* **2019**, *497*, 143722. [[CrossRef](#)]
78. Wang, Y.; Wang, S.; Xie, T.; Cao, J. Activated carbon derived from waste tangerine seed for the high-performance adsorption of carbamate pesticides from water and plant. *Bioresour. Technol.* **2020**, *316*, 123929. [[CrossRef](#)]

79. Neolaka, Y.A.B.; Lawa, Y.; Naat, J.; Riwu, A.A.P.; Darmokoesoemo, H.; Widyaningrum, B.A.; Iqbal, M.; Kusuma, H.S. Indonesian Kesambi wood (*Schleichera oleosa*) activated with pyrolysis and H₂SO₄ combination methods to produce mesoporous activated carbon for Pb(II) adsorption from aqueous solution. *Environ. Technol. Innov.* **2021**, *24*, 101997. [[CrossRef](#)]
80. Liu, B.; Wang, W.; Wanga, N.; Au, C.T. Preparation of activated carbon with high surface area for high-capacity methane storage. *J. Energy Chem.* **2014**, *23*, 662–668. [[CrossRef](#)]
81. Serafin, J.; Ouzzine, M.; Cruz, O.F.; Sreńscek-Nazzal, J.; Campello Gómez, I.; Azar, F.-Z.; Rey Mafull, C.A.; Hotza, D.; Rambo, C.R. Conversion of fruit waste-derived biomass to highly microporous activated carbon for enhanced CO₂ capture. *Waste Manag.* **2021**, *136*, 273–282. [[CrossRef](#)]
82. Tongpoothorn, W.; Sriuttha, M.; Homchan, P.; Chanthai, S.; Ruangviriyachai, C. Preparation of activated carbon derived from *Jatropha curcas* fruit shell by simple thermo-chemical activation and characterization of their physico-chemical properties. *Chem. Eng. Res. Des.* **2011**, *89*, 335–340. [[CrossRef](#)]
83. Sreńscek-Nazzal, J.; Kielbasa, K. Advances in modification of commercial activated carbon for enhancement of CO₂ capture. *Appl. Surf. Sci.* **2019**, *494*, 137–151. [[CrossRef](#)]
84. De Oliveira Brito, S.M.; Andrade, H.M.C.; Soares, L.F.; de Azevedo, R.P. Brazil nut shells as a new biosorbent to remove methylene blue and indigo carmine from aqueous solutions. *J. Hazard. Mater.* **2010**, *174*, 84–92. [[CrossRef](#)]
85. Thommes, M.; Kaneko, K.; Neimark, A.V.; Olivier, J.P.; Rodriguez-Reinoso, F.; Rouquerol, J.; Sing, K.S.W. Physisorption of gases, with special reference to the evaluation of surface area and pore size distribution (IUPAC Technical Report). *Pure Appl. Chem.* **2015**, *87*, 1051–1069. [[CrossRef](#)]
86. Serafin, J.; Ouzzine, M.; Cruz Junior, O.F.; Sreńscek-Nazzal, J. Preparation of low-cost activated carbons from amazonian nutshells for CO₂ storage. *Biomass Bioenergy* **2021**, *144*, 105925. [[CrossRef](#)]
87. Wang, S.; Zhu, Z.H. Effects of acidic treatment of activated carbons on dye adsorption. *Dye. Pigment.* **2007**, *75*, 306–314. [[CrossRef](#)]
88. Shim, J.-W.; Park, S.-J.; Ryu, S.-K. Effect of modification with HNO₃ and NaOH on metal adsorption by pitch-based activated carbon fibers. *Carbon N. Y.* **2001**, *39*, 1635–1642. [[CrossRef](#)]
89. Ania, C.; Parra, J.; Pis, J. Influence of oxygen-containing functional groups on active carbon adsorption of selected organic compounds. *Fuel Process. Technol.* **2002**, *79*, 265–271. [[CrossRef](#)]
90. Ünveren, E.; Gündüz, G.; Cakicioğlu-Özkan, F. Isomerization of Alpha-pinene Over Acid Treated Natural Zeolite. *Chem. Eng. Commun.* **2005**, *192*, 386–404. [[CrossRef](#)]
91. Allahverdiev, A.I.; Irandoust, S.; Murzin, D.Y. Isomerization of α -Pinene over Clinoptilolite. *J. Catal.* **1999**, *185*, 352–362. [[CrossRef](#)]